This electronic thesis or dissertation has been downloaded from the King's Research Portal at https://kclpure.kcl.ac.uk/portal/

Epidermal growth factor receptor ligands as modulators of peripheral nerve injury

Kiesewetter, Hannes

Awarding institution:
King's College London

The copyright of this thesis rests with the author and no quotation from it or information derived from it may be published without proper acknowledgement.

END USER LICENCE AGREEMENT

Unless another licence is stated on the immediately following page this work is licensed

under a Creative Commons Attribution-NonCommercial-NoDerivatives 4.0 International

licence. https://creativecommons.org/licenses/by-nc-nd/4.0/

You are free to copy, distribute and transmit the work

Under the following conditions:

- Attribution: You must attribute the work in the manner specified by the author (but not in any way that suggests that they endorse you or your use of the work).
- Non Commercial: You may not use this work for commercial purposes.
- No Derivative Works - You may not alter, transform, or build upon this work.

Any of these conditions can be waived if you receive permission from the author. Your fair dealings and other rights are in no way affected by the above.

Take down policy

If you believe that this document breaches copyright please contact librarypure@kcl.ac.uk providing details, and we will remove access to the work immediately and investigate your claim.

Download date: 08. Oct. 2023

Epidermal growth factor receptor ligands as modulators of peripheral nerve injury

Hannes Kiesewetter

Thesis presented for the degree of Doctor of Philosophy at the University of London

King's College London

2013

I. Abstract

Signalling between different cell types in the nervous system is a key element in the pathophysiology of peripheral nerve injury. Epidermal growth factor receptor ligands (EGFRLs) bind the EGF receptor (ErbB1) and its related protein ErbB4 forming an adaptable signalling system implicated in multiple biological processes. Ligands binding the EGF receptor have not yet been implicated in the pathophysiology of nerve injury.

In this thesis, I demonstrated differential expression of EGFR ligands following nerve injury in rats, such as Amphiregulin, Epidermal growth factor, Epiregulin, Heparin-binding EGF, Transforming growth factor-α and Betacellulin (BTC). In a medium-throughput quantitative PCR array screening of cytokines, BTC was one of the top differentially upregulated factors following partial sciatic nerve transection (SNT) at different timepoints. Given that its role in the nervous system is unknown I set out to elucidate its mechanism of action following injury. First I examined its ability to activate intracellular pathways. Although BTC activated ERK and p38 MAP kinases in relevant cell types (dorsal root ganglion neurons, macrophages) imaging experiments indicated no change in intracellular calcium levels. To investigate a potential neuronal effect I examined the growth promoting effect of BTC on dissociated DRG neurons. The growth factor did not affect neurite outgrowth. Interestingly, other EGFR ligands were also ineffective. In cultured peritoneal macrophages chemotaxis was not affected in vitro, but I demonstrated a chemotactic effect *in vivo.* Additionally, examination of a panel of macrophage phenotypic markers revealed a downregulation of the phagocytic scavenger receptor CD36 following stimulation with BTC.

Intrathecal injection of BTC in the spinal cord (L4-L5), was able to activate ERK but did not affect thermal (Hargreaves) and mechanical (von Frey) sensitivity. Moreover, blocking the EGF receptor in models of either inflammatory (formalin injection in the hindpaw) or neuropathic (SNT) pain did not alter thermal and mechanical hypersensitivity.

In summary, BTC is robustly upregulated following peripheral nerve injury. Although its role its not yet completely clarified, my data points towards a modulating effect on the macrophage phenotype and its an interesting target for future investigation on the pathophysiology of nerve injury.

II. Publications

CXCL5 mediates UVB irradiation-induced pain.

Dawes, J.M., M. Calvo, J.R. Perkins, K.J. Paterson, **H. Kiesewetter**, C. Hobbs, T.K. Kaan, C. Orengo, D.L. Bennett, and S.B. McMahon. 2011. Science translational medicine. 3:90ra60.

Sodium channels and mammalian sensory mechanotransduction

Raouf, R., F. Rugiero, **H. Kiesewetter**, R. Hatch, E. Hummler, M.A. Nassar, F. Wang, and J.N. Wood. 2012.. Molecular pain. 8:21.

Gene expression profiling of EGFR ligands following nerve injury.

Kiesewetter, H., Dawes J. M., Calvo M., McMahon S. B., Bennett D. L. H., SFN 2012, Poster

In vitro model of Bortezomib-induced peripheral neuropathy

La Russa F., **Kiesewetter H.,** Cavaletti G., Bennett D. L. H., IASP 2012, Poster

Profiling inflammatory mediators in peripheral tissues from MIA model of chronic joint pain.

Dawes, J. M., **Kiesewetter H.,** Bennett D.L.H., McMahon, S. B., Poster, SFN 2011

III. Acknowledgements

I am sincerely grateful to my supervisors Professor Stephen McMahon and Dr. David Bennett for giving me the opportunity to do a PhD with the London Pain Consortium. I want to express my deepest gratitude to both of them. Also, I want to thank my unofficial third supervisor Dr. Athanasios Didangelos, who supported me with invaluable knowledge, especially for my 4th Chapter but also for reading most of my thesis.

I would like to thank Dr. Andrew Grant for advice with the Ca^{2+} imaging experiments, Dr. Margarita Calvo for teaching me how to use the Boyden chamber and Dr. Ning Zhu for getting me started with Western blotting. Special thanks goes to Vivien Cheah, Caroline Abel and especially John Grist, who did most of the SNT surgeries for this thesis. For introducing me to the lab and teaching me how to do my first PCR, DRG neuron culture and behavioural testing I must thank Dr. John Dawes. Dr. Dawes also did the initial experiment using PCR array cards on injured sciatic nerve tissue, which was the start-up for this thesis. For introducing me to the InCell Analyser, I thank Dr. Thomas Hutson. Thanks, Tom and John for being excellent friends over the years.

I am extremely grateful to useful brainstorming with my colleagues in the office Dr. Lan Zhu, Dr. Franziska Denk, and especially Dr. Ana Antunes-Martins who also read some of my thesis. I also want to thank Dr. Katalin Bartus for brilliant help with immunocytochemistry. Especially, I have to thank Kathryn Paterson, who, as my desk neighbour, always had to listen and always did. A special thanks to Federica La Russa, who joined the lab halfway through, so we could team up measuring neurite outgrowth. Kathryn, Fede, Ana and Katalin all became good friends. Thank you Martina for the evenings in the climbing centre. Of course I would like to thank everyone from the Wolfson for making work such a pleasurable memory, but especially, Amelie, Maggie, Lisa, Patricia, Natalie, Costi, Emily, Seb, Rie, Tom P. and the friends from the café. Outside of the lab I would like to thank my amazing friends Johannes, Yves, Chrischi, Junne and Thanos who were always there for me, my parents, Beate and Reinhard Kiesewetter and of course my partner the lovely Joo-Hee Waelzlein (a BIG Thank You!, not only for proofreading). Last but not least, (although he did not do too much proofreading) I want to thank my little son Henry for arriving on this planet during my time here in London.

Table of contents

I. Abstract 2
II. Publications 3
III. Acknowledgements 4
IV. List of figures 9
V. List of tables 11
VI. Abbreviations 12

1. General introduction 16

1.1. History of Wallerian degeneration 17
1.2. Peripheral changes following nerve injury 18
1.3. Cellular components involved in peripheral nerve injury and Wallerian degeneration 21
1.3.1. Schwann cells 21
1.3.2. Immune cell response after peripheral nerve injury 24
1.3.2.1. Neutrophils/mast cells 24
1.3.2.2. Macrophages 24
1.3.2.3. T-Lymphocytes 26
1.3.2.4. Fibroblasts 26
1.3.2.5. Endothelial cells 27
1.3.3. Changes in primary neurons following nerve injury 28
1.4. Nerve injury and neuropathic pain 31
1.5. Effects of neurotrophic and growth factors following peripheral nerve injury 33
1.6. Epidermal growth factor receptor ligands 36
1.7. ADAMs - activating enzymes of EGFR ligands 37
1.8. The EGFR family 38
1.9. EGFR and peripheral nerve injury 40
1.10. Animal models of chronic pain 41
1.11. Spinal nerve transection model as a model for neuropathic pain and regeneration 42
1.12. Aims of this work 43

2. The regulation of EGFR ligands, their receptors and shedding enzymes in the DRG and sciatic nerve after injury 44

2.1. Introduction 45
2.1.1. Expression changes in the peripheral nerve following peripheral nerve injury 46
2.1.2. Expression changes in the DRG following peripheral nerve injury 47
2.1.3. Expression changes in the dorsal horn following peripheral nerve injury 48

2.2. Materials and Methods 49
2.2.1. Animals 49
2.2.2. Surgery 49
2.2.3. Tissue dissection 50
2.2.4. RNA extraction 51

2.2.5. Reverse transcriptase PCR 53
2.2.6. Taqman array set-up and quantitative real-time PCR 53
2.2.7. Quantitative real-time PCR 53
2.2.8. Statistical analysis 60

2.3. Results 61
2.3.1. Medium-throughput TaqMan RT-qPCR array cards 61
2.3.1.1. Timecourse following SNT 61
2.3.1.2. Functional clustering of co-expressed genes 65
2.3.1.3. Ranking of the most significant gene changes 67
2.3.2. Expression of EGFR ligands 71
2.3.2.1. Baseline expression of EGFR ligands 71
2.3.2.2. Expression changes of EGFR ligands in the sciatic nerve 73
2.3.2.3. Expression changes of ErB1 and ErbB4 and ADAM10 and ADAM17 in the sciatic nerve 77
2.3.2.4. Expression changes of EGFR ligands in the L5 DRG 79
2.3.2.5. Expression changes of ErB1 and ErbB4 and ADAM10 and ADAM17 in the L5 DRG 82
2.3.2.6. Expression changes of EGFR ligands in the dorsal horn 84
2.3.2.7. Expression changes of ErB1 and ErbB4 and ADAM10 and ADAM17 in the dorsal horn 87

2.4. Discussion 89

3. Behavioural evaluation of EGFR inhibition and BTC treatment rats 96

3.1. Introduction 97
3.1.1. BTC, a protein with diverse functions in biological processes 97
3.1.2. EGFR as a novel target for nociceptive modulation; EGFR inhibition 100
3.1.3. EGFR inhibition as a potential treatment for neuropathic pain 101

3.2. Methods 105
3.2.1. Animals 105
3.2.2. Intraplantar injections 105
3.2.3. Intrathecal injections 105
3.2.4. Oral gavaging 106
3.2.5. Preparation of drugs 106
3.2.6. Formalin Test 106
3.2.7. Surgery 107
3.2.8. Mechanical hypersensitivity 107
3.2.9. Thermal hypersensitivity 107
3.2.10. Protein extraction and protein immunoblotting 108
3.2.11. Statistical analysis 108

3.3. Results 109
3.3.1. BTC as a peripheral pain mediator 109
3.3.2. Intrathecal injection of BTC 111
3.3.3. Intrathecal injection of EGF and EREG 112
3.3.4. Inhibition of EGFR: physiological and pathological effects 114
3.3.4.1. Inflammatory pain model – formalin test 117
3.3.4.1.1. Intraperitoneal administration of Gefitinib 117
3.3.4.1.2. Oral administration of Gefitinib 117
3.3.4.2. Neuropathic pain – L5 SNT model 120

3.4. Discussion 124
3.4.1. BTC has no peripheral effect in nociception 124
3.4.2. The effects of BTC, EGF and EREG following intrathecal injection 126
3.4.3. Inhibition of EGFR in animal models of pain 126

4. The role of BTC following nerve injury – mechanistic studies 129

4.1. Introduction 130
4.1.1. The function of growth factors in neurons 130
4.1.2. The function of growth factors in SCs 132
4.1.3. The function of growth factors on macrophages in the peripheral nervous system 133

4.2. Methods 135
4.2.1. Animals 135
4.2.2. Cell culture 135
4.2.2.1. Sensory neuron culture 135
4.2.2.2. Macrophages 136
4.2.2.2.1. Peritoneal macrophages 136
4.2.2.2.2. Bone-marrow derived macrophages 136
4.2.2.3. Schwann cells 136
4.2.2.4. Cell lines 137
4.2.3. Calcium imaging 137
4.2.4. Protein biochemistry -Western blotting 138
4.2.5. Immunocytochemistry 141
4.2.6. Neurite outgrowth – InCell Analyser 141
4.2.7. Chemotaxis assay *in vitro* 143
4.2.8. Chemotaxis assay *in vivo* 144
4.2.9. RT-qPCR 144
4.2.10. Statistical analysis 144

4.3. Results 145
4.3.1. Downstream signalling of BTC 145
4.3.2. Evaluation of neurite outgrowth *in vitro* following BTC stimulation 150
4.3.3. Gefitinib inhibits ERK phosphorylation in sensory neurons *in vitro* 157
4.3.4. Effect of BTC on intracellular calcium signalling 159
4.3.5. Effect of BTC on Schwann cell function 163

4.3.6. Effect of BTC on macrophage function 167
4.3.6.1. Chemotaxis in peritoneal macrophages 167
4.3.6.2. Chemoattractive properties of BTC *in vivo* 168
4.3.6.3. Monocyte scavenger receptor 1B, CD36 is modulated by BTC 170
4.3.7. BTC and scavenger receptor expression following nerve injury 173

4.4. Discussion 178

5. General conclusion and future directions 182

5.1. General conclusions 183
5.2. Future directions 186
5.3. Summary 187

Bibliography 188

IV. List of Figures

Chapter 1

Figure 1.1. Schematic representation of cellular components in peripheral nerve injury 20

Figure 1.2. Neuronal response following nerve injury 30

Figure 1.3. Trk/p75 receptor signaling 34

Figure 1.4. EGFR ligands, receptors and cleavage sites 37

Figure 1.5. Simplified pathway of intracellular protein interactions following EGFR activation 39

Chapter 2

Figure 2.1. Anatomy of the sciatic nerve in rats 50

Figure 2.2. RNA purity 52

Figure 2.3. Testing for primer efficiency 56

Figure 2.4. Melting curve analysis 57

Figure 2.5. Equation $2^{-\Delta\Delta CT}$ 58

Figure 2.6. $2^{-\Delta\Delta CT}$ Analysis 59

Figure 2.7. Hierarchical clustering of medium-throughput RT-qPCR data from sciatic nerve following SNT 64

Figure 2.8. Group of genes with most uniform clustering 66

Figure 2.9. TaqMan medium-throughput RT-qPCR. Relative expression of BTC and HB-EGF in the sciatic nerve 70

Figure 2.10. Estimation of baseline expression of EGFR ligands 72

Figure 2.11. EGFR ligands in the sciatic nerve 74

Figure 2.12. Comparing expression of EGFR ligands in sciatic nerve 76

Figure 2.13. ErbB1 (EGFR), ErbB4 and shedding enzymes ADAM10 and ADAM17 in the sciatic nerve 78

Figure 2.14. EGFR ligands in L5 DRG 80

Figure 2.15. Comparing expression of EGFR ligands in L5 DRG 81

Figure 2.16. ErbB1 (EGFR), ErbB4 and shedding enzymes ADAM10 and ADAM17 in L5 DRG 83

Figure 2.17. EGFR ligands in the dorsal horn 85

Figure 2.18. Comparing expression of EGFR ligands in the dorsal horn at the level of L5 87

Figure 2.19. ErbB1 (EGFR), ErbB4 and shedding enzymes ADAM10 and ADAM17 in the dorsal horn at the level of L5 88

Chapter 3

Figure 3.1. Structure of BTC 97

Figure 3.2. Structure of Gefitinib 103

Figure 3.3. BTC (2µg) and NGF (500ng) s.c. injection 110

Figure 3.4. Intrathecal injection of BTC and MAPK activation *in vivo* 112

Figure 3.5. EGF intrathecal injection 113

Figure 3.6. EREG intrathecal injection 114

Figure 3.7. Experimental design, EGFR inhibition – sensitivity levels and Formalin test 115

Figure 3.8. EGFR inhibition – baseline sensitivity levels 116

Figure 3.9. EGFR inhibition – inflammatory pain 118

Figure 3.10. Experimental design – Gefitinib following SNT 120

Figure 3.11. EGFR inhibition – neuropathic pain 122

Figure 3.12. BTC orthologues in rat and mouse 125

Chapter 4

Figure 4.1. Automated image analysis 142

Figure 4.2. Design of Boyden chamber 143

Figure 4.3. Signalling in HEK293 cells 146

Figure 4.4. Signalling in peritoneal macrophages 147

Figure 4.5. ErbB1 (EGFR) and ErbB4 expression in DRG neurons *in vitro* 148

Figure 4.6. Signalling in DRG neurons 149

Figure 4.7. Neurite outgrowth on DRG neurons 24 hours *in vitro* 151

Figure 4.8. NGF and BDNF enhance neurite outgrowth in primary adult DRG neurons 152

Figure 4.9. BTC has no effect on neurite length or cell number 154

Figure 4.10. Neurite length and cell number with delayed BTC treatment 155
Figure 4.11. Neurite outgrowth with EGFR ligands 156
Figure 4.12. Gefitinib inhibits ERK activation in DRG neurons *in vitro* 158
Figure 4.13. Calcium imaging *in vitro* 161
Figure 4.14. PCR array SCs stimulated with BTC 164
Figure 4.15. ErbB1 (EGFR) expression in SCs 165
Figure 4.16. ErbB1 and ErbB4 expression in SCs 5 days *in vitro* 166
Figure 4.17. Chemotaxis assay peritoneal macrophages 168
Figure 4.18. BTC increases IBA1 positive cells *in vivo* 169
Figure 4.19. CD36 modulation in macrophages by BTC 171
Figure 4.20. IBA1 and BTC following SNT 173
Figure 4.21. Protein levels of BTC 14 days following nerve injury 175
Figure 4.22. IBA1, CD36 and CD68 expression in the nerve post SNL 177

V. List of tables

Table 1. Primer sequences 55
Table 2. Genes of the TaqMan RT-qPCR array card 62
Table 3. Top-ranking the 5 most upregulated genes in the sciatic nerve 68
Table 4. Expression of the EGF receptor in the human nervous system 100
Table 5. Solutions for Western blotting 140

VI. Abbreviations

ADAM	A disintegrin and metalloprotease
AKT	Protein kinase B
ANOVA	Analysis of variance
AP1 box	Activator protein 1 box
AREG	Amphiregulin
ATP	Adenosine triphosphate
ATP	Adenosine triphosphate
AUC	Area under the curve
BDNF	Brain-derived neurotrophic factor
bFGF	Basic fibroblast growth factor
BTC	Betacellulin
cAMP	Cyclic adenosine monophosphate
CD	cluster of differentiation ()
cDNA	Complementary DNA
CNS	Central nervous system
CNTF	Ciliary neurotrophic factor ()
CO_2	Carbondioxide
CPRS 1	Complex regional pain syndrome type 1
CR3	Complement receptor-3
C_T	Cycling threshold
DMEM	Dulbecco's modified eagle medium
DNA	Desoxyribonucleic acid
DRG	Dorsal root ganglion
e.g.	*exempli gratia* (lat.: for example)
ECM	Extracellular matrix
EDTA	Ethylene-diamine-tetra-acetic acid
EGF	Endothelial growth factor
EGFR	Endothelial growth factor receptor
ErbB	Receptor tyrosine-protein kinase ErbB
EREG	Epiregulin
ERK	Extracellular signal-regulated kinase
et al.	*Et alii* (lat.: and others)
etc.	Et cetera (lat.: and other things)

FBS	Foetal bovine serum
FC-γ-R	FC gamma receptors
FGF	fibroblast growth factor
FGFR	Fibroblast growth factor receptor
Fura-2-AM	Fura-2-acetoxymethyl ester
Gal-3	Galectin-3
GAP-43	Growth associated protein-43
GAPDH	Glyceraldehyde 3-phosphate dehydrogenase
GDNF	Glial cell-derived neurotrophic factor
GGF	Glial growth factor
GM-CFS	Granulocyte macrophage colony-stimulating factor
GOI	Gene of interest
GSK-3	Glycogen synthase kinase-3
GTP	Guanosine-5'-triphosphate
H_2O	Water
HB-EGF	Heparin binding-endothelial growth factor
HBSS	Hank’s balanced salt solution
HEK293	Human embryonic kidney 293
HEPES	4-(2-hydroxyethyl)-1-piperazineethanesulfonic acid
HNSCC	Head and neck squamous cell carcinoma
i.p.	Intraperitoneal
IBA1	Ionised calcium-binding adapter molecule 1 ()
IFN	Interferon
Ig	Immunoglobulin
IL	Interleukin
IP_3	Inositol-1,3,5-triphosphate
KCl	Potassium chloride
LIF	Leukemia inhibitory factor
LPS	Lipopolysaccharide of gram-negative bacteria
LRP-1	Low density lipoprotein receptor-related protein 1
MAG	Myelin associated glycoprotein
MAPK	Mitogen activated protein kinase
MBP	Myelin basic protein
MCL	Markov clustering algorithm
MCSF	Macrophages-culture stimulating factor

MHC	Major histocompatibility class
MIP-1α	Macrophage inflammatory protein 1α
MMP	Matrix metalloproteases
mRNA	Messenger RNA
NCAM	Neural cell adhesion molecule
NGF	Nerve growth factor
NO	Nitric oxide
NRG	Neuregulin 1
NSCLC	Non-small cell lung cancer
n.s.	*not significant*
NT	Neurotrophin
ON	Overnight
p-EGFR	Phosphorylated EGFR
p-ERK	Phosphorylated ERK
p-p38	Phosphorylated p38
p.o.	*per os* (lat.: Oral administration)
PBS	Phosphate buffered saline
PC12	Pheochromocytoma cell line 12
PCR	Polymerase chain reaction
PFA	Paraformaldehyde
PI3	Phosphoinositide-3-kinase
PKC	Protein kinase C
PLA_2	Phospholipase A_2
PLCγ	Phospholipase C-γ
PLL	Poly-L-lysine
PVDF	Polyvinylidene fluoride
RG	Reference gene
RNA	Ribonucleic acid
rpm	Revolutions per minute
RT	Room temperature
RT-PCR	Reverse transcriptase polymerase chain reaction
RT-qPCR	Quantitative real time polymerase chain reaction
SC	Schwann cell
SCI	Spinal cord injury
SDS-PAGE	Sodium dodecylsulfate polyacrylamide gel electrophoresis

SNT	Spinal nerve transection
SVZ	Subventricular zone
TACE	TNF-α converting enzyme
TGF-α	Transforming growth factor-α
TKI	Small-molecule tyrosine kinase inhibitor
TLR	Toll-like receptors
TNF-α	Tumour necrosis factor alpha
Trk	Tropomyosin-receptor-kinase
TRP	Transient receptor potential
Wld^{slow}	Slow Wallerian degeneration

CHAPTER 1

General Introduction

1.1. History of Wallerian degeneration

The first advances in understanding the physiology and pathophysiology of the function of neurons started in the beginning of the 19th century with the development of new microscopy techniques. Robert Remak (Lagunoff, 2002) made the first groundbreaking contributions - in the beginning at his kitchen table then as an assistant in Johannes Müller's laboratory - to the anatomical understanding of the nervous system, describing the unmyelinated nerve fibre (Remak, 1844). Other discoveries led to an exponential growth in knowledge about the anatomy of the nervous system at the beginning of the 20th century. Augustus Wolney Waller used frog glossopharyngeal and hypoglossal nerves to anatomically describe the "alterations produced thereby in the structure of their primitive fibres", observing "coagulation and curdling of the medulla (myelin) into separate particles of various size" (Waller, 1850). Following Waller's discovery that distal axons degenerate once they become detached from the proximal nerve, the corner stone was laid for research into peripheral nerve injury. New therapies, especially nerve grafting, the gold standard in treating peripheral nerve injuries until today, were progressively developed and refined during the two world wars where extremity injuries included trauma to peripheral nerves (Gaudet et al., 2011; Langley and Hashimoto, 1917).

1.2. Peripheral changes following nerve injury

When Augustus Waller described his model of peripheral nerve injury in 1850 his key findings described mainly anatomical changes, which were later specified by others, ranging from an initial swelling of the distant part of the nerve and subsequently a slow degeneration, which does not begin until 24 hours following the injury in rodents (Lubinska, 1977; Beirowski et al., 2005). Waller described the degenerative changes, which involve both, axon degeneration and myelin breakdown and are followed by a regenerative phase involving axon regeneration and remyelination. The timecourse of regeneration is different in different species. In humans the regenerative process can take up to several days (Chaudhry and Cornblath, 1992). In the adult peripheral nervous system nerve regeneration following injury can lead to functional recovery. Nevertheless, location (distal versus proximal) and severity of the injury (crush injury versus dissection) has a considerable impact on the clinical outcome (Burnett and Zager, 2004). In contrast to the periphery, central neurons have limited intrinsic regenerative capabilities and are much more exposed to inhibitory factors, which hinder the process of effective reinnervation (Rossi et al., 2007).

It is not clear what the exact molecular mechanisms are, that initiate an axon death programme. However, it has been proposed that axon death is regulated via an algorithm akin to the apoptotic cell death programme, but with a distinct molecular process. This controlled degeneration does not only reduce energy consumption of non-functional tissue but also helps to recycle essential molecules for reconstruction. This can be supported by the discovery of the *slow Wallerian degeneration* (Wld^{slow}) mutant mouse, in which the axotomised distal part of the nerve remains intact for much longer in comparison to the wildtype (Coleman and Freeman, 2010). The Wld^{slow} mouse has a gain of function mutation overexpressing the protein nicotinamide mononucleotide adenlyl transferase 1 fused to ubiquitination factor e4b. This mutation delays Wallerian degeneration in a lot of species, which suggests that the mutation inhibits a conserved axon destruction programme (Coleman and Freeman, 2010). Recently, Osterloh *et al.* described that the loss of *Drosophila* Toll receptor adaptor *dSarm* can suppress Wallerian degeneration, providing first evidence for a member of this endogenous axonal degeneration programme

which might be a promising therapeutic target for neurodegenerative diseases (Osterloh et al., 2012).

Peripheral nerve injury leads to an inflammatory but growth-promoting environment distal to the injury site to achieve reorganization of the injured tissue and reinnervation of the affected target. Functional recovery differs depending on the severity of the injury. Axonotmesis, which means that axonal injury occurs without disrupting the connective sheaths of a nerve, usually leads to more successful regeneration whereas neurotmesis, a transection of a whole nerve leads to poor recovery due to misrouting of regenerating axons or fibrosis of distal nerves (Burnett and Zager, 2004).

The main cell types involved in the processes at the denervated site of an injured peripheral nerve are Schwann cells (SCs) and cells which are part of the innate immune response such as neutrophils, macrophages or T-lymphocytes. Moreover, also fibroblasts and endothelial cells regulate changes following nerve injury.

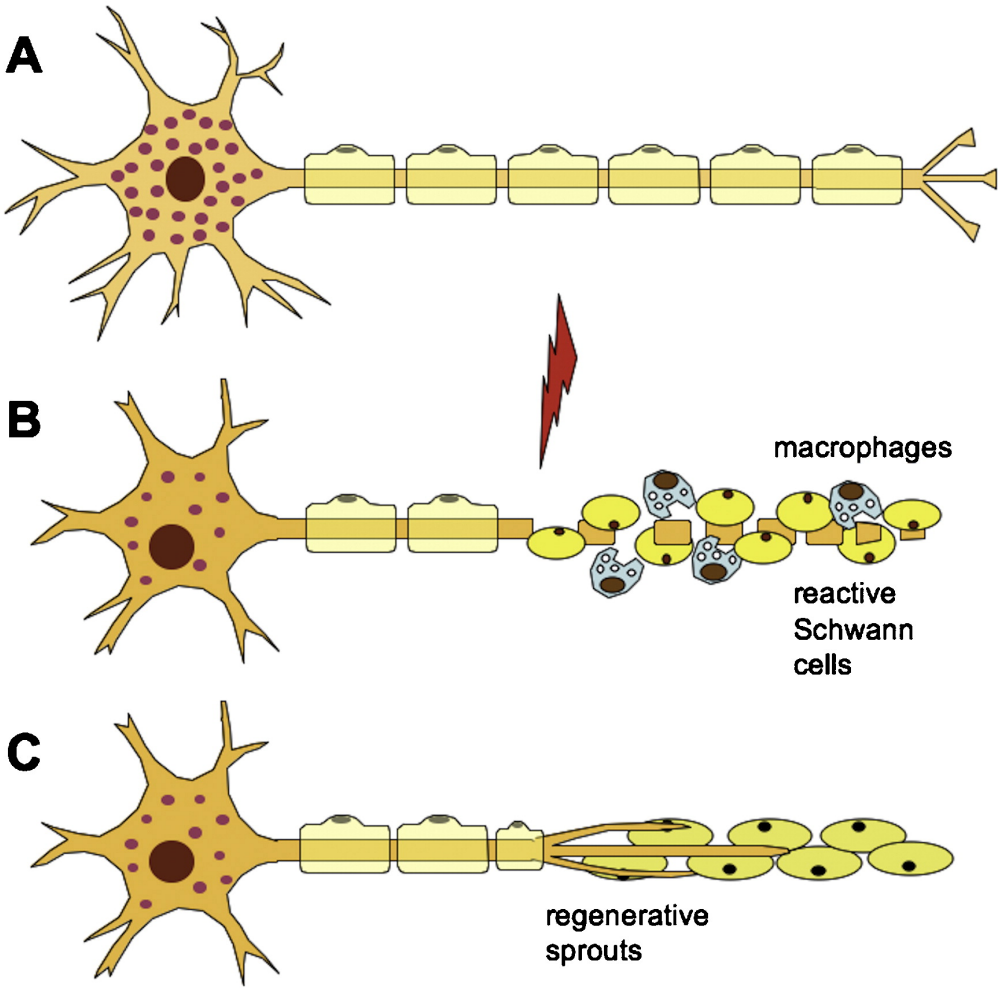

Figure 1.1. Schematic representation of cellular components in peripheral nerve injury. (Adapted from Allodi *et al.*) A) Neurons extend axons to the periphery and are myelinated by SCs. B) When injury occurs, SCs but also resident macrophages start to phagocytose and produce cytokines and chemokines to attract haematogenous monocytes, which then infiltrate the peripheral nerve to further clear myelin debris. C) SCs further de-differentiate and form Bands of Büngner (Allodi et al., 2012).

1.3. Cellular components involved in peripheral nerve injury and Wallerian degeneration

1.3.1. Schwann cells

Two types of SCs reside in the vicinity of peripheral nerve fibres. Myelinating SCs and non-myelinating, also referred to as ensheathing SCs, which loosely ensheath unmyelinated small diameter fibres (Griffin and Thompson, 2008). Myelinating SCs form a myelin sheath to allow fast action potential propagation. After peripheral nerve injury, SCs de-differentiate and acutely change expression levels of specific regeneration-associated genes like neurotrophins and neurotrophin receptors, neuregulins and their receptors of the ErbB family. SCs begin to proliferate with a maximum at three days and start to sequester myelin debris (Stoll et al., 1989). Moreover, the production of myelin is discontinued in the first two days following nerve injury (White et al., 1989, Trapp et al., 1988). In the first days following injury SCs proliferate and form Bands of Büngner as supportive structures for regenerative re-growth (Hoke, 2006, Chen et al., 2007). As mentioned before, SCs play a pivotal role in removing growth inhibiting myelin debris, mainly consisting of myelin associated glycoproteins (MAG) (McKerracher et al., 1994), as the myelin scavengers in the first days after injury (Stoll et al., 1989; Perry et al., 1995). The molecular mechanism of how SCs phagocytose degenerated myelin is unclear but involvement of galectin-3 (Gal-3), a well known monocyte antigen expressed mainly by phagocytosing macrophages, also known as MAC-2 (Ho and Springer, 1982), has been discussed (Reichert et al., 1994). MAC-2 stabilises the guanosine-5'-triphosphate (GTP)-ase K-Ras leading to phosphoinositide 3-kinase (PI3) dependent phagocytosis (Sato et al., 2009). MAC-2 is upregulated in SCs, detectable at 48 hours after injury (Reichert et al., 1994), in resident macrophages, and later on in the process, in invading macrophages. Fibroblasts seem to be involved in this pathway by producing granulocyte macrophage colony-stimulating factor (GM-CFS), thus driving MAC-2 expression (Saada et al., 1996).

Phospholipase A_2 (PLA_2) is considered one of the main enzymes regulating myelin breakdown (Lopez-Vales et al., 2008). PLA_2 is synthesised by two cell types, macrophages and SCs, shortly after injury and remains elevated for at

least two weeks (De et al., 2003). PLA_2 expression can be controlled by cytokines like Tumour necrosis factor α (TNF-α), suggesting that inflammatory mediators can modulate myelin clearance.

Denervated SCs are highly proliferative cells. Following injury SCs de-differentiate into a progenitor-like state, stop the production of myelin and begin to proliferate, forming long, parallel processes to form Bands of Büngner as a supportive structure for regenerative axons (Griffin and Thompson, 2008). SC de-differentiation is controlled by transcriptional programmes, which either support or inhibit myelinating properties. Positive regulators of myelination such as Krox-20, Oct-6, Sox-10, Brn2 and nuclear factor kappa-light-chain-enhancer of activated B cells (NF-κB) are expressed in the myelinating phenotype. In balance to those are negative transcriptional regulators such as c-Jun, Notch, Sox-2 and Pax-3 and Id2, which are expressed in the de-differentiated SCs (Jessen and Mirsky, 2008). Negative regulators of myelination are believed to drive the de-differentiation process of SCs and are likely to have a major role in processes following injury (Jessen and Mirsky, 2008). The transformation can be controlled by mitogen activated kinase (MAPK) activation, in particular Raf kinase (Napoli et al., 2012) together with extracellular signal-regulated kinases (ERK1/2) (Harrisingh et al., 2004). It has been shown *in vivo* that transcription factors regulated by the activation of the activator protein 1 box (AP1 box), e.g. c-Jun can programme denervated SCs into specialised cells, which support regeneration (Parkinson et al., 2008). When c-Jun is conditionally deleted in SCs, repair mechanisms following injury fail and the result is neuronal death and reduced functional recovery (Arthur-Farraj et al., 2012). Other mechanisms, which could promote SC de-differentiation such as activation by growth factors like Neurotrophin (NT)-3 or altered neuronal activity are discussed (Jessen and Mirsky, 2008). Once contact to re-growing axons is restored SCs can differentiate (Jessen and Mirsky, 2008) again into a myelinating phenotype. SCs are a main source for extracellular matrix proteins (ECM) (Chen et al., 2007), which are essential for structural support and attachment to the cells.

SCs, which are an important source for neurotrophic factors, upregulate the synthesis of nerve growth factor (NGF), brain-derived neurotrophic factor (BDNF) and NT-3 and NT-4 (Gordon, 2010, Terenghi, 1999), which are able to promote axonal outgrowth of the proximal end to reinnervate the target tissue.

It was suggested that tissue specific reinnervation might be regulated by upregulation of distinct molecular markers and antibodies promoting axonal re-growth to a specific target tissue. (Allodi et al., 2012). SCs associated with axons derived from motor neurons express the epitope L2/HNK1 rather than neural cell adhesion molecule (NCAM). NCAM is exclusively expressed in non-myelinating SCs, associated with sensory unmyelinated fibres (Saito et al., 2005). However, L2/HNK-1 and NCAM expression is lost following nerve injury due to Schwann cell de-differentiation (Martini et al., 1994) but may be re-expressed once the respective axon is restored, which may imply that SCs can retain specificity to axonal subtypes (Allodi et al., 2012). This finding was supported by Höke *et al.,* who described specific SC populations, which express distinct neurotrophic factors such as NGF and BDNF when ensheathing cutaneous nerves or pleiotropin and glial cell line-derived neurotrophic factor (GDNF) when ensheathing ventral roots, suggesting a specific sensory or motor phenotype (Hoke et al., 2006).

Denervated SCs produce cytokines and chemokines to attract haematogenous monocytes/macrophages (Gillen et al., 1998, Shamash et al., 2002) and other immune cells. Furthermore, pro-inflammatory cytokines can break down the blood nerve barrier and increase permeability of the vasculature. Examples are the pro-inflammatory cytokine TNF-α (Wagner and Myers, 1996) or interleukin (IL)-6, which can act as a pro and anti-inflammatory cytokine (Bolin et al., 1995).

SCs, as immune-competent cells, are able to process endogenous antigens to immune cells, expressing major histocompatibility class I and II molecules (MHC) and can also express receptors of the immune defence, in particular toll-like receptors (TLR), which recognise patterns of exogenous antigens such as lipopolysaccharide of gram-negative bacteria (LPS) (Meyer zu Horste et al., 2008). Recent findings have shown high expression of TLRs following axonal injuries. Especially TLR-3 and TLR-4 expression in SCs are regulated following injuries (Goethals et al., 2010). Recent research suggests SC loose regenerative support over time, which can lead to poor functional recovery in long-term (one to two months), chronically denervated areas (Sulaiman and Gordon, 2000).

In conclusion, following peripheral nerve injury, SCs are irreplaceable as supportive and growth promoting cells, secreting trophic factors and cytokines, but also through phagocytosing myelin debris and forming a structural scaffold for the regenerating nerve.

1.3.2. Immune cell response after peripheral nerve injury

1.3.2.1. Neutrophils/mast cells

Neutrophils and mast cells are considered the first invading immune cells following nerve injury (Gaudet et al., 2011). Their main functions is to activate other immune cells, mainly blood-derived monocytes, and attract them to the injury site (Zuo et al., 2003) via releasing a variety of cytokines and chemokines such as macrophage inflammatory protein 1α (MIP-1α) (Scapini et al., 2000).

Mast cells mainly invade the injury site and are sparsely distributed in the distal areas of the affected nerve (Perkins and Tracey, 2000). Mast cells are mostly studied in regards to their role in nerve injury induced neuropathic pain. They release histamine and TNF-α, which both can sensitise nociceptors in the absence of nerve injury but may also activate injured proximal nerve endings (Perkins and Tracey, 2000).

1.3.2.2. Macrophages

A small proportion of macrophages reside permanently in the peripheral nerve (Mueller et al., 2001). These cells express MHC class I and class II molecules and complement receptor 3 (CR3). Resident macrophages have been described as cells with an elongated morphology and small ramifications (Monaco et al., 1992).

Whereas SCs and resident macrophages are responsible for early myelin clearance, haematogenous monocytes/macrophages play a significant role in debris phagocytosis after the first week of peripheral nerve injury (Mueller et al., 2003). Axonal regeneration and functional recovery depends on myeloid cells (Barrette et al., 2008). In zebrafish it has been recently shown, using live cell

imaging, that macrophage infiltration can start as early as 120 minutes post-lesion (Rosenberg et al., 2012). Factors released from various sources lead to recruitment of macrophages, which peaks (Perry et al., 1987) at 14 days post-injury. Macrophages can be attracted by cytokines, chemokines and neurotrophic factors produced by denervated SCs in the distal segments of the nerve (Perrin et al., 2005, Shamash et al., 2002). Also, molecules which are cleaved and activated by matrix metalloproteases (MMP) and members of the complement system have been described as chemoattractants for blood-derived monocytes (Siebert et al., 2001), (Bruck and Friede, 1991).

Blood-derived monocytes enter the site of injury through diapedesis through the endothelium of the vasculature. Blood-derived monocytes/macrophages support and also replace SCs as the main scavengers for myelin debris. Different factors have been studied, which regulate the phagocytic mechanism in these cells. For example, phagocytosis can be initiated by CR3 (Bruck and Friede, 1990, Rotshenker, 2003) but also immunoglobulin FC gamma receptors (FC-γ-R). Those receptors interact with opsonised myelin and endogenous anti-myelin antibodies (Vargas et al., 2010), respectively. Also, non-opsonised myelin can be phagocytosed via the scavenger receptor-AI/II (Reichert and Rotshenker, 2003).

A recent series of discoveries might become of interest in the field of macrophage activation following nerve injury. Macrophages can be distinctively activated to form specific phenotypes, termed M1 or M2 population (Mantovani et al., 2004). During this form of polarization macrophages express different subsets of receptors and proteins like cytokines or chemokines. The M1 phenotype is considered inflammatory with the production of pro-inflammatory cytokines like TNF-α, IL1α and IL1β whereas the M2 phenotype is anti - inflammatory with the production of anti-inflammatory proteins, for example IL10 or scavenger receptors, like cluster of differentiation (CD)-163. Very simplified, the typical inflammatory response of these subspecialised macrophages starts with the infiltration of M1 macrophages, which over time convert into an M2 phenotype (Martinez et al., 2009). It has been shown that after spinal cord injury (SCI) the invading macrophage population is considered to be polarised towards the M1 phenotype (Kigerl et al., 2009), (David and Kroner, 2011) and lacks the change into the anti-inflammatory, M2 category,

which might explain the reduced regenerative capability described following SCI. The mechanism, through how those different subsets might effect regeneration in peripheral nerves remains to be elucidated.

1.3.2.3. T-lymphocytes

T-cells could be detected by day 3 following chronic constriction injuries and numbers reached a peak at 21 days (Moalem et al., 2004). Peripheral nerve injury leads to a rapid infiltration with CD3, CD11α (αL, LFA1α) and CD44 immunoreactive T-cells (Raivich et al., 1998).

The main types of invading T-cells, type 1 and type 2 helper cells, produce pro-inflammatory cytokines like TNF-α or Interferon (IFN)-γ and anti-inflammatory cytokines like IL4 and IL10, respectively. Those two cell types further modulate the infiltration of phagocytic cells but also regulate the phagocytic response in the affected area.

Evidence has been accumulated that T-cells play a role in the development of neuropathic pain after nerve injury. In the chronic constriction injury (CCI) model in rats, injection of T-cell subsets could alter the pain behaviour in rats. Type 1 T-cells can increase hypersensitivity whereas Type 2 T-cells can attenuate pain behaviour (Moalem et al., 2004). It has to be noted that hypersensitivity changes were small in those studies, suggesting just a limited effect of those cells in the numerous complex mechanisms promoting the development of neuropathic pain.

1.3.3. Fibroblasts

Fibroblasts, the structural cellular element in a lot of tissues, produce components of the ECM in the endoneurium. These proteins act as supportive scaffolding but can also function as a buffer substrate, binding and retaining soluble proteins, such as growth factors and cytokines (Frantz et al., 2010). Fibroblasts have essential functions supporting this structural reorganisation but also in forming scarring tissue at the injury site. Depending on the severity of the injury, fibroblasts of the endoneurial tubes and in the epineurium become

reactive and proliferate at the distal end of the injured nerve within 24 hours (Burnett and Zager, 2004). Proliferation leads to a fibrous scar around the site of the injury, which can cause swelling of the injured segment but can also develop intrafascicular if the injury is less severe (Burnett and Zager, 2004).

Fibroblasts also support the phagocytic response, releasing chemoattractive cytokines, like granulocyte macrophage colony stimulating factor (GM-CSF), which induces MAC-2 expression in SC and macrophages, initializing their phagocytic potential (see 1.3.1.) (Saada et al., 1996). Fibroblasts can also modulate the immune response by producing cytokines, such as, IL6, which can have both pro-inflammatory and anti-inflammatory functions (Bolin et al., 1995, Reichert et al., 1996).

Reorganisation of injured tissue includes reutilizing myelin-derived lipids for remyelination. It could be shown in mice that apolipoprotein D, a lipid binding protein, which accumulates in the distal stump after axotomy is expressed mainly by endoneurial fibroblasts (Spreyer et al., 1990), implicating a role of fibroblasts in the remyelination process.

1.3.4. Endothelial cells

Endothelial cells form the vasculature around and also within the nerve and ensure oxygenation of nervous tissue. Following nerve injury the vasculature regulates the concentration of inflammatory mediators and infiltration of immune cells into the injury site with increased perfusion and permeability. Furthermore, endothelial cells can have a direct function on the regenerative processes following peripheral nerve injury via producing injury related mediators. They are known to produce nitric oxide (NO) (Palmer et al., 1988), which potentially can participate in changes following injury, such as axon and myelin phagocytosis (Zochodne and Levy, 2005) or sensitivity changes as a nociceptive mediator following nerve injury (Levy et al., 2000).

Endothelial cells can also produce cytokines and chemokines and therefore directly modulate the inflammatory response following nerve injury. It has been described that seven days after injury endothelial cells express TNF-α in injured nerve tissue (Wagner and Myers, 1996), (Fabry et al., 1993). Other

factors released by endothelial cells are growth factors (Nakahashi et al., 2000), which can be released directly into the blood or act locally to support axonal regrowth.

1.3.5. Changes in primary neurons following nerve injury

When a peripheral nerve injury occurs the respective cell bodies of the affected axons undergo drastic changes. After a peripheral injury the affected neurons can be motor neurons in the spinal cord, sensory neurons in the dorsal root ganglion (DRG) or autonomic neurons in sympathetic ganglia. Anatomically, morphological changes, termed chromatolysis, have been described, which include nucleus displacement, swelling of the cell body and dissolution of the Nissl bodies (Kreutzberg, 1982) (Figure 1.2.). Peripheral axotomy triggers radical gene expression changes in genes regulating neuronal survival and regeneration (Raivich and Makwana, 2007). Peripheral nerves are capable of successful regeneration, whereas nerves in the central nervous system (CNS) cannot effectively regenerate (Hoffman, 2010) due to the non-permissive environment of the CNS. An intrinsic growth capacity regulated by peripheral injury has been shown in a rat injury model, where neurons switch into a regenerative state following axotomy. After a second injury to the same nerve, regeneration is even more pronounced (McQuarrie et al., 1977). This paradigm was described as the “conditioning” lesion paradigm and helped to characterise expression changes following nerve injury. Interestingly, in DRG neurons, where one neurite extends in the periphery and the other into the spinal cord, the peripheral branch regenerates, whereas the central process does not. Neumann and Woolf (1999) could show that a lesion to the peripheral branch can prime the neuron into a growth promoting state, which allows the central branch to regenerate into the permissive CNS (Neumann and Woolf, 1999). This is evidence, that retrograde transport of factors from the peripheral injury can increase this regenerative potential even into the permissive environment of the CNS (Rishal and Fainzilber, 2010).

After injury, changes in the cell body occur, which involve gene expression and expression of proteins. These changes can be conveyed by electrical impulses, which are the acute initial response of the injured nerve fibre (Mandolesi et al.,

2004). Rapid ionic changes usually depend on an increase of intracellular calcium levels, which is then conducted via voltage dependent sodium channels (Mandolesi et al., 2004). Interestingly, when peripheral nerves are electrically stimulated, a direct effect on neurite outgrowth can be shown. This increase in neurite outgrowth was accompanied by increased cyclic adenosine monophosphate (cAMP) levels, which let the authors conclude that this may be responsible for the increase in axonal outgrowth (Udina et al., 2008). Electrical signals from the injury site only account for relatively few gene changes in the cell body. In contrast, more prominent expression changes in the neuronal cell body have been observed, following retrograde transport of factors released at the injury site. Such locally synthesised neuropoietic proteins can be cytokines like, leukemia inhibitory factor (LIF) (Subang and Richardson, 2001), IL6 (Cao et al., 2006) or ciliary neurotrophic factor (CNTF) (Kirsch et al., 2003). Downstream mediators for these cytokines can be activated locally.

A recently discussed paradigm, described as an alternative to the energy demanding long distance transport of proteins, is local protein synthesis (Gumy et al., 2010). Axonal proteins, like extracellular signal-regulated kinases (ERK) or transcription factors can be activated and may also travel to the cell body from the injury site (Agthong et al., 2006, Ben-Yaakov et al., 2012). Locally synthesised proteins can have supportive functions in retrograde protein transport, like vimentin, which, after proteolysis binds to ERK and importin-β, thereby linking activated ERKs to importin-mediated retrograde transport. This complex of factors has been termed cargo binding complex (Perlson et al., 2005, Rishal and Fainzilber, 2010). Locally synthesised proteins can also be structural components, needed for local regeneration like β-Actin (Jung et al., 2012). Conversely to local protein synthesis, the lack of constituent retrogradely transported neurotrophic factors to the neuronal cell body can signal injury and induce a significant change in gene expression (Michaelevski et al., 2010). In the uninjured state, neurotrophic factors are permanently transported from the target tissue to the cell body. Loosing this essential signal can convey information about the injury to the cell body of the affected axon (Rishal and Fainzilber, 2010).

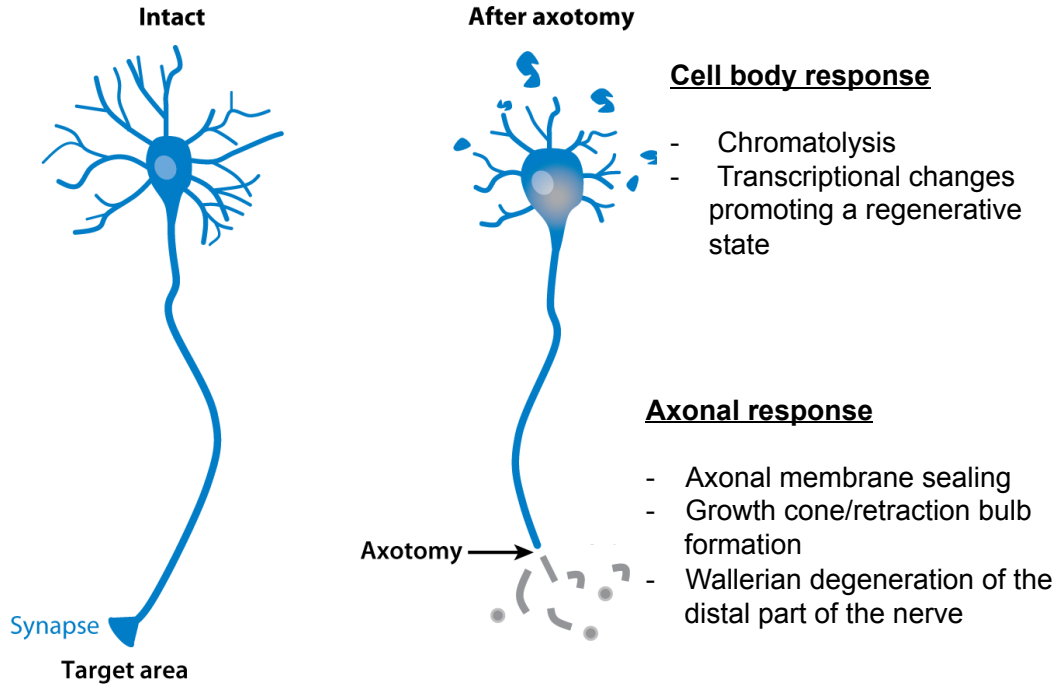

Figure 1.2. Neuronal response following nerve injury (Adapted from Liu *et al.*) Following injury the cell body changes morphologically termed, chromatolysis, whereas the affected axon degenerates and forms a growth cone (Liu et al., 2011a).

Whereas the distal part of the affected axon undergoes Wallerian degeneration the proximal part transforms anatomically and develops a growth cone, which has a specific protein expression profile to respond to diverse neurotrophic factors, which orchestrate regeneration (Tessier-Lavigne and Goodman, 1996). When the target tissue is reached by regenerating fibres, a complex mechanism leads to the reduction of axonal growth capabilities, which increases synaptic growth and synaptogenesis (Liu et al., 2011a).

1.4. Nerve injury and neuropathic pain

The cellular and molecular changes following peripheral nerve injury, including monocyte/macrophage activation and upregulation of neurotrophins and cytokines contributes to the sensitisation of the sensory nervous system and the generation of neuropathic pain. Neuropathic pain, defined by the International Association for the Study of Pain, is 'pain initiated or caused by a primary lesion in the nervous system'. Usually partial or incomplete nerve injury is cause for a nociceptive response but also complete transection of a nerve can be responsible for painful sensations originating from effects in higher sensory centres.

Myers *et al.* showed that Wld^{slow} mice display reduced hyperalgesia (Myers et al., 1996). This exemplifies the fact that the process of Wallerian degeneration is a key factor in the pathogenesis of neuropathic pain mostly due to inflammatory molecules, which can directly sensitise nociceptors. Cytokines like TNF-α or IL1β have repeatedly been associated with mediating nociceptive signals (Marchand et al., 2005). It has been shown that in Wld^{slow} mice, the onset of thermal hypersensitivity was also delayed, whereas mechanical hypersensitivity developed at the same time as in naïve animals (Sommer and Schafers, 1998). These differences were linked to differences in cytokine expression, suggesting a correlation between cytokine release following Wallerian degeneration and development of neuropathic pain.

McLachlan *et al.* showed that sprouting of noradrenergic perivascular axons sprout into the DRG and can account for neuropathic pain development (McLachlan et al., 1993). This sympathetic component of pain development is delayed in Wld^{slow} mice (Ramer et al., 1997).

It is debated that a partial nerve injury leads to a more severe nociceptive phenotype. This can be explained by the exposure of uninjured fibres to degenerating products of injured fibres, produced in their close proximity. Ectopic impulses can be due to excess of mediators, such as TNF-α or IL1β (Costigan et al., 2009) or other electrophysiological mechanisms. This hypothesis could be supported by experiments, where uninjured C-fibres in the L4 spinal nerve increase spontaneous activity after transection of a neighbouring spinal nerve, which contributes to the maintenance of neuropathic

pain (Wu et al., 2001). This can be explained by an accumulation of ion channels in uninjured axons (Gold et al., 2003). This imbalance of impulse activity can be summarised as the ectopic discharge hypothesis and can be origin for neuropathic pain (Devor, 2009).

The location of the initiation of those ectopic signals has not been determined. Additionally, ion channel accumulation in the growth cone might be responsible for pain sensations following nerve injury. For example, transient receptor potential channels (TRP), such as TRPC1, which has been described to mediate mechanical hyperalgesia (Alessandri-Haber et al., 2009), are highly expressed in the neuronal growth cones and can be responsible for the transmission of nociceptive signals (Shim and Ming, 2010).

As described in detail before, peripheral nerve injury leads to axon and myelin degradation by SCs and macrophages with a subsequent infiltration and activation of immune cells. All changes are orchestrated by a variety of neurotrophic factors. These can be responsible for several effects, such as supporting regeneration, but also activating nociceptors directly (Pezet and McMahon, 2006). Injury to peripheral nerves triggers infiltration of haematogenous macrophages and proliferation of SCs. Both cell types produce inflammatory mediators, which can directly activate nociceptors (Campana, 2007).

In conclusion, many mediators that are important for the regeneration of an injured nerve are also involved in the development of neuropathic pain (Nadeau et al., 2011). Therefore, the development of new drugs, which are effective in reducing neuropathic pain while not affecting successful regeneration, remains a challenging task.

1.5. Effects of neurotrophic and growth factors following peripheral nerve injury

The regulation of neurotrophic factors following injury is complex. Reduced transport of neurotrophic factors, due to an axotomy-induced lack of retrograde transport from the target tissue can account for reduced concentrations in affected neurons. One example is the dramatic reduction of NGF in neurons following sciatic nerve axotomy (Raivich et al., 1991). In uninjured neurons neurotrophic factors are retrogradely transported from the periphery to the cell body and serve as survival signals. Axon transection leads to their loss and might signal injury to the neuronal cell body (Rishal and Fainzilber, 2010).

Peripheral nerve injury also causes local release of neurotrophic factors from surrounding cells. Increased concentrations in the periphery can have local effects after binding to receptors at the injured end/growth cone of the nerve but also can be transported retrogradely, exerting effects in the cell soma of the neuron. Neuronal and non-neuronal cells, e.g. SCs or fibroblasts, can express growth factors. Neurotrophin protein levels usually increase seven days after injury (Gordon, 2009) but gene expression could be examined already within hours after axotomy (Heumann et al., 1987). Experimentally it could be shown that electrical stimulation can elevate growth factor levels in neurons, suggesting an interplay of injury induced electrical signals and growth factor production (Rishal and Fainzilber, 2010). Amongst others, NGF, BDNF and NT-4 are upregulated following peripheral nerve injury. They bind to the tyrosine kinase receptors, tropomyosin-receptor-kinase (Trk)-A/B and p75 (low affinity) neurotrophin receptors and activate intracellular signalling cascades, which can stimulate diverse cell functions (Figure 1.3.)

The adult DRG produces mRNA for growth and neurotrophic factors. NGF (Shelton and Reichardt, 1984) and BDNF (Ernfors et al., 1990) are expressed in the DRG at the mRNA level, suggesting constant growth factor synthesis and raising the possibility that these factors act permanently in an autocrine or paracrine way. Growth factors play an essential role in the way cells in the DRG respond to peripheral nerve injury. As described above, injured neurons regulate growth factor expression following injury, but also other cell types in the DRG, like fibroblasts or satellite cells are likely to affect axotomised

neurons with the release of growth factors. Amongst others, NGF is intensely regulated in the DRG, beginning at the first day following peripheral injury (Sebert and Shooter, 1993). Also BDNF mRNA levels change following injury, not only in the injured but also in adjacent uninjured DRGs (Fukuoka et al., 2001). GDNF is increased following injury in DRG neurons (Hoke et al., 2000) and satellite cells of the DRG, (Hammarberg et al., 1996). Also FGF-2 (Grothe et al., 1997) and members of the NRG family, e.g. glial growth factor (GGF), which binds to ErbB receptors (Li et al., 1997) are regulated in affected DRG neurons following nerve injury.

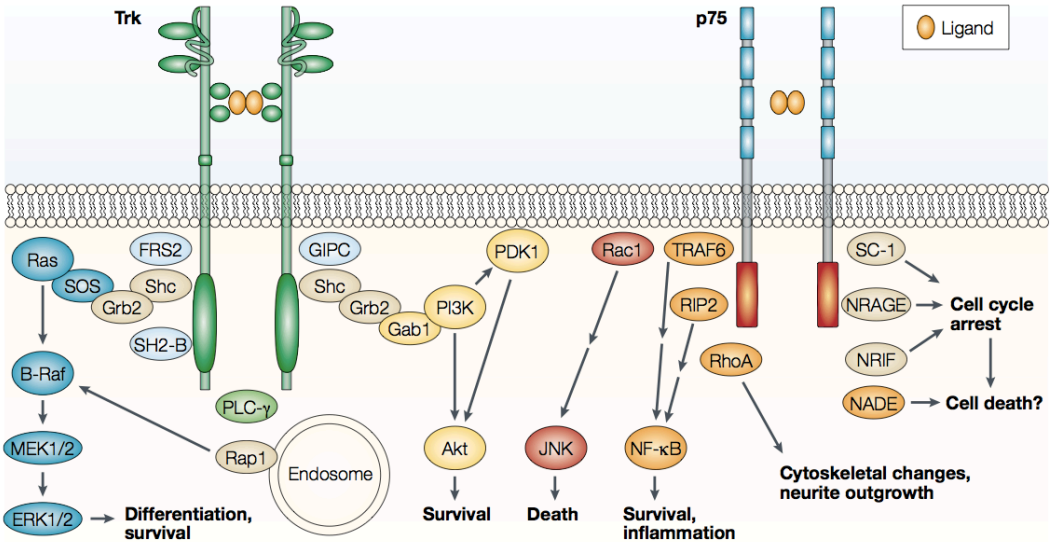

Figure 1.3. Trk/p75 receptor signalling. (Adapted from Chao *et al.*) Trk receptors signal through extracellular signal-regulated kinase (ERK), phosphatidylinositol 3-kinase (PI3K) and phospholipase Cγ (PLC-γ) pathways whereas p75 mainly activates NF-κB and Jun N-terminal kinase (JNK) (Chao, 2003).

The family of neurotrophins has been shown to alter neurite outgrowth in numerous *in vitro* findings. In contrast, *in vivo* findings revealed that regenerative properties of neurotrophins are more controversial. Some findings support the hypothesis that SC-derived or neuron-derived neurotrophic factors can promote axon regeneration in rodents (Hoke et al., 2002) and non-human primates (Ahmed et al., 1999). Others claim that neurotrophic factors can suppress regeneration in a time and concentration dependent manner (Boyd and Gordon, 2002). Efforts have been focused on the delivery of exogenous neurotrophins to aid regeneration following nerve injury (Wiberg et al., 1999, Whitworth et al., 1995). Also, combining surgical and pharmacological methods may be an approach to aid axon regeneration in patients with nerve injury.

Changes, involving immune cell activation (Colburn et al., 1997) and plasticity, can be regulated by growth and trophic factors. Growth factors have direct and indirect effects on cells in the dorsal horn. Changes in protein expression in the dorsal horn can be often explained by increased axonal transport from the sensory neurons (Pezet and McMahon, 2006). This is affected following nerve injury; two examples are the upregulation of NGF, which leads to sprouting of small diameter afferents following SCI (Krenz et al., 1999) and the increased BDNF expression in synaptic terminal in Lamina IV of the dorsal horn following axotomy, (Michael et al., 1999), suggesting involvement in synaptogenesis. The increase of BDNF protein in the dorsal horn can be explained by retrograde transport originating from sensory neurons in the DRG (Tonra et al., 1998). The interaction between immune cells and neurons can be regulated by growth factors. Jeffrey *et al.* showed that spinal microglia, which express BDNF following peripheral injury can affect neuronal excitability and eventually cause neuropathic pain (Coull et al., 2005).

Neurotrophic and growth factors have been investigated in their function promoting hypersensitivity changes as pain mediators (Pezet and McMahon, 2006). It seems that neurotrophic factors function specifically as nociceptive modulators in different types of pain models (Pezet and McMahon, 2006). The mechanisms of action for neurotrophins in nociceptive circuits can be diverse. In the periphery neurotrophins, especially NGF and BDNF can directly sensitise nociceptors, e.g. via upregulation of ion channels, such as transient receptor potential (TRP)-V1 channels in nociceptors. Also, receptors and

neurotransmitters can be increase expression in the spinal cord. Furthermore, neurotrophins can have effects on synaptic plasticity or modulate glial cell function (Pezet and McMahon, 2006), leading to central sensitisation.

1.6. Epidermal growth factor receptor ligands

The epidermal growth factor (EGF) family of peptides binds to the ErbB receptors (named after their homology to the erythroblastoma viral gene product v-erbB (Citri and Yarden, 2006) and can be categorised depending on their distinct receptor specificity. ErbB receptors, which include ErbB1 (EGFR), ErbB2, ErbB3 and ErbB4, are tyrosine kinase receptors, which regulate key processes in cell biology, such as proliferation, migration and apoptosis upon binding of diverse families of peptides. Several ligands, binding ErbB receptors, have been described.

The structural and functional commonality of all EGF receptor (EGFR) ligands is the EGF domain, a highly conserved protein motif that can be found in a variety of unrelated proteins, ECM and cell adhesion proteins, blood coagulation factors and even in pox viruses (Schneider and Wolf, 2009). The EGFR ligands comprise of seven related peptides, the epidermal growth factor (EGF) (Cohen, 1964), Aregulin (AREG) (Shoyab et al., 1988), Epiregulin (EREG) (Toyoda et al., 1995), Epigen (EPGN) (Strachan et al., 2001), Heparin-binding EGF (HB-EGF) (Higashiyama et al., 1992), Betacellulin (BTC) (Shing et al., 1993) and Transforming growth factor alpha (TGFα) (Massague, 1990) (Figure 1.4.).

EGFR ligands are processed as membrane-bound pro-forms, which are proteolytically released by a family of membrane bound metalloproteases known as ‘a disintegrin metalloprotease’ (ADAM) (Kataoka, 2009). Following proteolytic processing the cleaved extracellular fragment is released, which can then exert its function on neighbouring cells (paracrine) or activate in an autocrine manner (Singh and Harris, 2005). EGFR ligands can also activate receptors of adjacent cells without being cleaved off their membrane anchor (juxtacrine), which can account for different biological effects. (Brachmann et al., 1989; Singh and Harris, 2005). Ectodomain shedding leaves a cytoplasmic

tail. The cytoplasmic tail of the protein can be released into the cytoplasm and then utilise different cytoplasmic pathways (Hieda et al., 2008).

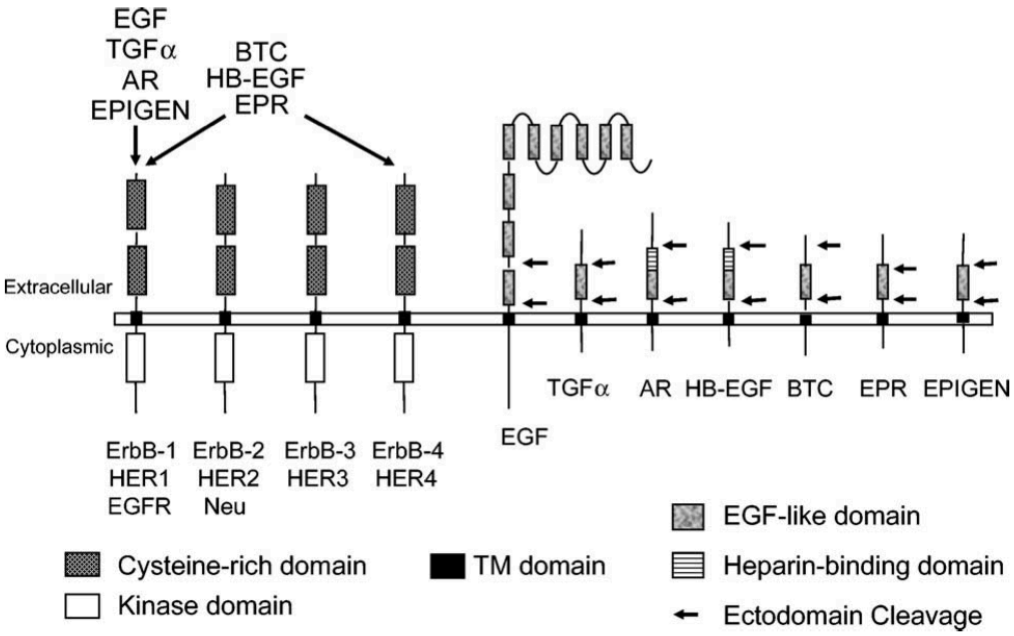

Figure 1.4. EGFR ligands, receptors and cleavage sites. (Adapted from Harris *et al*.) Left: EGFR ligands bind to the receptors ErbB1 (EGFR) and ErbB4. EGF, TGFα, AREG and Epigen only bind the ErbB1 (EGFR) receptor. BTC, HB-EGF and EREG can additionally bind to ErbB4. Right: All EGFR ligands have at least one EGF-like motif, which is crucial for receptor interaction. Each molecule also pocesses a specific cleavage site through which metalloproteases of the ADAM family release the mature form of the peptide (Harris et al., 2003).

1.7. ADAMs - activating enzymes of EGFR ligands

Activation of EGFR ligands is regulated by metalloproteases of the 'a disintegrin and metalloprotease' (ADAM) family. All EGFR ligands are synthesised as membrane anchored precursors. In experiments using knockout animals it could be shown that ADAM10 is the main sheddase enzyme for EGF and BTC whereas ADAM17, also known as TNF-α converting enzyme (TACE) is the main activator of TGFα, EREG and HB-EGF (Hinkle et

al., 2004; Sahin et al., 2004). Due to their various targets ADAMs have been implicated in a lot of biological processes (Blobel, 2005). Although various functions in the development of the nervous system have been described (Yang et al., 2006b), no detailed knowledge about their role following nerve injury exists. It has been proposed that they might regulate axonal behaviour and can affect neurite outgrowth (Yang et al., 2006b). ADAM10 is important for the development of motor axon pathways in developing *Drosophila* (Fambrough et al., 1996) and it has been shown that it is critical in axonal outgrowth and myelination of the peripheral nerve (Jangouk et al., 2009). ADAM17 has been found in naïve peripheral nerves localised in SCs, endothelial cells and axons. Chronic constriction injury pronounces expression in SCs and macrophages (Shubayev and Myers, 2002), making them potential candidates for further investigations.

1.8. The EGFR family

The receptors of the ErbB family, including ErbB1 (EGFR), are receptor tyrosine kinases, which have pleiotropic biological functions. They are known to regulate survival of cells, migration and proliferation and are widely expressed on a variety of cells. Activation of the ErbB receptors leads to dimerisation into hetero- or homodimers. ErbB1, 3 and 4 have a binding site for the EGF-motif, which is present in a lot of different protein structures. ErbB2 has no ligand binding domain and is considered a preferential dimerisation partner for other ErbB receptors (Olayioye, 2001). ErbB3 has no tyrosine kinase domain and therefore needs to form heterodimers with other receptors to promote intracellular signaling (Schneider and Wolf, 2009).

Intracellular signalling pathways of the EGFR are various and involve activation of MAPKs or the PI3 kinase/AKT and JAK/STAT3-5 pathway (Jorissen et al., 2003). Also the EGFR can be activated by transactivation from other G-protein-coupled receptors (Daub et al., 1996) (Figure 1.5.). Besides, cytokines can transactivate the EGFR via increasing the expression of EGFR ligands (Valyi-Nagy et al., 1992).

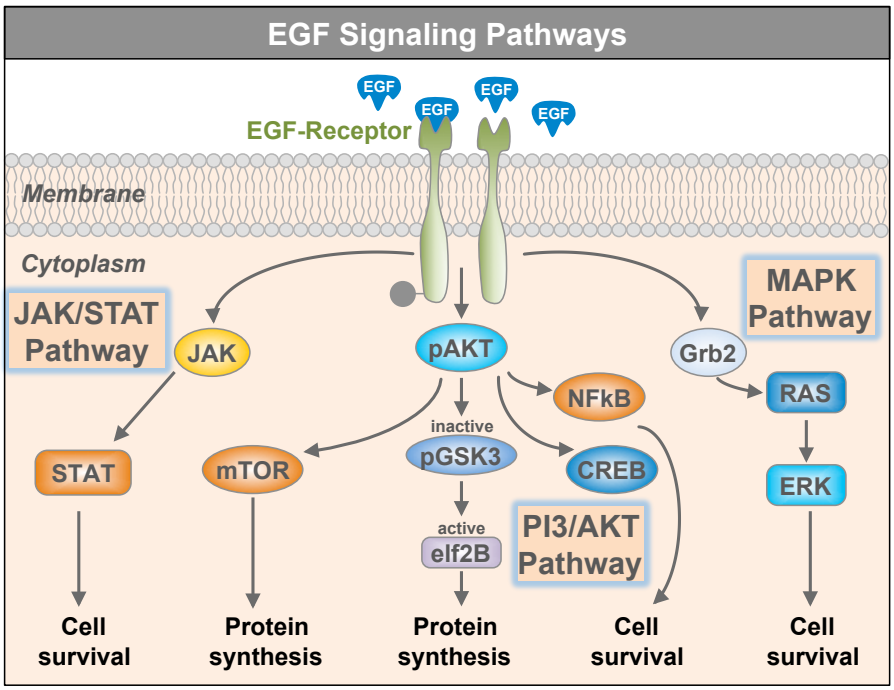

Figure 1.5. Simplified pathway of intracellular protein interactions following EGFR activation. Phosphorylation of the tyrosine kinase domain after dimerisation can lead to activation of various intracellular pathways, which can involve MAPK activation, PI3-kinase/Akt activation or activation of the JAK/STAT pathway. Therefore, phosphorylation of the EGFR can have diverse functional outcomes, affecting cellular growth, migration, cell survival, proliferation and differentiation.

A large body of evidence exists regarding the function of the EGFR in the development and maintenance of different types of cancer (Yarden and Pines, 2012). Several EGF inhibitors have been developed and could be translated successfully into clinical settings (for details see Chapter 3). Furthermore, the role of EGFR in inflammatory processes has been studied thoroughly. It has been shown in skin, that EGFR transactivation by increasing the availability of EGFR ligands via MMP activation can lead to an altered inflammatory response and increased keratinocyte cell migration (Pastore et al., 2008). Also, cytokines like TNF-α or IFN-γ can transactivate the EGFR by increasing the availability of EGFR ligands (Valyi-Nagy et al., 1992; Matsuura et al., 1999).

1.9. EGFR and peripheral nerve injury

In comparison to research dedicated on the EGFR family in other fields of science, it is surprising that little is known about expression changes of EGFR ligands in the peripheral nerve following injury. Cohen *et al.* investigated the expression of all ErbB receptors following injury in the sciatic nerve (Cohen et al., 1992). They found that, although ErbB4 was undetectable, ErbB1, ErbB2 and ErbB3 were present in the sciatic nerve at all timepoints. ErbB1 (EGFR) and the receptors ErbB2 and ErbB3 (7-fold at 7 days post-injury), which both, after binding to the ligand Neuregulin 1 (NRG), essential in the response to injury (Fricker et al., 2011; Stassart et al., 2013) are induced by axotomy of peripheral nerves (Carroll et al., 1997). This is in line with other findings: it has been shown that expression of the ErbB2 receptor, which does not have a ligand binding domain, but can heterodimerise with other members of the EGFR family is increased following injury (Guertin et al., 2005; Cohen et al., 1992). Additionally, Toma *et al.* characterised the spatiotemporal expression of the EGFR following peripheral nerve injury and were able to show that expression in SCs and fibroblasts increases following nerve injury (Toma et al., 1992).

In the peripheral nerve, it has been shown that nerve injury upregulates the expression of EGFR following nerve injury (Toma et al., 1992; Xian and Zhou, 1999a) on the mRNA level. Wildering *et al.* found that an EGF analogue in a model system for peripheral nerve injury, using *Lymnea stagnalis,* a gastropod mollusk, that EGFR activation can increase axonal outgrowth (Wildering et al., 2001). The same group suggested a mechanism for this trophic function, showing that EGFR activation supports survival of infiltrating macrophages following injury (Hermann et al., 2005). However, evidence from the mammalian physiology is contradictory. Dubuisson *et al.* could not show (Dubuisson et al., 1993) treatment effects of EGF activation in an experiment, where collagen tubes, supplemented with EGF, were used as scaffolding for injured sciatic nerve (Dubuisson et al., 1993). Further, Xian *et al.* could not show an effect of EGFR activation using TGFα on sensory or motoneuron regeneration in a sciatic nerve injury model (Xian et al., 2001).

Most findings were made in the context of traumatic injury to the CNS, e.g. SCI,

where activation of the EGFR has been shown to have beneficial effects. It promotes astrocyte proliferation (McGinn et al., 2004) after binding of TGFα (Zhang and Neufeld, 2005) and EGF. EGFR activation can differentiate neuroepithelial precursors into astrocytes, suggested as a potential therapeutic approach following traumatic injury. (Quinn et al., 1999). Following SCI, intrathecal administration of EGF promotes functional recovery via ependymal cell proliferation (Kojima and Tator, 2002). Erschbamer *et al.* showed that inhibiting the EGFR subsequently decreases the differentiation into reactive astrocytes, which can promote nerve regeneration (Erschbamer et al., 2007).

1.10. Animal models of chronic pain

There are many challenges in investigating molecules involved in pain processing in animal models.

Responses to nociceptive stimuli in animals lack subjective perception of the tested individuals. Therefore, the most reliable responses using behavioural observations are simple reflexes and innate responses, such as licking or lifting an inflamed paw (Mogil, 2009).

The Formalin test was firstly described by Dubuisson and Dennis (1977) as a behavioural pain measure, which is continuous for at least 30 minutes and does not involve restraining of the animal and therefore evaluates an ongoing habitual behaviour (Dubuisson and Dennis, 1977). The Formalin test is an assay of acute pain. Subcutaneous injection of 5% formalin (37% formaldehyde in H_2O) into the plantar hindpaw produces two phases of nocifensive behaviour with an interim period. The first phase is probably due to direct activation of nociceptors via TRP-A1 channels (McNamara et al., 2007). The second phase has been explained by an ongoing inflammatory response and subsequent central sensitisation (Coderre et al., 1993).

Surgery based neuropathic pain models mostly involve a partial injury to a peripheral nerve. Bennett and Xie described chronic constriction injury of the sciatic nerve as the first partial nerve injury model (Bennett and Xie, 1988). Partial injury involves axotomy of many but not all nerves, which generates long-standing mechanical and thermal hypersensitivity. Especially the reflex

response to cold stimuli is altered in partial nerve injury models. This can be tested by applying a droplet of acetone to cool the skin by evaporation or by a cooling metal plate beneath the animal (Allchorne et al., 2005). Hypersensitivity is measured as time spent for hindpaw lifting. Many different surgical alternatives have been developed, which in some cases produce dramatic differences in nociceptive response depending on the degree of peri- or intraneural inflammation (Cui et al., 2000).

Cellular and molecular changes distant to the peripheral nerve lesion (DRG, dorsal horn) are involved in the induction or maintenance of neuropathic pain. Nevertheless, animal models using rodents have been successfully exploited since the 1940s to analyse underlying mechanisms (Hardy et al., 1940).

1.11. Spinal nerve transection model as a model for neuropathic pain and regeneration

A commonly used rodent model of nerve injury is the spinal nerve transection (SNT) model, introduced by Kim and Chung (Kim and Chung, 1992) (Figure 2.1.). Since complete transection of the sciatic nerve will result in total loss of sensation, in SNTs only parts (L5/L6) of the nerve are transected following ligation of the stumps to prevent re-innervation. The consequence is development of neuropathic pain with a long-lasting hypersensitivity to thermal and mechanical stimuli. The pathological process involves peri- and intraneural inflammation affecting the peripheral part of the nerve, the DRG and the dorsal horn of the spinal cord. The tissue damage results in the infiltration of immune cells and production and release of cytokines and chemokines (Mogil, 2009).

These neuroimmune mechanisms, involving the release of growth factors, not only orchestrate the reorganisation of the injured tissue, but also contribute to abnormal pain sensation (Bennett, 1999). Besides investigating potential pain mediators for neuropathic pain this model can help to clarify the process of Wallerian degeneration, which involves release of cytokines, chemokines and growth factors. (Be'eri et al., 1998; Perrin et al., 2005; Shamash et al., 2002).

1.12. Aims of this work

The EGFR system of ligands and receptors has great importance in many physiological processes and only limited information about its role in the nervous system is available. With my thesis, I have set out to examine expression levels of EGFR ligands and receptors and investigate potential mechanisms by which this system may modulate nociceptive processing or regeneration following peripheral nerve injury.

First (Chapter 2): How do the expression levels of EGFR ligands, their receptors and activating enzymes change following peripheral nerve injury?

Second (Chapter 3): Do behavioural experiments contribute to the understanding of the potential function of the EGFR system in pain processing pathways in rats?

Third (Chapter 4): Unraveling the cellular mechanisms of BTC regulation by investigating its effects on macrophage function, phagocytosis, chemotaxis and neurite outgrowth DRG neuronal cultures in order to identify its function *in vivo* following peripheral nerve injury.

CHAPTER 2

The regulation of EGFR ligands, their receptors and shedding enzymes in the dorsal horn, DRG and sciatic nerve after injury

2.1. Introduction

Nerve injury leads to drastic and extensive changes in the peripheral nervous system. Anatomical changes were first described by Augustus Waller; 'Coagulation and curdling of the medulla' (*medulla* may have been used by Augustus Waller to describe myelin) (Waller, 1850), and start at 24 - 48 hours after the peripheral nerve is damaged (Koeppen, 2004). SCs change into a proliferative state, reorganise in Bands of Büngner (Tetzlaff, 1982) and together with macrophages phagocytose myelin debris (Gaudet et al., 2011). All these anatomical alterations are accompanied by molecular changes involving transcription of mRNA and protein expression. On a molecular level, changes occur in close temporal relationship with the injury (Dubovy, 2011).

The components affected by peripheral nerve injury are the peripheral nerve endings and nerve fibres and the neuronal cell bodies located in the DRG, autonomic ganglia, as well as in the spinal cord. In addition to axons, nerves consist of different cellular structures including SCs, endothelial cells, fibroblasts and resident immune cells. The DRGs and autonomic ganglia contain fibroblasts, immune cells and satellite cells. The spinal cord relays information to and from higher centres of the CNS and is composed of second order sensory neurons, motor- and interneurons, glial cells such as astrocytes and oligodendrocytes and microglia, which are the resident immune cells of the CNS.

2.1.1. Expression changes in the peripheral nerve following peripheral nerve injury

The injured peripheral nerve undergoes drastic changes following injury (see General Introduction). Functional recovery is achieved by removal of degenerating myelin but also by the orchestration of regeneration by activation of an intrinsic growth programme and extrinsic cues such as trophic factors. An interesting study, which was published more than 10 years ago, used microarray analysis to characterise changes in gene expression following nerve injury (Kubo et al., 2002). This study and others revealed that the expression of growth factors such as NGF, BDNF and GDNF and their receptors, are clearly regulated in the distal stump of the injured sciatic nerve. The examined tissue was enriched with SCs, which are an important source for growth factors following injury and are involved in the subsequent pathological reorganization and regeneration (Taniuchi et al., 1988).

Although the EGFR and its ligands are important regulators of multiple physiological processes and are also involved in tumourigenesis, little is known about their role or function following nerve injury.

2.1.2. Expression changes in the DRG following peripheral nerve injury

It is not only the environment of the injured nerve, which undergoes drastic changes following injury. The DRG, which comprises the neurons promoting sensory information to the dorsal horn, also shows clear expression changes. As described above, after nerve injury, there is differential protein expression of specific molecules (e.g. BDNF, GDNF, LIF etc.), which can modulate the intrinsic growth capacity of the neuronal cell body to allow successful regeneration (Rishal and Fainzilber, 2010).

Several high-throughput microarray studies have revealed that numerous mediators are regulated in the DRG following nerve injury (LaCroix-Fralish et al., 2011). A recently published microarray study of the rat DRG found hundreds of candidates, which might be involved in the pathophysiological process. Among these are several different types of receptors (G-Protein coupled receptors, tyrosine kinase receptors, ligand-gated ion channels), cytoskeletal proteins, transcription factors and ECM proteins. Furthermore, cytokines, such as IL1β, IL6 and TNF-α were regulated. As expected, in those experiments growth factors were regulated following injury, amongst others BDNF and basic fibroblast growth factor (FGF) (Costigan et al., 2002).

Information about the EGF growth factor family and its receptors is sparse. In humans the EGFR is expressed on the protein level in the DRG (Huerta et al., 1996) and it was shown in rats that it is regulated in response to a peripheral insult (Xian and Zhou, 1999a). However, it is not yet known whether EGFR ligand expression is altered in a long-term manner following nerve injury.

2.1.3. Expression changes in the dorsal horn following peripheral nerve injury

Alterations in sensory pathways of the central nervous system following nerve injury, especially in the dorsal horn, can affect nociceptive processes. Development of neuropathic pain as a result of nerve injury involves neurons, spinal microglia and astrocytes. In brief, nerve injury leads to activation, infiltration and proliferation of microglia and astrocytes in the dorsal horn of the respective spinal cord segment (Scholz and Woolf, 2007). In addition, neuronal cells in the dorsal horn undergo plasticity changes following nerve injury (Woolf and Salter, 2000). An indication for that is that the expression levels of ion channels, like sodium or potassium channels are altered (Hains et al., 2004). Additionally, more indirect mechanisms of neuronal excitability have been proposed, which can be due to an expression change of enzymes responsible for the supply of neurotransmitters (Moore et al., 2002). Furthermore, there are alterations in the mRNA expression of several markers for synaptogenesis, such as Synaptophysin, indicating plasticity changes (Chou et al., 2002) after injury.

Whether expression changes of key members of the EGF-family, including ligands, receptors and shedding enzymes occur in DRGs following peripheral injury is not yet known. In the present work my aim was to identify novel mediators of neuropathic pain development. In order to achieve this, I employed the SNT model in rats in combination with a medium-throughput gene expression array platform focused on EGFR ligands, their receptors and shedding enzymes, following nerve injury.

2.2 Materials and Methods

2.2.1. Animals

Experiments were performed using male Wistar rats (~250g, Harlan). Animals were housed under standard conditions with a 12 hour light/dark cycle and food and water was available *ad libitum*. All experiments were done in accordance to the United Kingdom Home Office regulations.

2.2.2. Surgery

The partial nerve injury model was generated by the transection of the L5 spinal nerve derived from a method introduced by Kim and Chung (Kim and Chung, 1992) (Figure 2.1.). The method was altered so that only L5 was injured, which differs from the original method where L5 and L6 are transected. Adult rats were anaesthetised with a combination of Medetomidine (Domitor®) (0.25mg/kg) and Ketamine (Vetalar®) (60mg/kg) given via intraperitoneal injection. Bilateral paramedian incisions next to the spinal column were made and one third of the L6 transverse process was removed which exposed the spinal nerves. Once identified the L5 spinal nerve was tightly ligated using 6-0 silk. Then, the L5 spinal nerve was transected and distal to the ligation first the muscle layer and then the skin was sutured with Vicryl 3-0. Surgery was performed under sterile conditions. Following the procedure and at least 45 minutes after anaesthetic induction, animals were given a subcutaneous injection of Atipamezole hydrochloride (1m/kg).

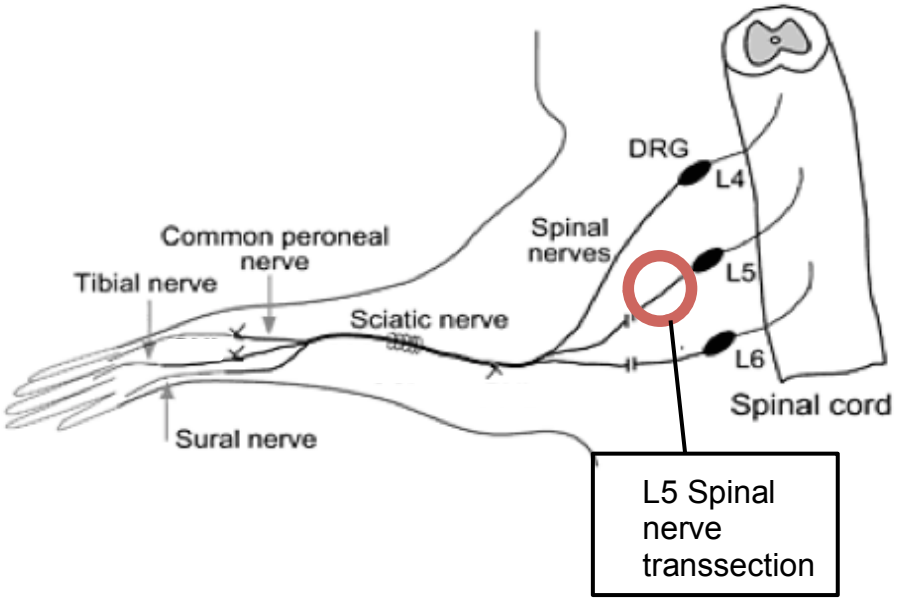

Figure 2.1. Anatomy of the sciatic nerve in rats. (Adapted from Ueda *et al.* (Ueda, 2006) Illustrated is the left hindpaw of a rat with the sciatic nerve and its branches. The circle indicates the L5 spinal nerve, which is first ligated and then transected in the SNT model used in this thesis.

2.2.3. Tissue dissection

Rats were terminally anaesthetised using 0.8ml of sodium-pentobarbital and then transcardially perfused with cold saline solution (0.9% in H_2O). Following careful exposure, a section of the sciatic nerve, the L5 DRG and the respective dorsal horn section L5 were carefully dissected out from the surrounding connective tissue, snap frozen in RNase-free tubes (Eppendorf) in liquid nitrogen and stored at -80°C. Tissue samples were taken from 3-4 rats per time point 3, 7 and 21 days after SNT and from naïve animals and individually used for the experiments.

2.2.4. RNA extraction

Tissue was extracted from 3-4 rats per time point. Tissue samples were individually homogenised in TRIZOL (Invitrogen) using an automated homogeniser. Samples were incubated in chloroform and ethanol and the RNA fraction was separated by centrifugation at 14,000 revolutions per minute (rpm) at 4°C for 15 minutes. A column purification assay (Qiagen, RNAeasy MiniKit) was used to further clean RNA samples from contamination with chemical reagents. All samples were treated with DNAse (Qiagen) to prevent genomic DNA contamination.

Following extraction, RNA concentration was determined using a spectrophotometer (Nanodrop1000). Only samples with a suitable photometric spectrum (Figure 2.2.) and high quality regarding purity and contamination of RNA samples (260:280 and 260:230 between 1.8-2.2) were used for further analysis. Samples, which were used for medium-throughput PCR array analysis were tested for RNA integrity (Fleige and Pfaffl, 2006) using RNA 6000 Nano Chip (Agilent). Only samples with integrity values >7 were included into further experiments.

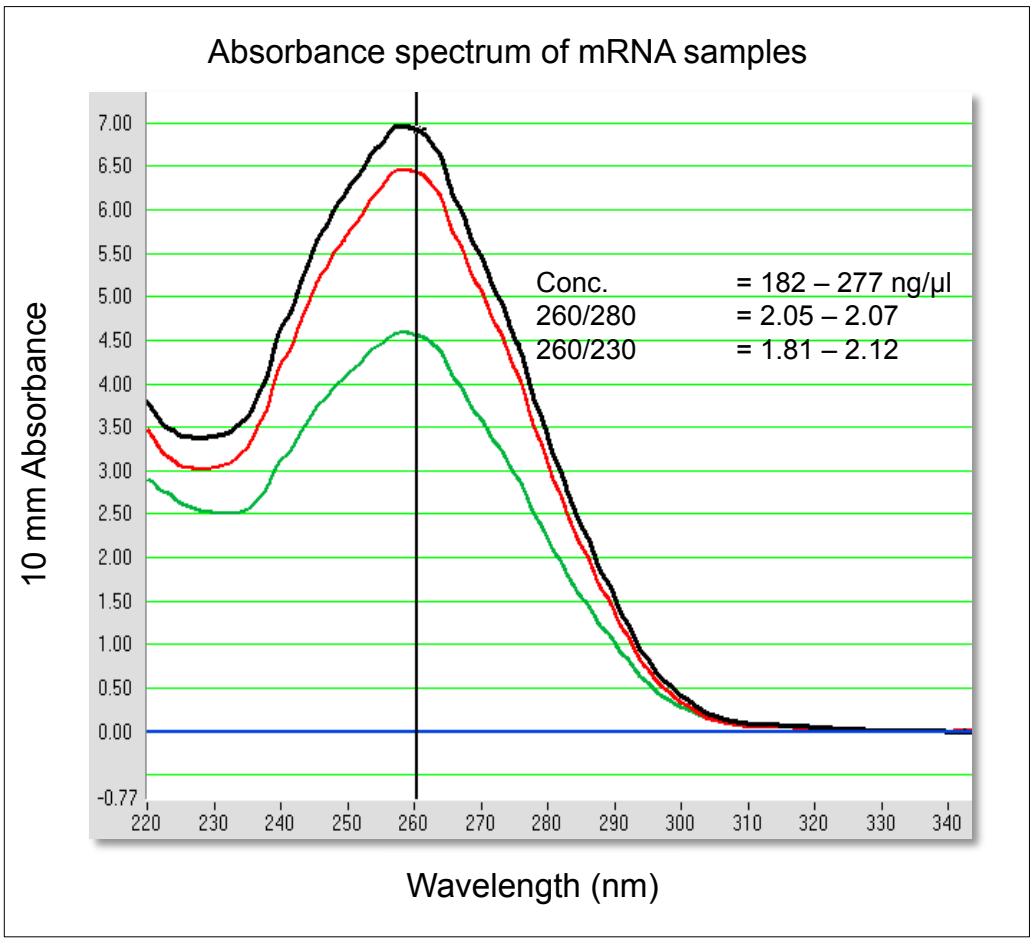

Figure 2.2. RNA purity. Photometric spectrum exemplifies three mRNA samples used for further experiments. Only samples with a suitable photometric spectrum (Figure) and high quality regarding contamination and purity (260:280 and 260:230 between 1.8-2.2) were used for further analysis

2.2.5. Reverse transcriptase PCR

RNA samples were reversely transcribed using a standardised kit, Superscript III (Invitrogen). Reverse transcription was done in batches of all samples for sciatic nerve, DRG or dorsal horn, respectively to reduce experimental variability. Complementary DNA (cDNA) samples were stored at -20°C.

2.2.6. Taqman array set-up and quantitative real-time PCR

Taqman array cards were designed using the Applied Biosystem website (http://www.appliedbiosystems.com). 96 different primer pairs, which included 4 reference genes (Glyceraldehyde 3-phosphate dehydrogenase (GAPDH), 18s, β-Actin and β-2-Microglobulin), were custom designed. Each cDNA sample was diluted with polymerase chain reaction (PCR) grade water and samples were transferred into the microfluidic based loading ports according to the manufacturer's guidelines. RT-qPCR reactions were performed in a 7900HT Fast Real-Time PCR system (Applied Biosystems) with 40 cycles of amplification per experiment. Expression of each transcript was measured using the delta delta CT ($2^{-\Delta\Delta CT}$) method (Schmittgen and Livak, 2008) normalised to the geometric mean of the 4 reference genes. Samples with an average cycling threshold (C_T) of >38 were defined as not detectable and not included into the analysis.

2.2.7. Quantitative real time PCR

Individual RT-qPCR was done using SYBR Green (Roche) as a fluorescent probe in a Rotor-Gene 6000 Corbett Research) and Roche Lightcycler 480. Each experiment was designed in triplicates for the gene of interest (GOI) primer and duplicates for the reference gene primer. The most stable reference gene was determined for each tissue (reference gene validation see below).

Primers were designed using Primer3 software (www.primer3.sourceforge.net) and Blast software (http://www.ncbi.nlm.nih.gov/tools/primer-blast/). Potential hairpin or primer dimer formations were analysed using Netprimer (premierbiosoft). Primers were tested for efficiency running a standard curve with a validated pool (6 different tissues) of rat cDNA (Figure 2.3.) and for specificity testing the PCR product using a melting curve protocol (Figure 2.4.) and determining product size with an agarose gel. All primer sequences and efficiency are presented in **Table 1**.

	forward	reverse	*R*
AREG	AAGCGTCGCAGCTATTGGCA	TTGCCGCAGCCTCCTTCTTTCT	
BTC	TGGGAACACAACCAGAACCCCT	TTCGTCCATCACGAAGCGGCAT	
EREG	TTTGCGAGCTGCACCGAGAGAA	TGTCCATGCAAGCAGTAGCCGT	
HB-EGF	TTCCACCTGGCTCAATGCCACA	ATCCATCCTTGCACTCCGACCA	
TGFα	CACGAGCGGCTGGCTGTGAA	GGCTGATGCTGGAGCTGGGC	
TACE	TGGCAGAGTGTGCCCCAAATGA	AGTTGCCGCACACCTTGTTGCT	
ADAM 10	GCCTATGTCTTCACGGACCG	TGCCAGACCAAGAACACCATC	**A**
ErbB1	GTACAGCGCCACCTGACGGG	ACGCCGGGAACATTGCTGGG	
ErbB2	CCTGCCTCCACTTCAATCAT	CAGGATCCCACTTCCGTAGA	
ErbB3	TGAAGATGTGTGAGCCTTGC	GGTCCAGTGCGGGTATCTTA	
ErbB4	ATGGCCTTCCAACATGACTC	CACCTGCCATCACATTGTTC	
GAPDH	GACCGGTTCTGTCATGTCG	ACCTGGTTCATCATCATAATCAC	**B**
UBC	CAGGACAAGGAGGGCATC	GCCATCTTCCAGCTGCTT	**B**
YWHAZ	GCTACTTGGCTGAGGTTGCT	TGCTGTGACTGGTCCACAAT	**B**
β-Actin	TGTCACCAACTGGGACGATA	ACCCTCATAGATGGGCACAG	**B**
β2MG*	TCTCTGGCCGTCGTGCTTGC	TCCCAGGTGACGGTTTTGGGC	
CD36	TCTCCTCGGATGGTTAGCTG	TGTGGCCTGGTTCAACTAATTC	
CD68	AAGCAGCACAGTGGACATTCT	GGGTAACGCAGAAGGCAATG	
MBP	CCACATGTACAAGGACTCACACACA	GAAGCTCTGCCTCCGTAGC	
IBA1	TCCCCACCTAAGGCCACCAGC	CGTCTCCTCGGAGCCACTGGA	

Table 1 Primer sequences. R = references for primer sequence. **A)** (Jangouk et al., 2009); **B)** (Xing et al., 2009). All other Primers were designed using Primer3 software (www.primer3.sourceforge.net). *β-2-Microglobulin (β2MG).

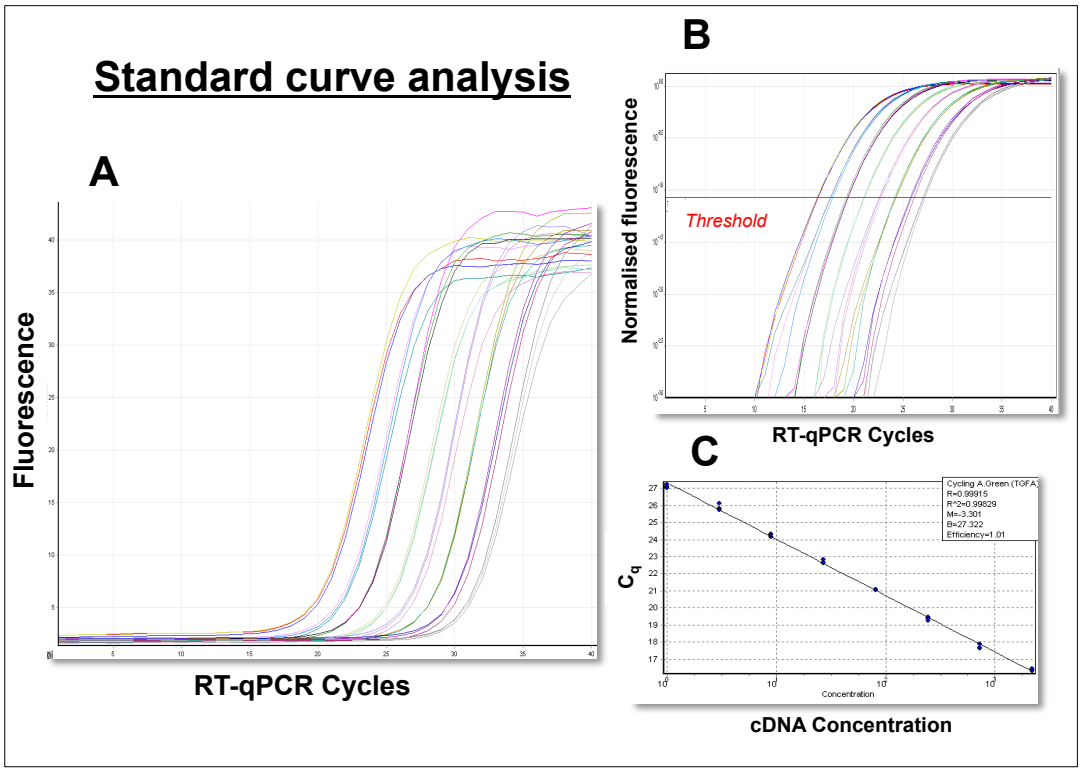

2.3. Testing for primer efficiency. **A)** Example of raw RT-qPCR traces using the BTC primer on increasing cDNA concentrations (1ng to 1ug) in triplicates. **B)** Data was log-normalised and an arbitrary threshold was set to determine C_T values. **C)** A standard curve plotting C_T values over cDNA concentration was used to determine the slope (efficiency of the reaction).

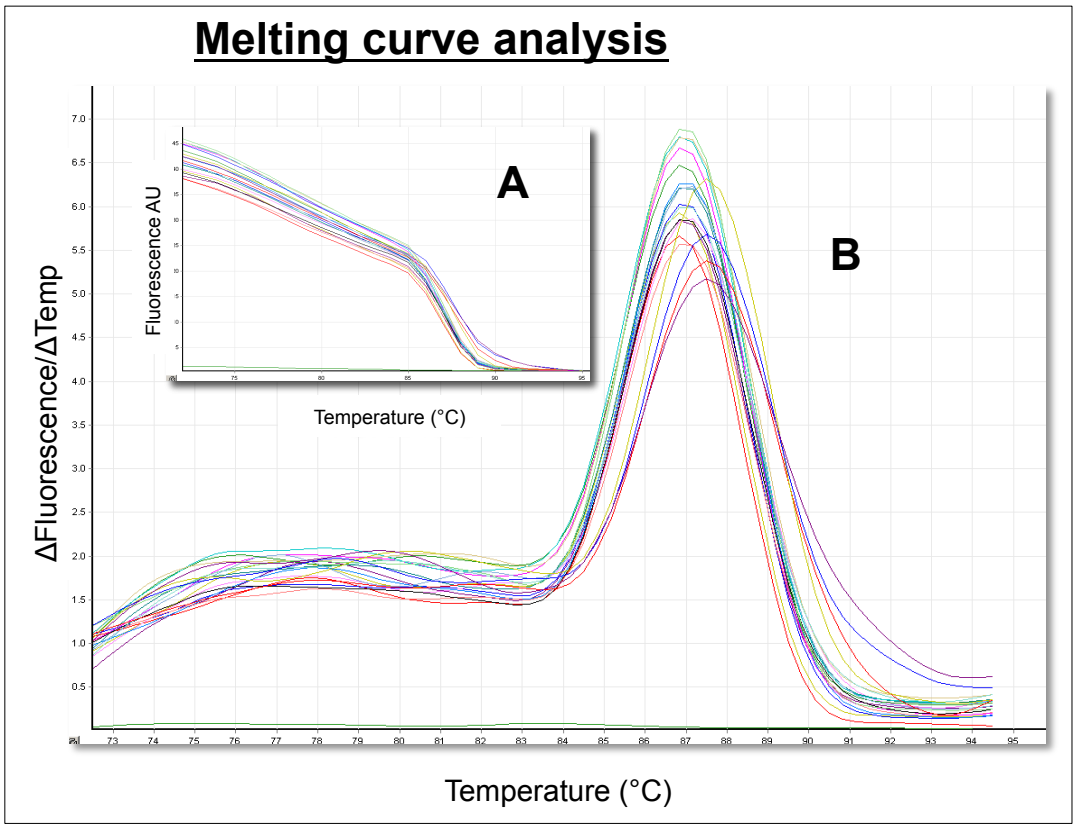

Figure 2.4. Melting curve analysis. Primer quality and amplification sensitivity was analysed with a melting curve analysis at the end of each RT-qPCR run. **A)** Raw fluorescent traces of BTC primer on cDNA samples at increasing temperatures **B)** Melting curve traces show one peak, suggesting one PCR product. Product size was also determined using agarose gel electrophoresis.

RT-qPCR data was analysed determining an arbitrary cycling threshold (C_T) for each sample from the log-linear plot of the PCR signal versus the cycle number. The C_T was used to calculate the $2^{-\Delta\Delta CT}$ (Schmittgen and Livak, 2008), which describes the fold change of mRNA/cDNA levels in different samples in relation to the expression of a suitable reference gene (Figure 2.6.).

$$2^{-\Delta\Delta CT} = [(C_T \text{ gene of interest} - C_T \text{ reference gene}) \text{ TREATMENT SAMPLE}) - (C_T \text{ gene of interest} - C_T \text{ reference gene}) \text{ CONTROL SAMPLE})]$$

Figure 2.5. Equation $2^{-\Delta\Delta CT}$

Reference genes were validated amplifying each sample with primers for at least 5 different well-known reference genes (RG) (primer sequences Table 1) (Vandesompele et al., 2002). The most stable reference gene was chosen for each tissue. As inter-run calibrator (Derveaux et al., 2010) a pool of validated rat tissue, including equal amounts of cDNA from lung, liver, spleen, heart, brain, spinal cord, kidney was used in each experiment to correct for run-to-run variation. With that approach expression of all GOIs could be compared to each other in the analysed tissues.

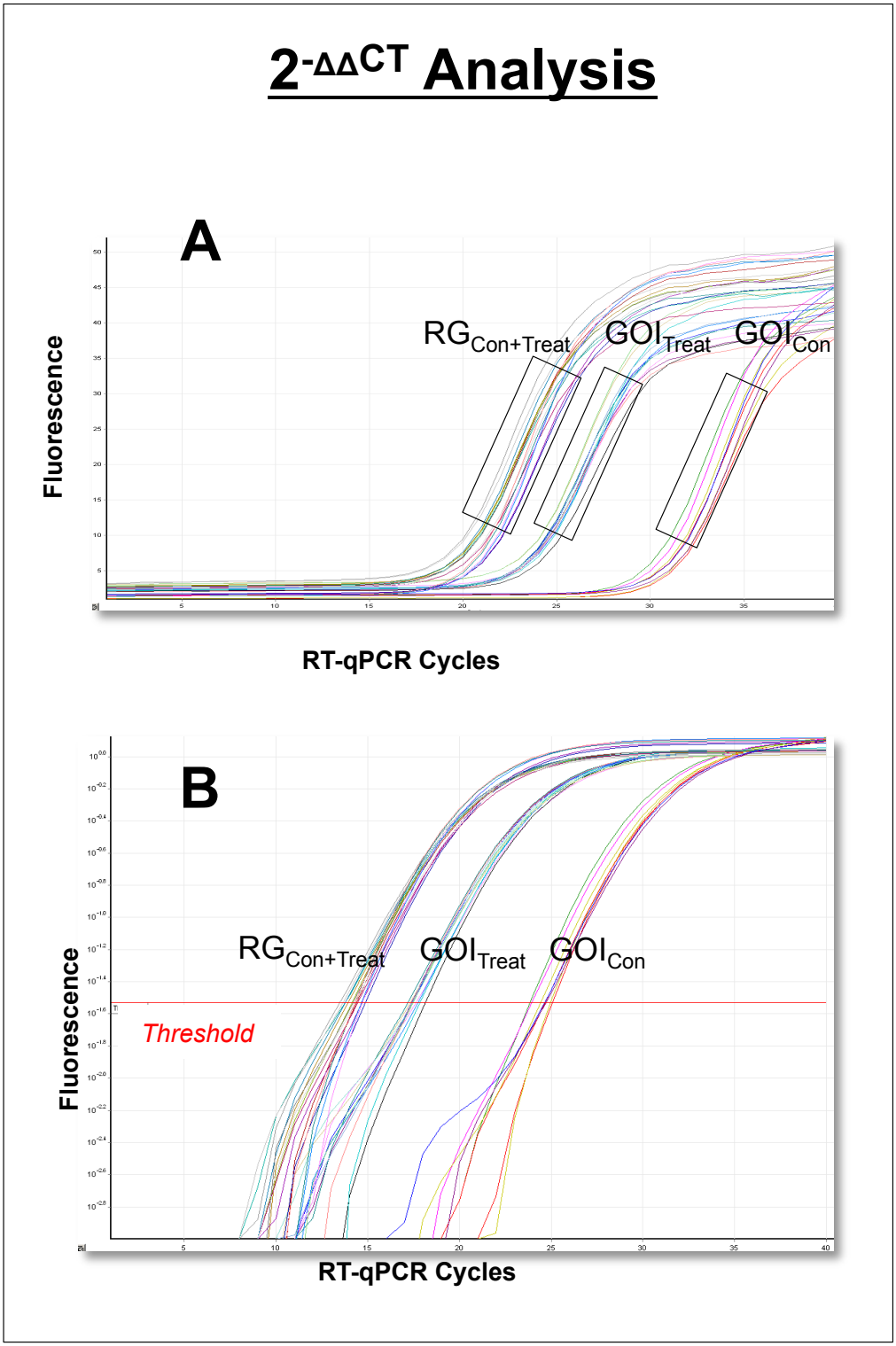

Figure 2.6. $2^{-\Delta\Delta CT}$ analyses. Illustrated are raw traces of one RT-qPCR experiment. **A)** Highlighted are groups including the RG of control and treatment samples, and traces for the GOI of control and treatment samples**. B)** After log normalization, an arbitrary threshold was determined and C_T values were analysed using $2^{-\Delta\Delta CT}$ method.

2.2.8. Statistical analysis

All statistical analyses were done on the $2^{-\Delta\Delta CT}$ values to avoid unnecessary underestimation of experimental variation among replicate reactions (Livak and Schmittgen, 2001). One-way Analysis of variance (ANOVA) was used to analyse data of more than two groups, where necessary Bonferroni's post-doc analysis was performed to characterise individual differences. A p-value <0.05 was defined as a significant result. Data was computed using GraphPad PRISM. For graphic data presentation, all charts represent arithmetic mean ± standard error of the mean (SEM).

2.3. Results

2.3.1. Medium-throughput TaqMan RT-qPCR array cards

2.3.1.1. Timecourse following SNT

Following peripheral nerve injury dramatic changes occur in the affected peripheral nerve, which consist of an acute and chronic inflammatory response, tissue remodeling as well as extensive spatial and temporal infiltration of different cell types. To study effector molecules of the pathological process following nerve injury, TaqMan probe-based, PCR array cards (Keys et al., 2010) as a medium-throughput screening of 96 genes, including chemokines, cytokines and growth factors (**Table 2**) were used (tissue extraction, mRNA extraction and TaqMan qPCR for this experiment were done by Dr. John Dawes).

Gene	full name	Gene	full name
IBA1	Allograft inflammatory factors -1	**FGF7**	Fibroblast growth factor 7
ARA5	Arachidonate 5 and 15- Lipoxygenase	**IFNγ**	Interferon gamma
HB-EGF	Heparin-binding EGF-like growth factor	**IL10**	Interleukin 10
AREG	Amphiregulin	**IL11**	Interleukin 11
ARTN	Artemin	**IL12a**	Interleukin 12a
BDNF	Brain-derived neurotrophic factor	**IL12b**	Interleukin 12b
BTC	Betacellulin	**IL13**	Interleukin 13
C3	Complement component 3	**IL15**	Interleukin 15
C5	Complement component 5	**IL16**	Interleukin 16
CL1	Chemokine (C motif) ligand 1	**IL18**	Interleukin 18
CCL1	Chemokine (C-C motif) ligand 1	**IL19**	Interleukin 19
CCL11	Chemokine (C-C motif) ligand 11	**IL1α**	Interleukin 1 alpha
CCL12	Chemokine (C-C motif) ligand 12	**IL1β**	Interleukin 1 beta
CCL17	Chemokine (C-C motif) ligand 17	**IL2**	Interleukin 2
CCL19	Chemokine (C-C motif) ligand 19	**IL20**	Interleukin 20
CCL2	Chemokine (C-C motif) ligand 2	**IL21**	Interleukin 21
CCL20	Chemokine (C-C motif) ligand 20	**IL23a**	Interleukin 23a
CCL21b	Chemokine (C-C motif) ligand 21b	**IL24**	Interleukin 24
CCL22	Chemokine (C-C motif) ligand 22	**IL27**	Interleukin 27
CCL24	Chemokine (C-C motif) ligand 24	**IL3**	Interleukin 3
CCL25	Chemokine (C-C motif) ligand 25	**IL33**	Interleukin 33
CCL26	Chemokine (C-C motif) ligand 26	**IL4**	Interleukin 4
CCL27	Chemokine (C-C motif) ligand 27	**IL5**	Interleukin 5
CCL28	Chemokine (C-C motif) ligand 28	**IL6**	Interleukin 6
CCL3	Chemokine (C-C motif) ligand 3	**IL7**	Interleukin 7
CCL4	Chemokine (C-C motif) ligand 4	**IL9**	Interleukin 9
CCL5	Chemokine (C-C motif) ligand 5	**c-Kit**	C-Kit ligand
CCL6	Chemokine (C-C motif) ligand 6	**LIF**	Leukemia inhibitory factor
CCL7	Chemokine (C-C motif) ligand 7	**IL17**	Interleukin -17 precursor
CCL9	chemokine (C-C motif) ligand 9	**CTLA-8**	Lymphocyte- associated antigen 8)
MCSF	Colony stimulating factor 1	**LTA4H**	Leukotriene A4 hydrolase
GCSF-1	Colony stimulating factor 2	**MIF**	Macrophage migration inhibitory factor
GCSF-2	Colony stimulating factor 3	**NGFβ**	Nerve growth factor (beta polypeptide)
CX3CL1	Chemokine (C- X3-C motif) ligand 1	**NOS2**	Nitric oxide synthase 2, inducible
CXCL1	Chemokine (C-X- C motif) ligand 1	**Nrgl-1**	Neuregulin-1 (1)
CXCL10	Chemokine (C-X- C motif) ligand 10	**Nrgl-2**	Neuregulin-1 (2)
CXCL11	Chemokine (C-X- C motif) ligand 11	**CXCL4**	Platelet factor 4
CXCL12	Chemokine (C-X- C motif) ligand 12	**CXCL7**	Pro-platelet basic protein
CXCL13	Chemokine (C-X- C motif) ligand 13	**PROK2**	Prokineticin 2
CXCL14	Chemokine (C-X- C motif) ligand 14	**PGE**	Prostaglandin E synthase
CXCL16	Chemokine (C-X- C motif) ligand 16	**PGI2**	Prostaglandin I2 (prostacyclin) synthase
CXCL17	Chemokine (C-X- C motif) ligand 17	**COX-2**	Prostaglandin- endoperoxide synthase 2
CXCL2	Chemokine (C-X- C motif) ligand 2	**TGFβ**	Transforming growth factor, beta 1
CXCL3	Chemokine (C-X- C motif) ligand 3	**TNF-α**	Tumor necrosis factor alpha
CXCL5	Chemokine (C-X- C motif) ligand 5	**TRPA1**	Transient receptor potential cation channel A1
CXCL9	Chemokine (C-X- C motif) ligand 9	**TRPV3**	Transient receptor potential cation channel V3
EBVG3	Epstein-Barr virus induced gene 3	**TRPV4**	Transient receptor potential cation channel V4
ET1	Endothelin 1	**β3T**	Tubulin, beta 3
EREG	Epiregulin	**IL14**	Taxilin-α

Table 2: Genes of the TaqMan RT-qPCR array card. Highlighted are members of the EGFR ligand family.

To evaluate gene expression changes in the sciatic nerve following nerve injury three different timepoints (3, 7, 21 days) were used and gene expression changes of injured versus uninjured sciatic nerves were compared. RNA from the injured sciatic nerve distal to the injury site was extracted from each animal separately (n=3-4 animals per time point equals 3-4 nerves, respectively).

Differential gene expression was computed using one-way ANOVA and Bonferroni's multiple comparison test. P-values ≤ 0.05 were considered significant. Hierarchical clustering of significantly regulated genes using Pearson Correlation Coefficient revealed excellent temporal clustering of genes and highlighted groups of clearly co-expressed mRNAs, mainly at 7 and 21 days post-injury (Figure 2.7. A). One group of genes with the most uniform and sharp clustering regulated at 7 days, was selected for further analysis (Figure 2.7. B).

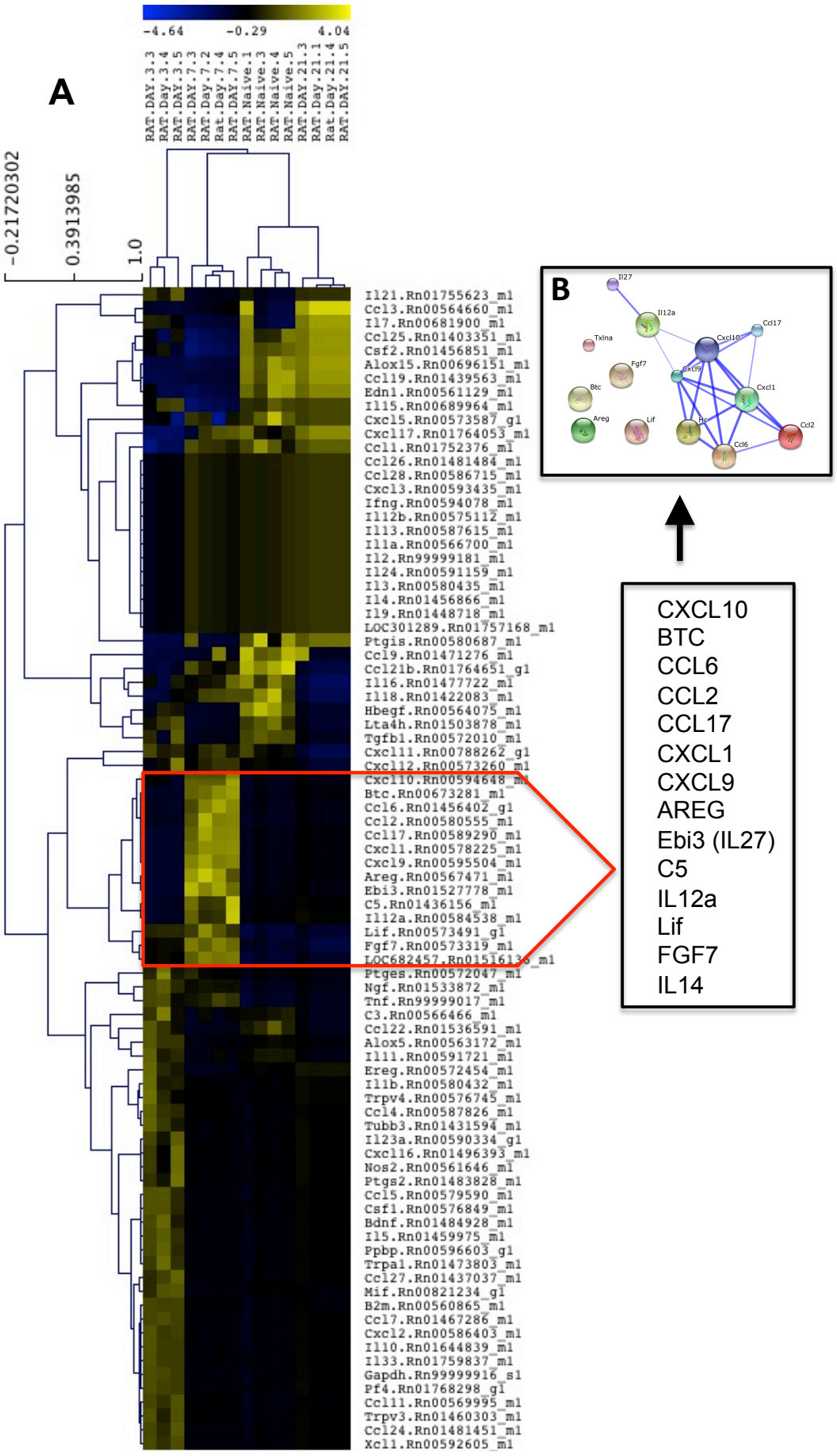
A
-4.64
-0.29
4.04
RAT.DAY.3.3
RAT.Day.3.4
RAT.DAY.3.5
RAT.DAY.7.3
RAT.Day.7.2
Rat.Day.7.4
RAT.DAY.7.5
RAT.Naive.1
RAT.Naive.3
RAT.Naive.4
RAT.Naive.5
RAT.DAY.21.3
RAT.Day.21.1
Rat.Day.21.4
RAT.DAY.21.5
-0.21720302
0.3913985
1.0
Il21.Rn01755623_m1
Ccl3.Rn00564660_m1
Il7.Rn00681900_m1
Ccl25.Rn01403351_m1
Csf2.Rn01456851_m1
Alox15.Rn00696151_m1
Ccl19.Rn01439563_m1
Edn1.Rn00561129_m1
Il15.Rn00689964_m1
Cxcl5.Rn00573587_g1
Cxcl17.Rn01764053_m1
Ccl1.Rn01752376_m1
Ccl26.Rn01481484_m1
Ccl28.Rn00586715_m1
Cxcl3.Rn00593435_m1
Ifng.Rn00594078_m1
Il12b.Rn00575112_m1
Il13.Rn00587615_m1
Il1a.Rn00566700_m1
Il2.Rn99999181_m1
Il24.Rn00591159_m1
Il3.Rn00580435_m1
Il4.Rn01456866_m1
Il9.Rn01448718_m1
LOC301289.Rn01757168_m1
Ptgis.Rn00580687_m1
Ccl9.Rn01471276_m1
Ccl21b.Rn01764651_g1
Il16.Rn01477722_m1
Il18.Rn01422083_m1
Hbegf.Rn00564075_m1
Lta4h.Rn01503878_m1
Tgfb1.Rn00572010_m1
Cxcl11.Rn00788262_g1
Cxcl12.Rn00573260_m1
Cxcl10.Rn00594648_m1
Btc.Rn00673281_m1
Ccl6.Rn01456402_g1
Ccl2.Rn00580555_m1
Ccl17.Rn00589290_m1
Cxcl1.Rn00578225_m1
Cxcl9.Rn00595504_m1
Areg.Rn00567471_m1
Ebi3.Rn01527778_m1
C5.Rn01436156_m1
Il12a.Rn00584538_m1
Lif.Rn00573491_g1
Fgf7.Rn00573319_m1
LOC682457.Rn01516136_m1
Ptges.Rn00572047_m1
Ngf.Rn01533872_m1
Tnf.Rn99999017_m1
C3.Rn00566466_m1
Ccl22.Rn01536591_m1
Alox5.Rn00563172_m1
Il11.Rn00591721_m1
Ereg.Rn00572454_m1
Il1b.Rn00580432_m1
Trpv4.Rn00576745_m1
Ccl4.Rn00587826_m1
Tubb3.Rn01431594_m1
Il23a.Rn00590334_g1
Cxcl16.Rn01496393_m1
Nos2.Rn00561646_m1
Ptgs2.Rn01483828_m1
Ccl5.Rn00579590_m1
Csf1.Rn00576849_m1
Bdnf.Rn01484928_m1
Il5.Rn01459975_m1
Ppbp.Rn00596603_g1
Trpa1.Rn01473803_m1
Ccl27.Rn01437037_m1
Mif.Rn00821234_g1
B2m.Rn00560865_m1
Ccl7.Rn01467286_m1
Cxcl2.Rn00586403_m1
Il10.Rn01644839_m1
Il33.Rn01759837_m1
Gapdh.Rn99999916_s1
Pf4.Rn01768298_g1
Ccl11.Rn00569995_m1
Trpv3.Rn01460303_m1
Ccl24.Rn01481451_m1
Xcl1.Rn00592605_m1
B
Il27
Il12a
Ccl17
Txlna
Cxcl10
Fgf7
Cxcl9
Btc
Cxcl1
Areg
Lif
Ebi3
Ccl2
Ccl6
CXCL10
BTC
CCL6
CCL2
CCL17
CXCL1
CXCL9
AREG
Ebi3 (IL27)
C5
IL12a
Lif
FGF7
IL14

Figure 2.7. Hierarchical clustering of medium-throughput RT-qPCR data from sciatic nerve following SNT. A) The dendrogram displays hierarchical clustering analysis (Pearson correlation coefficient) of the differentially expressed genes in samples from the sciatic nerve 3, 7, 21 days following SNT (L5). Differences in spectral counts are colour-coded as indicated. Displayed are n = 3 for day 3 samples and n = 4 for naïve, day 7 and day 21 samples. **B)** Network visualization of the group of similarly regulated target genes**.** Genes are displayed as protein-protein interactions from known and predicted associations using the STRING database.

2.3.1.2 Functional clustering of co-expressed genes

Using the STRING database I performed further network enrichment of the selected gene cluster (Figure 2.8. B). This cluster includes two members of the EGFR ligand group, BTC and AREG, the growth factors FGF7 (fibroblast growth factor) and leukemia inhibitory factor (LIF), the chemokines CXCL10, CCL6, CCL2, CCL17, CXCL1, CXCL9 and the cytokines Ebi3 (subunit of IL27) and IL35 (Devergne et al., 1996) IL12a and Taxilin-α (IL14) but also a gene for members of the complement (C) system, C5 -C9 (hemolytic complement gene, Hc), which are all similarly regulated following SNT (Figure 2.7. A).

The Markov clustering algorithm (MCL) generated three subnetworks based on functional inference. As expected, growth factors, including EGFR ligands and their receptors, chemokines and cytokines respectively, form an individual cluster. After functional enrichment of the network additional nodes are generated including two other ligands of the EGFR family, EREG, HB-EGF and also the EGFR. Apart from the EGFR ligands and FGF7, the enrichment cluster includes Grb2, an adaptor protein for the EGFR (Lowenstein et al., 1992) and EGFR substrate 15 (Eps15), involved in the receptor endocytosis of EGF (Benmerah et al., 1999). Fibroblast growth factor receptor 2 (FGFR2) is functionally linked to both EGF and FGF7. Similarly, the chemokine group was enriched with other effectors and receptors common to the inflammatory response. As expected, the two groups appear disconnected. Interestingly, the cytokines IL27 and IL12α, although similarly regulated are not linked to the EGFR ligands (Figure 2.8. A).

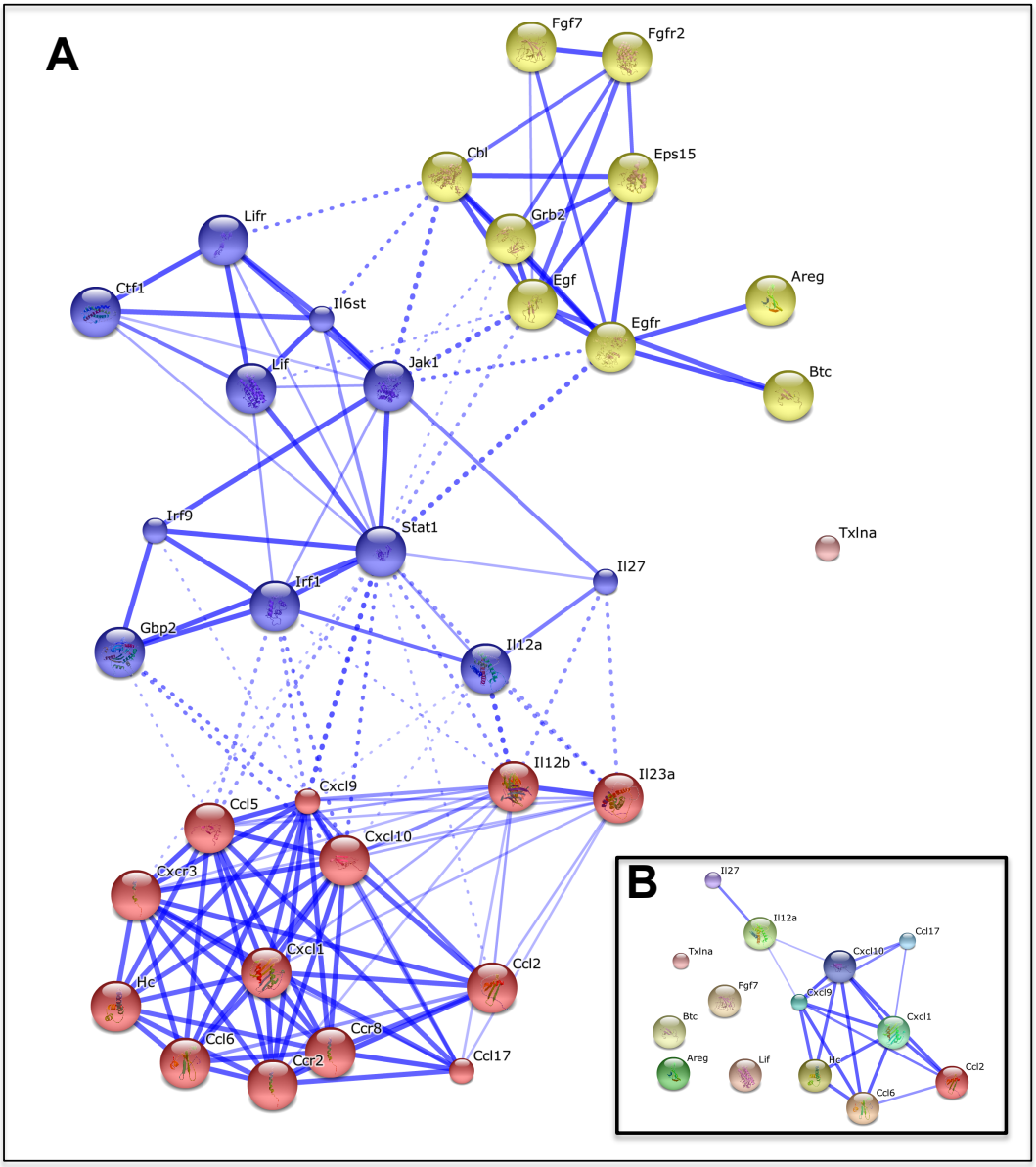

Figure 2.8. Group of genes with most uniform clustering. A) MCL analysis generated three subnetworks based on functional inference. Thickness of the lines represents a connection based on functional similarity and co-expression. Each node represents one gene. **B)** Network visualization of the group of genes with the most uniform and sharp clustering regulated at 7 days**.** Genes are displayed as protein-protein interactions from known and predicted associations using the STRING database.

2.3.1.3. Ranking of the most significant gene changes

As shown in Figure 2.7 (A) significant gene changes occur after injury. In order to evaluate the most differentially expressed genes a ranking method based on fold change was used. Table 3 shows the five most upregulated genes and reveals a combination of growth factors and inflammatory mediators. A striking observation is the significant regulation of BTC, a member of the EGFR ligand family (day 3 FC = 54.28 (37.71 – 70.86, $p < 0.05$); day 7 FC = 53.20 (49.42 – 56.98, $p < 0.05$) and day 21, FC = 95.29 (88.59 – 102.00, $p < 0.05$). BTC is the most upregulated gene at day 3 post-injury and ranked second at day 7 and day 21. BTC has not yet been implicated in nerve injury-related pathophysiology. BDNF, another highly regulated gene is a well-described growth factor in the physiology of nerve repair (Wilhelm et al., 2012). Other highly regulated genes are IL6, IFN-γ and the chemokines CXCL14 and CXCL10, suggestive of an inflammatory response.

DAY 3		
Rank	**Gene**	**FC**
1	BTC	54.28 (37.71 – 70.86)
2	IL6	12.4 (8.8 – 17.6)
3	CXCL14	8.1 (5.0 – 11.3)
4	LIF	6.9 (4.2 – 11.3)
5	BDNF	6.5 (-1.3 – 55.9)

DAY 7		
Rank	**Gene**	**FC**
1	BDNF	374.5 (103.1 – 1361.1)
2	BTC	53.20 (49.42 – 56.98)
3	IFNγ	18.5 (10.0 – 34.2)
4	IL6	16.5 (10.9 – 25.0)
5	CXCL10	11.3 (6.9 – 18.5)

DAY 21		
Rank	**Gene**	**FC**
1	BDNF	2145.0 (662.3 – 7394.1)
2	BTC	95.29 (88.59 – 102.00)
3	IL6	75.9 (43.6 – 132.1)
4	IFNγ	60.0 (25.3 – 142.4)
5	IL12b	44.3 (12.5 – 156.3)

Table 3. Top-ranking the five most upregulated genes in the sciatic nerve at three different timepoints following SNT (L5). Data derived from medium-throughput RT-qPCR cards. The data is shown as the mean fold change (±1 SD range), calculated using $2^{-\Delta\Delta CT}$ comparing SNT versus naïve nerve samples.

The increased expression of BTC is intriguing especially since other members of EGFR ligand family are either downregulated or could not be detected. AREG mRNA was only detectable 3 days post-injury, EREG was not expressed at any timepoint. The expression for BTC and HB-EGF changed significantly in a distinct manner (Figure 2.9.) HB-EGF showed a significant ($p < 0.0001$) downregulation at day 3 (4.64 ± 0.09), day 7 (17.6 ± 0.66) and day 21 (7.97 ± 1.97) post-injury in comparison to naïve tissue. BTC showed a marked upregulation ($p < 0.0001$) at 3 days (54.28 ± 16.58), 7 days (53.20 ± 3.78) and 21 days (95.29 ± 6.70). The distinct regulation of BTC prompted me to further investigate the EGFR family of ligands as well as their receptors and the relevant activating enzymes.

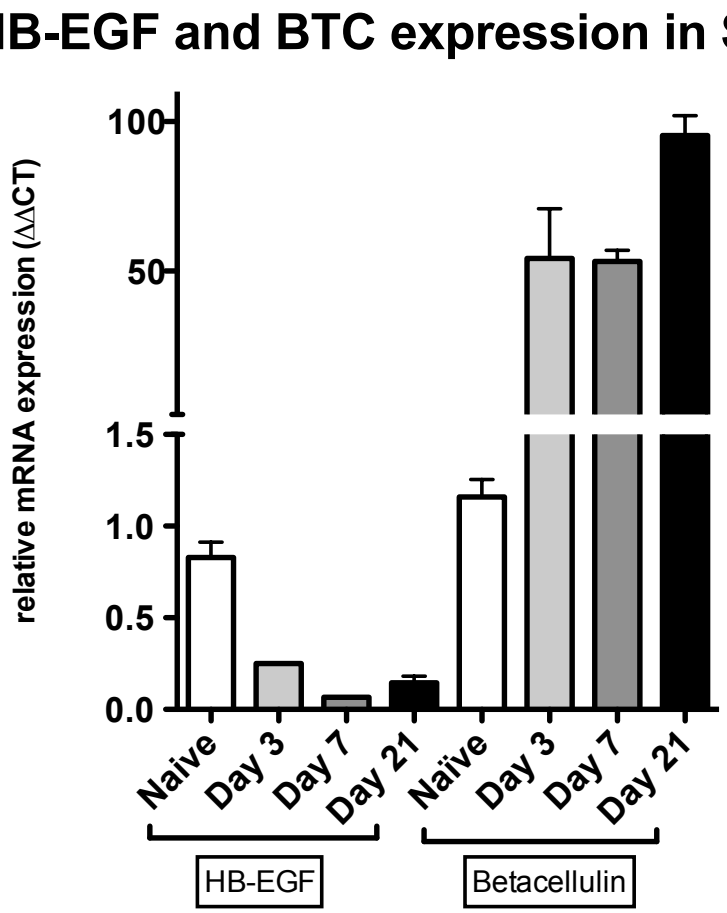

Figure 2.9. TaqMan medium-throughput RT-qPCR. Relative expression of BTC and HB-EGF in the sciatic nerve. Expression levels at three different timepoints following nerve injury. Graph represents fold changes relative to uninjured tissue. Data was analysed using the $2^{-\Delta\Delta CT}$ method with an n=3-4 per group and the mean of 4 reference genes was used for normalisation.

2.3.2. Expression of EGFR ligands

2.3.2.1. Baseline expression of EGFR ligands in naïve tissue

To date, the role of EGFR ligands following nerve injury is not well studied. To validate and further characterise the temporal and anatomical expression profile of EGFR ligands, individual RT-qPCRs were performed for AREG, BTC, EREG, HB-EGF, TGFα and EGF in tissue from sciatic nerve, DRG and dorsal horn taken at 3, 7 and 21 days after partial sciatic nerve transection surgery. First, to evaluate the baseline expression, I compared C_T values of uninjured samples with the C_T values of the appropriate reference gene (suitable reference gene C_T value between 15 and 25) Genes with $C_T \geq 35$ cycles were not included in the analysis. The expression profile can be seen in Figure 2.10.

Baseline expression constant= $\mathbf{C_T\ (GOI)/\ C_T\ (RG)}$

(C_T: cycling threshold; GOI: Gene of Interest; RG: Reference Gene)

Except for EREG and EGF in the dorsal horn all other ligands were expressed in all tissues. Similarly, expression for the receptors ErbB1 (EGFR) and ErbB4 and the shedding enzymes Adam10 and Adam17 could be confirmed (Figure 2.10.).

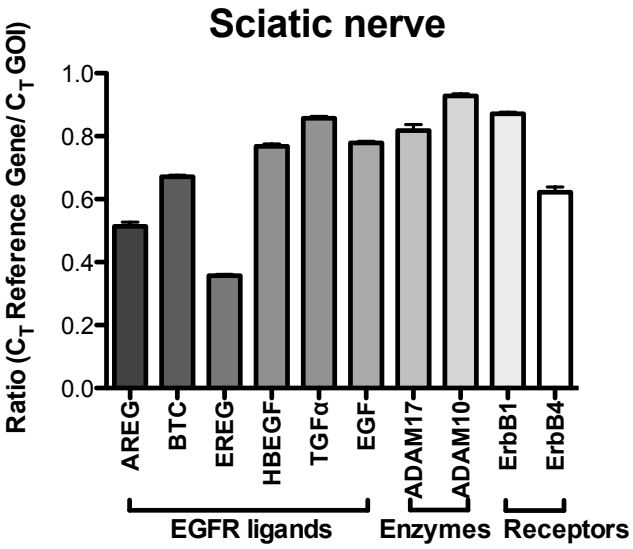
Sciatic nerve
Ratio (C_T Reference Gene/ C_T GOI)
1.0
0.8
0.6
0.4
0.2
0.0
AREG
BTC
EREG
HBEGF
TGFα
EGF
ADAM17
ADAM10
ErbB1
ErbB4
EGFR ligands
Enzymes
Receptors

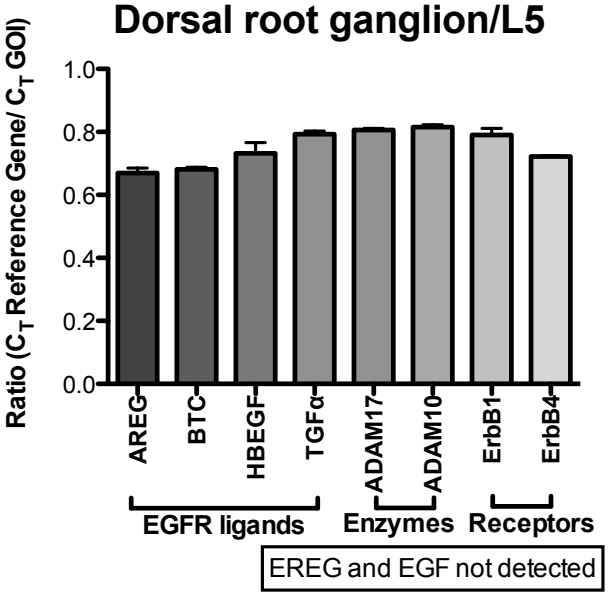
Dorsal root ganglion/L5
Ratio (C_T Reference Gene/ C_T GOI)
1.0
0.8
0.6
0.4
0.2
0.0
AREG
BTC
HBEGF
TGFα
ADAM17
ADAM10
ErbB1
ErbB4
EGFR ligands
Enzymes
Receptors
EREG and EGF not detected

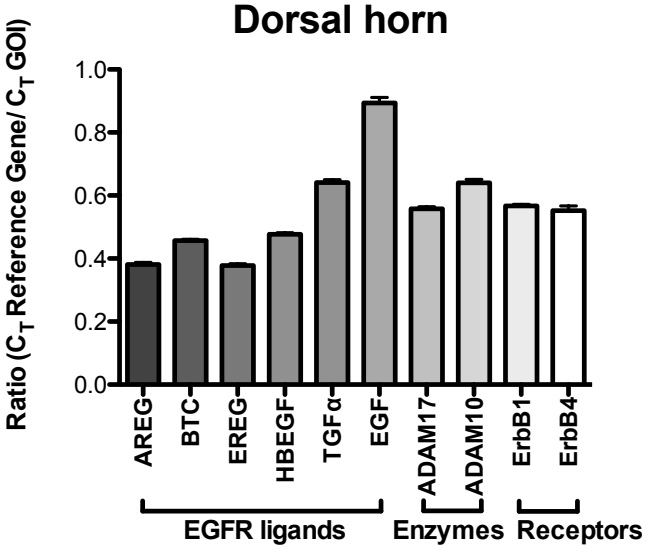
Dorsal horn
Ratio (C_T Reference Gene/ C_T GOI)
1.0
0.8
0.6
0.4
0.2
0.0
AREG
BTC
EREG
HBEGF
TGFα
EGF
ADAM17
ADAM10
ErbB1
ErbB4
EGFR ligands
Enzymes
Receptors

Figure 2.10. Estimation of baseline expression of EGFR ligands, receptors and shedding enzymes in naïve sciatic nerve, DRG and dorsal horn tissue. Comparing C_T values of naïve sample relative to the C_T values of the respective RG (suitable C_T value between 15 and 25) show an estimate of baseline expression of the GOI.

2.3.2.2. Expression changes of EGFR ligands in the sciatic nerve

After characterising the baseline expression, I evaluated mRNA levels of EGFR ligands, ErbB receptors and shedding enzymes ADAM10 and ADAM17 at different timepoints following injury.

Data shown in Figure 2.11 represent individual RT-qPCR experiments for each ligand. Confirming the findings of the medium-throughput RT-qPCR analysis, BTC levels were significantly increased after SNL (28-fold higher expression starting 3 days post-injury). Expression remained high until 21 days post-injury (day 3 FC ≈ 28.76 ± 0.94, day 7 FC ≈ 26.52 ± 0.77, day 21 FC ≈ 35.97 ± 1.39; $n = 3$, $p < 0.0001$) (Figure 2.11.).

The level of HB-EGF mRNA was significantly reduced (by 62.7 %, 91.44 % and 91.49 % at day 3, day 7 and day 21, respectively). TGFα mRNA was also significantly reduced (by 71.77 %, 57.97 % and 45.95 % at day 3, day 7 and day 21 respectively; $n = 3$, $p < 0.0001$).

No significant changes were observed in the expression of EREG, AREG and EGF, although AREG and EREG showed a trend with a 2-fold upregulation 21 days following injury and EGF a stable reduction of mRNA to ≈ 40 % starting at 3 days following injury, respectively (Figure 2.11.)

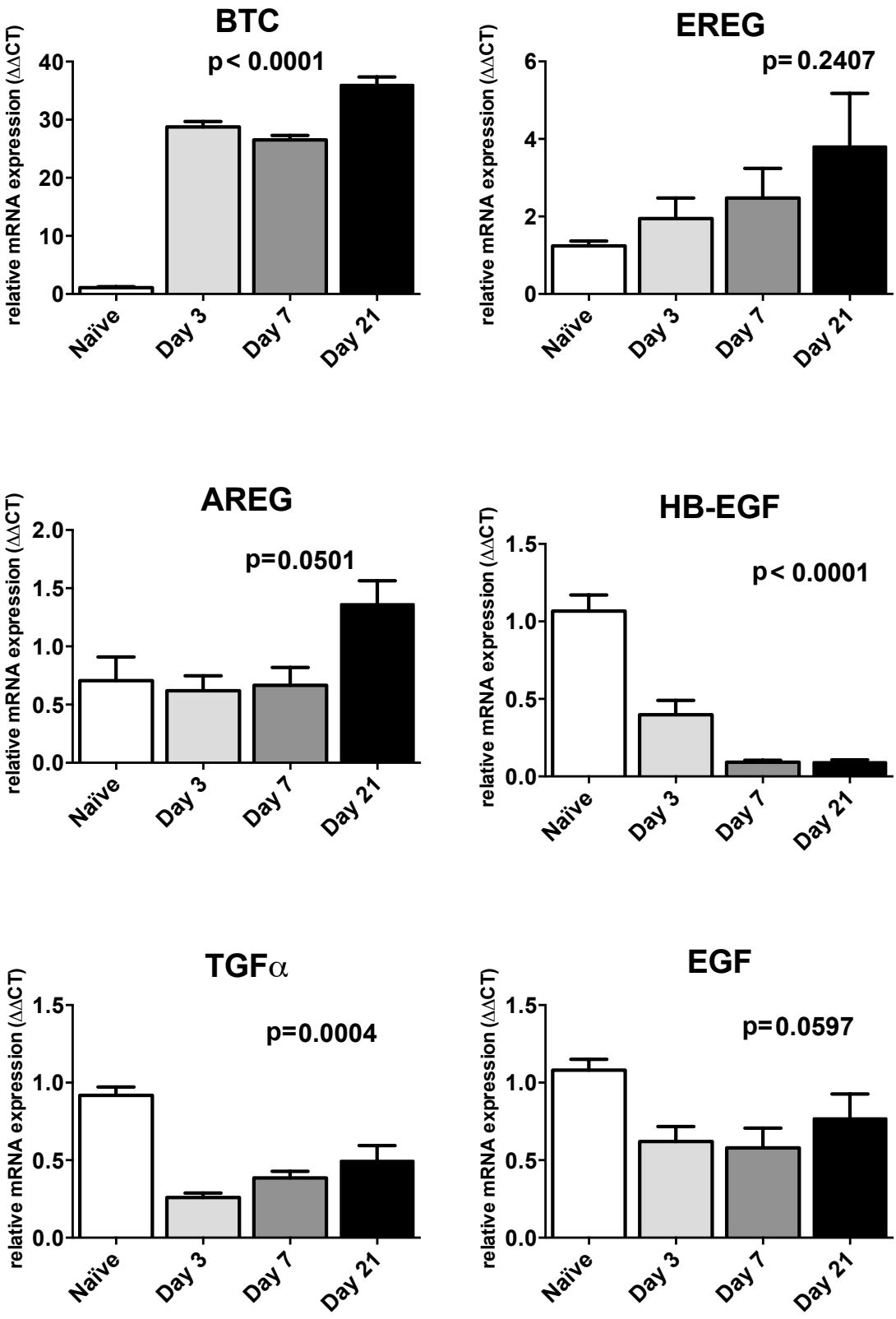
BTC
p< 0.0001
relative mRNA expression (ΔΔCT)
40
30
20
10
0
Naïve
Day 3
Day 7
Day 21
EREG
p= 0.2407
relative mRNA expression (ΔΔCT)
6
4
2
0
Naïve
Day 3
Day 7
Day 21
AREG
p=0.0501
relative mRNA expression (ΔΔCT)
2.0
1.5
1.0
0.5
0.0
Naïve
Day 3
Day 7
Day 21
HB-EGF
p< 0.0001
relative mRNA expression (ΔΔCT)
1.5
1.0
0.5
0.0
Naïve
Day 3
Day 7
Day 21
TGFα
p=0.0004
relative mRNA expression (ΔΔCT)
1.5
1.0
0.5
0.0
Naïve
Day 3
Day 7
Day 21
EGF
p=0.0597
relative mRNA expression (ΔΔCT)
1.5
1.0
0.5
0.0
Naïve
Day 3
Day 7
Day 21

Figure 2.11. EGFR ligands in the sciatic nerve. RT-qPCR data from three different timepoints following nerve injury. Each graph represents fold changes relative to naïve tissue. Data was analysed using the $2^{-\Delta\Delta CT}$ method with an n = 3-4 per group and YWHAZ as a reference gene. Data sets were computed using a one-way ANOVA; p-values indicate significant difference between groups within a given data set. Significance was defined as $p < 0.05$.

The transcript levels of the EGFR ligands were also compared using an inter-run calibrator to compare data of individual experiments. This analysis demonstrated that expression levels for EGFR ligands are regulated very distinctively in injured versus uninjured animals (Figure 2.12.). The genes, which are highly regulated are BTC (at all timepoints) and HB-EGF (at day 3).

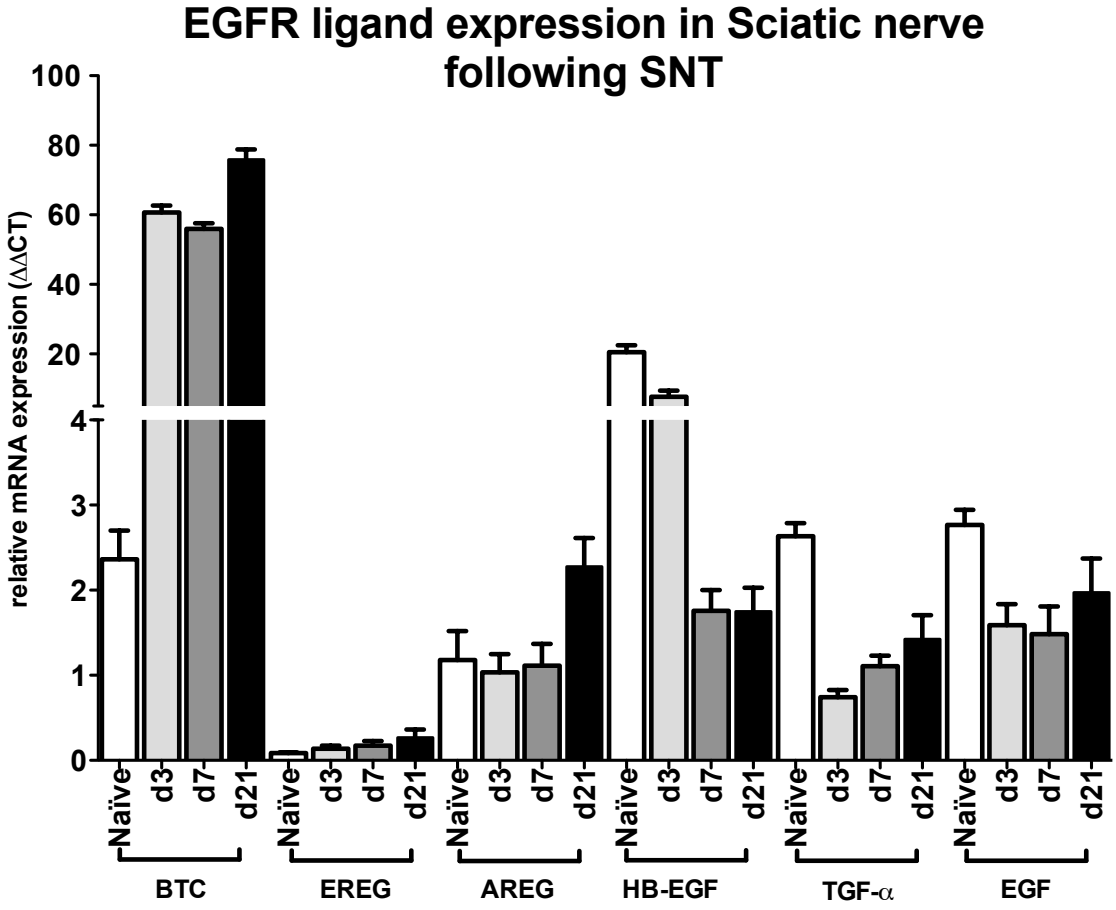

Figure 2.12. Comparing expression of EGFR ligands in sciatic nerve. RT-qPCR data from three timepoints following nerve injury normalised against reference gene YWHAZ. Individual RT-qPCR experiments were combined using an inter-run calibrator to compare real gene changes of individual EGFR ligands (n = 3-4 per group).

2.3.2.3. Expression changes of ErB1 and ErbB4 and ADAM10 and ADAM17 in the sciatic nerve

Receptor expression for growth factors can be altered following nerve injury (Terenghi, 1999). It was shown that receptors of the ErbB receptor family are distinctively regulated, not only in the acute phase of the injury but also during the regenerative processes (Li et al., 1997; Audisio et al., 2008).

EGFR ligands bind to the receptors ErbB1 (EGFR) and ErbB4, resulting in homo- or heterodimerisation. Although ErbB2 and ErbB3 can participate in the formation of dimers, ErbB2 lacks the binding site for the EGF domain and

ErbB3 lacks tyrosine kinase activity and hence were not included into the analysis (see General Introduction).

To characterise the role of ErbB1 (EGFR) and ErbB4 following nerve injury mRNA levels were measured in the sciatic nerve following injury (Figure 2.13.). Expression for both receptors was significantly reduced. In particular, ErbB1 (EGFR) was reduced by 73.6 % at day 3 following injury and remained low until 21 days (at day 7 expression was reduced by 76.84 % and at day 21 expression was reduced by 65.59 %, $p < 0.0001$). The expression of ErbB4 was reduced by 64.65 % and also remained low for the tested period (at day 7 expression was reduced by 63.44 % and at day 21 expression was reduced by 67.76 %, $p < 0.01$).

The enzymes, which cleave and subsequently activate EGFR ligands, can be regulated in close relationship to expression of their ligands (Blobel, 2005). The main activators for EGFR ligands are ADAM10 and ADAM17. They release the soluble ectodomain from the membrane-bound pro-form. The mRNA level for ADAM10, the main activator of BTC and EGF, was significantly reduced over the course of the injury (day 3, 67.7 %; day 7, 51.49 %; day 21, 43.68 %, $p < 0.0001$). In contrast, ADAM17 expression was not markedly altered following nerve injury (Figure 2.13.).

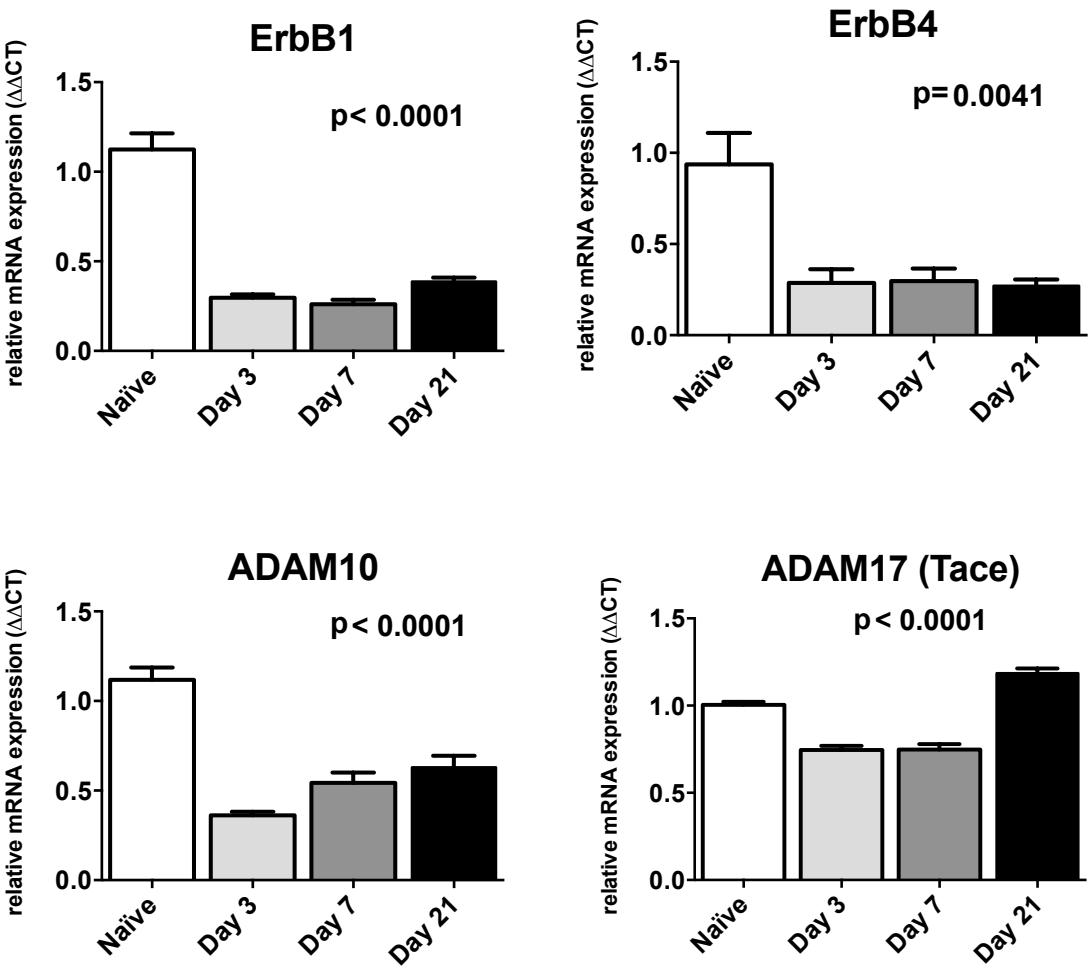

Figure 2.13. ErbB1 (EGFR), ErbB4 and shedding enzymes ADAM10 and ADAM 17 in the sciatic nerve. Each graph represents fold changes of mRNA levels for specific receptors or enzymes relative to naïve tissue (data from three different timepoints). Data were analysed using the $2^{-\Delta\Delta CT}$ method with an n = 3-4 per group and YWHAZ as a reference gene. Data sets were computed using a one-way ANOVA; p-values indicate significant difference between groups within a given data set. Significance was defined as $p < 0.05$.

2.3.2.4. Expression changes of EGFR ligands in the L5 DRG

Following SNT, gene expression changes at the injury site and in the respective DRG of the affected axons were analysed. mRNA from the L5 DRG was isolated at three different timepoints following nerve injury and gene expression for EGFR ligands, the shedding enzymes and the receptors ErbB1 (EGFR) and ErbB4 was quantified.

In the DRG EGFR ligands do not change as prominently as in the sciatic nerve. Out of the 6 ligands tested only BTC showed a significant increase with 6.95-fold upregulation at day 21 after SNL ($n = 3\text{-}4$, $p = 0.013$).

No significant changes were observed in the expression of AREG, TGFα and HB-EGF. EGF transcript also increased at a later timepoint (21 day, FC ≈ 6.17 ± 2.18, $p = 0.061$) but without reaching statistical significance. EREG mRNA was not detected in the DRG (Figure 2.14.).

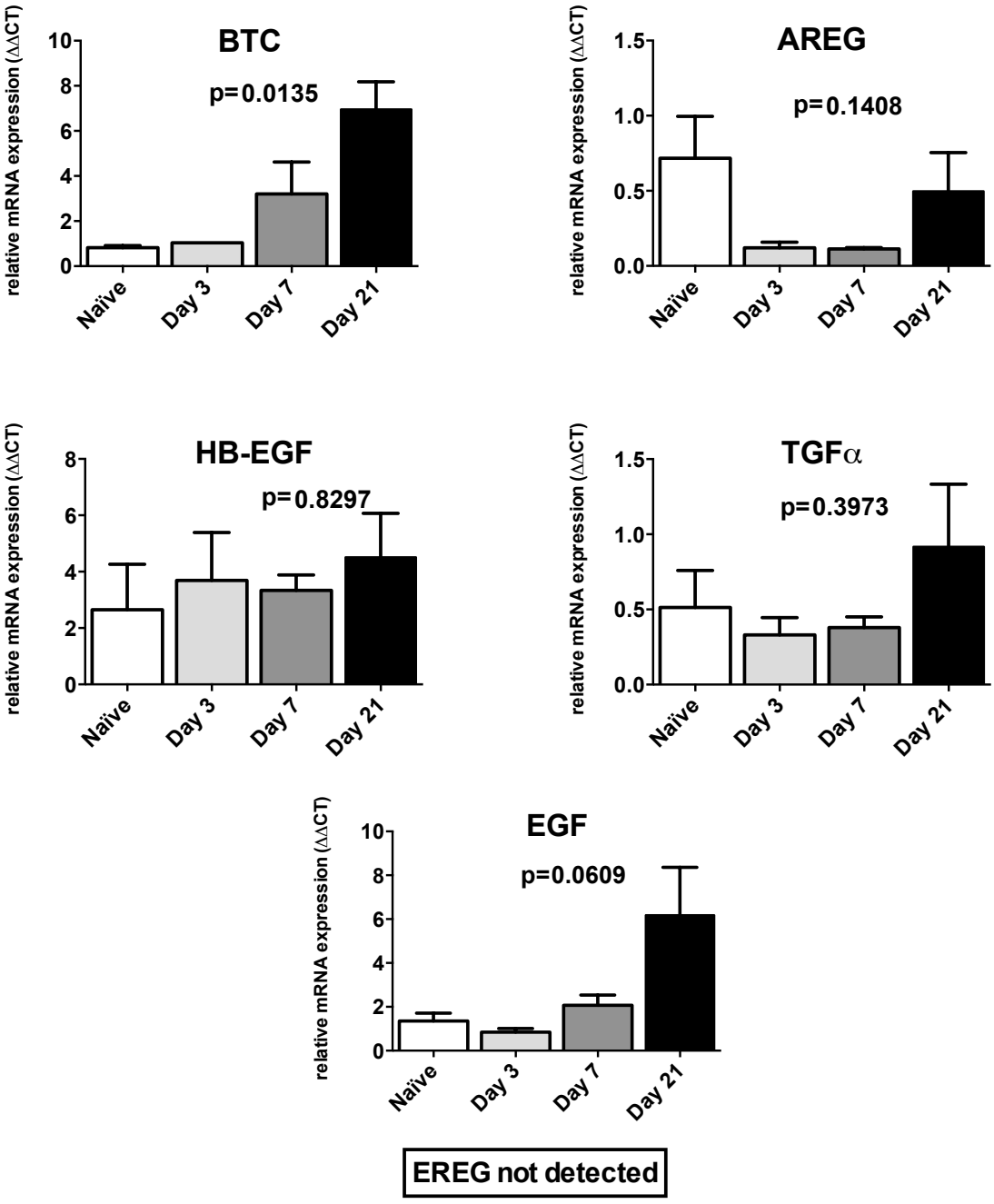

Figure 2.14. EGFR ligands in L5 DRG. Each graph represents fold changes of mRNA levels for specific EGFR ligands relative to naïve tissue (data of three different timepoints). Data was analysed using the $2^{-\Delta\Delta CT}$ method with an n = 3-4 per group and GAPDH as a reference gene. Data sets were computed using a one-way ANOVA; p-values indicate significant difference between groups within a given data set. Significance was defined as $p < 0.05$.

The transcript levels of the EGFR ligands were also compared using an inter-run calibrator to compare data of individual experiments. Similar to the changes in the sciatic nerve expression levels for EGFR ligands are regulated distinctively in injured versus sham animals (Figure 2.15.). EREG could not be detected in the DRG. BTC and HB-EGF expression is higher in comparison to other EGFR ligands but in contrast, not as prominent as in the sciatic nerve.

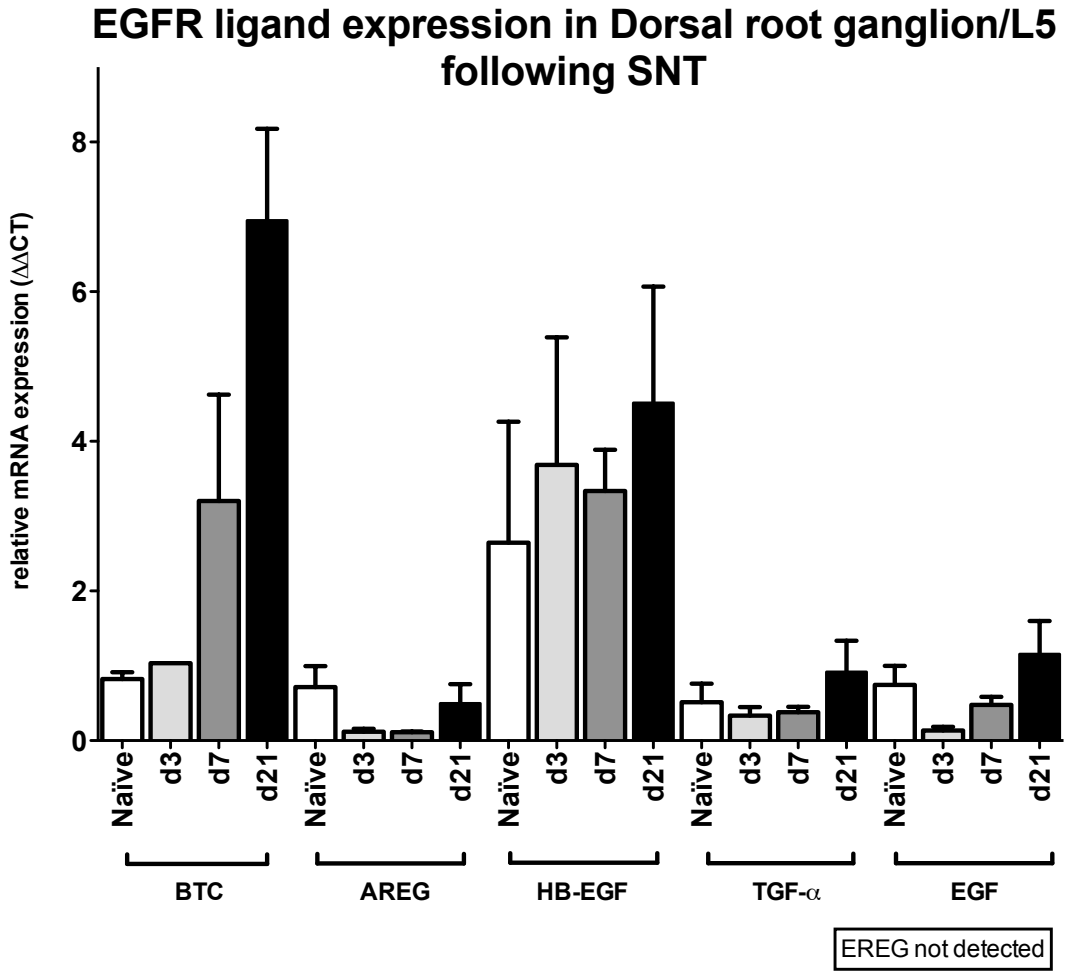

Figure 2.15. Comparing expression of EGFR ligands in L5 DRG. GOIs normalised against reference gene YWHAZ. Individual RT-qPCR experiments were combined using an inter-run calibrator to compare real gene changes of individual EGFR ligands.

2.3.2.5. Expression changes of ErbB1, ErbB4 and ADAM10 and ADAM17 in the L5 DRG

In the DRG changes of receptors and cleaving enzymes were clearly different in comparison to changes in the peripheral nerve. Whereas both receptors for the EGFR ligand family are significantly decreased in the sciatic nerve, only changes in mRNA levels for ErbB1 (EGFR) could be detected in the DRG. Overall, a significant increase is observed at 21 days after the injury (6.15-fold ± 0.04, $p < 0.0001$) (Figure 2.16.). ErbB4 expression does not change upon injury, neither does expression for the activation enzymes ADAM10 and ADAM 17 (Figure 2.16.)

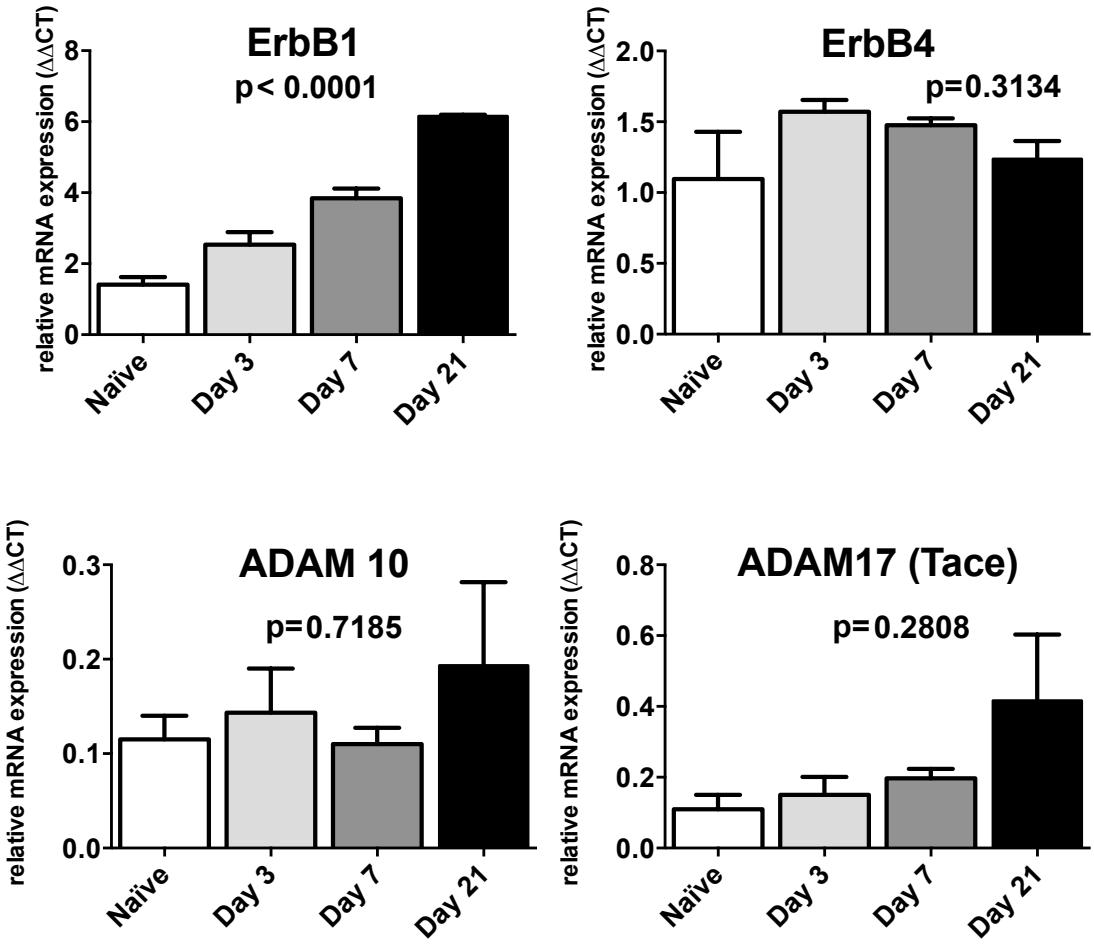

Figure 2.16. ErbB1 (EGFR), ErbB4 and shedding enzymes ADAM10 and ADAM17 in L5 DRG. RT-qPCR data from three different timepoints following nerve injury. Each graph represents fold changes of mRNA levels for specific receptors or enzymes relative to naïve tissue. Data was analysed using the $2^{-\Delta\Delta CT}$ method with an n = 3-4 per group and YWHAZ as a reference gene. Data sets were computed using a one-way ANOVA; p-values indicate significant difference between groups within a given data set. Significance was defined as $p < 0.05$.

2.3.2.6. Expression changes of EGFR ligands in the dorsal horn

After transection of the L5 spinal nerve pathological changes occur, not only in the peripheral nerve and in the DRG, but also in the dorsal horn of the spinal cord. As for the other anatomical locations, little is known about EGFR ligand regulation in the dorsal horn following peripheral nerve injury. Therefore, I set out to examine their mRNA levels in L5 spinal cord at our chosen timepoints after nerve injury.

Individual gene expression profiling reveals that BTC is the only EGFR ligand regulated in the spinal cord. It changes significantly at day 21 (FC ≈ 3.19 ± 0.53, $p < 0.01$) following injury. The regulation of BTC in the dorsal horn, quite distal from the site of injury, highlights the importance of this ligand in the pathological process of nerve injury (Figure 2.17.).

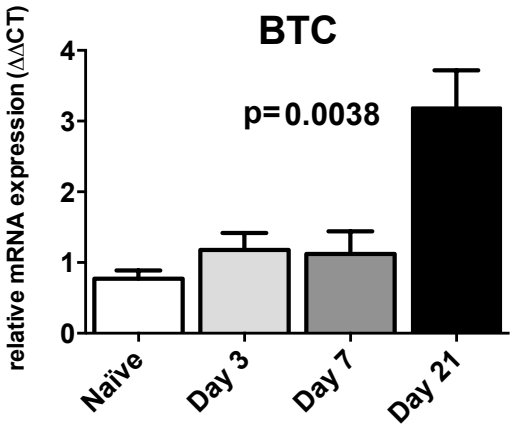
BTC
p=0.0038
relative mRNA expression (ΔΔCT)
0
1
2
3
4
Naïve
Day 3
Day 7
Day 21

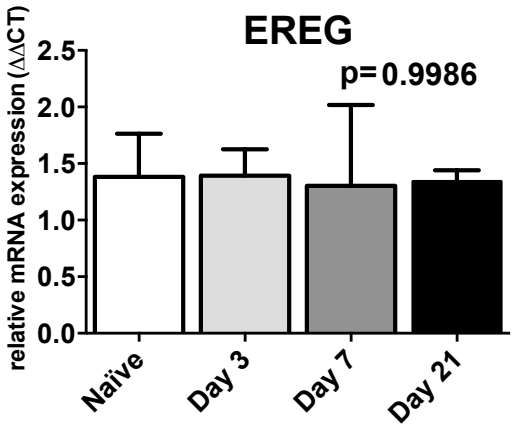
EREG
p=0.9986
relative mRNA expression (ΔΔCT)
0.0
0.5
1.0
1.5
2.0
2.5
Naïve
Day 3
Day 7
Day 21

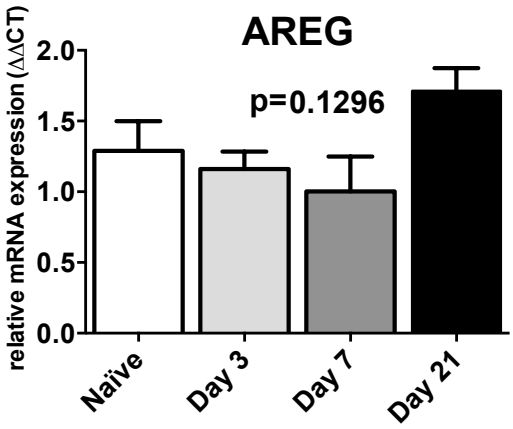
AREG
p=0.1296
relative mRNA expression (ΔΔCT)
0.0
0.5
1.0
1.5
2.0
Naïve
Day 3
Day 7
Day 21

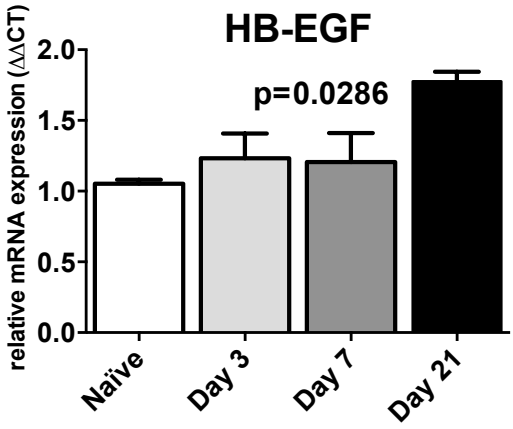
HB-EGF
p=0.0286
relative mRNA expression (ΔΔCT)
0.0
0.5
1.0
1.5
2.0
Naïve
Day 3
Day 7
Day 21

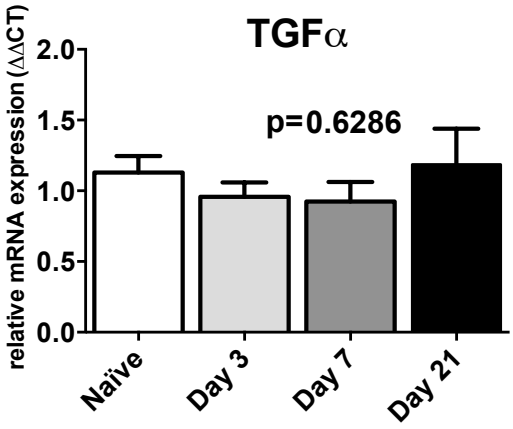
TGFα
p=0.6286
relative mRNA expression (ΔΔCT)
0.0
0.5
1.0
1.5
2.0
Naïve
Day 3
Day 7
Day 21

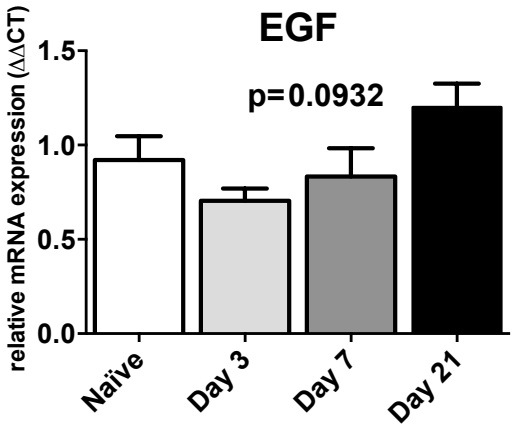
EGF
p=0.0932
relative mRNA expression (ΔΔCT)
0.0
0.5
1.0
1.5
Naïve
Day 3
Day 7
Day 21

Figure 2.17. EGFR ligands in the dorsal horn. Data from the dorsal horn at the level L5 at three different timepoints following nerve injury. Each graph represents fold changes of mRNA levels for specific EGFR ligands relative to naïve tissue. Data was analysed using the $2^{-\Delta\Delta CT}$ method with n = 3-4 per group and GAPDH as a reference gene. Data sets were computed using a one-way ANOVA; p-values indicate significant difference between groups within a given data set. Significance was defined as $p < 0.05$.

The transcript levels of the EGFR ligands were also compared using an inter-run calibrator to compare data from individual experiments. In contrast to changes in the sciatic nerve and the DRG, mRNAs for EGFR ligands are expressed but not regulated. An exception is BTC, which is regulated at 21 days, see above (Figure 2.18.). EREG is the EGFR ligand with the lowest expression in comparison to the other family members.

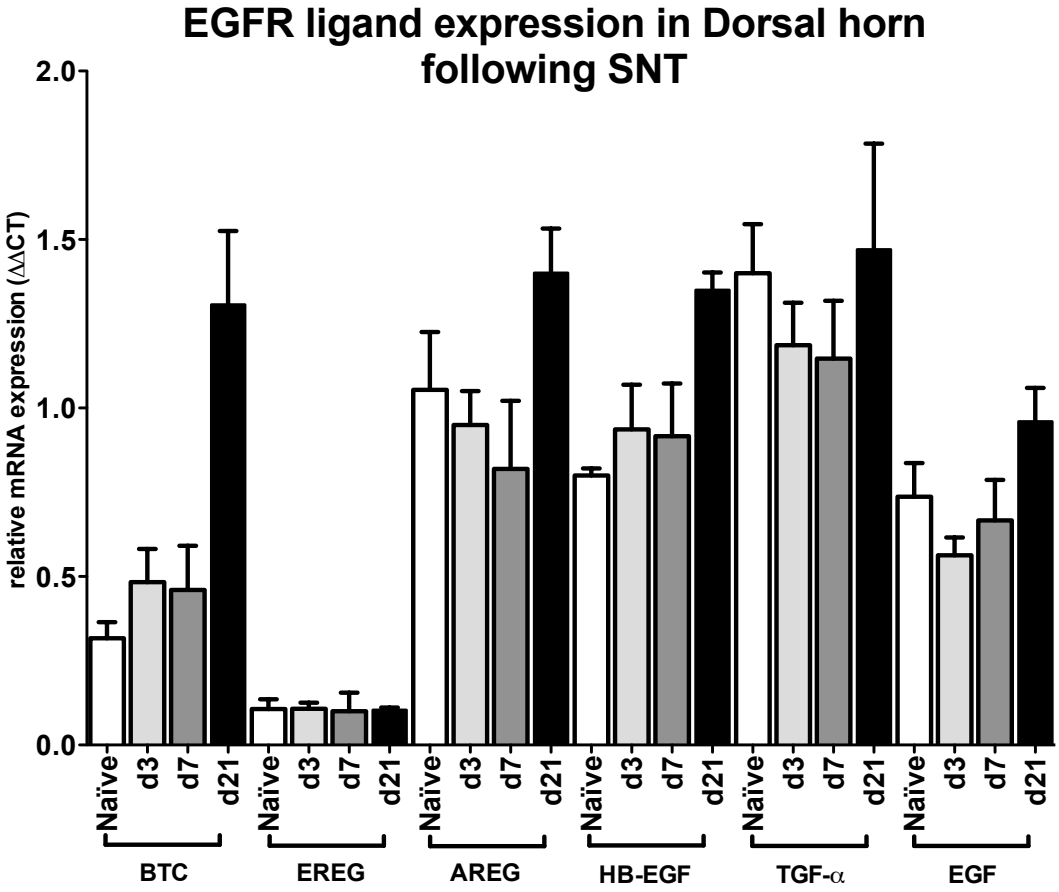

Figure 2.18. Comparing expression of EGFR ligands in in the dorsal horn at the level of L5. Data normalised against reference gene GAPDH. Individual RT-qPCR experiments were combined using an inter-run calibrator to compare real gene changes of individual EGFR ligands.

2.3.2.7. Expression changes of ErbB1, ErbB4 and ADAM10 and ADAM17 in the dorsal horn

Similar to the EGFR ligand expression, mRNA levels of ErbB1, ErbB4, ADAM10 and 17 in the dorsal horn of the spinal cord (L5) remain unchanged after injury. Interestingly, the baseline expression of the receptors and cleaving enzymes is higher than in the other tissues (Figure 2.10.) although no changes occur at the three different timepoints studied (Figure 2.19.).

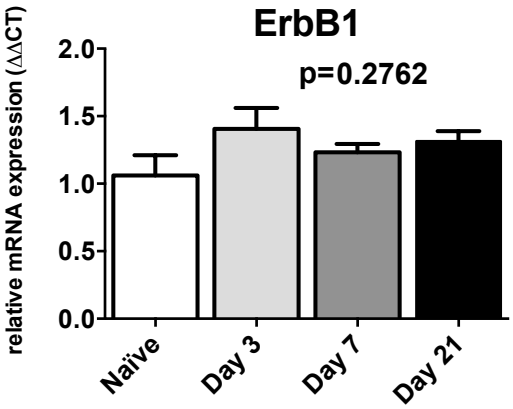
ErbB1
p=0.2762
relative mRNA expression (ΔΔCT)
2.0
1.5
1.0
0.5
0.0
Naïve
Day 3
Day 7
Day 21

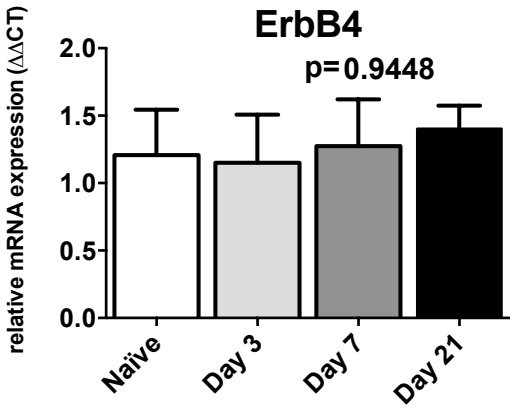
ErbB4
p=0.9448
relative mRNA expression (ΔΔCT)
2.0
1.5
1.0
0.5
0.0
Naïve
Day 3
Day 7
Day 21

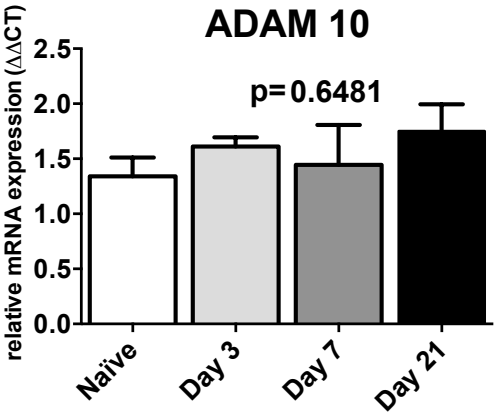
ADAM 10
p=0.6481
relative mRNA expression (ΔΔCT)
2.5
2.0
1.5
1.0
0.5
0.0
Naïve
Day 3
Day 7
Day 21

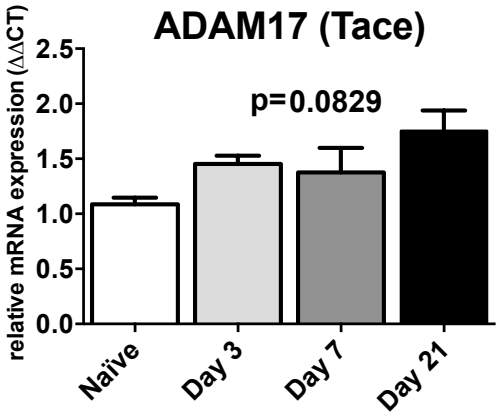
ADAM17 (Tace)
p=0.0829
relative mRNA expression (ΔΔCT)
2.5
2.0
1.5
1.0
0.5
0.0
Naïve
Day 3
Day 7
Day 21

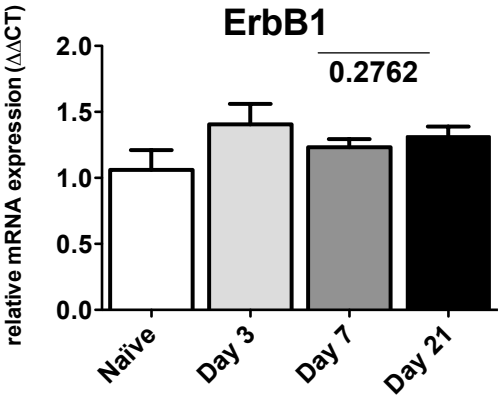
ErbB1
0.2762
relative mRNA expression (ΔΔCT)
2.0
1.5
1.0
0.5
0.0
Naïve
Day 3
Day 7
Day 21

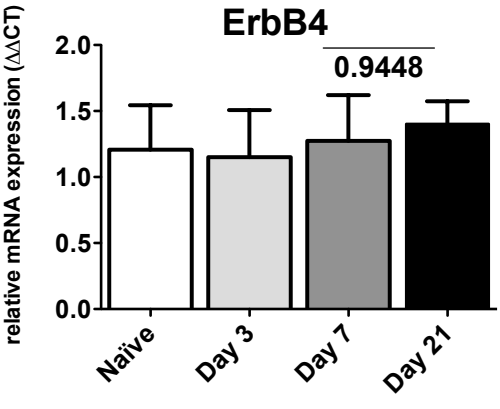
ErbB4
0.9448
relative mRNA expression (ΔΔCT)
2.0
1.5
1.0
0.5
0.0
Naïve
Day 3
Day 7
Day 21

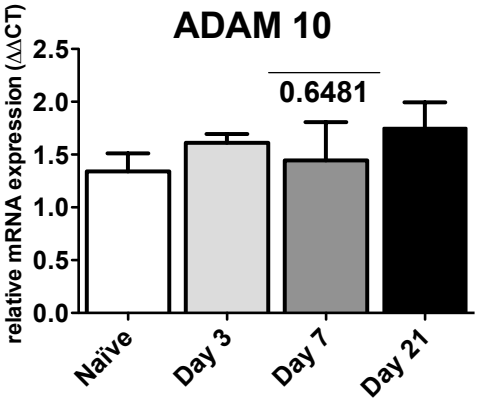
ADAM 10
0.6481
relative mRNA expression (ΔΔCT)
2.5
2.0
1.5
1.0
0.5
0.0
Naïve
Day 3
Day 7
Day 21

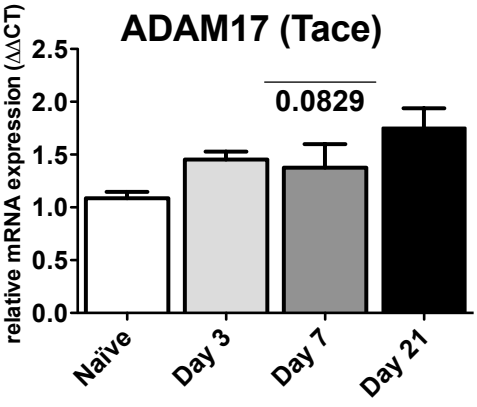
ADAM17 (Tace)
0.0829
relative mRNA expression (ΔΔCT)
2.5
2.0
1.5
1.0
0.5
0.0
Naïve
Day 3
Day 7
Day 21

Figure 2.19. ErbB1 (EGFR), ErbB4 and shedding enzymes ADAM10 and ADAM17 in the dorsal horn at the level L5. Data presented from three different timepoints following nerve injury. Each graph represents fold changes of mRNA for specific receptors or enzymes relative to naïve tissue. Data was analysed using the $2^{-\Delta\Delta CT}$ method with an n = 3-4 per group and YWHAZ as a reference gene. Data sets were computed using a one-way ANOVA; p-values indicate significant difference between groups within a given data set. Significance was defined as $p < 0.05$.

2.4. Discussion

The nervous system responds to peripheral injury in a very specific manner. Changes are orchestrated by different mediators, both at the level of transcription but also by activation of functional protein from “resting” pro-forms or intracellular stores.

Growth factors are important mediators of tissue homeostasis in healthy tissues and contribute to tissue remodeling following injury. They regulate the metabolic activity and proliferation of resident and infiltrating cells as well as promote or inhibit inflammatory activation, control vascularization and the phagocytosis of injury debris.

In this work, I focused on a group of growth factors, the EGFR ligands, which, despite being highly investigated in other fields, have so far received little attention in the field of neuroscience. Given that peripheral nerve injury directly affects the injured nerve as well as the DRG and the dorsal horn, I characterised the expression profile of EGFR ligands, their receptors and activating enzymes, using a model of partial nerve transection (SNT), at different timepoints and in all anatomical levels.

An initial medium-throughput gene expression screen using a microfluidic PCR-based approach revealed that two ligands, BTC and HB-EGF, were highly regulated following nerve injury. BTC was one of the most regulated genes in the sciatic nerve at day 3 post-injury. Cluster analysis revealed that its regulation clustered with a group of pro-inflammatory chemokines. Most of those chemokines regulate macrophage infiltration or T-cell function. CXCL9

and CXCL10 are structurally related chemokines and a great body of literature suggests involvement in chemotaxis of monocytes, induction of apoptosis, regulation of cell growth and angiostatic effects (Liu et al., 2011b). CCL2/MCP-1, a well-studied monocyte chemoattractant (Conductier et al., 2010), is regulated in a similar manner as BTC. Also CXCL1/MIP-2, a neutrophil chemoattractant clusters in this group (Armstrong et al., 2004). Given that BTC was co-expressed with these chemokines it is tempting to speculate that its expression is regulated by similar pro-inflammatory events. Perhaps, immune cell infiltration, which peaks at seven days after injury, is at least in part responsible for the increased expression of BTC. Interestingly, network analysis focused on known and predicted functional similarities and regulation patterns, found no connections between the clustered chemokines/cytokines and BTC. At this point it is important to highlight the limited nature of our preliminary screening, which although it covers an extensive list of injury-related genes is not broad enough to allow a more detailed characterisation of the BTC co-expression cluster. Interestingly, although BTC has not yet been implicated in regulating macrophage chemotaxis, some evidence links the group of EGFR ligands to monocyte/macrophage function (Vlaicu et al., 2013).

Although BTC, HB-EGF and EREG all bind ErbB1 (EGFR) and ErbB4 as their main receptor, expression changes over time suggest specific effects in regulating physiological function. BTC and HB-EGF have a striking differential regulation. Whereas BTC is increased in the injured nerve as shown before (Xian et al., 2001), HB-EGF is downregulated following injury. Whether downregulation in this case is a true reduction of mRNA in a specific cell type or a dilution effect as a result of infiltrating cells, which do not express HB-EGF is difficult to distinguish in these experiments. However, the reduced mRNA levels of HB-EGF in the injured nerve contradict findings by Xian *et al*. based on conventional RT-PCR (Xian et al., 2001). It has to be emphasised that RT-qPCR used for the presented data, offers higher sensitivity than RT-PCR and gel densitometry.

It was previously shown that regulation of EGFR ligands is highly complex and EGFR ligands can regulate their expression in a differential manner. For instance, BTC and HB-EGF show negative correlation in zebrafish and

chicken gametes following EGFR stimulation (Tse and Ge, 2009), (Wang et al., 2007).

Another ligand regulated significantly in the sciatic nerve following nerve injury is TGFα. TGFα has been studied to some extent in the peripheral and central nervous systems. In the central nervous system various functions were suggested from promoting proliferation and differentiation of neuronal and glial precursors to organizing injury-induced astrocytic gliosis (Xian and Zhou, 1999b). In the peripheral nervous system expression has been shown (Vega et al., 1994), but a functional mechanism on nerve regeneration could not be conclusively confirmed. Other research suggests potential functions of TGFα in the olfactory system (Herzog and Otto, 2002) but these findings could be related to the presence of the highly specialised olfactory glial cell, the 'olfactory ensheathing cell' (OEC).

My results show a clear downregulation of TGFα, contradicting the findings of Xian *et al.*, which showed increased expression of TGFα after sciatic nerve ligation and suggested that the growth factor is involved in repair following injury (Xian et al., 2001). Whether my observed downregulation is due to a negative feedback mechanism specific to the lesion model (e.g. partial nerve injury, SNT, versus sciatic nerve ligation) or a reduction of mRNA due to infiltration-related dilution of this specific gene is difficult to address in this study.

The expression for the two main receptors of the EGFR ligands, ErbB1 (EGFR) and ErbB4 is drastically reduced following nerve injury. Both receptors change concomitantly suggesting a potential functional similarity. It has been shown before that EGFR expression changes following nerve injury. Using *in situ* hybridization, Toma *et al.* demonstrated that SCs and fibroblasts express the EGFR, which is upregulated in both cell types following injury on the mRNA level, peaking at 72 hours (Toma et al., 1992). In contrast to that, Atanasoski *et al.* did not find ErbB1 (EGFR) and ErbB4 protein expression, neither in SCs, nor in sciatic nerves following sciatic nerve transection (Atanasoski et al., 2006). My results show a significant downregulation beginning at day 3 after injury. I measured mRNA levels in the whole nerve and was unable to distinguish what cell type is responsible for expression changes. It can only be hypothesised that infiltrating or proliferating cells, which do not express the EGFR dilute mRNA changes. Another interpretation might be that

acute gene upregulation, which is followed by translation into protein and incorporation of the receptor into the membrane ceases once the protein is assembled. Similar mechanisms of a feedback inhibition of mRNA expression by means of high protein levels have been proposed (Stapleton et al., 2012). With potentially very high levels of BTC, the main ligand for ErbB1 (EGFR) and ErbB4 in the peripheral nerve, a feedback mechanism may be proposed, conveying that the striking downregulation of the receptor expression could correlate with high levels of functional ligand. Similar mechanisms have been suggested for NGF and its receptor (Lindsay et al., 1990).

Sciatic nerve injury results in distinct expression changes in the DRG, consisting of neurons connected to the injured nerve. Dysregulation of EGFR ligands are not as striking as in the injured sciatic nerve. Again, BTC is one of the most regulated factors with a peak expression increase three weeks after the injury. One speculative role of BTC might be regulation of the vasculature in the DRG. It has been shown that the DRG is highly vascularised in comparison to other tissues (Jimenez-Andrade et al., 2008). Evidence for increased vascularisation in the DRG following injury is rare. Lubos *et al.* found an increase of RECA-1-positive capillaries within the DRG after nerve injury, suggesting intra-ganglionic angiogenesis (Kubicek et al., 2010). In the injured nerve it could be shown that endothelial cells respond with hypertrophy and proliferation (Podhajsky and Myers, 1993),(Wagner and Myers, 1996). Therefore BTC, a known stimulating factor for endothelial proliferation and angiogenesis (Kim et al., 2003) could have an effect on angiogenesis occurring after injury.

Another potential mechanism is based on the neurogenic properties, which have been described for BTC (Gomez-Gaviro et al., 2012) (see Chapter 3.1.1. for more general biology of BTC). In adult mammals neurogenesis is probably confined to two regions: the subventricular zone and the subgranular zone of the hippocampal dentate gyrus. Challenging this well accepted dogma, Namakaa *et al*. suggests neuronal precursors in the DRG, which can respond to injury with proliferation or differentiation (Namaka et al., 2001). Whether adult neurogenesis can occur outside the hippocampus or the subventricular zone and whether BTC plays a role in this system remains to be elucidated.

Other ligands showed no significant changes in gene expression, although EGF gene expression increases at 21 days post-injury suggesting a potential late-onset effect of this factor. EREG could not be detected in the DRG, which might be due to the sensitivity of the assay or to very low expression in only a subset of cells, e.g. a subset of DRG neurons (e.g. peptidergic or non-peptidergic neurons)

The mRNA levels for the ErbB receptors change differently in the DRG compared to the sciatic nerve. Whereas both receptors are consistently downregulated in the periphery, they are both significantly upregulated in the DRG. The EGFR is expressed in DRG neurons in humans (Werner et al., 1988) and in rodents (Xian and Zhou, 1999a). Sensory neurons could be the cells responsible for the expression change of the gene for the EGFR (Pearson and Carroll, 2004). Interestingly, ErbB4 is not regulated in the DRG suggesting a more prominent function for ErbB1 (EGFR).

Cleaving enzymes are not regulated in the DRG following the SNT model. ADAM10 is not only responsible for activating EGFR ligand pro-forms but is also a major cleaving enzyme for fractalkine/CX3CR1 ligand. It has been shown that nerve injury induces cleavage of fractalkine in the spinal nerve ligation model (Zhuang et al., 2007) in the dorsal horn. In the DRG, ADAM10 expression did not change following peripheral nerve injury. ADAM10 and ADAM17 have distinct functions in activating EGFR ligands. ADAM10 is critical for activating the pro-form of BTC and EGF whereas ADAM17 is activating EREG, AREG, HB-EGF and TGFα (Sahin et al., 2004; Hinkle et al., 2004).

Expression of ADAM17, also known as TNF-α-converting enzyme (TACE), is not regulated following SNT, which is surprising considering marked increase of TNF-α levels in the DRG following nerve injury (Wagner and Myers, 1996).

In the dorsal horn the only EGFR ligand, which changes expression following nerve injury, is BTC. Although the injury is spatially distant to the spinal cord, information of peripheral nerve damage is promoted via the DRG into the central nervous system either via electrical signals or via retrograde protein transport (see Chapter 1, General Introduction). Due to sparse knowledge about EGFR ligands in neuroscience functional implications of a late-onset upregulation of BTC can only be speculative. However, based on the data

shown in this work it is unlikely that BTC has an acute effect on the cells in the dorsal horn. As a growth factor, BTC could influence neuronal plasticity in the spinal cord and therefore could have an impact on nociceptive processing. The dorsal horn is composed of second order neurons of the sensory circuit, interneurons regulating the sensory input to higher centres of the circuit, glia cells and immune cells (Todd, 2010). In neuropathic pain conditions neuronal plasticity following peripheral nerve injury can be modulated by growth factors (Woolf and Salter, 2000). It has been described that EGF has the ability to directly modulate neuronal excitability via inhibiting potassium currents (Jia et al., 2007). ErbB4, one of the two receptors for BTC have been described to modulate synapse development (Krivosheya et al., 2008) and increase the intrinsic excitability of central interneurons (Li et al., 2012). Whether BTC is one of the growth factors responsible for excitability changes remains to be elucidated.

Also BTC could play a role in inflammatory processes in the spinal cord. Well studied are effects of growth factors on non-neuronal cell function following nerve injury. BDNF has been described to modulate microglial function (Coull et al., 2005) and a huge body of literature is describing NGF and other neurotrophins as key factors in the inflammatory response following peripheral nerve injury (Pezet and McMahon, 2006). In our group, Calvo *et al*. investigated NRG, which also binds receptors of the ErbB family of, namely ErbB3 and ErbB4, which directly modulates microglia function following peripheral nerve injury (Calvo et al., 2011; Calvo et al., 2010). Whether BTC can regulate the immune response after injury also remains to be clarified.

Another potential mechanism is based on stem cell activating properties of BTC, some of which have been described in the neural stem cell niche (Gomez-Gaviro et al., 2012). After SCI new cells, most likely astrocytes and oligodendrocytes proliferate into mature cells from residing precursors (Yang et al., 2006a). Neuronal death occurs in the dorsal horn after partial peripheral nerve injury (Moore et al., 2002). With a late-onset upregulation of BTC a regenerative mechanism is plausible but it is unclear if BTC might be a potential candidate.

Given that BTC expression is highly upregulated following nerve injury, I tested its role as a potential pain mediator, which is described in the following chapter.

CHAPTER 3

Behavioural evaluation of EGFR inhibition and BTC treatment in rats

3.1. Introduction

3.1.1. BTC, a protein with diverse functions in biological processes

As shown in Chapter 2, EGFR ligands and the ErbB receptor family are distinctively regulated in the sciatic nerve, DRG and dorsal horn following nerve injury. BTC is of particular interest because it is consistently upregulated in all three tissues.

BTC was discovered by Shing *et al.* in conditioned medium of a pancreatic tumour cell line (Shing et al., 1993). It is a 32kDa protein (Figure 3.1.), initially described to be a mitogen for retinal epithelial cells and vascular smooth muscle cells (Shing et al., 1993). BTC belongs to the group of EGFR ligands as it binds to ErbB1 (EGFR) and ErbB4 with its EGF like domain (Dunbar and Goddard, 2000). An ErbB2/ErbB3 heterodimer has also been proposed as a receptor for BTC (Pinkas-Kramarski et al., 1998). Binding of BTC to one of its receptors is related to the activation of intracellular signalling (Figure 1.5., Chapter 1). This aspect is further discussed in Chapter 4.

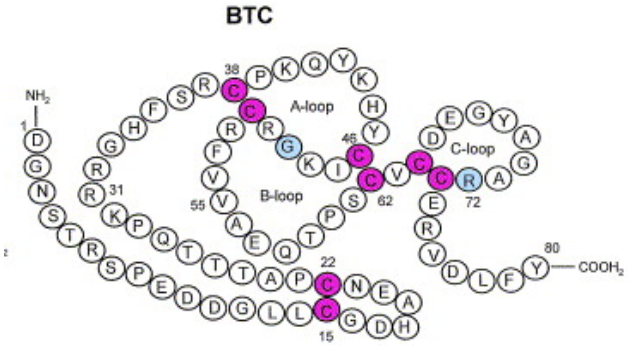

Figure 3.1. Structure of BTC. (Adapted from Dunbar and Goddard (Dunbar and Goddard, 2000) Schematic of the secondary structure of cleaved BTC.

BTC is produced as a membrane-bound precursor molecule, which is post-translationally activated by the metalloprotease Adam10 (Sahin et al., 2004). The released, activated fragment can signal in a paracrine and autocrine manner, but also juxtacrine signalling has been described (Tada et al., 1999).

BTC, like other EGFR ligands, has been extensively studied in different types of cancer. It has been shown that it is a mitogen in human pancreatic cancer (Kawaguchi et al., 2000). It is expressed in hepatocellular carcinoma cells (Moon et al., 2006), endometrial adenocarcinoma (Srinivasan et al., 1999) and was found to be expressed at low levels in breast cancer cells (McIntyre et al., 2010).

BTC stimulates the proliferation of various cell types. It promotes β-cell proliferation in the pancreas via activation of ErbB1 (EGFR) and ErbB2 receptors (Oh et al., 2011) and can differentiate embryonic pancreatic cells into insulin-producing β-cells (Thowfeequ et al., 2007).

Other functions have been described in the reproductive organs. Park *et al.* showed that BTC stimulates oocyte maturation (Park et al., 2004). Hence, it is a candidate protein for the modulation of fertility (Gratao et al., 2008).

The protein has been identified as a major growth factor in bovine milk, which raises the possibility of supporting development of the neonatal gastrointestinal tract (Dunbar and Goddard, 2000). This was supported by findings that BTC can stimulate the growth of mucosa cells in the gastrointestinal tract after long-term intravenous administration in rats (Howarth et al., 2003).

Furthermore, it has been described as a potent factor in keratinocyte proliferation (Schneider et al., 2008) and endothelial cell proliferation. It can promote angiogenesis in healthy skin (Kim et al., 2003) and following injury (Schneider et al., 2008). In vascular smooth muscle cells, BTC promotes growth and is chemotactic; it has been suggested that it might be involved in vascular remodeling (Mifune et al., 2004) following injury. BTC has been found in atherosclerotic lesions of the human aorta, most likely expressed by macrophages (Tamura et al., 2001).

Overexpression of BTC in mice has diverse effects. Postnatal mortality is high, due to increased risk of pulmonary haemorrhage and disproportionate bone growth. The latter is induced by the modulation of osteoblast precursors and gross alteration in osteogenic properties (Genetos et al., 2010). Moreover, complex eye pathology with abnormally shaped retinal layers has been described (Schneider et al., 2005). Overexpression increases insulin secretion and consequently improves glucose tolerance (Dahlhoff et al., 2009).

BTC knockout animals are viable and fertile and display no morphological differences to wildtype animals (Jackson et al., 2003).

Evidence for BTC expression and function in the peripheral and central nervous system is sparse. In a recent study, Gomez-Gaviro *et al.* showed that BTC promotes cell proliferation of neuronal progenitor cells in the stem cell niche (Gomez-Gaviro et al., 2012) proposing an interesting effect in adult neurogenesis. Byer *et al.* demonstrated that SCs express BTC and showed a concentration-dependent effect on SC migration *in vitro* (Byer et al., 2013).

These published findings and the striking regulation of BTC in the nerve, in the DRG and dorsal horn following nerve injury prompted me to investigate the role of BTC as a potential pain mediator. In order to do this, I used two well established behavioural tests, namely electronic von Frey and Hargreaves (Hargreaves et al., 1988) to investigate mechanical and thermal sensitivity after intraplantar and intrathecal injection of BTC in rats.

3.1.2. EGFRs as a novel target for nociceptive modulation; EGFR inhibition

As discussed before, BTC directly binds to the ErbB receptors, ErbB1 (EGFR) and ErbB4. Following binding, homo- or heterodimers are formed inducing receptor phosphorylation via trans-activation of receptor subunits in the cytoplasmic tail and initiation of intracellular signalling cascades.

The EGFR is expressed in the peripheral nerve, mainly in SCs (Cohen et al., 1992) in human dorsal root ganglia (Huerta et al., 1996) and in many neuronal cell types of the human central nervous system (Werner et al., 1988) (Table 4).

Nervous System		Normal Human Skin
Hippocampus	*Dorsal root ganglia*	*Thick, thin epidermis*
+ + Pyramidal cells	+ + Neurons	+ + S. basalis
− Granule cells	+ + Satellite cells	+ S. spinosum
	+ Schwann cells	+ / − S. granulosum
		− S. corneum
Parahippocampal gyrus	*Spinal cord*	*Pilosebaceous glands*
+ + Pyramidal cells	+ + Anterior horn cells	+ + Outer root sheath
	+ Dorsal nucleus of Clarke	+ + Sebocytes, basal
		+ + Arrector pilorum
Cerebellum	*Glial cells*	*Eccrine glands*
+ + Purkinje cells	− Oligodendrocytes	+ / − Eccrine sweat glands
+ Molecular layer	− Astrocytes	+ + Eccrine sweat ducts
Frontal cortex	*Ependymal cells*	*Apocrine glands*
+ Pyramidal cells, layers 3 and 5	+ + Choroidal	+ Epithelial cells
− Small neurons	+ + Extrachoroidal	+ + Myoepithelial cells
Thalamus		*Blood vessels*
+ + Internal capsule neurons		− Endothelial cells
+ Hypothalamus		+ + Vascular smooth muscle
Blood vessels		*Other*
+ / − Endothelial cells		+ / − Fibroblasts
+ + Vascular smooth muscle		

[4] Key: + +, strongly positive staining for immunoreactive EGF-R; +, positive; + / −, variably positive; −, no staining. S, stratum.

Table 4: expression of the EGFR in the human nervous system. (Adapted from (Werner et al., 1988)

Ligands binding the EGFR have been shown to affect various molecules in nociceptive pathways. EGFR can be trans-activated by cannabinoid receptor 1 (CB1) and transient receptor potential vanilloid (TRPV1) agonists (Yang et al., 2010). Both receptors are typical modulators of peripheral nociceptive processes (Agarwal et al., 2007).

Andres *et al*. described that EGFR activation leads to inhibition of prostaglandin E2 (PGE2) induced mechanical hyperalgesia (Andres et al., 2010). In contrast, it was shown that following SCI, reduced EGFR activation leads to a decrease in PGE2 release, speculating inhibition of the EGFR can affect pain attenuation after SCI (Xia and Zhu, 2011). Erschbamer *et al*. could show that following SCI, inhibition of the EGFR with PD168393, a tyrosine kinase inhibitor, not only improves functional recovery but also attenuates injury induced thermal and mechanical hypersensitivity (Erschbamer et al., 2007).

3.1.3. EGFR inhibition as a potential treatment for neuropathic pain

The EGFR family has been intensively investigated in human cancer development. Especially ErbB1 (EGFR) and ErbB2 are altered in many epithelial tumours (Hynes and Lane, 2005).

Two types of EGFR inhibitors have been developed: first, monoclonal antibodies directed against the extracellular domain of EGFR or ErbB2 and second, intracellular small-molecule tyrosine kinase inhibitors (TKIs), which compete with adenosine triphosphate (ATP) at the tyrosine kinase domain of the receptor (Hynes and Lane, 2005).

A recent case report indicated that treatment with Cetuximab, a chimeric IgG1 monoclonal antibody that binds to EGFR and inhibits its phosphorylation, considerably reduced pain in a 68 year old male patient with metastatic rectal cancer (from 8 to 2 on a ten point numeric rating scale) making the accompanying opioid treatment redundant (Kersten and Cameron, 2012).

A follow-up case series demonstrated that extracellular and intracellular EGFR inhibition can relieve therapy-resistant neuropathic pain (Kersten et al., 2013). In 4 out of 5 patients with severe neuropathic pain of different aetiologies, namely inflammatory polyneuropathy, complex regional pain syndrome type 1 (CRPS 1), radiculopathy after failed back surgery, malignant invasion of the sacral plexus by bladder cancer and phantom limb pain, EGFR inhibition with four different drugs resulted in effective pain relief. In some patients, intravenous drug administration led to pain relief within hours.

Given this potential involvement of the EGFR in pain processing, I tested the effect of EGFR inhibition in two animal models of neuropathic pain (L5 SNT model (Kim and Chung, 1992) and inflammatory pain (Formalin model (Coderre et al., 1993)). I have chosen the clinically approved drug Gefitinib.

Gefitinib (ZD1839/Iressa®), a small molecule tyrosine kinase inhibitor, was approved by the FDA in 2003 (Cohen et al., 2003) as a third line monotherapy for non-small cell lung cancer (NSCLC). In 2005 the FDA limited the use of Gefitinib as it was lacking a survival advantage in non-Asian NSCLC patients (Yarden and Pines, 2012). Clinical trials as a treatment for head and neck squamous cell carcinoma (HNSCC), gastrointestinal cancer and breast cancer are still ongoing (Hynes and Lane, 2005).

Inhibiting the tyrosine kinase domain of the EGFR was first described in the 1980s. Erbstatin, a small molecule inhibitor derived from gram-positive bacteria (Umezawa et al., 1986) is the predecessor for TKIs, which all compete with ATP on the intracellular tyrosine kinase domain.

Gefitinib is orally active and used in humans at a daily dose of 250mg with a low adverse event profile. The molecular structure is simplified in Figure 3.2. Gefitinib inhibits EGFR-induced MAPK activity in human cancer cell lines (Albanell et al., 2001) and delays cell-cycle progression in a HNSCC cell ine (Di Gennaro et al., 2003). It inhibits the Akt/NF-κB pathway in PC-9 cells, a NSCLC cell line (Culy and Faulds, 2002). In mice, treatment of NSCLC xenografts with 50 to 200mg/kg/day, Gefitinib produced 70-80% growth inhibition (Sirotnak et al., 2000); 40mg/kg/day of subcutaneous injection of Gefitinib increased apoptosis in a PC-9 xenograft grown in mice (Culy and Faulds, 2002).

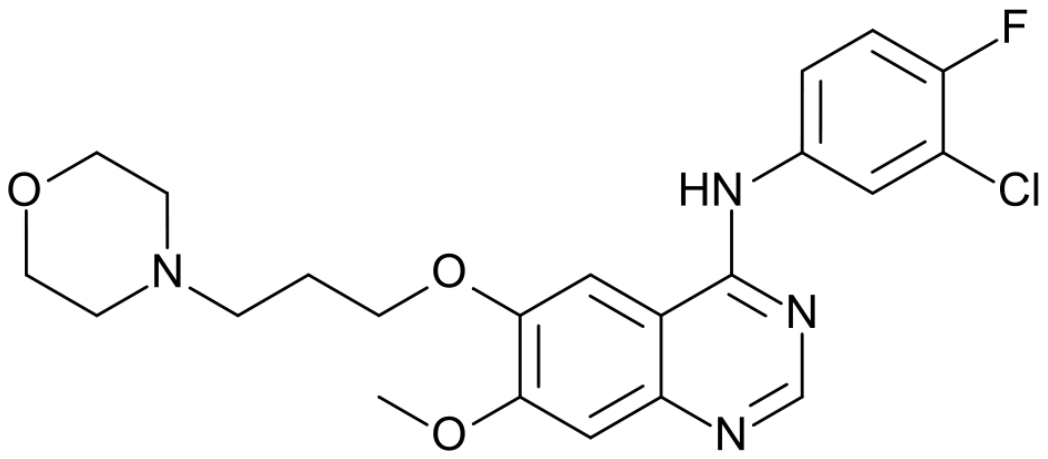

Figure 3.2. Structure of Gefitinib. (Retrieved from http://commons.wiki.org)

Mc Killop *et al*. described the pharmacokinetics in rats, which differ depending on the route of administration. The highest plasma concentration (C_{max}) following a single oral dose of 20mg/kg is reached after 2 hours and then declines with a half life of ≈ 10 hours with an oral availability of 40 – 60%. Following intravenous administration (20mg/kg) the C_{max} is 2 minutes with an elimination half-life of ≈ 14 hours. It has to be noted that bioavailability in female rats is greater than in male rats in both oral and intraveneous administration. (McKillop et al., 2004). The maximum tolerated oral dose in mice was determined as 150mg/kg without significant toxicity (Culy and Faulds, 2002).

Importantly, a recent case report showed that Gefitinib treatment could alleviate long-standing neuropathic pain in a 53 year old female CPRS1 patient. However, the treatment had to be discontinued due to elevated liver transaminases, which lead to reoccurrence of the symptoms within 48 hours (Kersten et al., 2013).

Here, I had two main objectives: first, to investigate whether BTC is a potential pain mediator and second, to examine the role of EGFR inhibition in pain sensation. The potential peripheral role of BTC in nociception was tested by subcutaneous administration into the hindpaw. To examine another mechanism of action, I injected BTC intrathecally into the cerebrospinal fluid (L4-L5 space). As described above, some evidence links EGFR inhibition to attenuation of pain. Consequently, I tested Gefitinib, a clinically approved TKI, in two standard pain assays, the acute inflammatory Formalin test and L5 spinal nerve transection (SNT) surgery as a model for neuropathic pain.

3.2. Methods

3.2.1. Animals

Experiments were performed using male Wistar rats (~250g, Harlan). Animals were housed under standard conditions with a 12 hour light/dark cycle and food and water was available *ad libitum*. All experiments were done in accordance to the United Kingdom Home Office regulations. For each experiment 8 animals were used per group.

3.2.2. Intraplantar injections

Rats were restrained and carefully injected under sterile conditions with either 2µg of recombinant mouse BTC (R&D systems) dissolved in 50µl sterile Phosphate buffered saline (PBS) (Sigma), or vehicle into the plantar surface of the right paw. A high dose of growth factor was chosen to observe activation of nociceptors because toxic effects of BTC after local application are unlikely. As a positive control another group of animals received 500ng of recombinant mouse NGF (R&D) in 50µl sterile PBS (Sigma). It has been described that NGF changes thermal sensitivity thresholds as a peripheral pain mediator (Andreev et al., 1995). The experimenter was blinded to the injected solution. For intraplantar injections 8 animals where used per group which were tested in both mechanical and thermal sensitivity thresholds.

3.2.3. Intrathecal injections

Rats were anaesthetised with a volatile anaesthetic, isoflurane/oxygen mix. Fur was removed over the spinal column at the level of L6, cleaned with 70% ethanol and placed on a sterile area. Once the intervertebral space was determined a micro-syringe (300µl) with a 29-gauge needle (Terumo) was used to inject recombinant mouse BTC (0.1 - 10µg/ml (5-500ng), EREG (50ng) and EGF (0.1 - 10µg/ml (5-500ng) (all from R&D) in PBS or vehicle. A successful injection was defined by an obvious tail flick. The experimenter was blinded to the injected solution. For intrathecal injections 8 animals where used per group which were tested in both mechanical and thermal sensitivity thresholds.

3.2.4. Oral gavaging

Rats were restrained and carefully gavaged (Turner et al., 2012) with a dose of 50mg/kg or 100mg/kg Gefitinib, emulsified in 5% methylcellulose to give a total volume of 1ml. Animals were treated daily at the same time. Following the first administration, animals were housed separately depending on their treatment. No differences have been observed in body weight or food consumption between the groups. The experimenter was blinded to the administered solution.

3.2.5. Preparation of the drugs

Recombinant proteins, BTC, EGF, EREG and NGF (all R&D) were dissolved in sterile PBS and stored in a stock concentration of 100µg/ml at -80°C.

For Gefitinib (LC Laboratories) treatment, two routes of administration were tested. Intraperitoneal (i.p.) injection of 10mg/kg Gefitinib in 20% DMSO was performed for 3 consecutive days every 24 hours to reach a baseline plasma concentration according to previously published work. Animals were Formalin tested 3 hours after the third injection. For oral administration (p.o.), Gefitinib was emulsified in 5 % methylcellulose and animals were treated with the same regime as for the i.p. injections (Figure 3.7.).

3.2.6. Formalin Test

A rat was placed in a transparent Plexiglas cube (30 x 30 x 30cm) and before each experiment habituated for 15 minutes. Then 50µl of a 5% formalin (37% formaldehyde in H_2O) solution was injected using a micro-syringe into the plantar region of the right hindpaw. The innate behavioural response, which is licking, flinching and biting of the affected paw was surveyed in real time. The animal was observed for 50 minutes following injection and time spent flinching and licking was measured. For analysis, the first phase was defined as 0-15 minutes post injection and the second phase as 20 to 50 minutes post injection. For the Formalin test 8 animals where used per group which were tested in both mechanical and thermal sensitivity thresholds.

3.2.7. Surgery

Partial nerve injury was generated by transection of the L5 spinal nerve slightly modified from a method introduced by Kim and Chung (1992). Adult rats were anaesthetised with a combination of medetomidine (Domitor®) (0.25mg/kg) and ketamine (Vetalar®) (60mg/kg) given via i.p. injection. A paramedian incision next to the spinal column was made and ⅓ of the L6 transverse process was removed, exposing the spinal nerves. Once identified, the L5 spinal nerve was tightly ligated using 6-0 silk. Then the L5 spinal nerve was transected distally to the ligation. Next, first the muscle layer and then the skin was sutured with vicryl 3-0. Surgery was performed under sterile conditions. Following the procedure and at least 45 minutes after anaesthetic induction, animals were given a subcutaneous injection of atipamezole hydrochloride (Antisedan®) (1ml/kg) to reverse anaesthesia.

3.2.8. Mechanical hypersensitivity

To assess mechanical sensitivity, I used an automatic Dynamic Plantar Aesthesiometer (electronic von Frey) (UgoBasile) with a 0.5mm filament, which exerts increasing strength (50g/20 seconds). Force at the time of the paw withdrawal reflex was measured four times (4 technical repeats) per paw at each timepoint. Following SNT surgery, mechanical thresholds were tested in ipsi- and contralateral hindpaws in both Vehicle-treated and Gefitinib-treated animals to verify the surgery and to investigate the effect of Gefitinib treatment on the unaffected nerve.

3.2.9. Thermal hypersensitivity

To assess thermal sensitivity I used Hargreaves Method (Hargreaves et al., 1988). Animals were habituated on a glass plate, where increase of temperature using an infrared source led to temperature-dependent paw withdrawal. Time was measured automatically four times (4 technical repeats) per paw by Hargreaves Plantar Test Instrument (UgoBasile). For cold sensitivity animals were placed on metal grit and 1ml of Acetone was squirted onto the plantar surface of the right hindpaw. As an index for sensitivity

changes the time spent licking or flinching of the treated paw was measured for four times (4 technical repeats) per paw at each timepoint.

3.2.10. Protein extraction and protein immunoblotting

Exactly 40 minutes after intrathecal BTC injection, rats were terminally anaesthetised using 0.8ml of sodium pentobarbital and then transcardially perfused with physiological saline (0.9%) and L5 and L6 dorsal root ganglia were dissected in PBS. Proteins were extracted in 0.2% SDS buffer, supplemented with 10μM EDTA and proteinase inhibitor cocktail (Sigma) for 2 hours at RT, samples were ultra-sonicated in a U400 Ultrasonicator (Ultrawave) at 50-60Hz for 30 minutes at RT. Finally, protein samples were electrophoresed and immunoblotted as described in detail in Chapter 4.2.4. For protein extractions 4 animals where used per group which were tested in both mechanical and thermal sensitivity thresholds.

3.2.11. Statistical analysis

All behavioural experiments were done blinded. Two-way repeated measures analysis of variance (ANOVA) was used to analyse data of more than two groups, tested at different timepoints. Where necessary, Bonferroni's post-doc analysis was performed to characterise individual differences. Area under the curve (AUC) analysis was compared using an unpaired T-test. A p-value < 0.05 was defined as a significant result. Data was computed using Graph Pad PRISM. For graphic data presentation, all charts represent arithmetic mean ± SEM.

3.3. Results

3.3.1. BTC as a peripheral pain mediator

Intraplantar injection of BTC: First, I determined whether BTC changes sensitivity when injected into peripheral healthy tissue. I performed plantar subcutaneous injection into the hindpaw of rats to characterise early and long-term effects measuring mechanical sensitivity (electronic von Frey) and thermal sensitivity (Hargreaves). NGF (500ng) was used as a positive control. It has been previously shown that NGF rapidly induces thermal hyperalgesia after subcutaneous injection (Andreev et al., 1995).

Figure 3.3. shows that 2µg/50µl BTC had no effect on the thermal sensitivity ($n = 8$ animals, $p = 0.3$) of the plantar region of the rat hindpaw. In contrast, NGF (500ng) produced a statistically significant ($n = 8$ animals, $p = 0.046$) hyperalgesia beginning at 30 minutes post injection, which lasted up to 6 hours post-injury (Figure 3.3. A) and confirmed findings by Andreev *et al*. (1995). The contralateral paw showed no differences in sensitivity levels (Figure 3.3. B).

No changes were observed after BTC ($n = 8$ animals, $p = 0.95$) or NGF injection ($n = 8$ animals, $p = 0.15$) when testing for mechanical sensitivity (Figure 3.3. C, D)

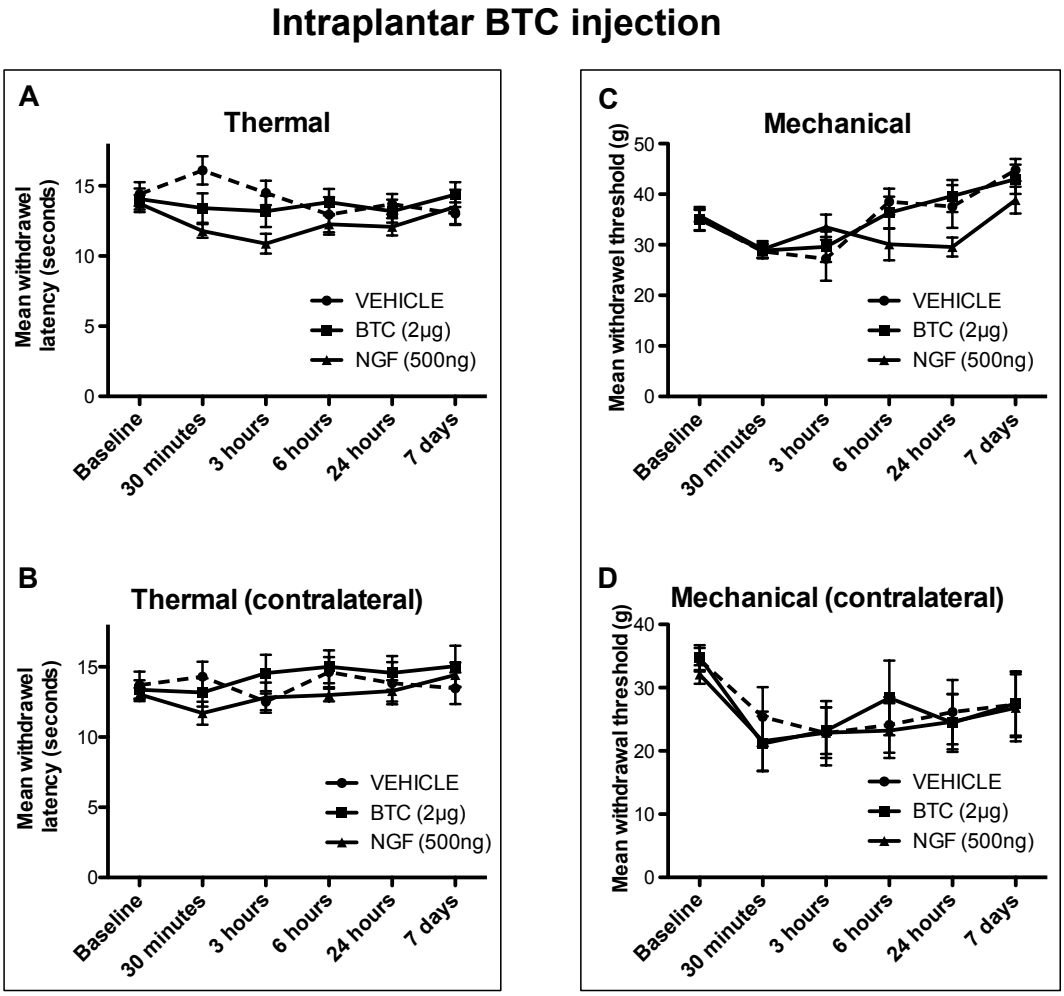

Figure 3.3. BTC (2µg) and NGF (500ng) s.c. injection. Injection into the plantar area of the hindpaw. Sterile saline was used as a control (dotted line). Mean withdrawal latencies in seconds of the ipsilateral **A)** and contralateral **B)** and mean withdrawal thresholds (ipsilateral **C)**, contralateral **D)** paw after thermal and mechanical stimulation at different timepoints following injection (n=8 animals per group).

3.3.2. Intrathecal injection of BTC

I then tested whether BTC can alter sensitivity levels when administered intrathecally. To do this, BTC was injected intrathecally into the L4/L5 space. Successful delivery of BTC (10µl/ml, 200ng per injection) into the CSF was demonstrated by the activation of the ERK MAPK, a typical EGFR/ErbB4 driven intracellular pathway. Indeed, L5 DRGs taken from BTC treated animals 40 minutes after injection, showed clear phosphorylation of ERK in comparison to PBS injected controls ($n = 4$, $p = 0.0076$) (Figure 3.4. A, B).

Although intrathecal BTC injection was able to activate ERK *in vivo*, no alteration in thermal ($n = 8$ animals, $p = 0.18$) or mechanical ($n = 8$, $p = 0.88$) sensitivity was observed with three different concentrations (0.1, 1, 10µg/ml) (Figure 3.4. C, D).

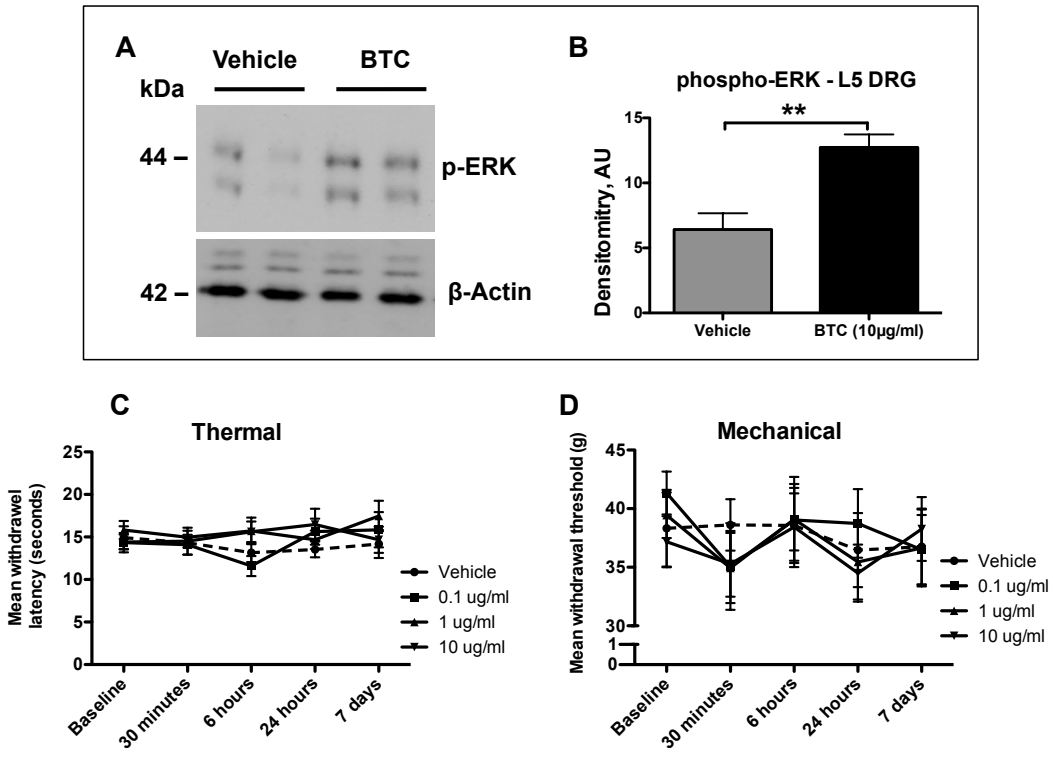

Figure 3.4. Intrathecal injection of BTC and MAPK activation *in vivo.* Intrathecal injection of BTC leads to clear phosphorylation of ERK in L5. **A)** Western Blot of vehicle versus BTC treated samples. **B)** Quantification of protein immunoblot (n = 4, p = 0.0076) comparing vehicle with BTC treated DRG. **C)** and **D)** sensitivity levels following intrathecal BTC administration with three different concentrations (n=8 animals per group).

3.3.3. Intrathecal injection of EGF and EREG

To investigate whether activation of the EGFR by other ligands can induce behavioural responses I tested the effect of EREG and EGF. EGF binds solely to the EGFR and could have distinct effects in comparison to other ligands. For example, it activates different ErbB dimerisation patterns always including ErbB1. Intrathecal injection of three concentrations of EGF (0.1, 1 and 10µg/ml) had no effect on thermal (n = 8 animals, p = 0.59) or mechanical (n = 8 animals, p = 0.68) sensitivity (Figure 3.5. A, B)

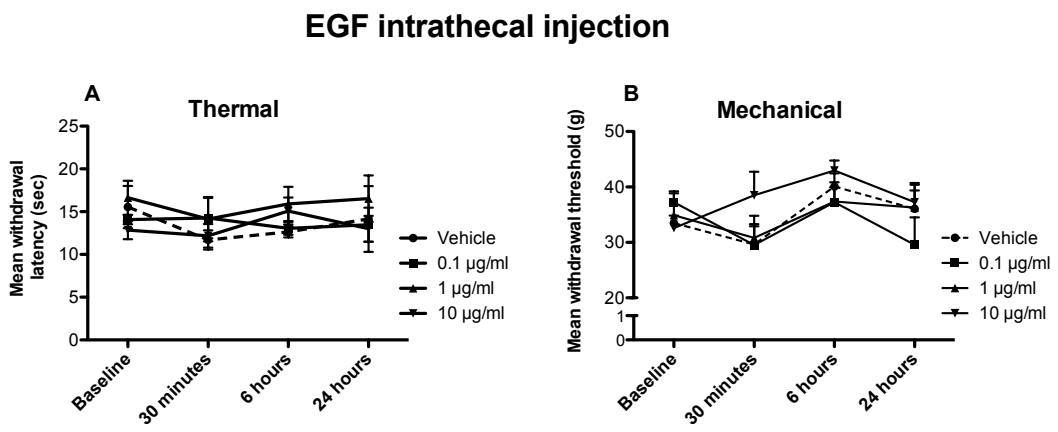

Figure 3.5. EGF intrathecal injection. Thermal **A)** and mechanical **B)** sensitivity levels following intrathecal EGF administration with three different concentrations (n=8 animals per group).

Although EREG is not expressed following nerve injury (see Chapter 2) it has some functional relationship to BTC since it also binds EGFR and ErbB4 as its main target receptors. Preliminary examination of EREG is shown in Figure 3.6. EREG (50ng) administration had no effect 24 hours following intrathecal injection (thermal $p = 0.79$, mechanical $p = 0.56$, $n = 8$ animals per group) (Figure 3.6. A, B).

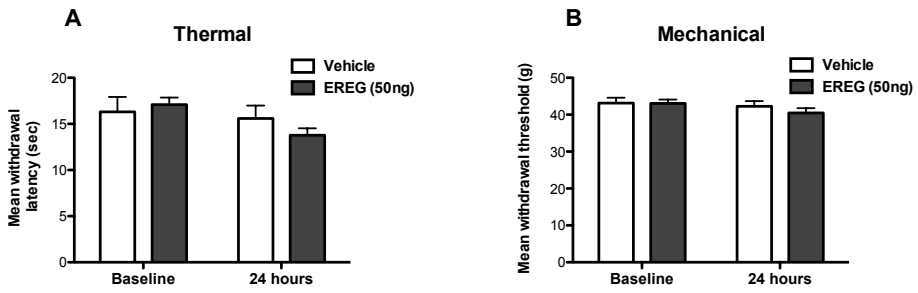

Figure 3.6. EREG intrathecal injection. Thermal **A)** and mechanical **B)** sensitivity levels following intrathecal EREG administration after 24 hours with 50ng EREG (n=8 animals per group).

3.3.4. Inhibition of the EGFR: physiological and pathological effects

The effect of EGFR inhibition on nociception was examined using Gefitinib. Mechanical and thermal sensitivity were tested following systemic drug delivery either into the peritoneum or orally. Due to its low solubility, Gefitinib was dissolved in 20% DMSO for peritoneal injections. For oral delivery, 5% methylcellulose was used as an emulsifier. The experimental design is presented in Figure 3.7. A. Due to an elimination half life of 10 hours (McKillop et al., 2004) animals were re-dosed 24 hours after drug administration.

No differences in thermal or mechanical sensitivity levels could be observed following i.p. Gefitinib administration (n = 8 animals per group, thermal, p = 0.23, mechanical, p = 0.6) (Figure 3.8. A, B).

Given differences in bioavailability following different application methods, Gefitinib, as an orally active drug (bioavailability in male rats 77–88% at doses > 20mg/kg (McKillop et al., 2004)), was also tested following oral gavage at concentrations of 50mg/kg and 100mg/kg in 5% methylcellulose.

Experimental design is presented in Figure 3.7. B. Sensitivity baselines were tested at 30 minutes, 3, 6 and 24 hours following oral administration of Gefitinib. No alteration of thermal (p = 0.48) or mechanical (p = 0.91) sensitivity levels could be observed (n = 8 per group) (Figure 3.8. C, D).

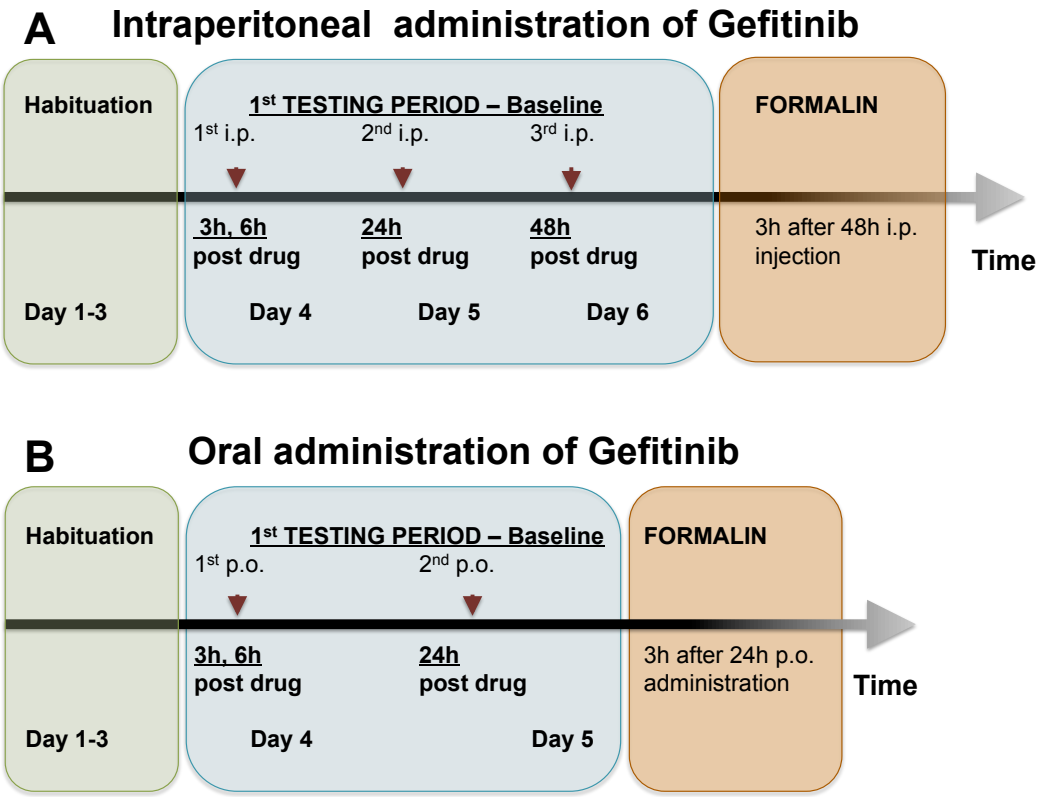

Figure 3.7. Experimental design, EGFR inhibition – sensitivity levels and Formalin. Schematic representation of the experimental design used to study the effect of Gefitinib in pain sensitivity. **A)** For intraperitoneal delivery, an initial phase of 3 days habituation, which included baseline measurements for thermal and mechanical sensitivity was followed by intraperitoneal injection of the drug (▼) Sensitivity levels were measured at different timepoints. The drug was re-dosed every 24 hours for 2 days. 3 hours after the last dose the Formalin test was conducted. **B)** For oral administration, experimental design slightly changed. Following the habituation phase sensitivity levels were measured at different timepoints after drug delivery. The drug was re-dosed 24 hours after the first dose. 3 hours later the Formalin test was conducted.

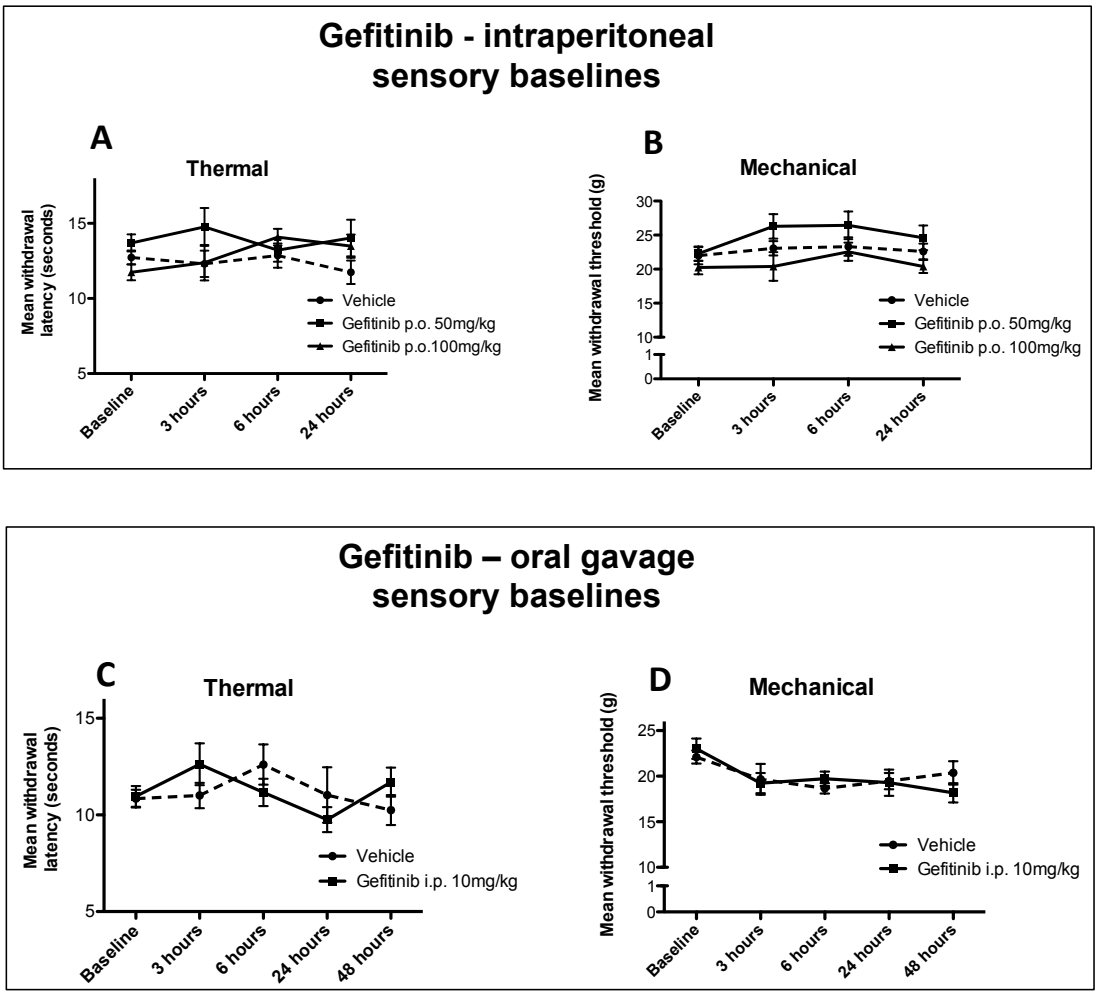

Figure 3.8. EGFR inhibition – baseline sensitivity levels. Baseline sensitivity is not affected by i.p. or p.o. Gefitinib treatment. **A)** and **B)** show thermal (Hargreaves) and mechanical (electronic von Frey) sensitivity levels at different timepoints following intraperitoneal Gefitinib treatment. **C)** and **D)** show no changes in baseline sensitivity following p.o. Gefitinib emulsified in 5% methylcellulose (n=8 animals per group).

3.3.4.1. Inflammatory pain model – Formalin test

Given that inhibition of the EGFR is a clinically approved cancer treatment and has been shown to be effective in human pain conditions, I set up experiments to determine whether EGFR inhibition alters the behavioural response in the Formalin test.

3.3.4.1.1. Intraperitoneal administration of Gefitinib

As a model for acute pain, the Formalin test was used to examine the effect of EGFR inhibition. Following the i.p. dosing regime, which consisted of 3 doses of Gefitinib every 24 hours (Figure 3.7. A), animals were injected 5% formalin into the right hindpaw three hours after the last drug application and time spent on licking, flinching or biting was measured as an index for the nociceptive response. No differences could be observed in the Gefitinib treated group compared to vehicle treated animals ($p = 0.9$, $n = 8$ animals per group) (Figure 3.9. A). AUC analysis showed no difference of drug treatment compared to vehicle treatment in the first ($p = 0.96$) or second phase ($p = 0.78$) of the Formalin test (Figure 3.9. B).

3.3.4.1.2. Oral administration of Gefitinib

Given that Gefitinib is used as an orally active drug, I also administered Gefitinib in two different concentrations 50mg/kg and 100mg/kg via oral gavaging. After administering Formalin in the drug treated and vehicle treated animals, no significant response could be observed at the tested timepoints for the two tested Gefitinib concentrations. (50mg/kg $p = 0.38$, 100mg/kg $p = 0.73$, $n = 8$ animals per group) (Figure 3.9. C, D). No differenced could be observed in the first or in the second phase of the Formalin test after performing an AUC analysis (50mg/kg, 1^{st} phase $p = 0.93$, 2^{nd} phase $p = 0.13$; 100mg/kg, 1^{st} phase $p = 0.68$, 2^{nd} phase $p = 0.53$) (Figure 3.9. E, F).

Intraperitorial administration

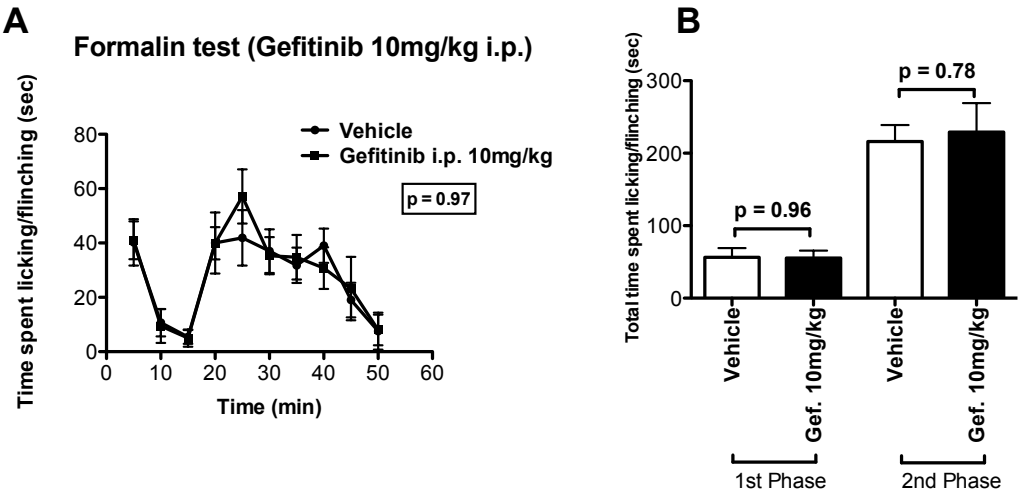

Oral administration

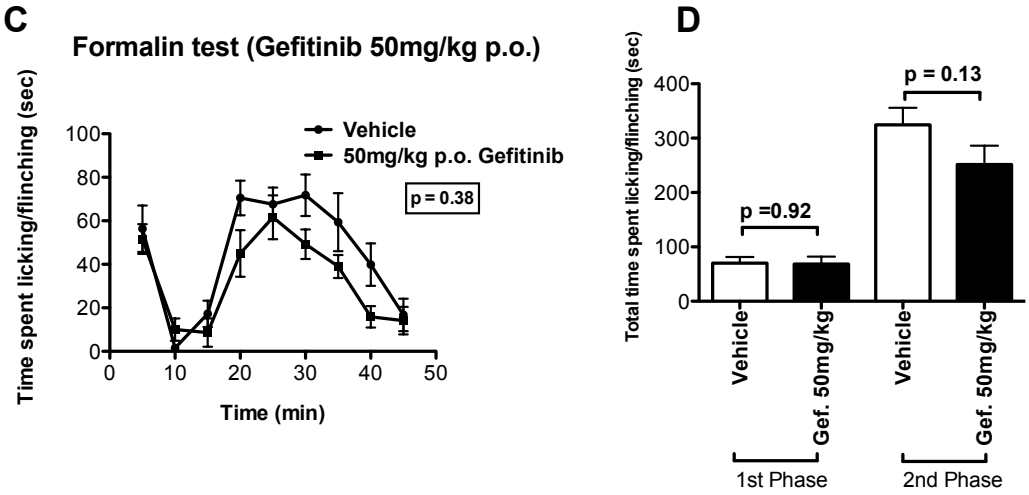

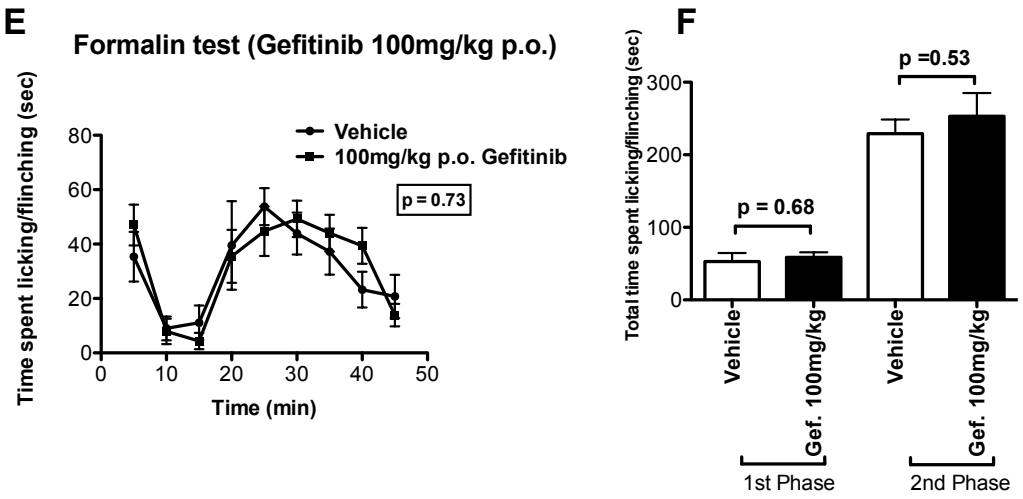

Figure 3.9. EGFR inhibition – inflammatory pain. Rats were injected with Formalin following systemic treatment with Gefitinib. **A)** Intraperitoneal drug delivery: Typical two-phase response of Formalin test without any differences in the treatment compared to the vehicle treated group. Index for nociceptive behaviour was the time spent flicking/licking/biting of the affected paw in seconds. **B)** AUC analysis of the first and second phase of the Formalin test. No significant differences between drug treated and vehicle treated group. **C)** and **E)** Oral drug delivery: no alteration in 50mg/kg and 100mg/kg Gefitinib administered via oral gavage in formalin induced behaviour. **D)** and **F)** AUC analysis of 1^{st} and 2^{nd} phase of this data did not reveal any change of behaviour in the treated compared to the untreated group (n=8 animals per group).

3.3.4.2. Neuropathic pain – L5 SNT model

Inhibiting the EGFR in humans suffering severe neuropathic pain conditions had a striking effect in a recent case series (Kersten et al., 2013). The EGFR has never been evaluated in neuropathic pain animal models. Therefore, EGFR inhibition was evaluated in rats, which had SNT surgery and developed cold and mechanically hypersensitivity. Experimental design is shown in (Figure 3.10.).

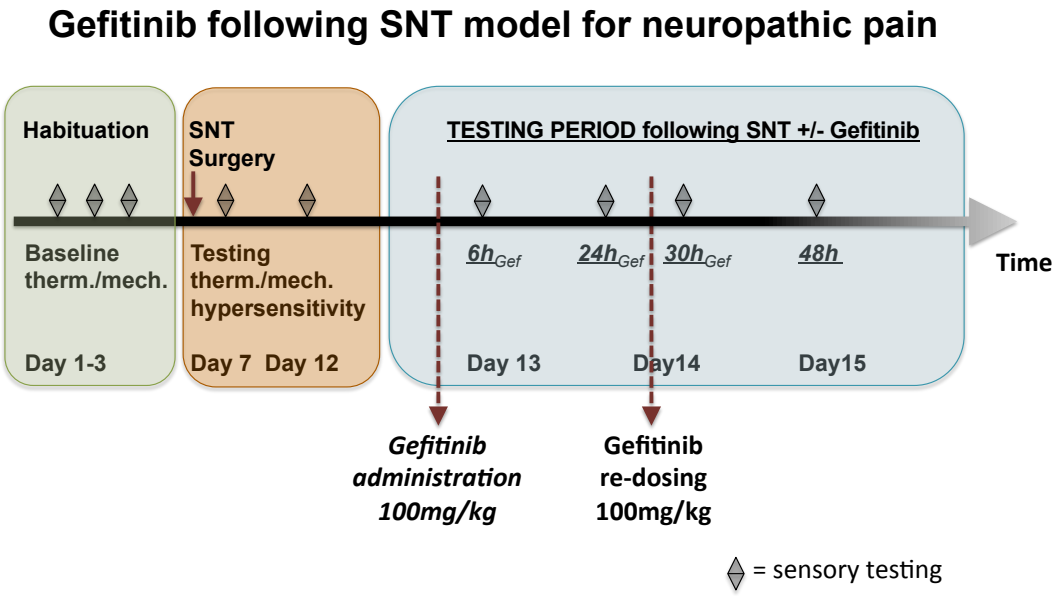

Figure 3.10. Experimental design – Gefitinib following SNT. An initial phase of 3 days habituation, which included baseline measurements for cold and mechanical sensitivity was followed by L5 SNT surgery. Subsequent hypersensitivity levels were confirmed at day 7 and day 12 following surgery. Gefitinib treatment (p.o.) was started at day 13 following SNT and at 6, 24, 30, and 48 hours sensitivity levels were measured. The drug was re-dosed once after data for the 24 hour timepoint was acquired.

In neuropathic animals, which show clear cold and mechanical hypersensitivity at 7 and 12 days following L5 SNT, 100mg/kg Gefitinib were administered via oral gavage. Sensitivity levels following cold stimulation with Acetone and electronic von Frey stimulation were measured. No differences in cold sensitivity (Acetone test) ($p = 0.97$, $n = 8$ animals) or mechanical sensitivity (electronic von Frey) ($p = 0.84$, $n = 8$ animals) could be observed (Figure 3.11. A, B). To test whether Gefitinib treatment affects mechanical thresholds on the contralateral nerve to the injury, sensitivity levels in both hindpaws were tested in all animals (Vehicle and Gefitinib treated group). As expected, after the transection surgery of L5, neither sensitivity levels changed in the uninjured nerve nor Gefitinib treatment had an affect on mechanical sensitivity on the contralateral side of the injury ($p = 0.64$, $n =$ animals) (Figure 3.11. C).

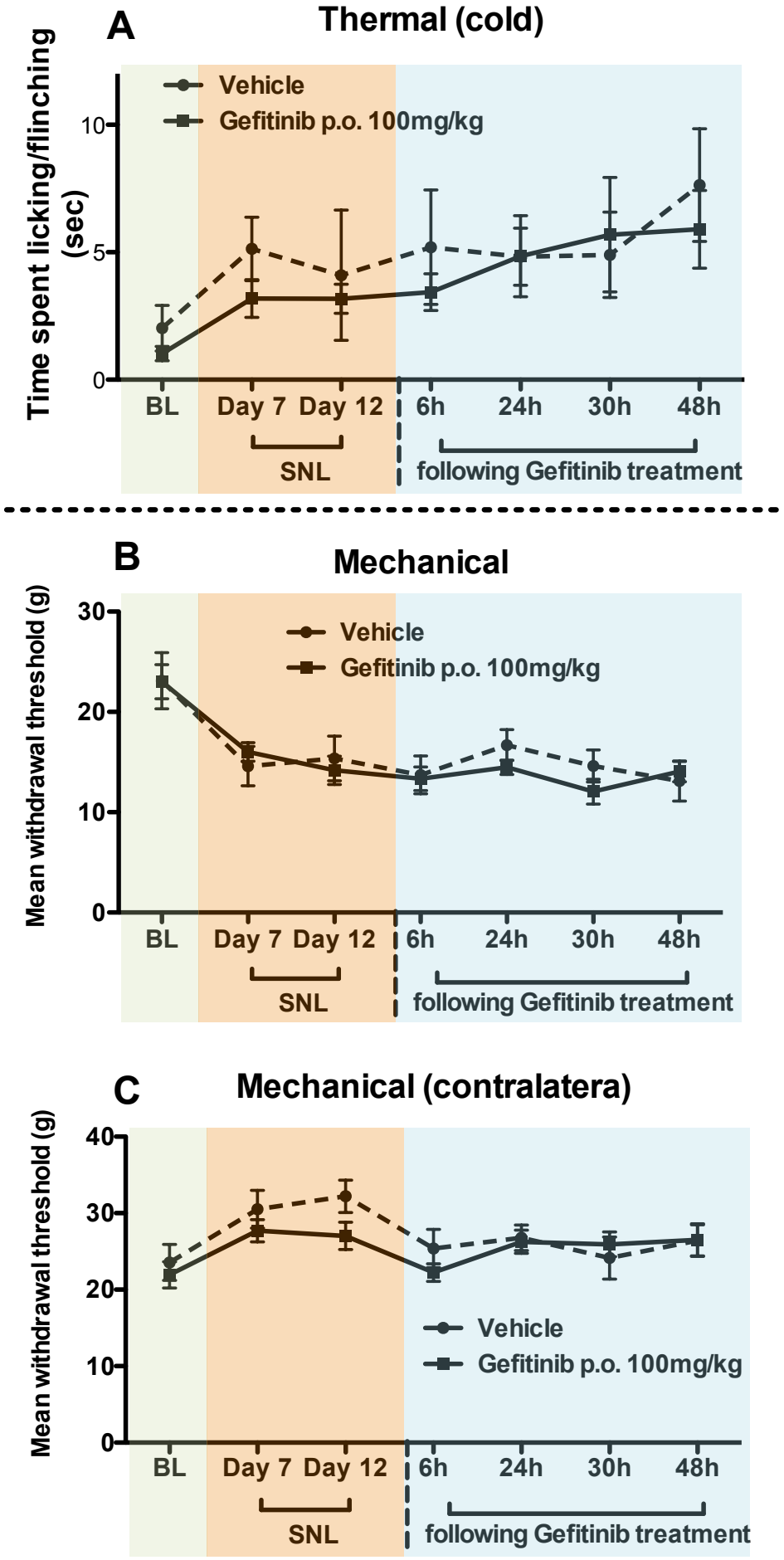
A
Thermal (cold)
Time spent licking/flinching (sec)
Vehicle
Gefitinib p.o. 100mg/kg
10
5
0
BL
Day 7
Day 12
6h
24h
30h
48h
SNL
following Gefitinib treatment
B
Mechanical
Mean withdrawal threshold (g)
30
20
10
0
C
Mechanical (contralatera)
40

Figure 3.11. EGFR inhibition – neuropathic pain. Graphs are colour-coded (see Figure 3.10.) for baseline sensitivity (green), neuropathic hypersensitivity (red) and EGFR inhibition (blue). Animals developed a clear increase in cold **A)** sensitivity and developed a mechanical hypersensitivity **B)** in the ipsilateral side of the L5 SNT, which was not affected by Gefitinib treatment. C) To test whether Gefitinib treatment affects mechanical thresholds on the contralateral nerve to the injury side, sensitivity levels in both hindpaws were tested in all animals (Vehicle and Gefitinib treated group). As expected, after the transection surgery of L5, neither sensitivity levels changed in the uninjured nerve nor Gefitinib treatment had an affect on mechanical sensitivity on the contralateral side of the affected nerve (n=8 animals per group).

3.4. Discussion

3.4.1. BTC has no peripheral effect in nociception

Nociceptive sensitisation in the periphery is mediated by a myriad of molecules, amongst others growth factors. In the previous chapter I discovered that BTC is highly regulated following injury. To test whether BTC is a candidate molecule involved in the sensitisation of peripheral nociceptors, it was injected into the hindpaw of healthy animals. No changes in thermal or mechanical hypersensitivity were seen at early timepoints and 7 days after the injection. Various different mechanisms could explain the lack of sensitisation. For instance, the recombinant protein could be immobilised on extracellular matrix molecules, thereby reducing its bioavailability. Binding of growth factors and cytokines on the ECM is well known. Apparently, the growth factor interacts with sulphated glycoproteins and its heparan sulphate binding is greater than that of EGF (Mummery et al., 2007). Another possible mechanism is receptor inactivation via endocytosis. This could be a protective effect following high ligand concentrations (Citri and Yarden, 2006).

In this study recombinant mouse BTC was used in rats. The protein sequence is highly conserved in both species at 93%. A ClustalW multiple sequence alignment is shown in (Figure 3.12.). Based on high levels of sequence similarity functional differences are unlikely.

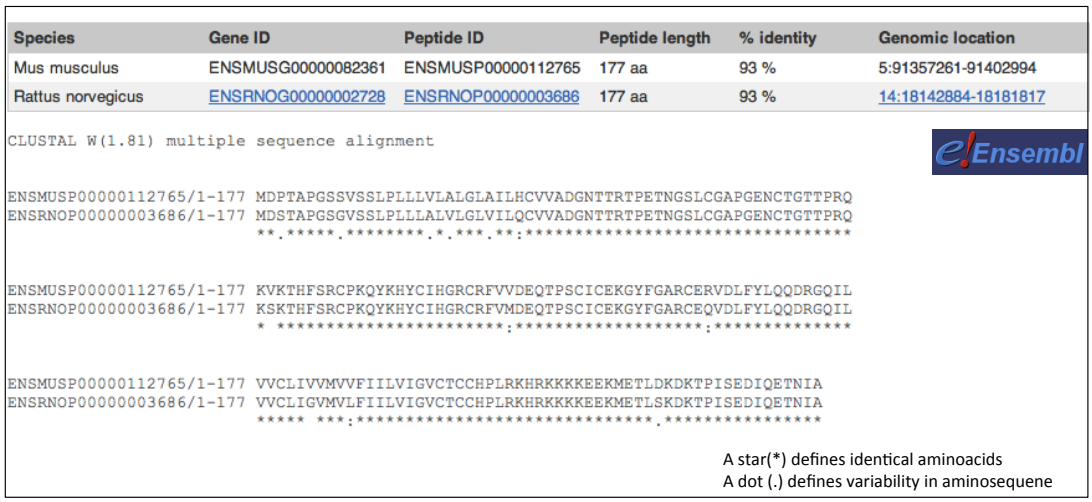

Species	Gene ID	Peptide ID	Peptide length	% identity	Genomic location
Mus musculus	ENSMUSG00000082361	ENSMUSP00000112765	177 aa	93 %	5:91357261-91402994
Rattus norvegicus	ENSRNOG00000002728	ENSRNOP00000003686	177 aa	93 %	14:18142884-18181817

```
CLUSTAL W(1.81) multiple sequence alignment

ENSMUSP00000112765/1-177 MDPTAPGSSVSSLPLLLVLALGLAILHCVVADGNTTRTPETNGSLCGAPGENCTGTTPRQ
ENSRNOP00000003686/1-177 MDSTAPGSGVSSLPLLLALVLGLVILQCVVADGNTTRTPETNGSLCGAPGENCTGTTPRQ
                         **.*****.********.*.***.**:**********************************


ENSMUSP00000112765/1-177 KVKTHFSRCPKQYKHYCIHGRCRFVVDEQTPSCICEKGYFGARCERVDLFYLQQDRGQIL
ENSRNOP00000003686/1-177 KSKTHFSRCPKQYKHYCIHGRCRFVMDEQTPSCICEKGYFGARCEQVDLFYLQQDRGQIL
                         * ***********************:*******************:***************


ENSMUSP00000112765/1-177 VVCLIVVMVVFIILVIGVCTCCHPLRKHRKKKKEEKMETLDKDKTPISEDIQETNIA
ENSRNOP00000003686/1-177 VVCLIGVMVLFIILVIGVCTCCHPLRKHRKKKKEEKMETLSKDKTPISEDIQETNIA
                         ***** ***:*******************************.****************
```

A star(*) defines identical aminoacids
A dot (.) defines variability in aminosequene

Figure 3.12. BTC orthologues in rat and mouse. Protein sequence conservation for mouse and rat orthologues of BTC (derived from www.ensembl.org; Ensembl release 72 – June 2013). Mouse and rat BTC orthologues are 93% conserved on the protein level.

Furthermore, a recombinant protein like BTC, generated *in vitro,* might have different folding properties affecting its function *in vivo.* In addition, I injected only a single dose of BTC into the hindpaw (2µg/50ul), which although high might be ineffective *in vivo*.

In contrast, using a different growth factor the findings of Andreev *et al.* (1995), who showed that subcutaneous injection of NGF leads to thermal hypersensitivity in the first 6 hours, could be confirmed.

3.4.2. The effects of BTC, EGF and EREG following intrathecal injection

Intrathecal injection of BTC leads to phosphorylation of the ERK MAPK pathway in the L5 DRG. Activation of ErbB receptors leads to dimerization and activation of several intracellular pathways (Figure1.5.). Erk 1 and Erk 2 are MAPKs, involved in diverse biological functions mediated mainly by the regulation of the AP1 (activator protein 1) box, including the fos, jun and ATF transcription factors amongst others (Chang and Karin, 2001). Activation of ERK by growth factors and trophic stimuli is generally associated with cellular proliferation, survival but also inflammatory processes (Johnson and Lapadat, 2002).

Activation of the EGFR can induce phosphorylation of other intracellular pathways such as the JAK/STAT and the PI3/Akt (Yarden and Sliwkowski, 2001). Whether BTC injection into the CNS can have downstream effects following activation of these pathways remains to be elucidated.

To test a potential role of BTC as an active mediator of nociception following intrathecal administration, I tested sensory thresholds for thermal and mechanical stimuli. EGF and EREG were used for comparison. BTC, EGF and EREG did not show any alterations at any of the timepoints tested, ranging from 30 minutes to 48 hours post-injection.

From these data it can be concluded that BTC, EREG or EGF do not affect sensory levels if applied peripherally or intrathecally, suggesting that they do not play a role as pain mediators, at least not in the models tested.

3.4.3. Inhibition of EGFR in animal models of pain

Inhibition of the EGFR in humans has been shown in a recent case series (Kersten et al., 2013) to be beneficial in treating resistant neuropathic pain conditions. Given that EGFR ligands and receptors are regulated following SNT, I tested whether EGFR inhibition, using the small molecule TKI Gefitinib, can alter behavioural responses in a rat model for acute inflammatory and neuropathic pain.

To mimic acute pain in animals, the Formalin test was used. Two routes of administration, intraperitoneal injection and oral gavage had no effect in the behavioural response. Neither the first phase, which is due to direct activation of TRPA1 nor the second phase, which was described as an ongoing inflammatory input with subsequent sensitisation (Mogil, 2009), showed any differences.

In a neuropathic pain model, L5 SNT, which leads to the development of a neuropathic phenotype with apparent increase in mechanical and cold sensitivity, Gefitinib treatment had no effect. Whether this lack of pharmacological effect is due to biological or technical limitations cannot be concluded at this stage.

A long-standing conflict in the field of pain is the limited translational success with the failure to convert findings from animal models into clinical drug development and *vice versa* (Mogil, 2009) (see Introduction, Chapter 3). With regards to that, I want to point out that animal models might not always be suitable to test drug effects. Animal models have a poor sensitivity in assessing ongoing pain since the responses measured are acute reflex responses on acute stimuli. In contrast, in humans, especially in neuropathic pain patients, ongoing pain is the main clinical symptom assessed. All experiments presented in this chapter have been conducted in young male rats, whereas beneficial effects of EGFR inhibition in humans involved aged patients with great comorbidity. Furthermore, human studies usually involve prescribed co-medication, which might interfere with the effectiveness of the experimental drug. All patients described in the above case series (Kersten et al., 2013) were treated with various drugs, e.g., non-steroidal anti-inflammatory drugs and opioids, which continued while the EGFR was inhibited. Additionally, the statistical impact from this case study is low. Further evaluation, such as a randomised controlled trial, analysing EGFR inhibition in neuropathic pain patients is essential to gain more specific evidence.

Furthermore differences in the specific animal model can account for a high variation. It has been shown that using slightly altered partial nerve ligation models in the same species can have clear differences in behavioural measurements. This could be generally explained by varying degrees of peri- or intraneural inflammation (Cui et al., 2000).

The bioavailability of Gefitinib *in vivo* can vary and this is dependent on many different factors (Cohen et al., 2003). I examined the effectiveness of Gefitinib *in vitro* in DRG neurons (see Chapter 4 Figure 4.12.), but its bioavailability in the injured nerve is uncertain. I attempted to test whether Gefitinib could inhibit the phosphorylation of the EGFR in the injured nerve using antibodies from different suppliers but my efforts were hampered by either lack of antigenicity or specificity in the extracted rat tissues. I also tried to measure ERK phosphorylation following drug treatment. However, baseline ERK activation was too high to examine group differences and to allow a conclusive statement.

In conclusion, BTC is upregulated in the nerve, DRG and dorsal horn following nerve injury but has no effect as a direct nociceptive mediator, at least not in the experimental setup used in this study. This was shown by injecting BTC directly and observing sensitivity levels in naïve animals. Also, inhibiting EGFR has no effect in inflammatory and neuropathic pain models. Given that the highest regulation of BTC mRNA expression could be found in the nerve, a role in regeneration or regulation of the immune response following injury is likely. In Chapter 4, I describe experiments, which focus on the effect of BTC on different cell types implicated in nerve injury.

CHAPTER 4

The role of BTC following nerve injury - mechanistic studies

4.1. Introduction

I spent a substantial amount of my PhD project evaluating the role of BTC as a potential pain mediator. However, BTC does not seem to be involved in nociception. In the following chapter I want to describe my approaches to reveal alternative biological functions using a variety of *in vitro* methods.

4.1.1. The function of growth factors in neurons

As described in the General Introduction, the regenerative properties of injured neurons are dependent on changes of the expression profile towards a regenerative phenotype (Chen et al., 2007). Growth factors play an important role in the process of peripheral nerve regeneration and specifically influence neurons and their regenerating axons (Terenghi, 1999). Two main functions have been described. First, neurotrophic and growth factors play a critical role in the survival of neurons, which increases the potential for successful regeneration and second, neurotrophic factors can have direct effects on the growth process of neurites. BDNF has been shown to protect motor neurons from axotomy-induced cell death (Yan et al., 1992) and NGF has been shown to protect axotomised sensory neurons from apoptosis (Miyata et al., 1986). The growth factor EGF enhances the survival of primary cultured dopaminergic neurons (Casper et al., 1991). Neuronal survival has been well studied in the context of development, which depends on controlled apoptosis of neuronal cell populations. The EGFR has been implicated in developmental cell survival pathways, for example in photoreceptor neurons of the developing *Drosophila* eye (Baker and Yu, 2001). Its family member ErbB4 can inhibit apoptosis in a pheochromocytoma (PC12) cells line, which is derived from a rat adrenal medullary pheochromocytoma and is commonly used to study the regulation of neural differentiation and survival (Erlich et al., 2001). The effect of EGFR ligands on cell viability following injury in adult neuronal cells is unknown.

In the context of neurite regeneration, growth factors like NGF, BDNF or NT-3 can induce axon growth through activation of PI3-Kinase, localised directly in the growth cone of the regenerating nerve (Zhou et al., 2004; Zhou et al., 2006). This leads to phosphorylation of the second messenger AKT and Glycogen synthase kinase (GSK)-3β, which then leads to cytoskeleton assembly and axon elongation (Zhou et al., 2004). Moreover, NGF, which is

well characterised, is important in axon extension in embryonal neurons, e.g. sensory neurons (Campenot, 1977), (Lentz et al., 1999).

The role of EGFR ligands and their receptors as neurotrophic or growth promoting factors is still subject of debate. For instance, activation of the EGFR of the mollusc *Lymnaea stagnalis* by EGF has neurotrophic actions (Hermann et al., 2000). Data from research in mammals is rare. EGF stimulates neurite outgrowth in cultured dopaminergic neurons (Ferrari et al., 1991) and it has been shown that the growth factor can induce neurite outgrowth after specific activation of protein kinase C (PKC)-ε (Brodie et al., 1999). In PC12 cells, EGF activation triggers axonal growth (Wu and Bradshaw, 1996). This finding is interesting, since it describes synergistic effects of growth factors in the biology of neurite outgrowth. When PC12 cells were treated with EGF or NGF alone, only modest changes could be observed, whereas combinational treatment was much more beneficial. The authors explained this finding with activation of specific intracellular pathways by the respective growth factor, which, when activated together by a synergistic treatment, have a much more pronounced effect (Wu and Bradshaw, 1996). Another example for this synergistic action is transactivation receptors. For example, Piiper *et al.* showed that high intracellular cAMP levels can increase concomitant phosphorylation of both, Trk_A and EGFR. This correlates with activation of distinct intracellular messengers, such as Akt for Trk_A and ERK1/2 for EGF, which in combination increased neurite outgrowth in PC12 cells (Piiper et al., 2002).

Also, ErbB4 activation can promote neurite outgrowth, accompanied by the activation of MAP kinases and induction of the neural differentiation marker Growth Associated Protein 43 (GAP-43) (Vaskovsky et al., 2000). In primary neuronal subpopulations such as cerebellar granule cells, neurite outgrowth can be regulated via activation of ErbB4 (Rieff et al., 1999).

Sparse knowledge exists about the effect of other EGFR ligands on neurite outgrowth. In a SCI model it has been shown that TGFα increases astrocyte invasion and promotes axonal growth in mice (White et al., 2008). Using PC12 cells, it was shown that treatment with recombinant HB-EGF stimulates neurite outgrowth (Mishima et al., 1996). In AR42J cells, a pancreatic cell line, stimulation with BTC leads to extension of neurite-like processes, which contain neurofilament, an intermediate filament found in neurons (Mashima et al., 1996).

4.1.2. The function of growth factors in SCs

SCs, the peripheral glia provide trophic support and in some case insulation to axons. As described in Chapter 1 nerve injury changes myelination properties of the cells. Following injury SCs loose their ability to myelinate and start to proliferate along a basal lamina to form Bands of Büngner. Once the target tissue is reinnervated SCs change phenotype back, acting as a myelinating, supportive cell (Jessen and Mirsky, 2008). This remarkable capacity of phenotypic modulation is orchestrated by a complex array of trophic factors. Another example is, that based on their association with sensory or motor neurons SCs express a different and specific set of growth factors (see Chapter 1) (Hoke et al., 2006).

Following injury, Schwann cell function is regulated by neurotrophic factors and their receptors (Chen et al., 2007). For example BDNF promotes remyelination (Zhang et al., 2000). and FGF2 induces Schwann cell proliferation but inhibits remyelination following injury. . (Jungnickel et al., 2004; Jungnickel et al., 2006). Growth factors can be mitogens for SCs, such as platelet derived growth factor (PDGF) (Davis and Stroobant, 1990) or vascular endothelial growth factor (VEGF) (Sondell et al., 1999). In contrast, also apoptosis can be regulated by growth factors, e.g. NGF can activate the low affinity p75 receptor, inducing apotosis (Soilu-Hanninen et al., 1999).

Although, substantial discoveries have been made about the interaction of NRG with ErbB receptors in the SC response to nerve injury (Fricker and Bennett, 2011), knowledge about EGFR ligand biology in SCs is sparse. Interestingly, in one of the few reports on the cellular function of BTC, Byer *et al.* found a chemotactic response and proliferation of SCs following BTC stimulation in nerve sheath tumours (Byer et al., 2013).

4.1.3. The function of growth factors on macrophages in the peripheral nervous system

Two main mechanisms can describe macrophage function in the periphery following nerve injury. First, infiltration of a haematogenous pool of macrophages regulated by chemoattractive factors released into the vicinity of the injured nerve and second, phagocytosis of myelin debris.

Macrophages accumulate at the site of injury following nerve injury. They can be attracted by signals from resident cells like SCs (Vargas and Barres, 2007) but also by factors released from the injured tissue, which are unrelated to SCs (Rosenberg et al., 2012). Nevertheless, the process of macrophage recruitment is not clearly defined yet. Neurotrophic factors can promote chemotaxis in macrophages. *In vitro* it was shown that NGF and NT-3 but not BDNF could attract macrophages (Kobayashi and Mizisin, 2001). In other experimental settings, growth factors of the EGFR ligand family have been implicated in macrophage chemotaxis. In atherosclerotic plaques, EGF mediates proliferation and chemotaxis of monocytes and macrophages (Lamb et al., 2004). In cutaneous wound healing EGF, TGFα and HB-EGF have been shown to affect macrophage motility and proliferation (Singer and Clark, 1999).

The other important role of macrophages in injured nerves is phagocytosis. In fact, most of the removal of degenerated myelin is performed by blood-derived monocytes (Bruck et al., 1996), (Beuche and Friede, 1984). Macrophages get activated by inflammatory cytokines and chemokines such as IL1 and TNF-α. This initiates the process of phagocytosis (Rotshenker, 2011). Growth and neurotrophic factors have been described to modulate the phagocytic function of monocytes/macrophages in the nervous system. For example, application of

exogenous BDNF has been shown to increase the phagocytic response of microglia following axotomy of the intraorbital optic nerve in mice (Galindo-Romero et al., 2013). BDNF has also been shown to increase the phagocytosis of latex beads in microglia (Elkabes et al., 1996) and peritoneal macrophages (Asami et al., 2006) *in vitro,* and the authors speculate that growth factors contribute to phagocytosis following injury. Another study showed that GDNF has a similar effect (Hashimoto et al., 2005).

Thus far, little is known about the potential function of the growth factor BTC on macrophages. Notably, Matsuzawa *et al.* found BTC protein expression in macrophages populating the atherosclerotic core of human aortas (Tamura et al., 2001).

In this chapter I strive to examine the function of BTC in DRG neurons, SCs and macrophages using several *in vitro* approaches.

4.2. Methods

4.2.1. Animals

All primary cells were extracted from adult (DRG neurons, macrophages) or postnatal (SCs) male Wistar rats. Animals were housed under standard conditions with a 12 hour light/dark cycle and food and water was available *ad libitum*. All experiments were done in accordance to the United Kingdom Home Office regulations.

4.2.2. Cell culture

4.2.2.1. Sensory neuron culture

Adult rats were killed by intraperitoneal injection of pentobarbital. DRGs were dissected and placed in HBSS (Hank's buffered salt solution, Sigma) without Ca^{2+} and Mg^{2+}. DRGs were micro-dissected to remove residual tissue and then digested in 1.25% collagenase at 37°C for 2 hours. Following trituration in Ham's F12 culture medium (Gibco) using different diameter glass pipettes, the cell suspension was placed onto a 12% bovine serum albumin (Sigma) cushion and centrifuged at 600rpm for 6 minutes at room temperature. Cells were resuspended in modified Bottenstein and Sato's culture medium and cultured either on glass cover slips or in 96-well plates, which were coated with 10µg/ml poly-L-lysine (PLL) and 10µg/ml laminin at 37°C under 5% CO_2.

For neurite outgrowth experiments neurons were fixed in 4% paraformaldehyde (PFA) and stained for 1 hour at room temperature with antibodies against β-III-tubulin (1:1000, Promega) diluted in PBS with 10% normal goat serum (Invitrogen, UK) and 0.3% Triton-X (Sigma). After 3 washes with PBS (Invitrogen) cells were incubated with secondary goat anti-mouse antibody, conjugated to Alexa-488 (1:1000, Molecular Probes) and 4', 6-diamidino- 2-phenylindole (DAPI) in PBS with 0.3% Triton-X for 45 minutes at room temperature. After three more washes with PBS 100µl PBS containing 0.02% sodium azide (Sigma, UK) were added and neurite outgrowth was measured. (details of quantification given below).

4.2.2.2. Macrophages

4.2.2.2.1. Peritoneal macrophages

Adult male Wistar rats were sacrificed using CO_2. 20-50ml of sterile HBSS was injected into the peritoneal cavity. After mobilising the peritoneal cavity for 5 minutes the buffer was retrieved and centrifuged at 1000rpm for 10 minutes. The cell pellet was resuspended in Dulbecco's modified eagle medium (DMEM) complemented with 10ml/l penicillin/streptomycin and 10% fetal bovine serum (FBS) and cultured at 37°C under 5% CO_2.

4.2.2.2.2. Bone-marrow derived macrophages

Cells were obtained from both femur and tibia previously cleaned from adherent tissues. The bone ends of femur and tibia of male adult rats were cut and flushed with PBS (5ml each bone). The cell suspension was filtered (70µm) and centrifuged at room temperature for 7 minutes at 2000rpm. The pellet was re-suspended in DMEM supplemented with 10ml/l penicillin/streptomycin, 10% FBS and 25ng/ml macrophages-culture stimulating factor (MCSF) (Peprotech). Cells were plated directly on 96-well plates and cultured at 37°C under 5% CO_2 for at least 7 days. Prior to each experiment cells were serum starved for 3 hours.

4.2.2.3. Schwann cells

Sciatic nerves were extracted from postnatal (P5) rat pups and microdissected in HBSS without Ca^{2+} and Mg^{2+} to remove the epineurium. Nerves were then digested in 0.1% collagenase and 0.25% trypsin for 30 minutes at 37°C. After trituration, using four different diameter fire polished glass pipettes, cells were centrifuged at 1000rpm for 2 minutes and the pellet was resuspended in DMEM supplemented with 10ml/l penicillin/streptomycin, 10% FBS and 2% pituitary gland extract (Invitrogen). Cells were plated in 4-well plates (500,000 per well), coated with poly-L-lysine (10µg/ml) and laminin (10µg/ml) and cultured at 37°C under 5% CO_2.

4.2.2.4. Cell lines

The THP1 monocytic cell line (ATCC) was maintained floating in DMEM supplemented with penicillin/streptomycin (10ml/l) and 10% FBS. For experiments, cells were plated in 96-well plates (250,000 per well). Prior to each experiment cells were serum starved for 3 hours.

Human Embryonic Kidney 293 (HEK293, Invitrogen) cells were maintained in DMEM supplemented with penicillin/streptomycin (10ml/l) and 10% FBS. For experiments, cells were plated in 96-well plates (250,000 per well). Prior to each experiment cells were serum starved for 3 hours.

4.2.3. Calcium imaging

For calcium imaging cultured macrophages and SCs were incubated for 60-90 minutes and DRG neurons for 30 minutes at 37°C with 2μM Ca^{2+} indicator Fura-2-AM (Invitrogen) in HBSS. For macrophages Probenicide (10mM) was added to inhibit Fura-2 sequestration (Di Virgilio et al., 1990). Cells were transferred to a perfusion system attached to an inverted microscope (Nikon) equipped with a monochromator (Photon Technology). Recordings were carried out using a standardised protocol. Baseling Ca^{2+} concentration based fluorescent ratios (340/380nm excitation) were taken over the first minute of each run under continuous perfusion (3ml/min) with HBSS buffer solution (containing 10mM 4-(2- hydroxyethyl)-1-piperazineethanesulfonic acid (HEPES), pH 7.4). HBSS perfusion buffer for recordings with DRG neurons contained 10mM HEPES and 15mM glucose. A single manual application of EGFR ligands (100nM) was followed by 2 minutes without continuous perfusion. After a 2-minute washout period, 25μM ATP (Sigma) or 20mM potassium chloride (KCl) (Sigma) were used as a positive control to define viable macrophages or DRG neurons respectively. For each ligand, experiments were done on at least three different days with independently cultured cells. Presented are example traces for one experiment.

4.2.4. Protein biochemistry: Western blotting

Protein extraction from sciatic nerve tissue or cultured cells: Nerves were weighed and washed (3x) in PBS with 12.5mM Ethylene-diamine-tetra-acetic acid (EDTA) prior to transfer to appropriate lysis buffer in a 1:10 ratio. Samples were agitated using a desktop vortex at room temperature for 120 minutes at 14rpm. Cultured cells were washed in PBS and transferred to lysis buffer. Lysates were subjected to 45 minutes of ultrasonification and the protein concentration was measured using a spectrophotometer (Nanodrop 1000 Version 3.3.1.). Only samples with appropriate reflectance profiles were used for subsequent experiments. Finally, protein samples were denatured for 5 minutes at 95^{o}C, reduced in ß-Mercaptoethanol containing sample buffer (see Table 5 for composition) and stored at -20 ^{o}C.

Gel electrophoresis: Proteins were separated using precast 12% or 16% Bis-Tris Gels (Novex, Invitrogen) in a sodium dodecyl sulfate polyacrylamide gel electrophoresis (SDS-PAGE) system (Cell SureLock, Carlsbad, CA) in Tris-glycine migration buffer (see Table 5) together with a molecular weight marker (Page ruler Plus, Thermoscientific).

Protein transfer: Proteins were transferred onto (methanol dehydrated) polyvinylidene fluoride (PVDF) membranes using a BioRad transfer system buffered by migration buffer containing 20% methanol (see Table 5). Protein loading was confirmed by a 5-minute incubation with Ponceau S Red (Sigma) at room temperature. Membranes were then washed three times in deionised water and any non-specific background binding was blocked for at least 60 minutes in 5% non-fat milk in phosphate buffered saline with 0.1% Tween-20 (PBS-T) (see Table 5). Next, membranes were incubated with primary antibodies against p-EGFR at 1:200 (Abcam), p-ERK at 1:1000 (R&D), p-p38 at 1:1000 (R&D), BTC at 1:200 (R&D) or β-Actin at 1:500 (Abcam) in PBS-T (+ 5% albumin + 0.2% sodium azide) at 4°C overnight. Following three washes with PBS-T membranes were incubated with secondary antibodies (polyclonal rabbit anti-mouse immunoglobulin HRP (Dako) 1:2000 in PBS-T) or goat anti-rabbit immunoglobulin HRP (Dako) 1:2000 in PBS-T) for 60 minutes at RT.

Protein visualisation: Membranes were washed three times with PBS-T prior to a 5-minute incubation with Amersham ECL Prime (GE Healthcare) at room temperature. Proteins were visualised using the UVP Multispectral Imaging System and Vision Works Software Version 7.1.

For timecourse experiments, examining phosphorylation of EGFR, ERK and p38, experiment were done at least 3 times; for primary cultured cells from at least 3 independent cultures. Presented is one example for the respective experiment. Control cells were not stimulated (labelled with C).

If membranes were reprobed with different antibodies, stripping buffer (Restore Plus, Thermo Scientific) was applied for 15 min at RT. After washing in PBS-T and reapplication of 5% non-fat milk in PBS-T, the next immunoblot experiment was performed.

Buffer	Composition (in H_2O)
RIPA lysis buffer	50mM Tris (pH 7.5) 150mM sodium chloride (NaCl) 100µM sodium beta-glycerophosphate (NaβGlyP) 0.1% sodium dodecyl sulphate (SDS) 1% sodium vanadate 2.5% Empigen BB™ Detergent 0.1% sodium fluoride
SDS lysis buffer	0.2% SDS 10mM EDTA 1:100 proteinase inhibitor
Sample buffer	2% w/v SDS 2mM β-mercaptoethanol 4% glycerol 40mM Tris-hydrochloride (Tris-HCl) 0.01% Bromophenolblue
Migration buffer	25mM Trizma BASE (2-Amino-2-(hydroxymethyl)-1,3-propanediol) 200mM glycine 0.1% w/v SDS
Transfer buffer	25mM Trizma BASE 200mM glycine 20% methanol
Phosphate Buffered Saline with Tween-20 (PBS-T)	10mM sodium phosphate dibasic (Na_2HPO_4) 2mM potassium phosphate dibasic (KH_2PO_4) 2.7mM potassium chloride (KCl) 137mM NaCl 0.1% Tween-20, pH 7.4

Table 5: Buffer solutions for Western blotting (All components were purchased from Sigma)

4.2.5. Immunocytochemistry

DRG neurons and SCs were fixed in 4% PFA for 15 minutes RT and incubated with primary antibodies against ErbB1 (EGFR) at 1:200 (Abcam), ErbB4 1:200 (Abcam), β-3-tubulin at 1:1000 (Promega), Schwann cells were visualised with S100 staining using rabbit S100 polyclonal antibody (1:400; Z0311; Dako) incubated for 120 minutes RT and secondary Alexa Fluor 546 goat anti-rabbit (1:1000; Invitrogen) incubated for 60 minutes RT. All reagents were diluted in PBS containing 0.2% Triton X-100 and 0.1% sodium azide. Images were taken using a Carl Zeiss Imager.Z1 microscope or a confocal Carl Zeiss LSM 700 laser-scanning microscope.

4.2.6. Neurite outgrowth – InCellanalyser

DRG neurons, cultured on PLL- and laminin-coated 96-well plates for 24 or 48 hours, were fixed with 4% PFA and stained for 120 minutes RT with β-3-tubulin at 1:1000 (Promega) in PBS containing 0.2% Triton X-100 and 0.1% sodium azide and and secondary Alexa Fluor 488 goat anti-rabbit (1:1000; Invitrogen) incubated for 60 minutes RT. From each well, images from 16 random fields of view per well were captured using a semi-automated image capturing system (InCell Analyzer 1000, GE Healthcare Life Sciences). For automated image analysis, each image was computed using a custom-written algorithm for Developer Toolbox 1.0 software (GE Healthcare Life Sciences). Images were analysed following optimisation to selectively detect neurites and cell bodies according to fluorescence intensity and size parameter (Figure 4.1). Both the number of cells stained positive for β-3-tubulin and the length of neurites per image were quantified in order to obtain neurite length per neuron per well. After optimization, only experiments with a positive effect of NGF on neurite length per neuron were used for further analysis. Per experiment, each condition was tested in quadruplicates. One-way ANOVA followed by Tukey's post hoc analysis was used on the raw values of experimental data.

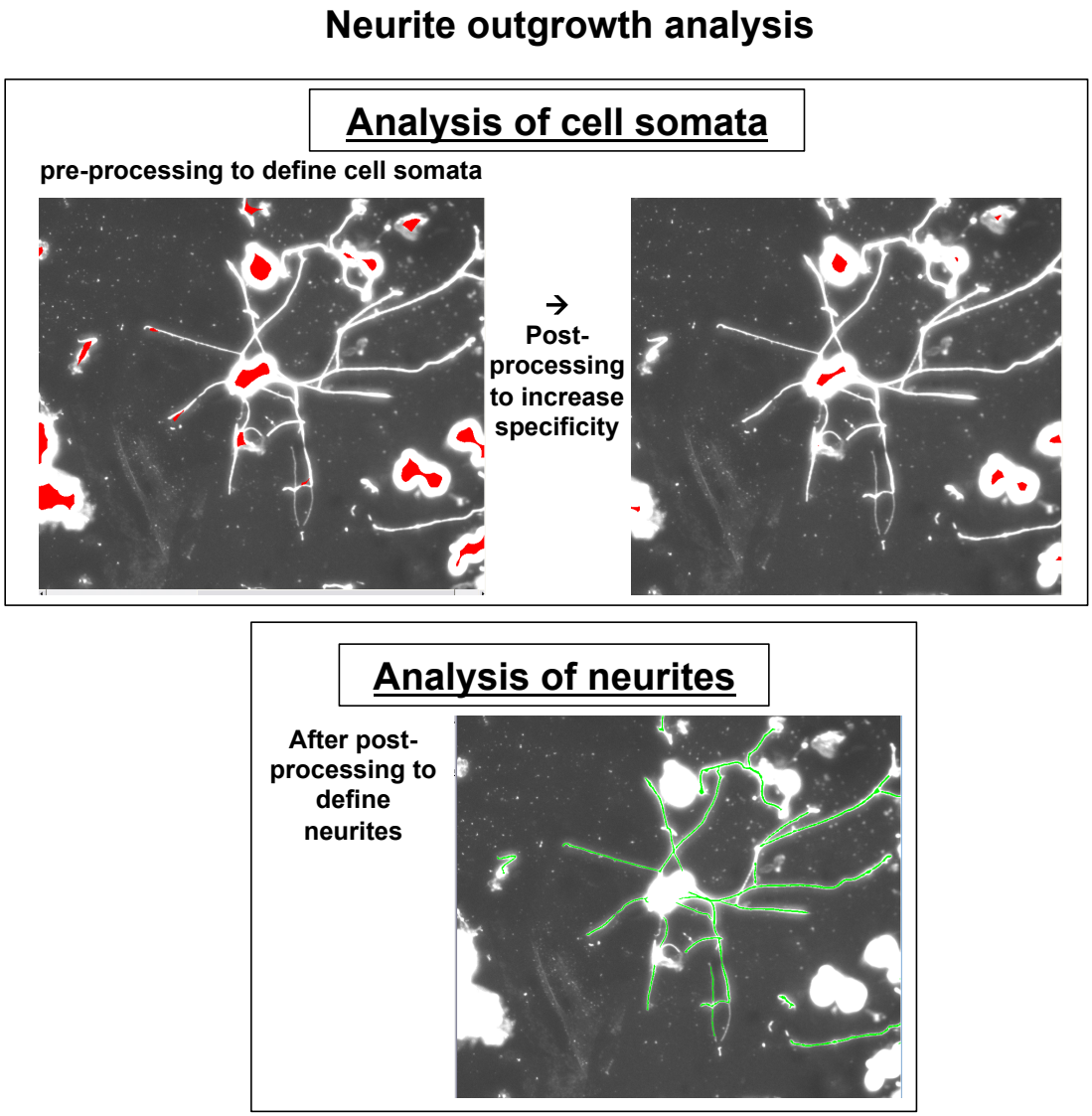

Figure 4.1. Automated image analysis. (Top) An automated custom written algorithm defined β-3-Tubulin positive cell somata, based on size and circumference (red) and (Bottom) β-3-Tubulin positive neurites (green) based on an area to distance ratio.

4.2.7. Chemotaxis assay *in vitro*

Chemotaxis was assessed using a Boyden chamber (Neuroprobe Bethesda) (Figure 4.2.) and a polycarbonate filter with a 5µm pore size. Prior to each experiment macrophages were serum-starved for 3 hours. The bottom wells were filled with different concentrations of BTC (100, 500ng/ml) and macrophages were added on top of the membrane in the top wells ($5x10^4$ cells per well). After 3 hours incubation at 37°C under 5% CO_2, the filter membrane was removed and the migrated cells on the bottom side were fixed in 100% methanol for 10 minutes and stained with RapiDiff (Biostain RRL). Images of the membrane were taken using a light microscope (Axioskop X-cite 120, Zeiss). Migrated cells were counted and analysed blinded.

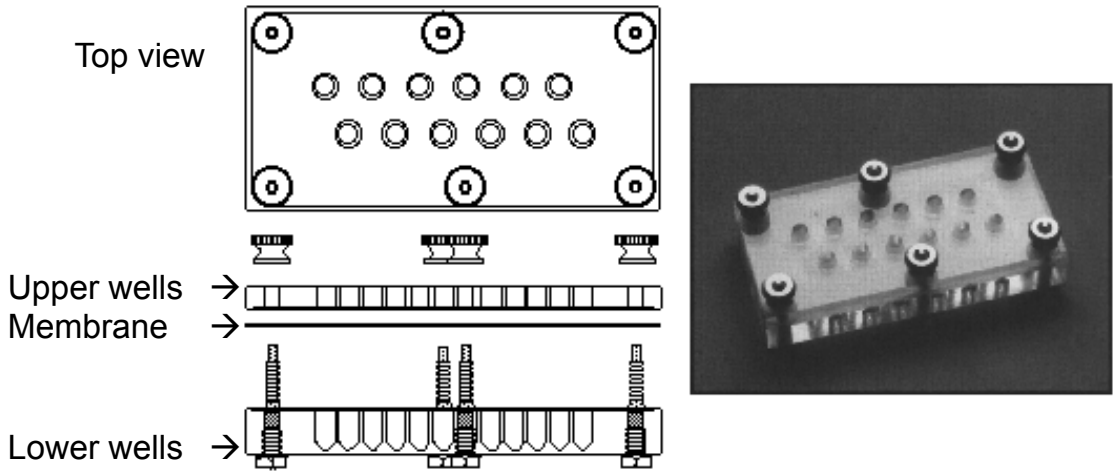

Figure 4.2. Design of Boyden chamber. (Adapted from Zigmond *et al.* (Zigmond et al., 2001)

4.2.8. Chemotaxis assay *in vivo*

To investigate *in vivo* chemotaxis, a method previously described to assess *in vivo* angiogenesis was adapted from Passaniti *et al*. (Passaniti et al., 1992). Matrigel, an extract of basement membrane proteins (mainly collagen and laminin), which cures at RT but is liquid at 4°C, was enriched with 200ng/ml BTC, injected subcutaneously into male Wistar rats and subsequently formed a solid gel plug (0.5ml with 100ng BTC). After 10 days mice were sacrificed and the Matrigel plugs were removed, fixed in 4% PFA in PBS, embedded in Optimal Cutting Temperature compound (OCT) and cryo-sectioned. For visualisation slides were then incubated with rabbit anti-IBA1 (1:1,000, WAKO). Following primary antibody incubation slides were washed and incubated for 1.5 hours with secondary antibody solution (Cy3 1:400, from Stratech). All antibodies were diluted in PBS containing 0.2% Triton X-100 and 0.1% sodium azide. Images were taken using a Carl Zeiss Z1 microscope. IBA1 positive cells were counted and quantified. For Western blot analysis Matrigel plugs were extracted after 10 days, washed in PBS with 12mM EDTA and protein was extracted using 0.2% SDS lysis buffer (see Table 5).

4.2.9. RT-qPCR

For RNA extraction please refer to Chapter 2.2.6. For RT-qPCR please refer to Chapter 2.2.7.

4.2.10. Statistical analysis

One-way Analysis of variance (ANOVA) was used to analyse data of more than two groups; where necessary Tukey's post-doc analysis was performed to characterise individual differences. A p-value <0.05 was defined as a significant result. Data was computed using GraphPad PRISM. For graphic data presentation, all charts represent arithmetic mean ± SEM.

4.3. Results

4.3.1. Downstream signalling of BTC

In order to study activation of the EGFR and intracellular signalling pathways, levels of kinase phosphorylation were measured by Western blotting. Before studying the effect of BTC and EGF stimulation on different primary cultured cells, I had to establish a reproducible working protocol. I used HEK293 cells to determine optimal antibody concentrations against the phosphorylated form of the EGFR and phosphorylation sites for downstream partners ERK and p38. In HEK293 cells stimulation with BTC (100ng/ml) or EGF (100ng/ml) lead to phosphorylation of the EGFR with a peak after 1 minute. Membranes were stripped and reprobed for antibodies against the phosphorylation site for either p38 or ERK MAPK. Phosphorylation was detected 5 minutes after stimulation and peaked at 15 minutes. At 60 minutes phosphorylation levels returned to baseline for both kinases. β-Actin was used as a loading control (Figure 4.3.)

Intracellular signalling in HEK cells

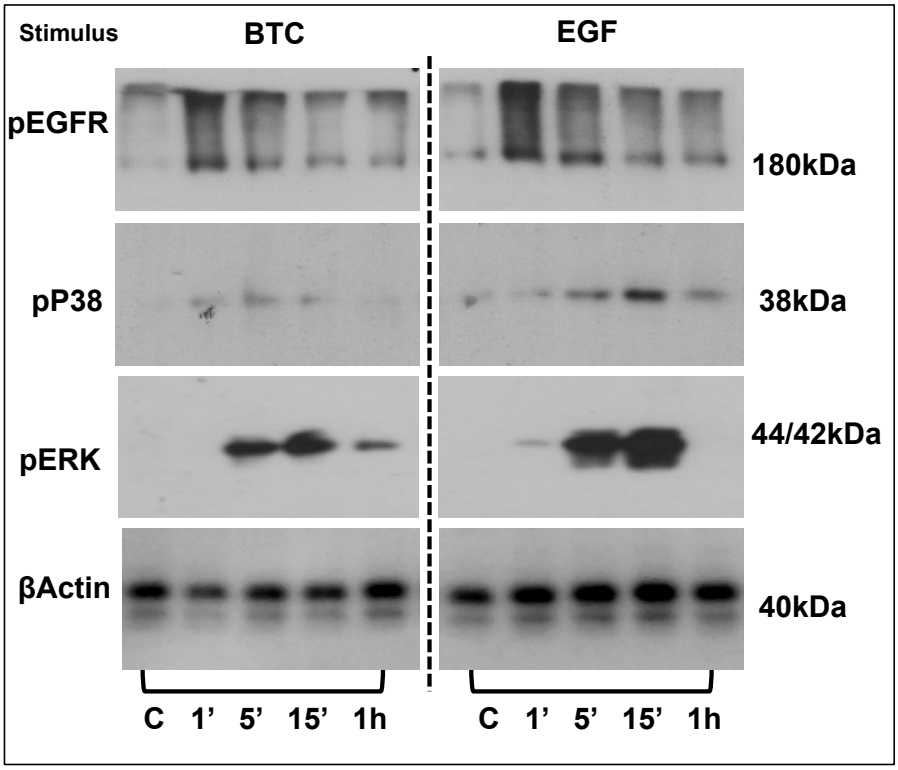

Figure 4.3. Signalling in HEK293 cells. HEK293 cell explants were extracted in RIPA buffer after 3 hour serum starvation and stimulation with either BTC (100ng/ml) or EGF (100ng/ml). Control cells were not stimulated (labelled with C). Protein lysates were protein blotted and blots immunostained for phosphorylated EGFR (p-EGFR), and reprobed for phosphorylated p38 (p-p38) and phosphorylated ERK (p-ERK) and βActin. Membranes of one experiment were reprobed with the different antibodies after using stripping buffer. Results are representative of at least 3 independent experiments.

The effect of EGF (100ng/ml) and BTC stimulation (100ng/ml) was then tested on cells of the monocyte/macrophage lineage. Primary rat macrophages were collected from the peritoneum, with a saline buffer lavage. Cells were left in culture for 5 days to adjust to tissue culture conditions. After a 3-hour serum starvation, cells were stimulated with EGF and BTC and protein was extracted at different timepoints (1, 5, 15, 60 minutes). Western blotting was used to detect the levels of p-EGFR and p-ERK. p-p38 was not detected, either due to antibody limitations (antibodies to p-ERK were found to be consistently

superior), or due to the fact that activation of the EGFR by EGF and BTC does not lead to p38 activation in the *in vitro* macrophage culture used. Moreover, in contrast to the HEK293 cell experiments shown above, it was not feasible to obtain a clear blot for the p-EGFR using rat peritoneal macrophages. Nevertheless, although the results are not as clean as the results in HEK293 cells, it appears that BTC does not phosphorylate EGFR but clearly activates ERK. EGF induces EGFR phosphorylation at 5 minutes followed by ERK activation. These data might suggest that ErbB4 dimers are the primary receptors for BTC in this cell type (Jones et al., 1999) (Figure 4.4.). This is an interesting hypothesis that needs to be further investigated.

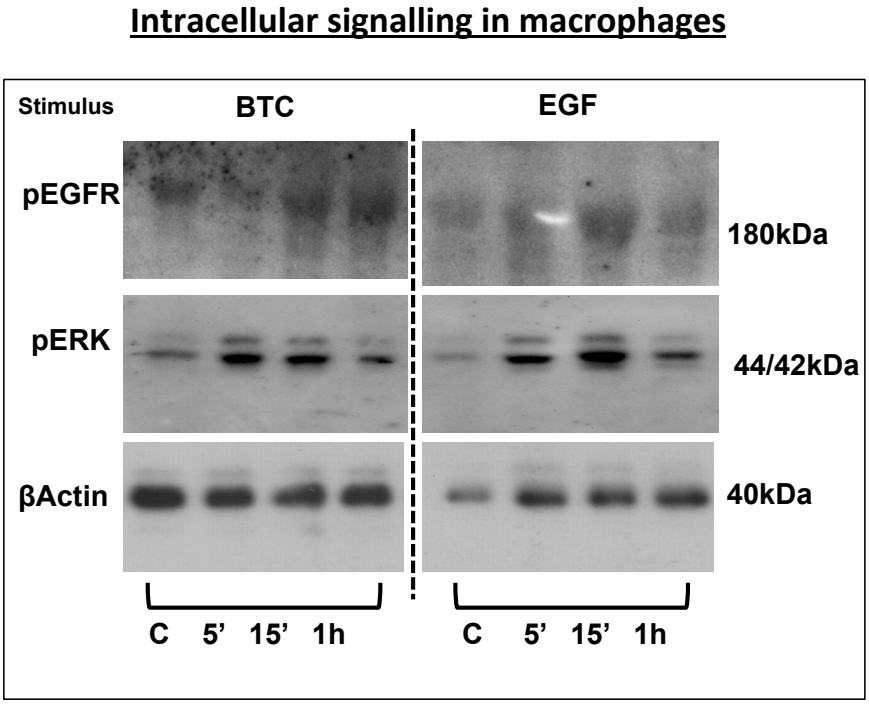

Figure 4.4. Signalling in peritoneal macrophages. Activation of ERK after BTC and EGF stimulation. Macrophages were extracted from the peritoneum of adult rats. After 5 days in culture, cells were serum-starved for 3 hours and then stimulated with either BTC (100ng/ml) or EGF (100ng/ml). Control cells were not stimulated (labeled with C). Protein lysates were blotted and stained for p-EGFR and reprobed for p-ERK and β-Actin as a loading control using stripping buffer. . Results are representative of at least 3 independent experiments.

The original working hypothesis was that activation of the EGFR and more specifically, activation by BTC, would have an effect on the function of sensory neurons. First, it was necessary to establish that the relevant receptors are expressed on the cells of interest; primary cultures of adult isolated DRG neurons were fixed and labeled with antibodies against ErbB4 (Figure 4.5. A). Some immunolabelling was found associated with neuronal cell bodies but these experiments did not provide clear evidence for the presence of ErbB4 receptors on DRG neurons. However, detecting the receptor in 24 hour-cultured cells was important given that DRGs were stimulated after they had adapted to culture conditions. Cells were also tested for expression of the ErbB1 (EGFR). Interestingly, ErbB1 (EGFR) was found on freshly isolated DRGs *ex vivo* but detection by immunocytochemistry was impossible in DRGs, which were in culture for 24 hours (Figure 4.5. B).

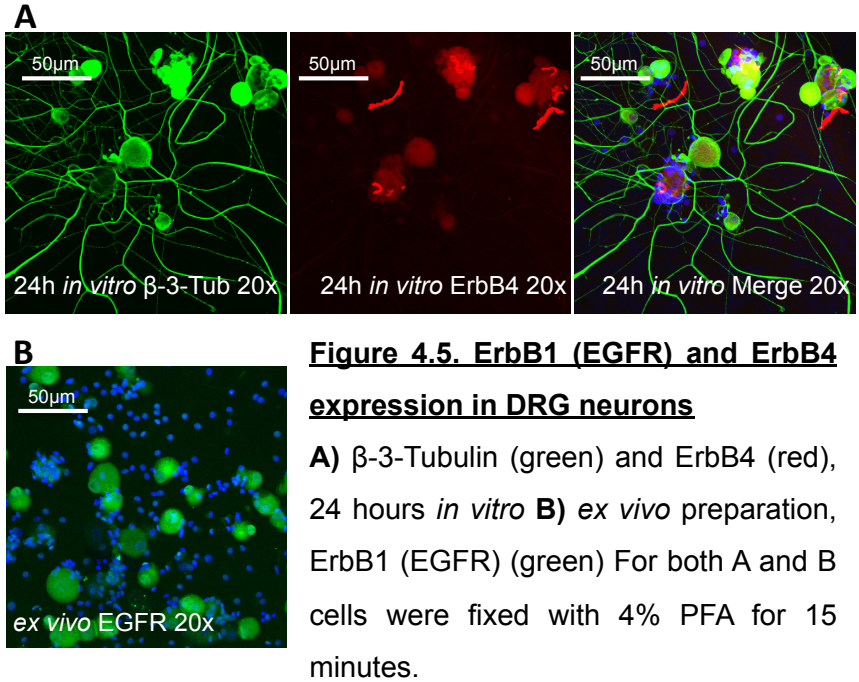

Figure 4.5. ErbB1 (EGFR) and ErbB4 expression in DRG neurons

A) β-3-Tubulin (green) and ErbB4 (red), 24 hours *in vitro* **B)** *ex vivo* preparation, ErbB1 (EGFR) (green) For both A and B cells were fixed with 4% PFA for 15 minutes.

To evaluate the effect of BTC on DRG neurons, I examined whether stimulation (100ng/ml) results in phosphorylation of the EGFR or downstream effectors ERK and p38; EGF (100ng/ml) was used as a positive control. In my experimental setup, BTC was ineffective on ErbB1 (EGFR) while EGF

activated the receptor after 5 minutes. Nevertheless, BTC was able to activate ERK and p38 with a peak after 15 minutes (Figure 4.6.), as in the macrophages (see Figure 4.4.), which might suggest that the growth factor is signalling not via ErbB1 (EGFR) but a different ErbB receptor, which is most likely ErbB4 (Jones et al., 1999). However, I was not able to demonstrate phosphorylation of ErbB4 using a few different commercially available antibodies.

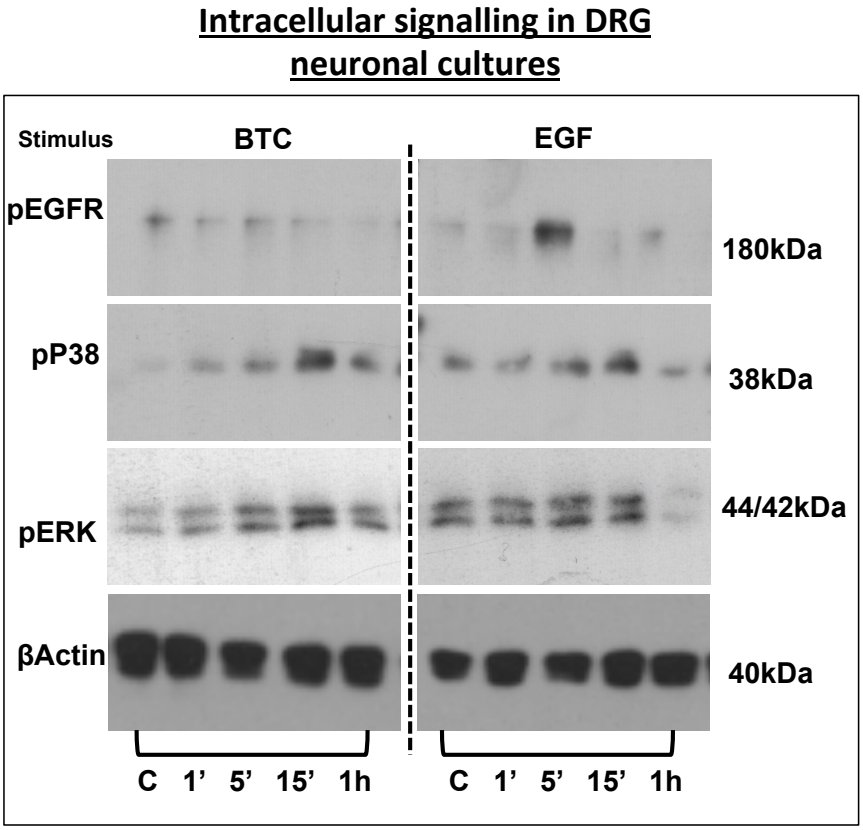

Figure 4.6. Signalling in DRG neuronal cultures. DRG neurons were extracted from adult rats. After 24 hours in culture, cells were stimulated with either BTC (100ng/ml) or EGF (100ng/ml). Control cells were not stimulated (labeled with C). Protein lysates were blotted and stained for p-EGFR and reprobed for p-ERK and β-Actin as a loading control using stripping buffer. Results are representative of at least 3 independent experiments.

4.3.2. Evaluation of neurite outgrowth *in vitro* following BTC stimulation

After it has been shown that BTC can at least activate signalling on sensory neurons, I wanted to test whether BTC and other EGFR ligands can promote neurite outgrowth on axotomised sensory neurons *in vitro*. I opted for this readout because neurite growth is an important event in the regeneration of a peripheral nerve following injury. DRG neurons were extracted from adult rats and cultured for 24 or 48 hours. A semi-automated system was used for counting cells and measuring neurite length. For details refer to (Chapter 4.2.6.). Briefly, as an objective and standardised way to measure neurite outgrowth and assess cell viability a computer-controlled microscope imaging system combined with semi-automated quantitative analysis software were used. This is the first time that adult sensory neurons have been examined with this method. Initially, the experimental procedure was optimised and different concentrations of two well-known neurotrophic factors, namely NGF and BDNF were tested. Both have been shown to enhance axonal outgrowth without affecting survival of adult sensory neurons (Lindsay, 1988). In a typical DRG neuron preparation and in the absence of mitotic inhibitors, fibroblasts and/or SCs start to proliferate and produce endogenous growth promoting factors. Hence, to minimise contamination with supporting cells experiments were done in the first 24 – 48 hours following dissociation. DRG neurons were cleaned from cell debris using a bovine serum albumin cushion. Neurons were plated in medium enriched with different concentrations of NGF (1,10,100ng/ml). Neurons were then plated at low density in 96-well plates (1,500 – 2,000 cells per 0.32cm^2). Wells were coated with PLL and laminin in order to promote rapid adherence of neurons and initiate axonal growth. First, cells were treated for 24 hours to allow clear distinction of neurite morphology (Figure 4.7.). This timepoint was selected because pilot experiments revealed that after 24-48 hours excessive neurite growth complicated the automated analysis.

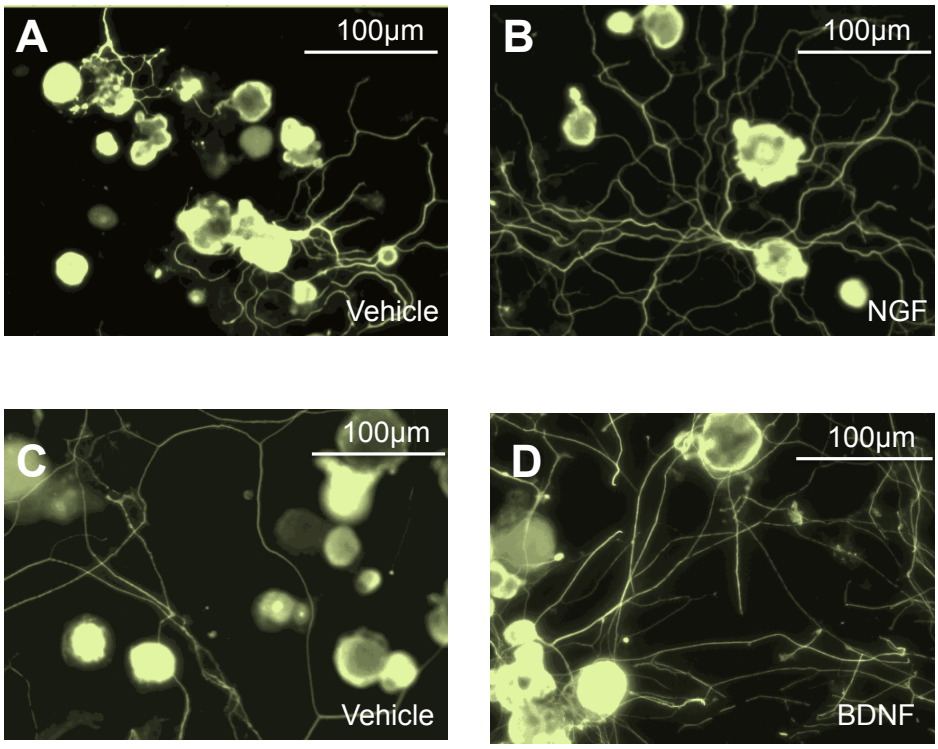

Figure 4.7. Neurite outgrowth on DRG neurons 24 hours in culture. Example images for DRG neuronal cultures in **B)** 10ng/ml NGF for 24 hours compared to **A)** vehicle treated cells and DRG neurons cultured in **D)** 100ng/ml BDNF for 24 hours compared to **C)** vehicle treated cells.

Supplementation with NGF significantly increased neurite outgrowth (Figure 4.8. A), even at low doses: neurite length per neuron changed from 172.7µm/cell in the vehicle group to 297.8µm/cell, 291.6µm/cell and 269.2µm/cell with 1, 10 or 100ng/ml NGF (n=4 individual experiments with quadruplicates per treatment, One-way ANOVA, Tukey's post-hoc, p=0.0019). BDNF treatment (100ng/ml) similarly increased neurite outgrowth from 30.8µm/cell to 70.9µm/cell (n=3 individual experiments with quadruplicates per treatment, One-way ANOVA, Tukey's post-hoc, p<0.0001) (Figure 4.8. C). With both treatments the number of cells counted per well did not change significantly (Figure 4.8. B, D) For all experiments PBS was used as vehicle.

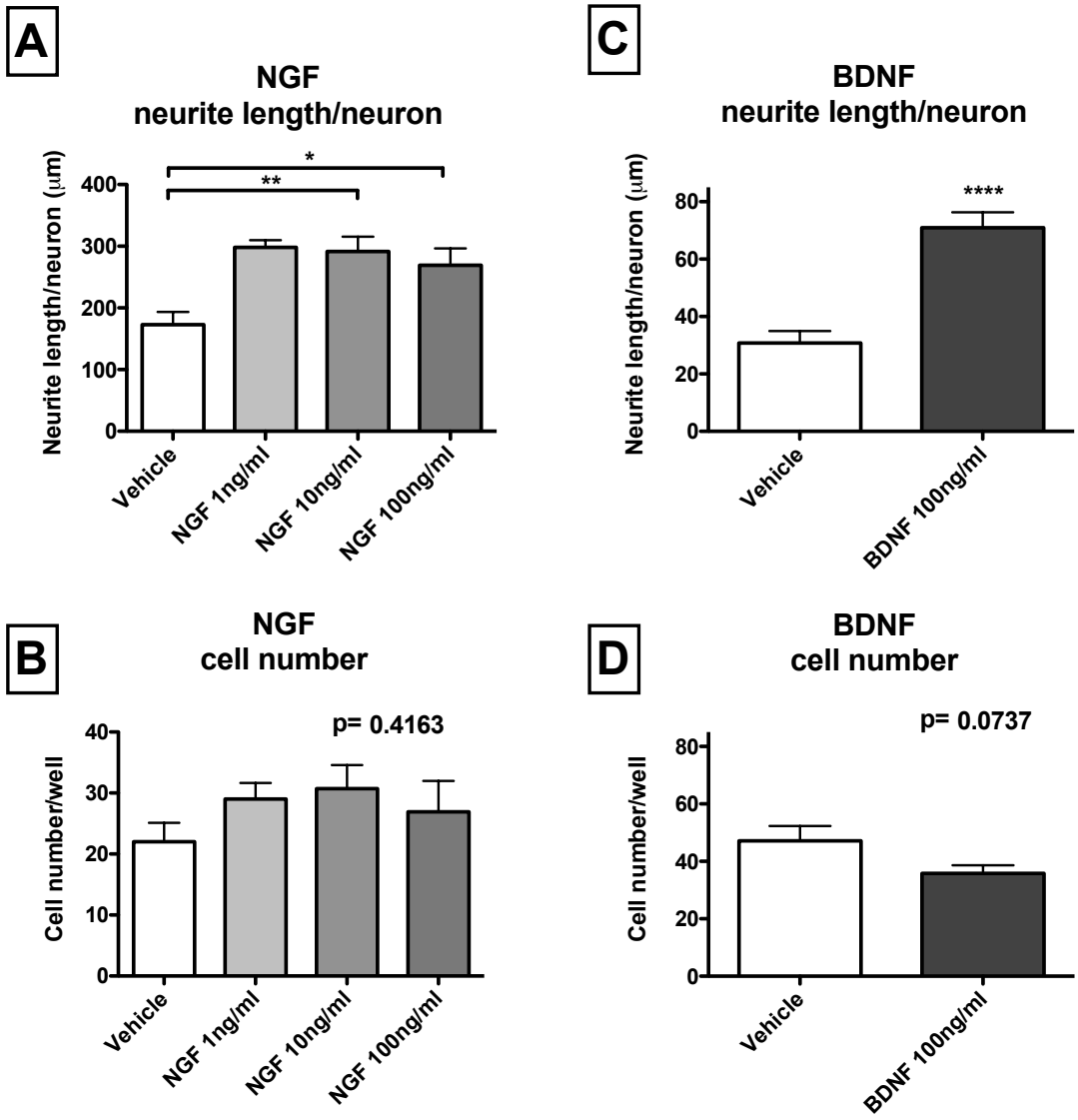

Figure 4.8. NGF and BDNF enhance neurite outgrowth in primary adult DRG neurons. **A)** Neurite length per neuron in NGF treated neurons (n=4 individual experiments with quadruplicates per treatment, One-way ANOVA, Tukey's post-hoc, p=0.0019) and BDNF **C)** (n=3 individual experiments with quadruplicates per treatment, One-way ANOVA, Tukey's post-hoc, p<0.0001) treated cells. **B)** Absolute cell number per well for NGF (n=14-18 in 4 individual experiments, One-way ANOVA, Tukey's post-hoc, p=0.4163) and **D)** BDNF (n=4 in 2 individual experiments, One-way ANOVA, Tukey's post-hoc, p=0.07) treated cells.

In order to evaluate the effect of BTC on neurite outgrowth in sensory neuronal cultures, four different conditions have been tested. First, to determine whether BTC affects the initiation phase of neurite growth *in vitro*, cells were treated for 24 hours immediately after dissociation. Second, it was examined whether treatment with BTC affects the "maintenance" of the neurite growth process after neurons have adapted to culture conditions for 24 hours.

Treatment of neuronal cultures with BTC for 24 hours immediately after dissociation, showed no significant effect (1, 10, 100, 500ng/ml, n=8 per concentration with quadruplicates per treatment (One-way ANOVA, p=0.58). NGF alone (used as a positive control for each experiment, see Methods) and in combination with BTC showed a significant increase of neurite outgrowth compared to vehicle. Combined treatment of 100ng/ml BTC and 10ng/ml NGF was tested to examine if BTC can potentiate or reduce the growth promoting effect of NGF. However, the combination of BTC and NGF did not alter neurite growth in comparison to NGF alone (Figure 4.9.) (n=8 per concentration with quadruplicates per treatment, One-way ANOVA; vehicle to NGF/BTC with NGF alone, Tukey's post hoc analysis, p=0.003).

Additionally, treatment with BTC did not affect cell numbers (n=8 per concentration with quadruplicates per treatment,, One-way ANOVA, p=0.802) (Figure 4.9.).

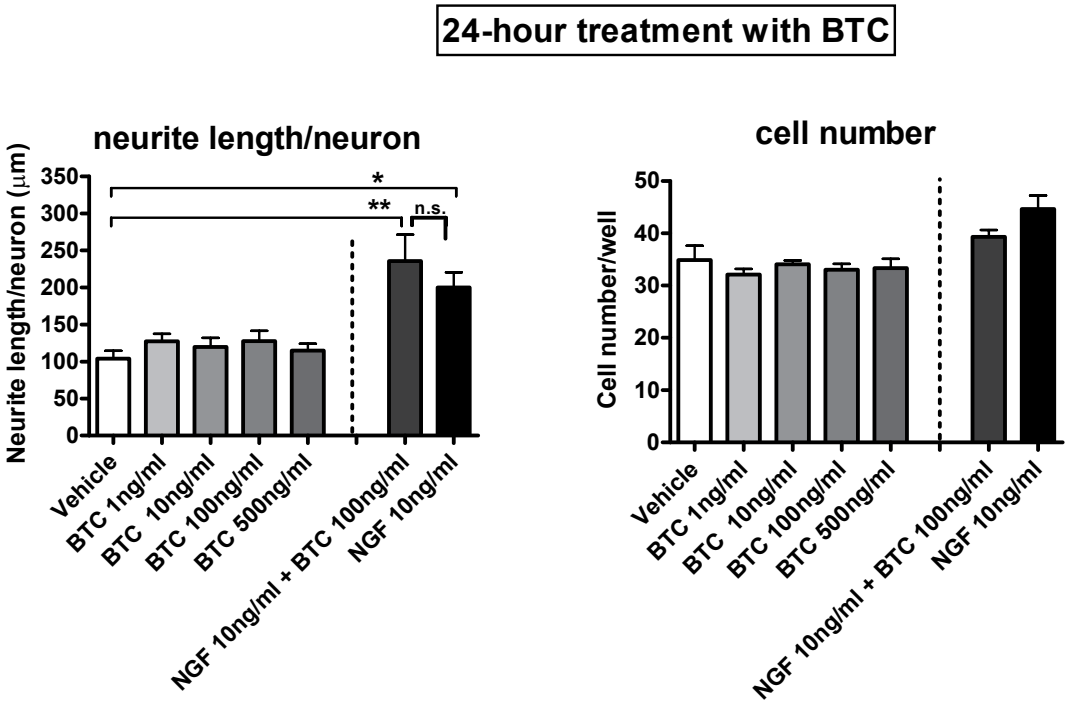

Figure 4.9. BTC has no effect on neurite length or cell number. Neurite length per neuron in BTC treated neurons (1, 10, 100, 500ng/ml, n=8 per concentration, One-way ANOVA, p=0.58). Absolute cell number per well for BTC treated neurons ((n=8 per concentration with quadruplicates per treatment, One-way ANOVA, p=0.802). NGF treatment was used as a positive control, which showed a significant difference compared to vehicle, both alone and in combination with BTC. However, the combination of BTC and NGF did not alter neurite growth in comparison to NGF alone (n.s.: not significant).

As described before, the method used to determine changes in neurite outgrowth has limited sensitivity when cells are cultured for a long period. Growth factors produced by neurons and non-neuronal cells can account for changes independent of exogenous growth factor treatment. Stimulating cells for longer than 48 hours produced variable results and the excessive neurite growth obscured the analysis. However, to test whether neurite outgrowth can be altered by BTC after cells have adapted to culture conditions, cells were cultured for 24 hours and then stimulated with BTC for another day. As shown in Figure 4.10., neurite outgrowth is not affected by BTC in this delayed treatment paradigm (Figure 4.10.) (n=4 with quadruplicates per treatment,,

One-way ANOVA p=0.22). Yet, treatment with NGF had a positive effect, although this finding was not significant (n=4 with quadruplicates per treatment,, unpaired t-Test p=0.0647). Interestingly, treatment with the two higher doses of BTC (100, 500ng/ml), induced a significant increase in cell number (n=4 with quadruplicates per treatment, One-way ANOVA, Tukey's post hoc analysis p=0.0012); NGF administration had no effect on cell numbers (Figure 4.9.)

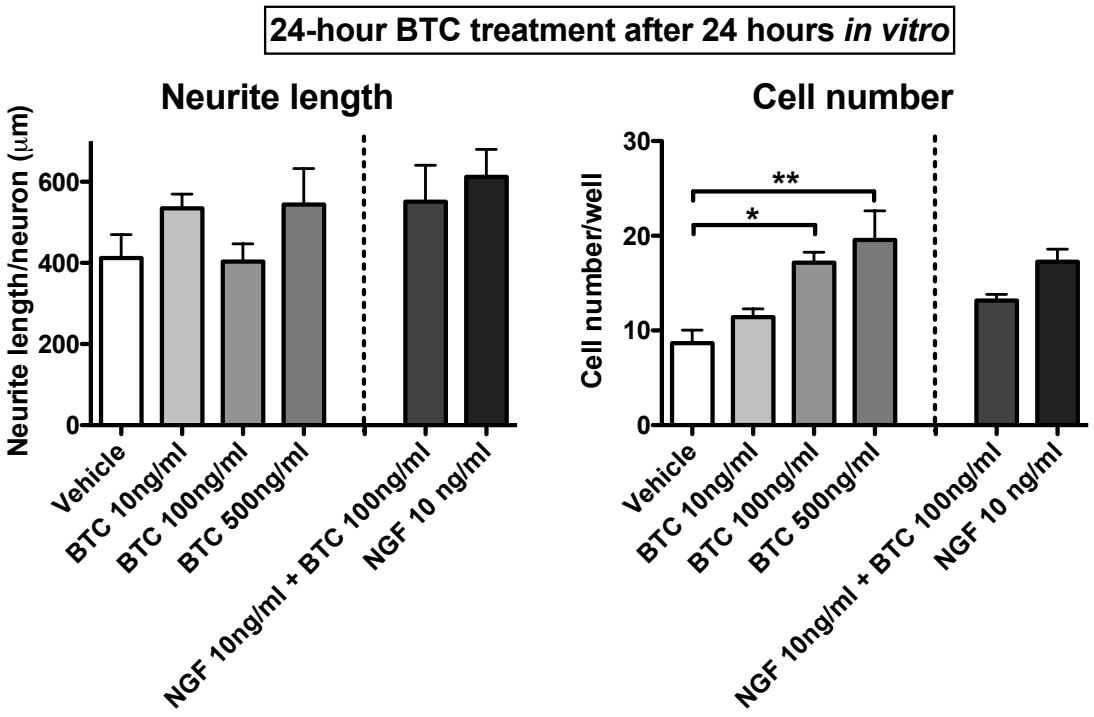

Figure 4.10. Neurite length and cell number with delayed BTC treatment. Cells were treated for 24 hours with BTC after 1 day in culture. Neurite length in BTC treated neurons. (n=4 with quadruplicates per treatment, One-way ANOVA, p=0.22, NGF versus vehicle unpaired T-Test p=0.0647) and absolute cell number (n=4 with quadruplicates per treatment, One-way ANOVA, Tukey's post hoc analysis p=0.0012).). NGF treatment was used as a control, and showed no significant difference compared to vehicle.

In addition, five other ligands of the EGFR family, EGF, EREG, AREG, HB-EGF, TNF-α were examined regarding their ability of affecting neurite outgrowth or cell number alteration. Cells were treated for 24 hours immediately after plating. No effects of either EGFR ligand treatment have been seen in neurite outgrowth (n=3, quadruplicates per treatment, One-way ANOVA with Tukey's post hoc analysis, $p<0.0001$) or cell number (n=3, quadruplicates per treatment, One-way ANOVA, $p=0.88$). NGF was used as a positive control (Figure 4.11.).

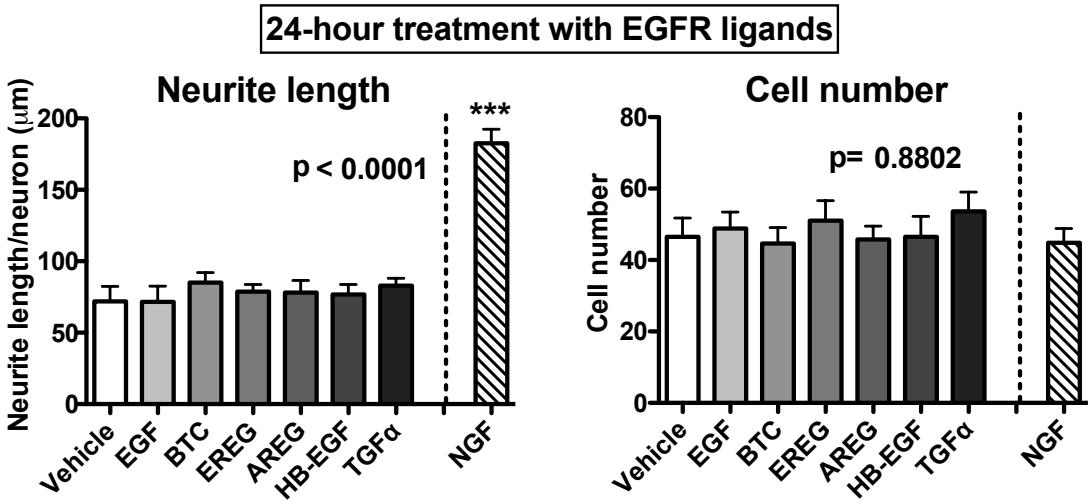

Figure 4.11. Neurite outgrowth with EGFR ligands. Graphs represent neurite length/neuron and cell number per image after 100ng/ml of each EGFR ligand. NGF was used as a positive control. Data was analysed using One-way ANOVA with Tukey's post hoc analysis (n=3 per group, quadruplicates per treatment); p-values are stated in the respective graph. NGF treatment was used as a positive control, which showed a significant difference in neurite length compared to vehicle.

4.3.3. Gefitinib inhibits ERK phosphorylation in sensory neuronal cultures *in vitro*

In Chapter 3 (Figure 3.9. and Figure 3.11.), I used the EGFR inhibitor Gefitinib following injury, working under the hypothesis that EGFR inhibition affects sensory thresholds. To validate the activity of the inhibitor at least *in vitro*, I tested its ability to block ERK activation following stimulation with BTC in DRG neuronal cultures cultured for 24 hours. Cells were pre-treated with Gefitinib (1mM) for 30 minutes in serum-free conditions, followed by stimulation with BTC (100ng/ml). EGF (100ng/ml) was used as a positive control (Figure 4.12. B). Western-blot analysis indicated that BTC activates ERK in a time-dependent manner. In the presence of Gefitinib, ERK phosphorylation is almost completely abolished in BTC-treated sensory neuronal cultures (n=3/group, One-way ANOVA with Tukey's post hoc analysis, p=0.05) (Figure 4.12. A). Gefitinib also reduced EGF-induced ERK activation (One-way ANOVA with Tukey's post hoc analysis, n=3/group p=0.089) (Figure 4.12. B).

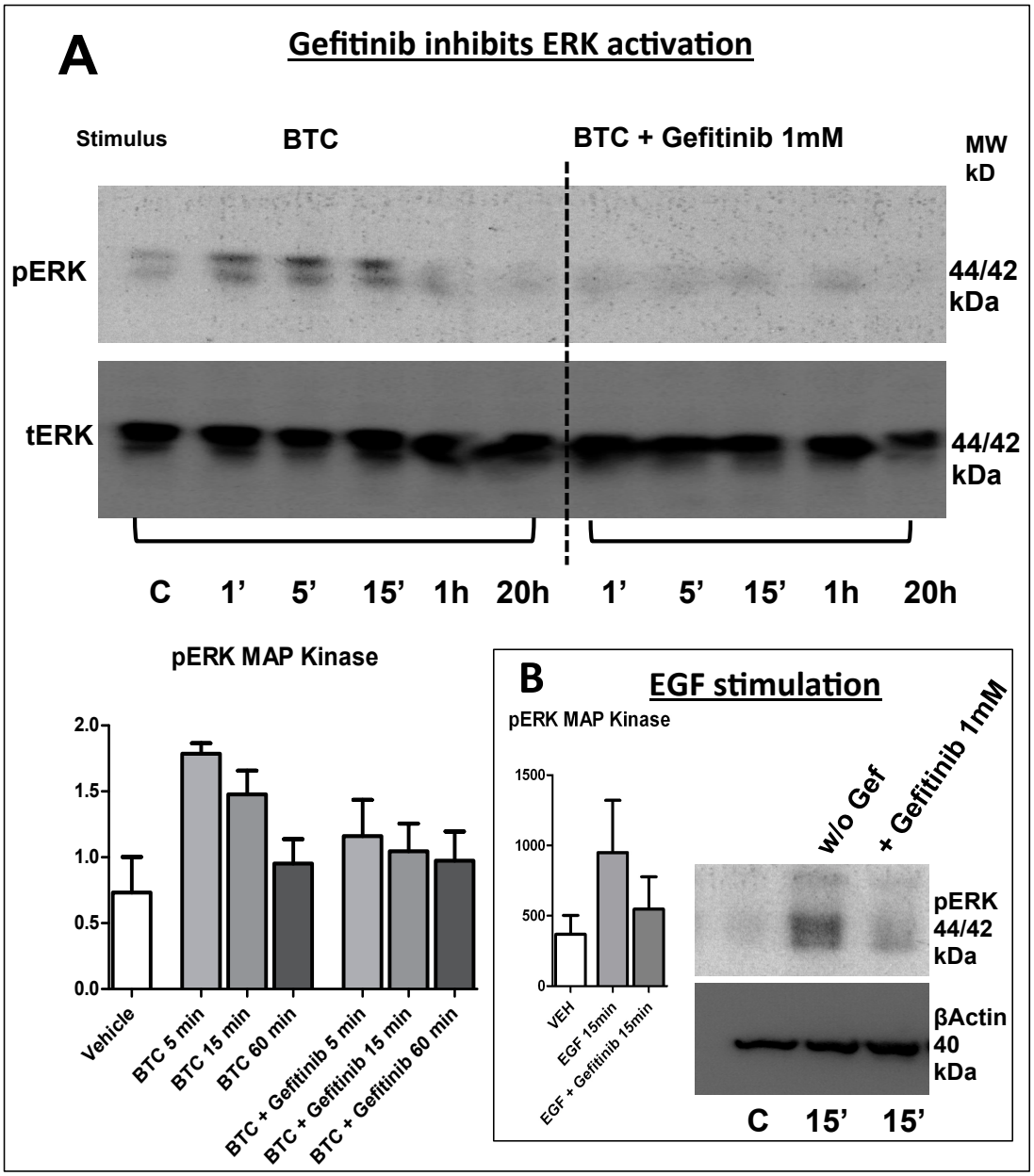

Figure 4.12. Gefitinib inhibits ERK activation in DRG neuronal cultures *in vitro.* Adult DRG neurons were stimulated for the indicated timepoints with either **A)** 100ng/ml BTC, **B)** 100ng/ml EGF or with **A)** 100ng/ml (10nM) BTC + 1mM Gefitinib. Control cells were not stimulated (labelled with C). Subsequently, protein extracts were immunoblotted with antibodies against p-ERK. ERK phosphorylation was quantified using densitometry. Values were normalised against total ERK and β-Actin (BTC treatment: One-way ANOVA with Tukey's post hoc analysis, n=3/group p=0.05; EGF treatment One-way ANOVA with Tukey's post hoc analysis, n=3/group p=0.089)

4.3.4. Effect of BTC on intracellular Calcium signalling

The intracellular Ca^{2+} concentration can be used to characterise a direct effect of tyrosine kinase receptor activation on Phospholipase C-γ (PLCγ) and Inositol-1,3,5-triphosphate (IP_3) mediated pathways (Scaltriti and Baselga, 2006). The dye Fura-2 was chosen based on its ability to bind to free intracellular Ca^{2+}. Fura-2 is first internalised as an acetomethyl-ester and then trapped in the cell after removal of the hydrophobic ester by intracellular esterases (Tsien, 1981). The ratio of the emissions at two wavelengths, 340nm and 380nm, is directly correlated to the intracellular calcium concentration. Using a ratiometric approach, compensates for loading variability and differences in cell size.

In DRG neurons a change of the intracellular Ca^{2+} concentration occurs very fast and can characterise a direct signalling mechanism, which is regulated by a complex system of Ca^{2+} channels (Grienberger and Konnerth, 2012).

To test whether BTC can activate calcium signalling in DRG neurons, cells were directly stimulated with either 100nM, 500nM or 1µM BTC for 1 minute, followed by a washout period of 2 minutes (Figure 4.13.). At these concentrations, BTC did not result in any increase of intracellular calcium. At the end of each stimulation, a high concentration of potassium chloride (KCl) (20 mM) was used as a positive control and only experiments with a positive response to KCl were included into the analysis.

Calcium responses were also tested in SCs following stimulation with BTC but with a different experimental setup. Cells were first treated with 10nM of BTC for 1 minute followed by a washout period of 2 minutes. The same cells were then treated with increasing concentrations of BTC (100nM, 1µM) (Figure 4.13.). None of the concentrations tested had an effect on intracellular calcium levels. SCs express purinergic receptors (Verkhratsky and Kettenmann, 1996) and therefore should respond with calcium signals following ATP stimulation. However, in the experimental setting used it was not possible to establish ATP as a positive control for calcium signalling in cultured SCs.

I also looked into the effect of BTC on calcium signalling in rat peritoneal macrophages. As for neurons and SCs, BTC at 100nM had no effect but ATP (25μM) showed a clear positive response. In addition to BTC five other EGFR growth factors were examined in macrophages regarding their ability to alter intracellular calcium levels, namely EGF, EREG, AREG, HB-EGF and TGFα (100nM per treatment) but no effect could be seen (Figure 4.13.)

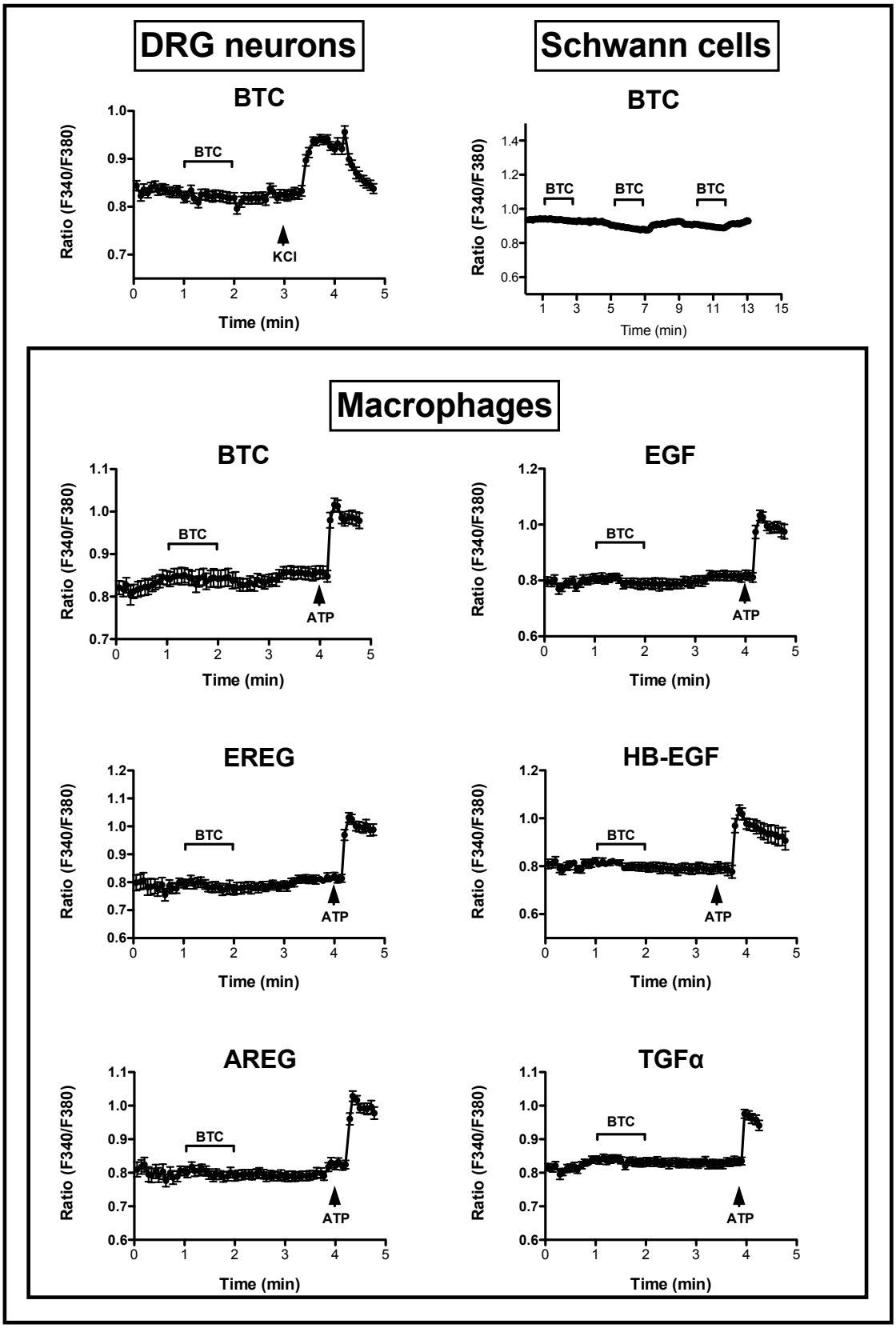
DRG neurons
Schwann cells
BTC
BTC
Ratio (F340/F380)
BTC
KCl
Time (min)
BTC
BTC
BTC
Time (min)
Macrophages
BTC
EGF
EREG
HB-EGF
AREG
TGFα
ATP
Time (min)

Figure 4.13. Calcium imaging *in vitro*. DRG neurons, SCs and macrophages do not respond with a intracellular Ca^{2+} response following BTC stimulation. (Top left) In the presented trace, neurons were treated with a single dose of 100nM BTC for 1 minute followed by a 2-minute washout period. Only cells with a positive response to 20mM KCl, which was used as a positive control, were included in the analysis. (bottom) Macrophages were treated with the same treatment regime, with ATP (25μM) as a positive control. SCs were treated with repetitive doses with increasing concentrations of BTC (10nM, 100nM, 1μM). All traces represent the arithmetic mean ± SEM for n=40 cells (DRG neurons), n=8-14 cells (macrophages), n=28 (SCs). Graphs represent data of one representative experiment.

4.3.5. Effect of BTC on Schwann cell function

SCs are the first cells responding following nerve injury and can participate in the inflammatory regulation (Meyer zu Horste 2008). In order to screen for a potential regulatory role of BTC on SCs, I tested the effect of the growth factor using a medium-throughput PCR array card for screening various inflammatory and growth factors released by SCs following nerve injury. Primary cultured SCs from postnatal (P5) rats were cultured for 5 days and following serum starvation, stimulated with BTC (100ng/ml) at two different timepoints (3 hours and 12 hours) evaluating acute and prolonged gene expression changes. mRNA expression of 96 genes, including chemokines, cytokines, and growth factors (Table 2) was evaluated.

Relatively few genes are differentially expressed in SCs following BTC stimulation. Hierarchical clustering of significantly regulated genes (One-way ANOVA with Bonferroni's multiple comparisons test, $p \leq 0.05$) using Pearson Correlation Coefficient revealed changes in IL16, β-Actin, HB-EGF and NRG at 3 hours after treatment (Figure 4.14.). I decided to validate IL16 (FC=42.1±17.2) , a cytokine with chemoattractive functions on CD4-bearing cells such as T-lymphocytes. IL16 also showed the highest fold change in the 3-hour timepoint. Nevertheless, validation with conventional RT-qPCR, did not show reproducible differences in IL16 levels following BTC stimulation (n=4 per group, One-way ANOVA, p=0.36) (Figure 4.14.). The increase of NRG, β-Actin and HB-EGF following BTC treatment also seemed particularly interesting, however, it has to be noted that fold changes, although significant (NRG, FC=1.2±0.17; β-Actin FC=1.16±0.15; HB-EGF FC=1.33±0.21), were so small, that its unlikely to be a biological effect, rather than a technical bias.

To investigate whether BTC has an effect on fundamental Schwann cell physiology, mRNA levels for myelin basic protein (MBP) were examined but showed no difference following BTC stimulation (n=4 per group, One-way ANOVA, p=0.19) (Figure 4.14.).

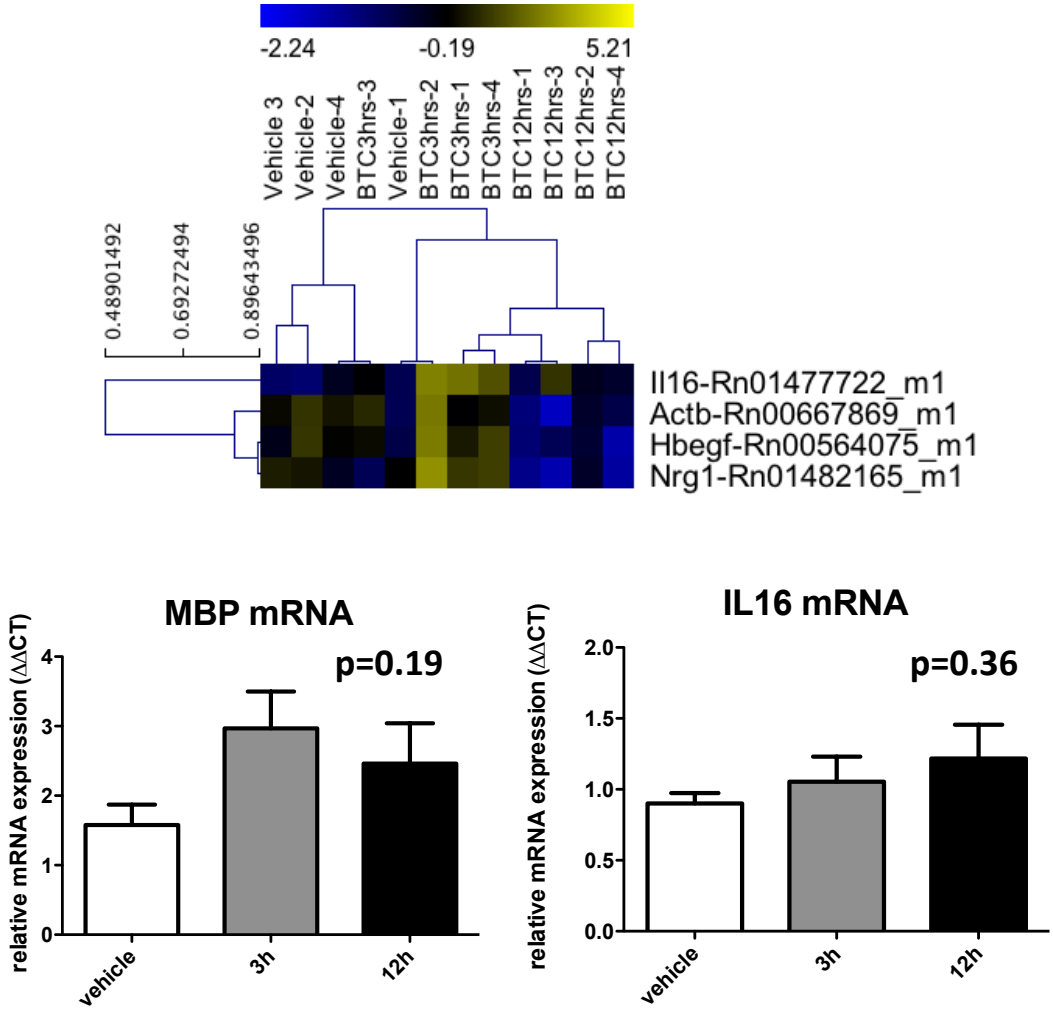

Figure 4.14. PCR array SCs stimulated with BTC. The dendrogram (top) displays hierarchical clustering analysis (Pearson correlation coefficient) of the differentially expressed genes in SCs treated with BTC (100ng/ml) for 3 hours, or 12 hours. Differences in spectral counts are color-coded as indicated. Displayed are n=4 per group of statistically significant gene changes. Validation RT-qPCR (bottom right) for IL16 gene changes 3 hours and 12 hours following BTC stimulation (n=4 per group, One-way ANOVA, p=0.36). RT-qPCR for MBP (bottom left) expression at 3 hours and 12 hours following BTC stimulation (n=4 per group, One-way ANOVA, p=0.19)

For confirmation that primary cultured SCs express the EGFR, I stained cells, dissected at postnatal day 5, after they have been adapted to culture conditions for 5 days (Figure 4.15.). EGFR is found in all SCs whereas staining for ErbB4 with a commercially available antibody was unsuccessful.

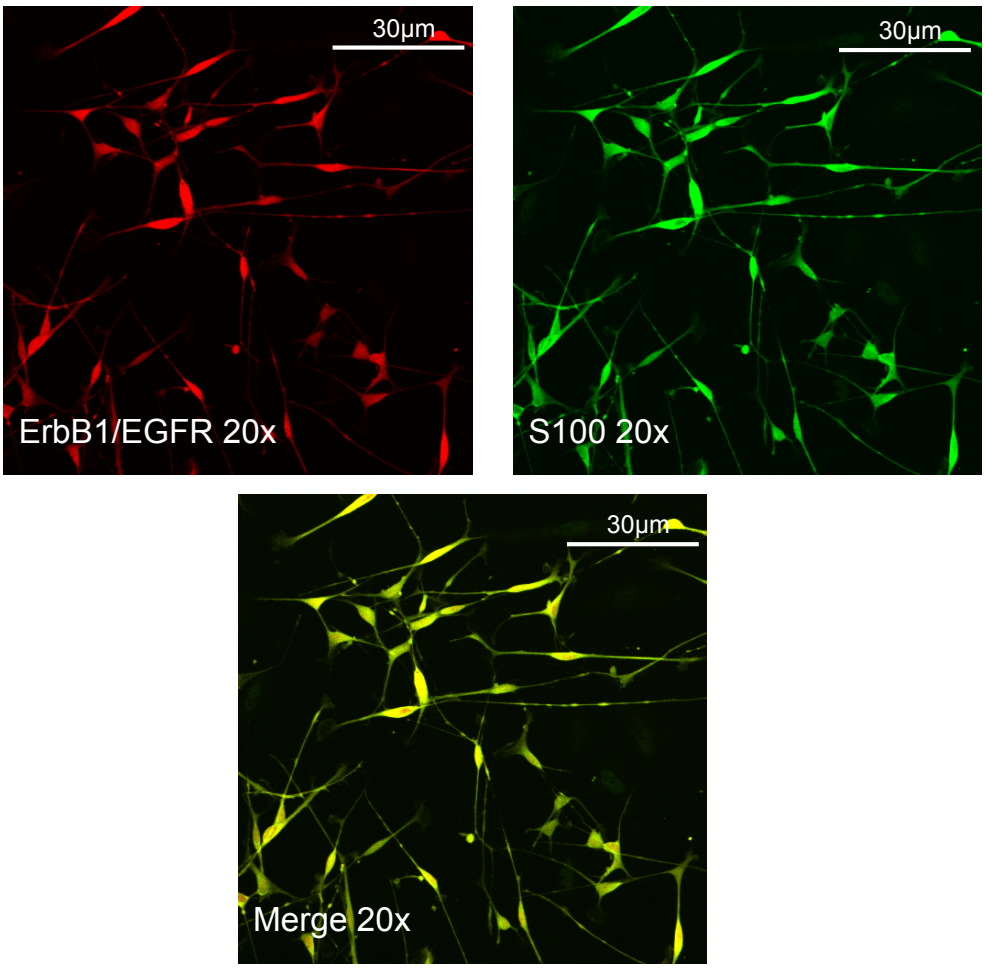

Figure 4.15. ErbB1 (EGFR) expression in SCs. Cells were cultured for 5 days and stained for ErbB1 (red), S100 (green), merged (bottom).

However, ErbB4 expression was found at the mRNA level. Using RT-qPCR I compared the ratio of C_T RG/C_T GOI (see Chapter 2.3.2.1.) as an estimate of baseline receptor expression (reference gene GAPDH). No difference could be observed comparing ErbB1 (EGFR) with ErbB4 expression levels (n=3, unpaired T-Test, p=0.3094) (Figure 4.16.).

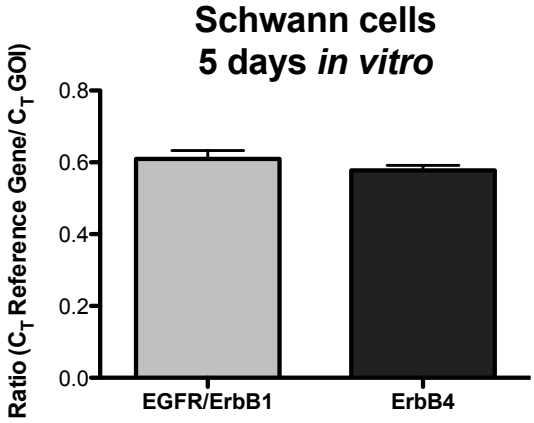

Figure 4.16. ErbB1 and ErbB4 expression in SCs 5 days *in vitro*. Estimation of baseline expression of ErbB1 (EGFR) and ErbB4 in primary cultured postnatal SCs presented as a ratio of C_T reference gene to C_T gene of interest. (n=3, unpaired T-Test, p=0.3094)

4.3.6. Effect of BTC on Macrophage function

Given the importance of macrophages in various processes following nerve injury, I designed experiments to study a possible role of BTC on macrophage function. Previously it was shown that stimulation of macrophages with BTC has downstream effects on the phosphorylation of MAPKs (Figure 4.4.). Since BTC expression is highest in the nerve following injury (Figure 2.12. Chapter 2.3.2.2.), I first looked into whether BTC plays a role in chemotaxis of macrophages to the injury site. As a model cell type, macrophages derived from the peritoneum of adult Wistar rats were used.

4.3.6.1. Chemotaxis in peritoneal macrophages

The chemotaxis response to BTC was assessed using a Boyden chamber. Cells migrated through a polycarbonate filter with a specific pore size across a concentration gradient of BTC. At two different concentrations (100 and 500ng/ml), BTC does not induce chemotaxis of peritoneal rat macrophages (n=5 per group, experiments were conducted in quadruplicates, One-way ANOVA, p=0.9609) (Figure 4.17.).

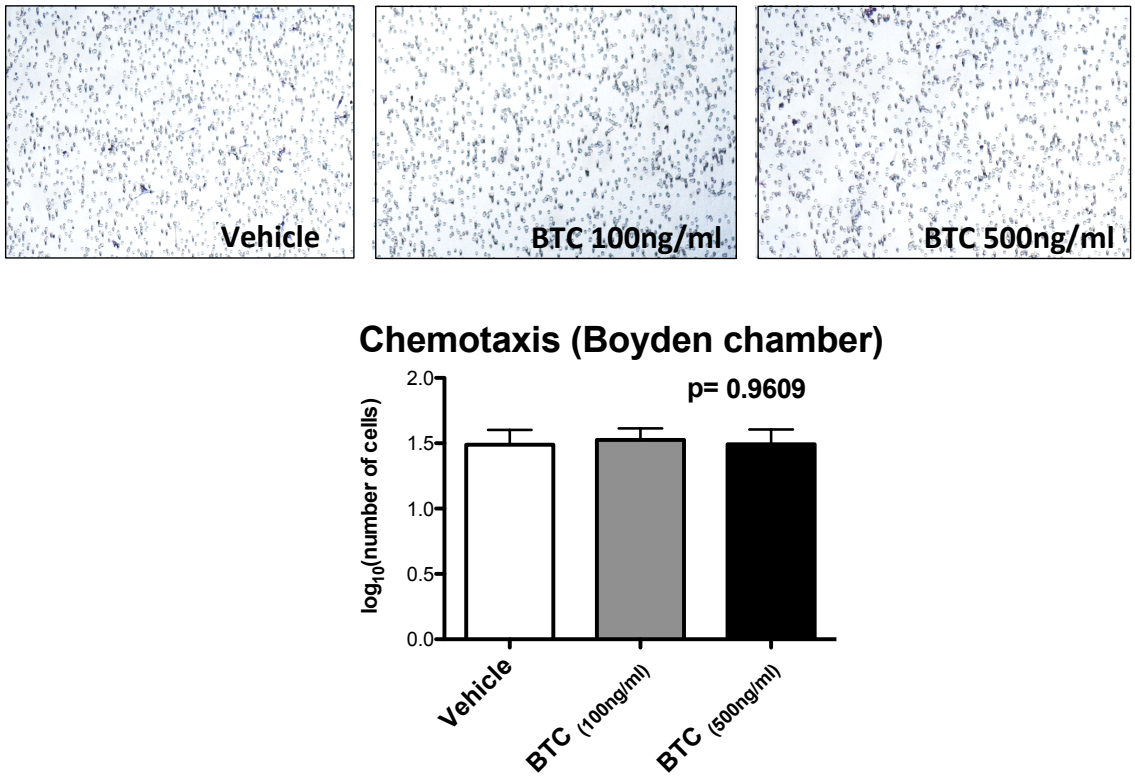

Figure 4.17. Chemotaxis assay peritoneal macrophages. BTC does not affect chemotaxis in peritoneal macrophages. Presented are example pictures for two different concentrations of BTC (100ng/ml and 500ng/ml) and quantification (n=5 per group, experiments were conducted in quadruplicates, One-way ANOVA, p=0.9609).

4.3.6.2. Chemoattractive properties of BTC *in vivo*

It is known that different populations of macrophages reside in different tissue microenviroments (Gordon and Taylor, 2005). Because it was not possible to observe a clear chemotactic effect of BTC on macrophages using primary cultured peritoneal cells, I decided to investigate chemotaxis *in vivo.* BTC (100ng) was mixed with 0.5ml of liquid Matrigel and was then subcutaneously applied to form a solid pouch (Kim et al., 2003) Matrigel is a mix of basement membrane proteins, such as laminin (60%) and collagen IV (30%) and has the ability to bind and release growth factors. 10 days after injection pouches were extracted and used for immunohistochemistry and Western blot analysis. BTC induced a significant increase in ionised calcium-binding adapter molecule 1 (IBA1)-positive cells in the extracted Matrigel (n=3, unpaired T-Test, $p<0.001$)

(Figure 4.18. A, B). Immunoblotting of protein extracts showed an increase of IBA1 protein expression in the BTC treated group (n=3, unpaired T-Test, p<0.001) (Figure 4.18. C, D).

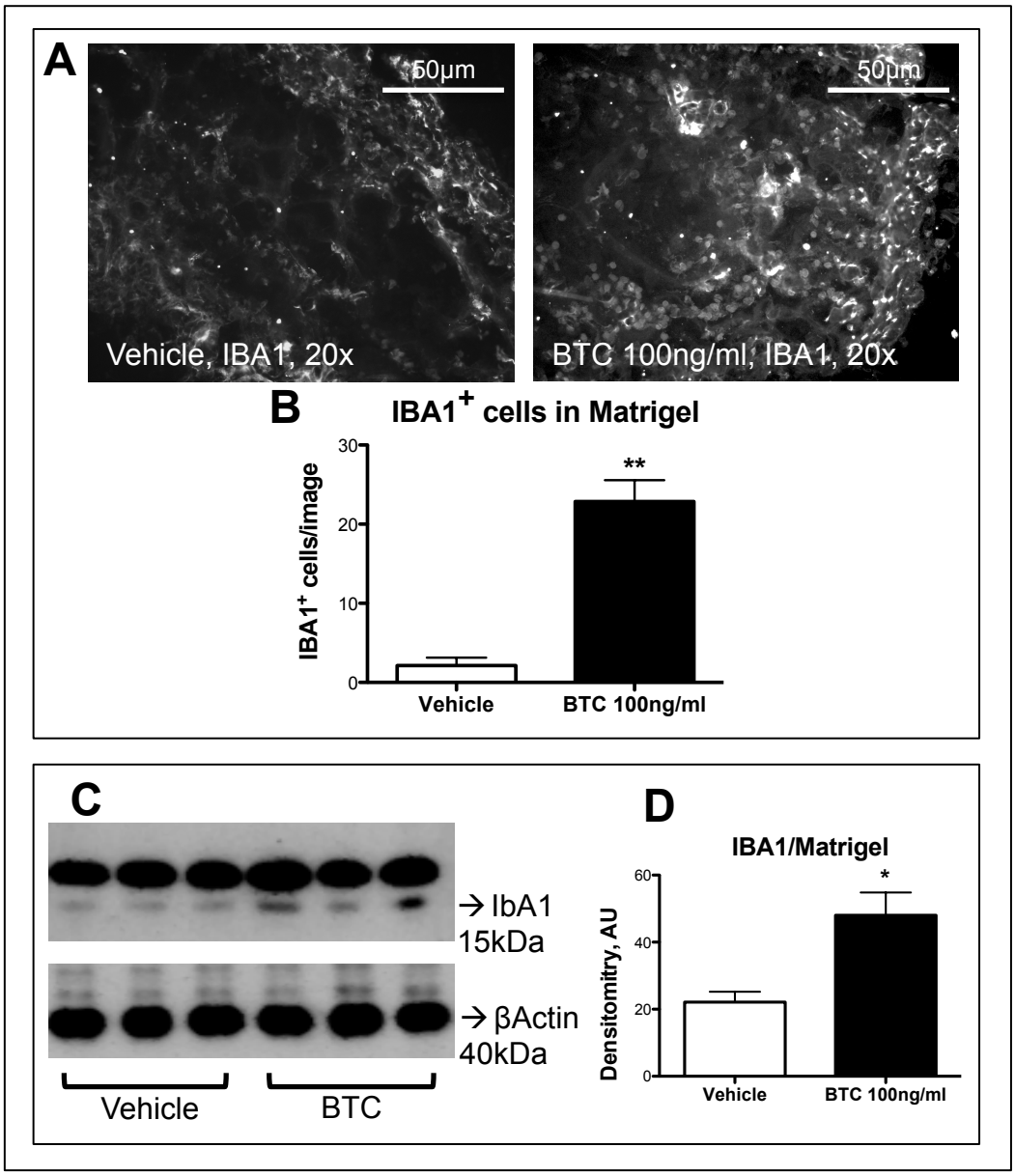

Figure 4.18. BTC increased IBA1 positive cells *in vivo*. A) Example pictures of Matrigel stained for IBA1. **B)** shows quantification of IBA1 positive cells in Matrigel after 10 days *in vivo* (n=3, unpaired T-Test, p<0.001). **C)** immunoblot stained for IBA1; quantification in **D)** (n=3, unpaired T-Test, p<0.025).

4.3.6.3. Monocyte scavenger receptor 1B, CD36 is modulated by BTC

The other main function of macrophages in the peripheral nerve is the phagocytosis of myelin debris following injury. Phagocytosis is mediated by scavenger receptors such as CD36 and CD68 as well as other complex mechanisms for the recognition of degenerated cellular material (Silverstein and Febbraio, 2009). Other receptors involved are complement C3 (CD11b/CD18), Fc receptors (CD16, CD32) and the lipoprotein receptor (LRP-1) (Flannagan et al., 2012; Hirata and Kawabuchi, 2002; Rotshenker, 2011). Given its prominence in phagocytosis and the availability of appropriate expertise and reagents in our lab, I decided to examine the expression of CD36. Since CD36 expression could change depending on the activation state of macrophages, I chose to study the effect of BTC in THP-1 cells, a human monocytic cell line, which closely resembles the phenotypic features of naïve, unpolarised monocytes. THP-1 cells are maintained in suspension and do not produce inflammatory cytokines. In addition, THP-1 cells are highly phagocytic and are often used to study macrophage function. After serum starvation cells were treated with BTC (100ng/ml) for 24 hours. Cells were also treated with either LPS (100ng/ml) to induce classic inflammatory activation or with a combination of LPS and BTC. Protein extracts were immunoblotted for CD36 and COX-2, a prominent inflammatory response gene. THP-1 cells express CD36 at baseline and interestingly, its expression was significantly decreased following BTC treatment similar to the effect observed with LPS (n=3-4 per group, One-way ANOVA with Tukey's post hoc analysis, p= 0.0002) (Figure 4.19. A). Given their resting baseline, THP-1 cells did not express COX-2 until inflammatory activation with LPS. BTC did not affect its baseline levels or its induction by LPS. In order to test CD36 modulation in primary cells, bone-marrow derived and peritoneal macrophages were used. Bone marrow derived macrophages, which are unpolarised, express CD36 and it could be demonstrated that expression levels were decreased by BTC (Figure 4.19. B). However, it was not possible to detect CD36 expression in peritoneal macrophages by Western-blot analysis. To investigate this further, I examined CD36 mRNA levels by RT-qPCR. Analysis revealed that BTC does not effect CD36 expression but these results should be considered with caution since baseline expression of the receptor was very low (~34 C_T) (Figure 4.19. C).

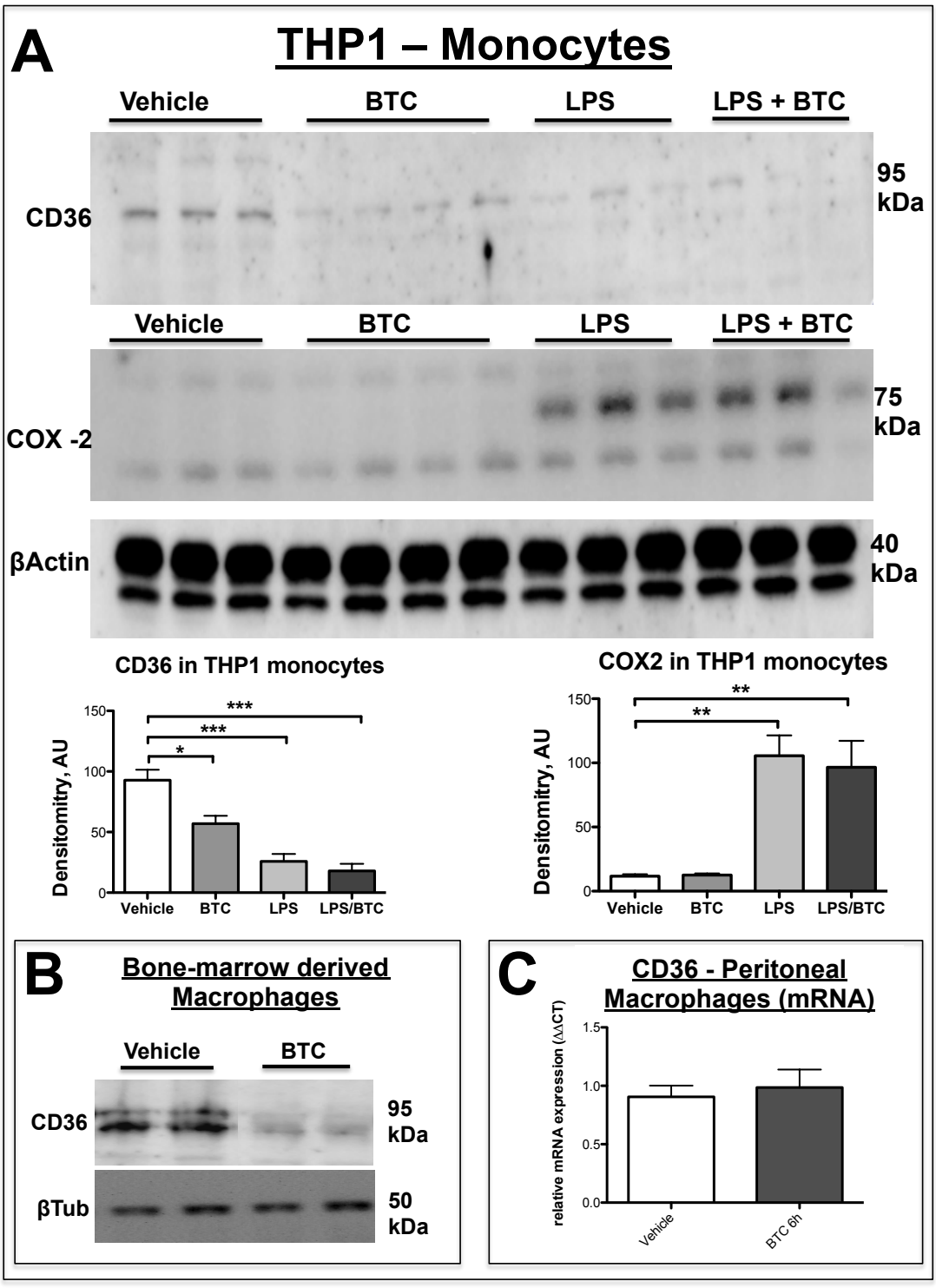
A
THP1 – Monocytes
Vehicle
BTC
LPS
LPS + BTC
CD36
95 kDa
Vehicle
BTC
LPS
LPS + BTC
COX -2
75 kDa
βActin
40 kDa
CD36 in THP1 monocytes
Densitomitry, AU
150
100
50
0
***
***
*
Vehicle
BTC
LPS
LPS/BTC
COX2 in THP1 monocytes
Densitomitry, AU
150
100
50
0
**
**
Vehicle
BTC
LPS
LPS/BTC
B
Bone-marrow derived Macrophages
Vehicle
BTC
CD36
95 kDa
βTub
50 kDa
C
CD36 - Peritoneal Macrophages (mRNA)
relative mRNA expression (ΔΔCT)
1.5
1.0
0.5
0.0
Vehicle
BTC 6h

Figure 4.19. CD36 Modulation in macrophages by BTC. A) BTC (100ng/ml) decreases CD36 protein levels in THP-1 monocytes. The levels of COX-2 were instead unaffected. Cells were also stimulated with LPS for comparison. Results were quantified by densitometry (n=3-4, One way ANOVA with Tukey's post hoc analysis, CD36 p=0.0002, COX-2 p=0.0003). **B)** In mature bone marrow derived macrophages, BTC decreases CD36 protein. **C)** mRNA levels of CD36 in mature peritoneal macrophages following BTC stimulation (100ng/ml) for 6 hours.

4.3.7. BTC and scavenger receptor expression following nerve injury

In chapter 2, I demonstrated increased expression of BTC (Figure 2.11.) in injured nerve. I subsequently wanted to relate these changes to alterations in macrophage markers. Macrophage infiltration following L5 SNT was confirmed by measuring the expression of IBA1 in sciatic nerve tissue. mRNA was extracted from sciatic nerve at three different following L5 SNT. IBA1 levels are highest at day 3, suggesting that, macrophage infiltration peaks at 3 days post-injury. IBA1 is then progressively reduced, possibly due to resolution of the acute inflammatory response (Figure 4.20. A) (n = 3-6, One-way ANOVA with Tukey's post hoc analysis, p=0.0026. These data confirm the generally accepted notion of macrophage infiltration (Rotshenker, 2011) following injury. For comparison the BTC expression following L5 SNT is plotted (identical to Figure 2.11.).

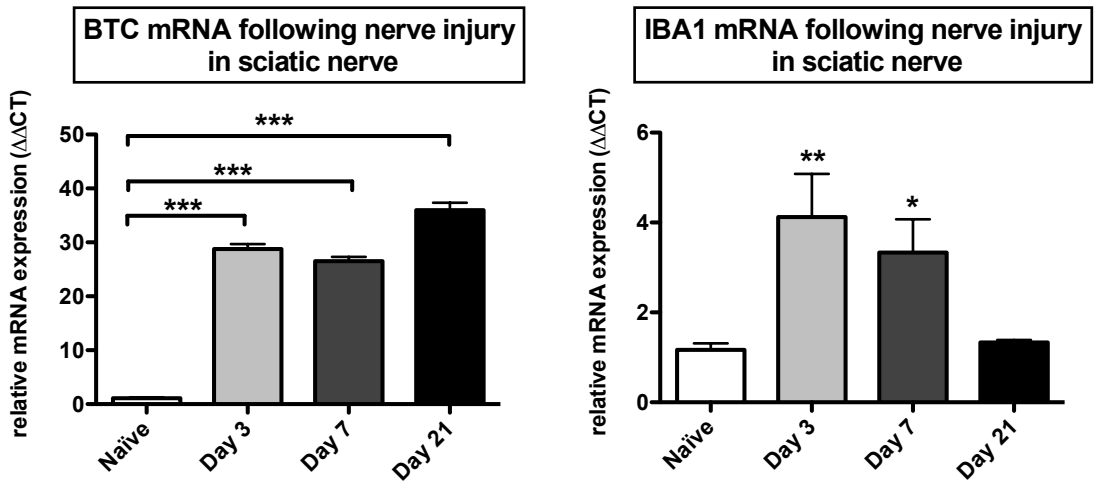

Figure 4.20. IBA1 and BTC following SNT. IBA1 and BTC mRNA levels change in the sciatic nerve following injury. Left, relative BTC expression at different timepoints (3, 7, 21 days) following injury (n=3-4 per group, One-way ANOVA with Tukey's post hoc analysis, p<0.001; identical to Figure 2.11.) and right, relative IBA1 expression at the same timepoints (n=3-4 per group, One-way ANOVA with Tukey's post hoc analysis, p<0.0026).

I then attempted to validate IBA1 and BTC expression, at the protein level. This was particularly important for understanding the functional properties of BTC in the injured tissue, e.g. is the growth factor present as a pro-form or as a mature protein? Protein was extracted from sciatic nerve tissue in 0.2% SDS extraction buffer (Table 5) 14 days post-injury and Western blot analysis was performed. At the site of injury (ipsilateral) IBA1 increased, as expected, indicating macrophage infiltration in the injured nerve (n=3, unpaired T-Test, p=0.031). For comparison, the contralateral nerve showed no increase in IBA1 (Figure 4.21.).

When I probed the same membrane, using an antibody that recognises the processed, mature form, I found strong immunoreactivity at around 26kDa. This was increased ipsilaterally, although it did not reach significance (n=3, unpaired T-Test, p=0.222). This could be the major fragment of the mature growth factor. ADAM10 is responsible for processing BTC (Sahin et al. 2004) from pro-BTC (40kDa). It generates a major (26–28kDa), two minor (20 and 15kDa) soluble forms and a cellular remnant lacking the ectodomain (12kDa) (Sanderson et al., 2005). I was not able to consistently detect the major fragment of BTC (26kDa) in the sciatic nerve (Figure 4.21.). Interestingly, the antibody was able to detect the recombinant mouse BTC at 9kDa (the same preparation used in stimulation experiments described above), run on adjacent lanes. This data raises interesting questions. It was possible to detect one fragment (26kDa) of the mature protein *in vivo* at the selected time point, suggesting soluble BTC protein in the nerve. Alternatively, it could be also possible that the antibody detects a non-specific antigen at 26kD and fragments of the mature form are not retained in the extracellular space due to its small size.

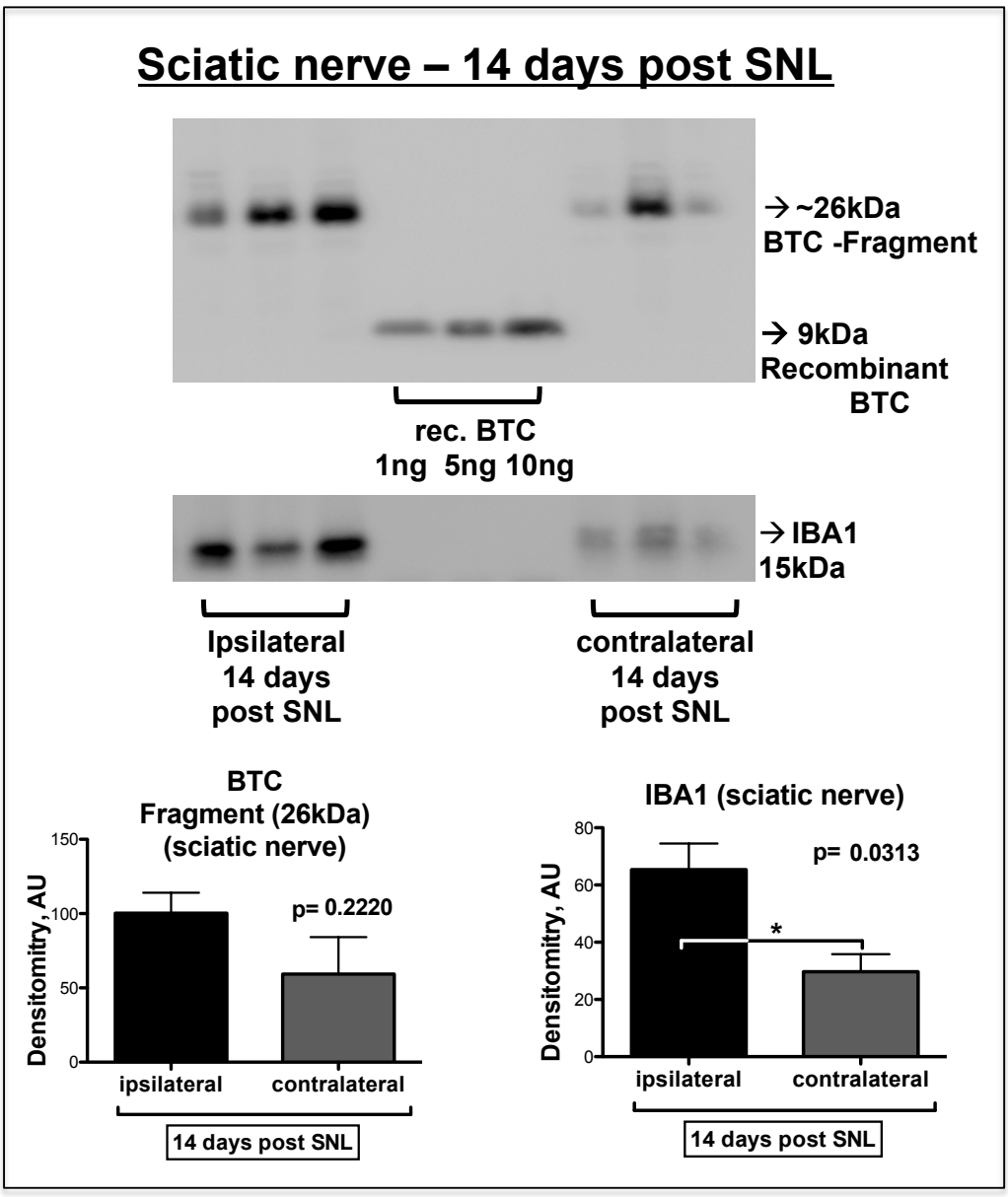

Figure 4.21. Protein levels of BTC 14 days following nerve injury. Western Blot for BTC in the sciatic nerve 14 days following injury. (post SNL). The 26kDa fragment of mature BTC was detectable and showed an increase in the ipsilateral side, although not significant. Densitometry of 26kDa-BTC (p=3, unpaired T-Test, n=0.22). For comparison 3 concentrations (1, 5, 10ng/ml) of recombinant BTC (9kDa). The same membrane was incubated with antibodies for IBA1. Densitometry for IBA1 (p=3, unpaired T-Test, n=0.0313) sciatic nerve.

In order to test the effect of EGFR inhibition on macrophage infiltration, IBA1 levels were examined in the injured tissue in animals treated with Gefitinib; mRNA expression was tested after 14 days. This timepoint was selected because the reproducible pain phenotype observed previously (see, Figure 3.11.) and to be comparable with Gefitinib treatment regimes, used before. It could be shown that inhibition of the EGFR via Gefitinib had no effect on the expression of IBA1 (n=3-4 One-way ANOVA with Tukey's post hoc analysis, p=0.001) (Figure 4.22. top).

It was demonstrated that in THP-1 monocytes and bone marrow derived macrophages the expression of CD36 following BTC stimulation decreases *in vitro* (Figure 4.18.), which brings up the question what is the expression level of CD36 in the nerve following injury?

Surprisingly, mRNA levels of CD36 are reduced after injury (3, 7, 21 days), which negatively correlates with the expression of IBA1 (n=3-4, One-way ANOVA with Tukey's post hoc analysis, p=0.0026) indicating phenotypic modulation of macrophages at the site of injury. CD36 expression is minimum at 3 days and progressively recovers to 50% of baseline expression after 21 days (n=3-4, One-way ANOVA with Tukey's post hoc analysis, p=0.0007) (Figure 4.22.). Interestingly, EGFR inhibition rescues the loss of CD36 at the 14-day time point. Is it possible that BTC or another EGFR ligand regulate, at least in part, the expression of CD36 in the nerve after injury. Interestingly, the expression of the other scavenger receptor CD68 (ED1) followed exactly the same trend (n=3-4, One-way ANOVA with Tukey's post hoc analysis, p=0.0164) (Figure 4.22.).

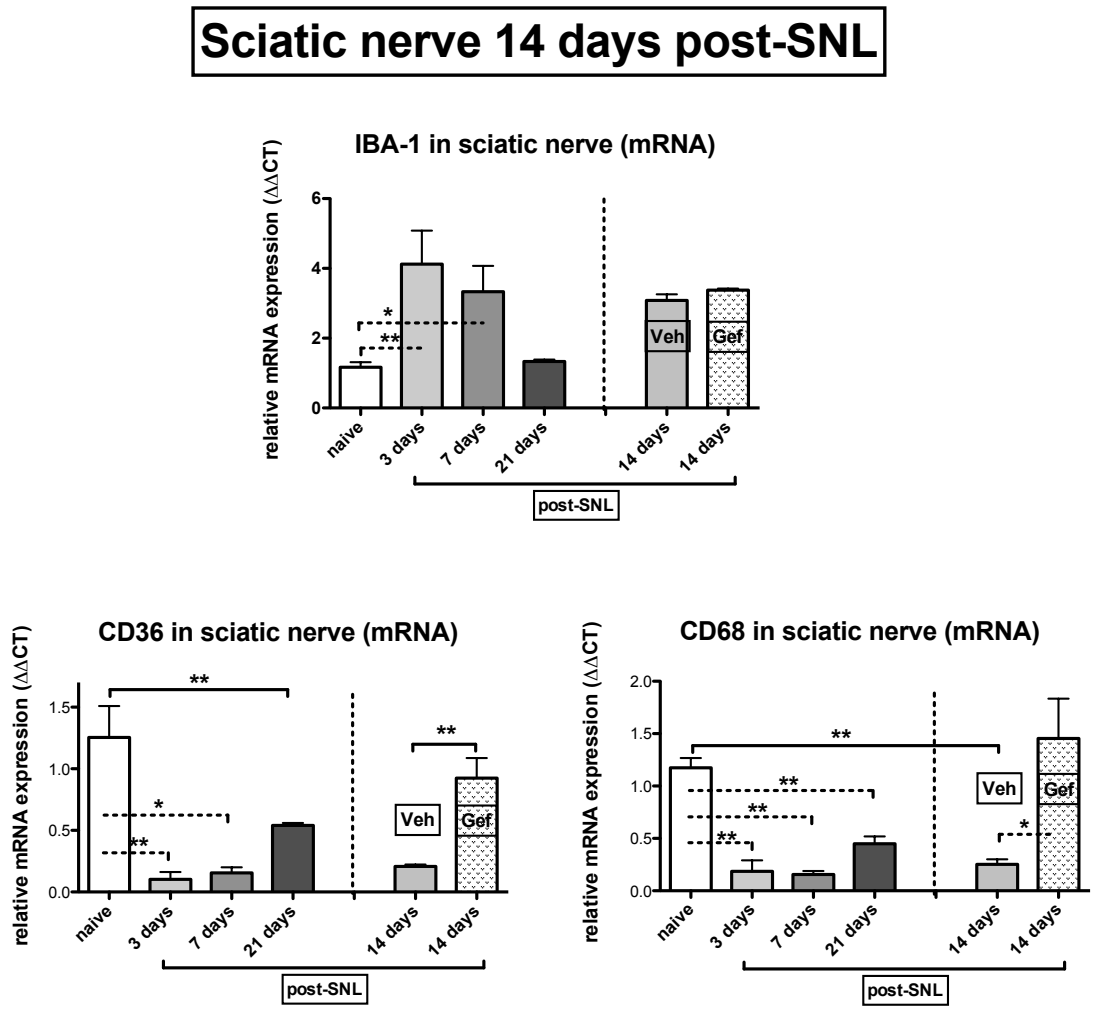

Figure 4.22. IBA1, CD36 and CD68 expression in the nerve post SNL. Top, relative expression levels of IBA1 at different timepoints (3, 7, 21 days) in the sciatic nerve following injury and at day 14 following injury +/-Gefitinib treatment (n=3-4, One-way ANOVA with Tukey's post hoc analysis, p=0.0026). Bottom, relative expression levels of CD36 (n=3-4, One-way ANOVA with Tukey's post hoc analysis, p=0.0007) and CD68 (n=3-4, One-way ANOVA with Tukey's post hoc analysis, p=0.0164) at the same timepoints following injury.

4.4. Discussion

In this chapter I described different *in vitro* assays, based on cell types involved in the process of peripheral nerve injury, to find a potential function for BTC.

First, to establish functionality of receptors in DRG neurons, and macrophages, I examined MAPK activation following BTC stimulation. BTC activates ERK and p38 in primary cultured DRG neurons and peritoneal macrophages. However, BTC did not induce EGFR phosphorylation. Activation of the EGFR was only seen after stimulation with recombinant EGF, suggesting that BTC is acting via an alternative ErbB receptor (Sahin et al. 2004). The interaction of EGFR ligands and ErbB receptors is known to be complex. Both low and high affinity receptor populations exist, which have distinct effects depending on the specific ligand (Ullrich and Schlessinger, 1990). EGFR ligands form heterodimers consisting of all four ErbB receptors with distinct functional outcome. BTC signals mainly via ErbB1 (EGFR) and ErbB4 but each receptor can form heterodimers with ErbB2 or ErbB3 (Jones et al., 1999). My data suggests that BTC is acting via a homodimer of ErbB4 or heterodimers of ErbB4 together with ErbB2 or ErbB3, also a ErbB2/ErbB3 dimer has been described to act a main receptor (Alimandi et al., 1997). However, both BTC and EGF activate ERK and p38, suggesting that the signalling effect might be the same.

To examine whether BTC is a neurotrophic factor, I tested neurite outgrowth in cultured DRG neurons. I optimised an automated microscope and image analysis system for measuring neurite outgrowth in adult sensory neurons. This system has been reported to measure neurite outgrowth in cerebellar granule cells (Hutson et al., 2011) and Neuro-2a cells, a neuroblastoma derived cell line from mice (Ramm et al., 2003).

I optimised the system for adult sensory neurons and used NGF as a positive control, as it is known to enhance neurite outgrowth (Lindsay, 1988). BDNF was also able to increase neurite outgrowth, confirming findings by other groups (Kimpinski et al., 1997; Lindsay, 1988). No effect on cell survival of adult sensory neurons was observed over 24 hours. In developing, but not adult neurons, it has been shown that neurotrophic factors, such as NGF can promote survival via activation of p75 (Barrett and Bartlett, 1994) or TrkA

receptors (Patapoutian and Reichardt, 2001). I found that this automated system could be beneficial to characterise the effect of neurotrophic factors on neurite outgrowth and cell survival of adult sensory neurons *in vitro,* and I am currently in the process of publishing this work.

In contrast to NGF and BDNF, the EGFR ligands, did not affect neurite outgrowth in adult neurons *in vitro*. Evidence from published literature is puzzling. Although, a neurite growth promoting effect has been described for EGFR activation in a model system (the mollusk *Lymnea stagnalis,* (Hermann et al., 2005)), in mammals it was shown that local administration of EGFR inhibitors increased neurite regeneration of injured optic nerve fibers, pointing towards a promising therapeutic option for enhancing axon regeneration after injury (Koprivica et al., 2005).

24-hour treatment with BTC had no effect on DRG cell numbers, however, after 48 hours there was a significant increase in the number of viable cells in comparison to vehicle treatment. This effect suggests that BTC was able to decrease the neuronal cell death occurring during the 48-hour culture. This finding suggests a neuroprotective effect of BTC, which needs to be further evaluated. In the context of nerve injury, the increase in BTC could suggest a role as an endogenous neuroprotective factor. Interestingly, Kim et al, reported that BTC can increase endothelial cell survival by activation of MAPKs, PI3 Kinase and Akt and consequently promote angiogenesis (Kim et al., 2003).

In this chapter I briefly examined the effect of BTC on SCs, after establishing their isolation and culture from postnatal sciatic nerves in the group. Given time I would have liked to extend these studies (see Future directions). SCs are known to produce cytokines, chemokines and growth factors following injury and can have antigen-presenting properties (Meyer zu Horste et al., 2008). BTC did not affect expression of inflammatory mediators and it did not alter the expression of MBP, the main myelin protein. It has to be noted that the postnatal SCs that I used *in vitro*, might respond differently than mature SCs *in vivo*, especially following injury. Interestingly, it was previously shown that BTC promotes Schwann cell migration *in vitro* suggesting that the growth factor could influence Schwann cell function following nerve injury (Byer et al., 2013).

The recruitment of macrophages and phagocytosis of myelin in the injury site is regulated by a complex system of mediators. By using Matrigel, I showed that BTC-infused Matrigel had a greater number of IBA1 positive cells in comparison to plain Matrigel. This data suggests that BTC could act as a macrophage chemottractant *in vivo.* Although a chemotactic effect for BTC has been proposed in endothelial cells (Kim et al., 2003) and vascular smooth muscle cells (Mifune et al., 2004) this is the first time that BTC appears to affect migration of macrophages. Interestingly, I was not able to show a chemoattractive effect in peritoneal macrophages using the Boyden chambers. This could be explained by functional differences of specific tissue specific macrophage subpopulations (Gordon and Taylor, 2005). Moreover, this could be an *in vitro* limitation; perhaps to exert its full effect, BTC needs to act in concert with other factors present *in vivo*, especially following injury. This was partially addressed using the Matrigel model *in vivo*. Additionally, EGFR activation by EGF mediates monocyte chemotaxis (Lamb et al., 2004) in the setting of atherosclerotic plaque formation. The authors concluded, that other factors of the EGFR ligand family could affect recruitment of macrophages, but they did not provide any mechanistic evidence. It is an interesting hypothesis that BTC, which is highly expressed in the nerve following injury, modulates macrophage recruitment.

In this chapter I demonstrated that BTC reduces the expression of class B scavenger receptor, CD36 in a monocyte cell line but also in bone marrow derived macrophages. Scavenger receptors are essential effectors of the phagocytic machinery in macrophages. CD36 binds to a variety of ligands, such as oxidised LDL, anionic phospholipids, thrombospondin and collagen. It is expressed on macrophages but also on platelets, microvascular endothelial cells and in adipose tissue (Eto et al., 2003). CD36 functions as a myelin receptor due to the high anionic lipid binding capacity that could account for the extensive uptake of non-opsonised myelin (Mosley and Cuzner, 1996). Eto *et al*. demonstrated that CD36 knockout animals show delayed phagocytosis and subsequently delayed remyelination after a peripheral nerve crush injury, indicating that CD36 plays a role in the clearance of degenerated myelin (Eto et al., 2003). In the context of phagocytosis following apoptosis, CD36 and a lysosomal protein, CD68, are receptors for phosphatidylserine, released from apoptotic cells (Fadok et al., 1998). CD68 (also known as ED1 in the rat)

commonly used as a macrophage marker, is also expressed by non-professional phagocytes, such as SCs in nerves that undergo Wallerian degeneration (Kaiserling et al., 1993). Importantly, given its key role in lipid scavenging, CD36 has been studied extensively in atherosclerosis. It is one of the best markers of lipid-laden macrophages *in vivo* but whether its presence is protective or detrimental is still a matter of debate (Febbraio et al., 2000; Moore et al., 2005).

I showed that CD36 was downregulated at the mRNA level following nerve ligation. This was surprising, given the established consensus on the expression of classic macrophage markers following injury. Interestingly, inhibition of the EGFR using Gefitinib *in vivo,* rescued this effect. Therefore, it can be postulated that EGFR inhibition either affects expression of the scavenger receptor or impacts on the infiltration of $CD36^+$ cells. Yet, Gefitinib did not affect the expression of IBA1 in the injured nerve. Is BTC, at least in part, responsible for the modulation of CD36? In an attempt to address this, I tested the effect of BTC on cultured monocytic cells and found that the growth factor was able to reduce the protein levels of CD36. Interestingly, I was not able to detect CD36 protein in mature peritoneal macrophages and its mRNA expression was close to baseline (~34 cycles). The difference in receptor expression between primary monocytes and mature macrophages is interesting. Could this explain the loss of CD36 mRNA following nerve injury? Interestingly, Fernandez *et al.* showed that CD36 expression is reduced in macrophages stimulated with IFN-γ and LPS, to induce M1 polarization (Martinez et al., 2006). Similarly, I found that the unpolarised THP-1 monocytes, lost CD36 expression when stimulated with either BTC or LPS. Yet, BTC was not able to induce COX2, indicating that it is not a classic inflammatory mediator.

CHAPTER 5

General conclusion and future directions

5. General conclusions and future directions

5. 1. General Conclusion

The work presented in this thesis addresses expression changes and potential mechanisms of the EGFR ligand BTC and implicates the ErbB family of receptors in inflammatory modulation following peripheral nerve injury.

At the beginning of my studies, I screened the expression of cytokines, chemokines and EGFR ligands after peripheral nerve injury and found that BTC was highly regulated in the sciatic nerve at all timepoints tested. BTC expression in the affected DRG and dorsal horn was also significantly increased, although not as prominently as in the nerve. I used changes in mRNA expression as the starting point for further investigations. However, a potential function as a pain mediator or a ligand involved in regeneration is mediated by functional protein. mRNA expression is therefore only a surrogate and cannot be utilised to generate conclusive statements about biological function. However, significant developments in the medium/high-throughput techniques to measure mRNA expression make it a sensitive and less time consuming option to screen a broad range of factors in one experiment.

I tried to correlate altered mRNA and protein levels with limited success. Although, I found an increase in the major fragment of mature BTC protein with Western blotting (Figure 4.21.), this finding was not significant. Correlating protein abundance with mRNA expression levels is challenging. Post-transcriptional mechanisms can account for mRNA increase without affecting protein expression. One major example is the function of endogenous microRNAs, which control the translational repression of transcripts, (Huntzinger and Izaurralde, 2011). The most important posttranslational mechanism in the biology of EGFR ligands, including BTC, is the shedding process by metalloproteases, resulting in the proteolytic release of the active fragment containing the EGF module (Schneider and Wolf, 2009). Once the mature growth factor is released, its active concentration is dependant on protein half-life. This is affected by intracellular or extracellular degradation (Pratt et al., 2002), but also by binding and retention of the growth factor in the ECM (Frantz et al., 2010). In my studies I showed that mRNA levels of the major shedding enzymes are unchanged following injury. Nevertheless, it is

possible that their activity or bioavailability is changed in the remodeling nerve. Investigating their mechanism of control in this context might be interesting. Gene deletion or chemical inhibition strategies could be used in future experiments. Therefore measuring gene expression with RT-qPCR will benefit from validation at the protein level to conclude a potential functional role.

Given that upregulation of BTC occurred in a classic animal model of neuropathic pain, I spent a substantial amount of my PhD testing whether BTC is a novel pain mediator and/or a potential role of the EGFR in pain processing. This hypothesis was supported by recent evidence, suggesting that EGFR inhibition can alleviate severe neuropathic pain symptoms in humans (Kersten et al., 2013). I used different tests to characterise the behavioural response of rats either after injection of BTC (intrathecal and subcutaneous) or systemic treatment with the EGFR inhibitor Gefitinib in a model of acute inflammatory/neuropathic pain. I was not able to detect an effect for either BTC or EGFR inhibition in nociceptive behaviour of healthy or injured animals. The lack of behavioural responses can be explained by different theories, one of which might be the translational limitations frequently discussed in the pain field (Mogil, 2009). In animal models it is not the perception of pain which is assessed, but reflex responses to sensory stimuli. Furthermore, in humans differences in the specific genotype could account for different “pain phenotypes” (Arning and Baron, 2009). This could also be true for the variability in behavioural responses in different strains of animals. Finally, BTC might play an important role in the nociceptive circuits in rats. Although I was able to show that intrathecal administration of BTC was sensed by target cells and induced activation of ERK, the “black box” of functional complexity, involving various cell types, a complicated system of growth factors and EGFR ligands with redundant activity might explain, at least in part, the outcome of those experiments. Importantly, EGFR inhibition was tested using only one receptor blocker to ErbB1 (EGFR). It would be beneficial to repeat these experiments using tissue specific genetic deletion of the receptor or members of the receptor family to obtain more specific results. Apart from ErbB1 (EGFR), BTC is also known to bind to ErbB4 (Sahin et al., 2004). Hence, for effective inhibition of its activity ErBb4 needs to be inhibited too. Unfortunately, I was not able to find appropriate inhibitors for *in vivo* experiments.

Apart from nociception, a highly regulated growth factor could have other important functions after nerve injury. The *in vitro* experiments presented in this project were designed to test this. I first established for the first time a 96-well medium-throughput screening of neurite outgrowth in adult DRG neurons and tested the ability of BTC and other EGFR ligands to act as neurotrophins, altering neurite outgrowth. Although BTC did not increase neurite outgrowth, it supported cell survival in cultured neurons. Moreover, *in vitro* neurite outgrowth assays are essential and provide invaluable information on specific growth promoting effects, it is indispensable to validate those findings in the much more complex *in vivo* environment, e.g. is BTC promoting or inhibitory to neuronal repair? This could be tested *in vivo* by selective blocking of the growth factor following injury and subsequent histological assessment of the regenerating nerve. Limitations in finding a specific BTC blocking reagent, as well as time, did not permit me to examine this further. Nevertheless, automated medium thoughput analysis of neurite outgrowth can be used as a powerful tool to screen neurotrophic properties for other mediators in adult sensory neurons.

I also hypothesised that BTC could have an effect in the inflammatory response. I gathered some interesting and reproducible evidence that BTC increases chemotaxis of macrophages in Matrigel plugs and decreases the expression of CD36 in cultured macrophages. These data are in line with the general function of growth factors and cytokines. Given its role in the scavenging and phagocytosis of myelin debris, the inhibition of CD36 could be very important. In agreement with this hypothesis, the expression of CD36 decreased significantly after nerve injury, although macrophages accumulated. Is BTC a negative regulator of phagocytosis? Moreover, EGFR inhibition rescued CD36 expression, but whether this is functionally related to the high expression of BTC following nerve injury *in vivo,* remains elusive. Again, this could be tested *in vivo* with specific BTC blockers or neutralising antibodies.

The EGFR ligands represent a highly complex biological system of ligand-receptor interaction and subsequent intracellular signalling activation. After revealing a distinct upregulation of BTC in the nerve following injury, I tried to study functional effects in appropriate *in vitro* models. Yet, in culture, it is very

difficult to reproduce the complex conditions present in the injured nerve. This could account for the lack of clear and potent effects in these experiments.

Nevertheless, the EGFR system remains an interesting target. Not only in the context of pain research, *inter alia* in the light of the current clinical use of potent EGFR inhibitors as therapeutic cancer treatment, but also as potentially important molecules in the process of modulating the macrophage response following injury. The striking upregulation of BTC following nerve injury as well as its potential role in regulating macrophage function deserves further investigation.

5.2. Future Directions

To further the studies presented in this thesis, several key experiments could be performed:

Using conditional gene deletion or specific chemical blockers/antibodies against the growth factor or its receptors could be used to further study their function *in vivo.* These approaches have been successfully used to characterise an interesting effect of BTC on neurogenesis *in vivo* (Gomez-Gaviro et al., 2012).

I also tested the effect of BTC in macrophages and showed its ability to alter scavenger receptor expression. Is it possible that BTC changes macrophage phenotypic properties or function? The classification of macrophage phenotype in either the cytotoxic M1 or reparative M2 subtypes, is an emerging concept in the field of nerve regeneration. Notably, in humans, CD36 is a marker of M2 macrophage polarization. Although BTC reduced CD36 expression it had no effect on COX-2 expression (a classic marker of M1 activation, Figure 4.19.), suggesting that it is not a classic inflammatory mediator. Perhaps its effect on the scavenger receptor is specific or it may somehow regulate the phagocytic potential of macrophages. Nevertheless, its specific function on macrophage phenotypic modulation is an interesting direction for additional studies. Recently, It was shown that acute peripheral nerve injury triggers the induction of the M2 phenotype of macrophages (Ydens et al., 2012; Mokarram et al., 2012).

BTC has been described as an angiogenic factor involved in tumour angiogenesis (Kim et al., 2003) and wound healing (Schneider et al., 2008). Further investigation of the potential role of BTC in angiogenesis following nerve injury could be an important research direction. Angiogenesis is a prominent feature following injury (Greenberg and Jin, 2005). Hobson *et al*. demonstrated that vascular endothelial growth factor (VEGF) delivered to injured nerves using a matrigel-infused silicone chambers had a beneficial effect on regeneration (Hobson et al., 2000). The authors showed a clear correlation of increased angiogenesis with axonal regeneration. This particular experiment could help to investigate effects of BTC in the setting of angiogenesis following peripheral nerve injury. I tried to examine the role of BTC in vivo using Matrigel. Although BTC induced macrophage infiltration in the matrigel plugs, I was not able to see a difference in the formation of neovessels, in comparison to vehicle treated controls. Nevertheless, a proangiogenic effect of BTC has been previously shown (Kim et al., 2003), in a comparable Matrigel experimental setting.

The effect of BTC stimulation on SCs could only be examined preliminary, using a medium-throughput PCR array to screen for expression changes of cytokines, growth factors and MBP following stimulation *in vitro.* Unfortunately, a limited amount of time did not allow any further investigations. Nevertheless, it remains an interesting hypothesis, that BTC can directly modulate SC function. Potential future experiments could involve analyzing transcriptional regulators of myelination (see Chapter 1.3.1.) following BTC stimulation. Additionally, BTC has been shown to increase migration of SCs *in vitro* (Byer et al. 2013). To further elucidate the role of SC migration following injury *in vivo,* using a conditional knockout approach would be very interesting.

5.3. Summary

In summary, I showed that BTC is robustly upregulated in the nerve following injury. In my experimental settings, the growth factor does not appear to have a role as a pain mediator. However, it potentially modulates macrophage infiltration and function in the complex system of Wallerian degeneration.

Bibliography

Agarwal, N., P. Pacher, I. Tegeder, F. Amaya, C.E. Constantin, G.J. Brenner, T. Rubino, C.W. Michalski, G. Marsicano, K. Monory, K. Mackie, C. Marian, S. Batkai, D. Parolaro, M.J. Fischer, P. Reeh, G. Kunos, M. Kress, B. Lutz, C.J. Woolf, and R. Kuner. 2007. Cannabinoids mediate analgesia largely via peripheral type 1 cannabinoid receptors in nociceptors. *Nature neuroscience*. 10:870-879.

Agthong, S., A. Kaewsema, N. Tanomsridejchai, and V. Chentanez. 2006. Activation of MAPK ERK in peripheral nerve after injury. *BMC neuroscience*. 7:45.

Ahmed, Z., R.A. Brown, C. Ljungberg, M. Wiberg, and G. Terenghi. 1999. Nerve growth factor enhances peripheral nerve regeneration in non-human primates. *Scandinavian journal of plastic and reconstructive surgery and hand surgery / Nordisk plastikkirurgisk forening [and] Nordisk klubb for handkirurgi*. 33:393-401.

Albanell, J., J. Codony-Servat, F. Rojo, J.M. Del Campo, S. Sauleda, J. Anido, G. Raspall, J. Giralt, J. Rosello, R.I. Nicholson, J. Mendelsohn, and J. Baselga. 2001. Activated extracellular signal-regulated kinases: association with epidermal growth factor receptor/transforming growth factor alpha expression in head and neck squamous carcinoma and inhibition by anti-epidermal growth factor receptor treatments. *Cancer research*. 61:6500-6510.

Alessandri-Haber, N., O.A. Dina, X. Chen, and J.D. Levine. 2009. TRPC1 and TRPC6 channels cooperate with TRPV4 to mediate mechanical hyperalgesia and nociceptor sensitization. *The Journal of neuroscience : the official journal of the Society for Neuroscience*. 29:6217-6228.

Alimandi, M., L.M. Wang, D. Bottaro, C.C. Lee, A. Kuo, M. Frankel, P. Fedi, C. Tang, M. Lippman, and J.H. Pierce. 1997. Epidermal growth factor and betacellulin mediate signal transduction through co-expressed ErbB2 and ErbB3 receptors. *The EMBO journal*. 16:5608-5617.

Allchorne, A.J., D.C. Broom, and C.J. Woolf. 2005. Detection of cold pain, cold allodynia and cold hyperalgesia in freely behaving rats. *Molecular pain*. 1:36.

Allodi, I., E. Udina, and X. Navarro. 2012. Specificity of peripheral nerve regeneration: interactions at the axon level. *Progress in neurobiology*. 98:16-37.

Andreev, N., N. Dimitrieva, M. Koltzenburg, and S.B. McMahon. 1995. Peripheral administration of nerve growth factor in the adult rat produces a thermal hyperalgesia that requires the presence of sympathetic post-ganglionic neurones. *Pain*. 63:109-115.

Andres, C., S. Meyer, O.A. Dina, J.D. Levine, and T. Hucho. 2010. Quantitative automated microscopy (QuAM) elucidates growth factor specific signalling in pain sensitization. *Molecular pain*. 6:98.

Armstrong, D.A., J.A. Major, A. Chudyk, and T.A. Hamilton. 2004. Neutrophil chemoattractant genes KC and MIP-2 are expressed in different cell populations at sites of surgical injury. *Journal of leukocyte biology*. 75:641-648.

Arning, K., and R. Baron. 2009. Evaluation of symptom heterogeneity in neuropathic pain using assessments of sensory functions. *Neurotherapeutics : the journal of the American Society for Experimental NeuroTherapeutics*. 6:738-748.

Arthur-Farraj, P.J., M. Latouche, D.K. Wilton, S. Quintes, E. Chabrol, A. Banerjee, A. Woodhoo, B. Jenkins, M. Rahman, M. Turmaine, G.K.

Wicher, R. Mitter, L. Greensmith, A. Behrens, G. Raivich, R. Mirsky, and K.R. Jessen. 2012. c-Jun reprograms Schwann cells of injured nerves to generate a repair cell essential for regeneration. *Neuron*. 75:633-647.

Asami, T., T. Ito, H. Fukumitsu, H. Nomoto, Y. Furukawa, and S. Furukawa. 2006. Autocrine activation of cultured macrophages by brain-derived neurotrophic factor. *Biochemical and biophysical research communications*. 344:941-947.

Atanasoski, S., S.S. Scherer, E. Sirkowski, D. Leone, A.N. Garratt, C. Birchmeier, and U. Suter. 2006. ErbB2 signaling in Schwann cells is mostly dispensable for maintenance of myelinated peripheral nerves and proliferation of adult Schwann cells after injury. *The Journal of neuroscience : the official journal of the Society for Neuroscience*. 26:2124-2131.

Audisio, C., S. Nicolino, A. Scevola, P. Tos, S. Geuna, B. Battiston, and I. Perroteau. 2008. ErbB receptors modulation in different types of peripheral nerve regeneration. *Neuroreport*. 19:1605-1609.

Baker, N.E., and S.Y. Yu. 2001. The EGF receptor defines domains of cell cycle progression and survival to regulate cell number in the developing Drosophila eye. *Cell*. 104:699-708.

Barrett, G.L., and P.F. Bartlett. 1994. The p75 nerve growth factor receptor mediates survival or death depending on the stage of sensory neuron development. *Proceedings of the National Academy of Sciences of the United States of America*. 91:6501-6505.

Barrette, B., M.A. Hebert, M. Filali, K. Lafortune, N. Vallieres, G. Gowing, J.P. Julien, and S. Lacroix. 2008. Requirement of myeloid cells for axon regeneration. *The Journal of neuroscience : the official journal of the Society for Neuroscience*. 28:9363-9376.

Be'eri, H., F. Reichert, A. Saada, and S. Rotshenker. 1998. The cytokine network of wallerian degeneration: IL-10 and GM-CSF. *The European journal of neuroscience*. 10:2707-2713.

Beirowski, B., R. Adalbert, D. Wagner, D.S. Grumme, K. Addicks, R.R. Ribchester, and M.P. Coleman. 2005. The progressive nature of Wallerian degeneration in wild-type and slow Wallerian degeneration (WldS) nerves. *BMC neuroscience*. 6:6.

Ben-Yaakov, K., S.Y. Dagan, Y. Segal-Ruder, O. Shalem, D. Vuppalanchi, D.E. Willis, D. Yudin, I. Rishal, F. Rother, M. Bader, A. Blesch, Y. Pilpel, J.L. Twiss, and M. Fainzilber. 2012. Axonal transcription factors signal retrogradely in lesioned peripheral nerve. *The EMBO journal*. 31:1350-1363.

Benmerah, A., M. Bayrou, N. Cerf-Bensussan, and A. Dautry-Varsat. 1999. Inhibition of clathrin-coated pit assembly by an Eps15 mutant. *Journal of cell science*. 112 (Pt 9):1303-1311.

Bennett, G.J. 1999. Does a neuroimmune interaction contribute to the genesis of painful peripheral neuropathies? *Proceedings of the National Academy of Sciences of the United States of America*. 96:7737-7738.

Bennett, G.J., and Y.K. Xie. 1988. A peripheral mononeuropathy in rat that produces disorders of pain sensation like those seen in man. *Pain*. 33:87-107.

Beuche, W., and R.L. Friede. 1984. The role of non-resident cells in Wallerian degeneration. *Journal of neurocytology*. 13:767-796.

Blobel, C.P. 2005. ADAMs: key components in EGFR signalling and development. *Nature reviews. Molecular cell biology*. 6:32-43.

Bolin, L.M., A.N. Verity, J.E. Silver, E.M. Shooter, and J.S. Abrams. 1995. Interleukin-6 production by Schwann cells and induction in sciatic nerve injury. *Journal of neurochemistry*. 64:850-858.

Boyd, J.G., and T. Gordon. 2002. A dose-dependent facilitation and inhibition of peripheral nerve regeneration by brain-derived neurotrophic factor. *The European journal of neuroscience*. 15:613-626.

Brachmann, R., P.B. Lindquist, M. Nagashima, W. Kohr, T. Lipari, M. Napier, and R. Derynck. 1989. Transmembrane TGF-alpha precursors activate EGF/TGF-alpha receptors. *Cell*. 56:691-700.

Brodie, C., K. Bogi, P. Acs, P. Lazarovici, G. Petrovics, W.B. Anderson, and P.M. Blumberg. 1999. Protein kinase C-epsilon plays a role in neurite outgrowth in response to epidermal growth factor and nerve growth factor in PC12 cells. *Cell growth & differentiation : the molecular biology journal of the American Association for Cancer Research*. 10:183-191.

Bruck, W., and R.L. Friede. 1990. Anti-macrophage CR3 antibody blocks myelin phagocytosis by macrophages in vitro. *Acta neuropathologica*. 80:415-418.

Bruck, W., and R.L. Friede. 1991. The role of complement in myelin phagocytosis during PNS wallerian degeneration. *Journal of the neurological sciences*. 103:182-187.

Bruck, W., I. Huitinga, and C.D. Dijkstra. 1996. Liposome-mediated monocyte depletion during wallerian degeneration defines the role of hematogenous phagocytes in myelin removal. *Journal of neuroscience research*. 46:477-484.

Burnett, M.G., and E.L. Zager. 2004. Pathophysiology of peripheral nerve injury: a brief review. *Neurosurgical focus*. 16:E1.

Byer, S.J., N.M. Brossier, L.T. Peavler, J.M. Eckert, S. Watkins, K.A. Roth, and S.L. Carroll. 2013. Malignant peripheral nerve sheath tumor invasion requires aberrantly expressed EGF receptors and is variably enhanced by multiple EGF family ligands. *Journal of neuropathology and experimental neurology*. 72:219-233.

Calvo, M., N. Zhu, J. Grist, Z. Ma, J.A. Loeb, and D.L. Bennett. 2011. Following nerve injury neuregulin-1 drives microglial proliferation and neuropathic pain via the MEK/ERK pathway. *Glia*. 59:554-568.

Calvo, M., N. Zhu, C. Tsantoulas, Z. Ma, J. Grist, J.A. Loeb, and D.L. Bennett. 2010. Neuregulin-ErbB signaling promotes microglial proliferation and chemotaxis contributing to microgliosis and pain after peripheral nerve injury. *The Journal of neuroscience : the official journal of the Society for Neuroscience*. 30:5437-5450.

Campana, W.M. 2007. Schwann cells: activated peripheral glia and their role in neuropathic pain. *Brain, behavior, and immunity*. 21:522-527.

Campenot, R.B. 1977. Local control of neurite development by nerve growth factor. *Proceedings of the National Academy of Sciences of the United States of America*. 74:4516-4519.

Cao, Z., Y. Gao, J.B. Bryson, J. Hou, N. Chaudhry, M. Siddiq, J. Martinez, T. Spencer, J. Carmel, R.B. Hart, and M.T. Filbin. 2006. The cytokine interleukin-6 is sufficient but not necessary to mimic the peripheral conditioning lesion effect on axonal growth. *The Journal of neuroscience : the official journal of the Society for Neuroscience*. 26:5565-5573.

Carroll, S.L., M.L. Miller, P.W. Frohnert, S.S. Kim, and J.A. Corbett. 1997. Expression of neuregulins and their putative receptors, ErbB2 and ErbB3, is induced during Wallerian degeneration. *The Journal of*

neuroscience : the official journal of the Society for Neuroscience. 17:1642-1659.

Casper, D., C. Mytilineou, and M. Blum. 1991. EGF enhances the survival of dopamine neurons in rat embryonic mesencephalon primary cell culture. *Journal of neuroscience research*. 30:372-381.

Chang, L., and M. Karin. 2001. Mammalian MAP kinase signalling cascades. *Nature*. 410:37-40.

Chao, M.V. 2003. Neurotrophins and their receptors: a convergence point for many signalling pathways. *Nature reviews. Neuroscience*. 4:299-309.

Chaudhry, V., and D.R. Cornblath. 1992. Wallerian degeneration in human nerves: serial electrophysiological studies. *Muscle & nerve*. 15:687-693.

Chen, Z.L., W.M. Yu, and S. Strickland. 2007. Peripheral regeneration. *Annual review of neuroscience*. 30:209-233.

Chou, A.K., R. Muhammad, S.M. Huang, J.T. Chen, C.L. Wu, C.R. Lin, T.H. Lee, S.H. Lin, C.Y. Lu, and L.C. Yang. 2002. Altered synaptophysin expression in the rat spinal cord after chronic constriction injury of sciatic nerve. *Neuroscience letters*. 333:155-158.

Citri, A., and Y. Yarden. 2006. EGF-ERBB signalling: towards the systems level. *Nature reviews. Molecular cell biology*. 7:505-516.

Coderre, T.J., M.E. Fundytus, J.E. McKenna, S. Dalal, and R. Melzack. 1993. The formalin test: a validation of the weighted-scores method of behavioural pain rating. *Pain*. 54:43-50.

Cohen, J.A., A.T. Yachnis, M. Arai, J.G. Davis, and S.S. Scherer. 1992. Expression of the neu proto-oncogene by Schwann cells during

peripheral nerve development and Wallerian degeneration. *Journal of neuroscience research*. 31:622-634.

Cohen, M.H., G.A. Williams, R. Sridhara, G. Chen, and R. Pazdur. 2003. FDA drug approval summary: gefitinib (ZD1839) (Iressa) tablets. *The oncologist*. 8:303-306.

Cohen, S. 1964. Isolation and Biological Effects of an Epidermal Growth-Stimulating Protein. *National Cancer Institute monograph*. 13:13-37.

Colburn, R.W., J.A. DeLeo, A.J. Rickman, M.P. Yeager, P. Kwon, and W.F. Hickey. 1997. Dissociation of microglial activation and neuropathic pain behaviors following peripheral nerve injury in the rat. *Journal of neuroimmunology*. 79:163-175.

Coleman, M.P., and M.R. Freeman. 2010. Wallerian degeneration, wld(s), and nmnat. *Annual review of neuroscience*. 33:245-267.

Conductier, G., N. Blondeau, A. Guyon, J.L. Nahon, and C. Rovere. 2010. The role of monocyte chemoattractant protein MCP1/CCL2 in neuroinflammatory diseases. *Journal of neuroimmunology*. 224:93-100.

Costigan, M., K. Befort, L. Karchewski, R.S. Griffin, D. D'Urso, A. Allchorne, J. Sitarski, J.W. Mannion, R.E. Pratt, and C.J. Woolf. 2002. Replicate high-density rat genome oligonucleotide microarrays reveal hundreds of regulated genes in the dorsal root ganglion after peripheral nerve injury. *BMC neuroscience*. 3:16.

Costigan, M., J. Scholz, and C.J. Woolf. 2009. Neuropathic pain: a maladaptive response of the nervous system to damage. *Annual review of neuroscience*. 32:1-32.

Coull, J.A., S. Beggs, D. Boudreau, D. Boivin, M. Tsuda, K. Inoue, C. Gravel, M.W. Salter, and Y. De Koninck. 2005. BDNF from microglia causes the

shift in neuronal anion gradient underlying neuropathic pain. *Nature*. 438:1017-1021.

Cui, J.G., S. Holmin, T. Mathiesen, B.A. Meyerson, and B. Linderoth. 2000. Possible role of inflammatory mediators in tactile hypersensitivity in rat models of mononeuropathy. *Pain*. 88:239-248.

Culy, C.R., and D. Faulds. 2002. Gefitinib. *Drugs*. 62:2237-2248; discussion 2249-2250.

Dahlhoff, M., P.M. Dames, A. Lechner, N. Herbach, L. van Burck, R. Wanke, E. Wolf, and M.R. Schneider. 2009. Betacellulin overexpression in transgenic mice improves glucose tolerance and enhances insulin secretion by isolated islets in vitro. *Molecular and cellular endocrinology*. 299:188-193.

Daub, H., F.U. Weiss, C. Wallasch, and A. Ullrich. 1996. Role of transactivation of the EGF receptor in signalling by G-protein-coupled receptors. *Nature*. 379:557-560.

David, S., and A. Kroner. 2011. Repertoire of microglial and macrophage responses after spinal cord injury. *Nature reviews. Neuroscience*. 12:388-399.

Davis, J.B., and P. Stroobant. 1990. Platelet-derived growth factors and fibroblast growth factors are mitogens for rat Schwann cells. *The Journal of cell biology*. 110:1353-1360.

De, S., M.A. Trigueros, A. Kalyvas, and S. David. 2003. Phospholipase A2 plays an important role in myelin breakdown and phagocytosis during Wallerian degeneration. *Molecular and cellular neurosciences*. 24:753-765.

Derveaux, S., J. Vandesompele, and J. Hellemans. 2010. How to do successful gene expression analysis using real-time PCR. *Methods*. 50:227-230.

Devergne, O., M. Hummel, H. Koeppen, M.M. Le Beau, E.C. Nathanson, E. Kieff, and M. Birkenbach. 1996. A novel interleukin-12 p40-related protein induced by latent Epstein-Barr virus infection in B lymphocytes. *Journal of virology*. 70:1143-1153.

Devor, M. 2009. Ectopic discharge in Abeta afferents as a source of neuropathic pain. *Experimental brain research. Experimentelle Hirnforschung. Experimentation cerebrale*. 196:115-128.

Di Gennaro, E., M. Barbarino, F. Bruzzese, S. De Lorenzo, M. Caraglia, A. Abbruzzese, A. Avallone, P. Comella, F. Caponigro, S. Pepe, and A. Budillon. 2003. Critical role of both p27KIP1 and p21CIP1/WAF1 in the antiproliferative effect of ZD1839 ('Iressa'), an epidermal growth factor receptor tyrosine kinase inhibitor, in head and neck squamous carcinoma cells. *Journal of cellular physiology*. 195:139-150.

Di Virgilio, F., T.H. Steinberg, and S.C. Silverstein. 1990. Inhibition of Fura-2 sequestration and secretion with organic anion transport blockers. *Cell calcium*. 11:57-62.

Dubovy, P. 2011. Wallerian degeneration and peripheral nerve conditions for both axonal regeneration and neuropathic pain induction. *Annals of anatomy = Anatomischer Anzeiger : official organ of the Anatomische Gesellschaft*. 193:267-275.

Dubuisson, A.S., R.W. Beuermann, and D.G. Kline. 1993. Sciatic nerve regeneration across gaps within collagen chambers: the influence of epidermal growth factor. *Journal of reconstructive microsurgery*. 9:341-346; discussion 346-347.

Dubuisson, D., and S.G. Dennis. 1977. The formalin test: a quantitative study of the analgesic effects of morphine, meperidine, and brain stem stimulation in rats and cats. *Pain*. 4:161-174.

Dunbar, A.J., and C. Goddard. 2000. Structure-function and biological role of betacellulin. *The international journal of biochemistry & cell biology*. 32:805-815.

Elkabes, S., E.M. DiCicco-Bloom, and I.B. Black. 1996. Brain microglia/macrophages express neurotrophins that selectively regulate microglial proliferation and function. *The Journal of neuroscience : the official journal of the Society for Neuroscience*. 16:2508-2521.

Erlich, S., Y. Goldshmit, Z. Lupowitz, and R. Pinkas-Kramarski. 2001. ErbB-4 activation inhibits apoptosis in PC12 cells. *Neuroscience*. 107:353-362.

Ernfors, P., C. Wetmore, L. Olson, and H. Persson. 1990. Identification of cells in rat brain and peripheral tissues expressing mRNA for members of the nerve growth factor family. *Neuron*. 5:511-526.

Erschbamer, M., K. Pernold, and L. Olson. 2007. Inhibiting epidermal growth factor receptor improves structural, locomotor, sensory, and bladder recovery from experimental spinal cord injury. *The Journal of neuroscience : the official journal of the Society for Neuroscience*. 27:6428-6435.

Eto, M., H. Yoshikawa, H. Fujimura, I. Naba, H. Sumi-Akamaru, S. Takayasu, H. Itabe, and S. Sakoda. 2003. The role of CD36 in peripheral nerve remyelination after crush injury. *The European journal of neuroscience*. 17:2659-2666.

Fabry, Z., K.M. Fitzsimmons, J.A. Herlein, T.O. Moninger, M.B. Dobbs, and M.N. Hart. 1993. Production of the cytokines interleukin 1 and 6 by

murine brain microvessel endothelium and smooth muscle pericytes. *Journal of neuroimmunology*. 47:23-34.

Fadok, V.A., D.L. Bratton, S.C. Frasch, M.L. Warner, and P.M. Henson. 1998. The role of phosphatidylserine in recognition of apoptotic cells by phagocytes. *Cell death and differentiation*. 5:551-562.

Fambrough, D., D. Pan, G.M. Rubin, and C.S. Goodman. 1996. The cell surface metalloprotease/disintegrin Kuzbanian is required for axonal extension in Drosophila. *Proceedings of the National Academy of Sciences of the United States of America*. 93:13233-13238.

Febbraio, M., E.A. Podrez, J.D. Smith, D.P. Hajjar, S.L. Hazen, H.F. Hoff, K. Sharma, and R.L. Silverstein. 2000. Targeted disruption of the class B scavenger receptor CD36 protects against atherosclerotic lesion development in mice. *The Journal of clinical investigation*. 105:1049-1056.

Ferrari, G., G. Toffano, and S.D. Skaper. 1991. Epidermal growth factor exerts neuronotrophic effects on dopaminergic and GABAergic CNS neurons: comparison with basic fibroblast growth factor. *Journal of neuroscience research*. 30:493-497.

Flannagan, R.S., V. Jaumouille, and S. Grinstein. 2012. The cell biology of phagocytosis. *Annual review of pathology*. 7:61-98.

Fleige, S., and M.W. Pfaffl. 2006. RNA integrity and the effect on the real-time qRT-PCR performance. *Molecular aspects of medicine*. 27:126-139.

Frantz, C., K.M. Stewart, and V.M. Weaver. 2010. The extracellular matrix at a glance. *Journal of cell science*. 123:4195-4200.

Fricker, F.R., and D.L. Bennett. 2011. The role of neuregulin-1 in the response to nerve injury. *Future neurology*. 6:809-822.

Fricker, F.R., N. Lago, S. Balarajah, C. Tsantoulas, S. Tanna, N. Zhu, S.K. Fageiry, M. Jenkins, A.N. Garratt, C. Birchmeier, and D.L. Bennett. 2011. Axonally derived neuregulin-1 is required for remyelination and regeneration after nerve injury in adulthood. *The Journal of neuroscience : the official journal of the Society for Neuroscience*. 31:3225-3233.

Fukuoka, T., E. Kondo, Y. Dai, N. Hashimoto, and K. Noguchi. 2001. Brain-derived neurotrophic factor increases in the uninjured dorsal root ganglion neurons in selective spinal nerve ligation model. *The Journal of neuroscience : the official journal of the Society for Neuroscience*. 21:4891-4900.

Galindo-Romero, C., F.J. Valiente-Soriano, M. Jimenez-Lopez, D. Garcia-Ayuso, M.P. Villegas-Perez, M. Vidal-Sanz, and M. Agudo-Barriuso. 2013. Effect of brain-derived neurotrophic factor on mouse axotomized retinal ganglion cells and phagocytic microglia. *Investigative ophthalmology & visual science*. 54:974-985.

Gaudet, A.D., P.G. Popovich, and M.S. Ramer. 2011. Wallerian degeneration: gaining perspective on inflammatory events after peripheral nerve injury. *Journal of neuroinflammation*. 8:110.

Genetos, D.C., R.R. Rao, and M.A. Vidal. 2010. Betacellulin inhibits osteogenic differentiation and stimulates proliferation through HIF-1alpha. *Cell and tissue research*. 340:81-89.

Gillen, C., S. Jander, and G. Stoll. 1998. Sequential expression of mRNA for proinflammatory cytokines and interleukin-10 in the rat peripheral nervous system: comparison between immune-mediated demyelination and Wallerian degeneration. *Journal of neuroscience research*. 51:489-496.

Goethals, S., E. Ydens, V. Timmerman, and S. Janssens. 2010. Toll-like receptor expression in the peripheral nerve. *Glia*. 58:1701-1709.

Gold, M.S., D. Weinreich, C.S. Kim, R. Wang, J. Treanor, F. Porreca, and J. Lai. 2003. Redistribution of Na(V)1.8 in uninjured axons enables neuropathic pain. *The Journal of neuroscience : the official journal of the Society for Neuroscience*. 23:158-166.

Gomez-Gaviro, M.V., C.E. Scott, A.K. Sesay, A. Matheu, S. Booth, C. Galichet, and R. Lovell-Badge. 2012. Betacellulin promotes cell proliferation in the neural stem cell niche and stimulates neurogenesis. *Proceedings of the National Academy of Sciences of the United States of America*. 109:1317-1322.

Gordon, S., and P.R. Taylor. 2005. Monocyte and macrophage heterogeneity. *Nature reviews. Immunology*. 5:953-964.

Gordon, T. 2009. The role of neurotrophic factors in nerve regeneration. *Neurosurgical focus*. 26:E3.

Gordon, T. 2010. The physiology of neural injury and regeneration: The role of neurotrophic factors. *Journal of communication disorders*. 43:265-273.

Gratao, A.A., M. Dahlhoff, F. Sinowatz, E. Wolf, and M.R. Schneider. 2008. Betacellulin overexpression in the mouse ovary leads to MAPK3/MAPK1 hyperactivation and reduces litter size by impairing fertilization. *Biology of reproduction*. 78:43-52.

Greenberg, D.A., and K. Jin. 2005. From angiogenesis to neuropathology. *Nature*. 438:954-959.

Grienberger, C., and A. Konnerth. 2012. Imaging calcium in neurons. *Neuron*. 73:862-885.

Griffin, J.W., and W.J. Thompson. 2008. Biology and pathology of nonmyelinating Schwann cells. *Glia*. 56:1518-1531.

Grothe, C., C. Meisinger, A. Hertenstein, H. Kurz, and K. Wewetzer. 1997. Expression of fibroblast growth factor-2 and fibroblast growth factor receptor 1 messenger RNAs in spinal ganglia and sciatic nerve: regulation after peripheral nerve lesion. *Neuroscience*. 76:123-135.

Guertin, A.D., D.P. Zhang, K.S. Mak, J.A. Alberta, and H.A. Kim. 2005. Microanatomy of axon/glial signaling during Wallerian degeneration. *The Journal of neuroscience : the official journal of the Society for Neuroscience*. 25:3478-3487.

Gumy, L.F., C.L. Tan, and J.W. Fawcett. 2010. The role of local protein synthesis and degradation in axon regeneration. *Experimental neurology*. 223:28-37.

Hains, B.C., C.Y. Saab, J.P. Klein, M.J. Craner, and S.G. Waxman. 2004. Altered sodium channel expression in second-order spinal sensory neurons contributes to pain after peripheral nerve injury. *The Journal of neuroscience : the official journal of the Society for Neuroscience*. 24:4832-4839.

Hammarberg, H., F. Piehl, S. Cullheim, J. Fjell, T. Hokfelt, and K. Fried. 1996. GDNF mRNA in Schwann cells and DRG satellite cells after chronic sciatic nerve injury. *Neuroreport*. 7:857-860.

Hardy, J.D., H.G. Wolff, and H. Goodell. 1940. Studies on Pain. A New Method for Measuring Pain Threshold: Observations on Spatial Summation of Pain. *The Journal of clinical investigation*. 19:649-657.

Hargreaves, K., R. Dubner, F. Brown, C. Flores, and J. Joris. 1988. A new and sensitive method for measuring thermal nociception in cutaneous hyperalgesia. *Pain*. 32:77-88.

Harris, R.C., E. Chung, and R.J. Coffey. 2003. EGF receptor ligands. *Experimental cell research*. 284:2-13.

Harrisingh, M.C., E. Perez-Nadales, D.B. Parkinson, D.S. Malcolm, A.W. Mudge, and A.C. Lloyd. 2004. The Ras/Raf/ERK signalling pathway drives Schwann cell dedifferentiation. *The EMBO journal*. 23:3061-3071.

Hashimoto, M., A. Nitta, H. Fukumitsu, H. Nomoto, L. Shen, and S. Furukawa. 2005. Involvement of glial cell line-derived neurotrophic factor in activation processes of rodent macrophages. *Journal of neuroscience research*. 79:476-487.

Hermann, P.M., J.J. Nicol, G.T. Nagle, A.G. Bulloch, and W.C. Wildering. 2005. Epidermal growth factor-dependent enhancement of axonal regeneration in the pond snail Lymnaea stagnalis: role of phagocyte survival. *The Journal of comparative neurology*. 492:383-400.

Hermann, P.M., R.E. van Kesteren, W.C. Wildering, S.D. Painter, J.M. Reno, J.S. Smith, S.B. Kumar, W.P. Geraerts, L.H. Ericsson, A.B. Smit, A.G. Bulloch, and G.T. Nagle. 2000. Neurotrophic actions of a novel molluscan epidermal growth factor. *The Journal of neuroscience : the official journal of the Society for Neuroscience*. 20:6355-6364.

Herzog, C.D., and T. Otto. 2002. Administration of transforming growth factor-alpha enhances anatomical and behavioral recovery following olfactory nerve transection. *Neuroscience*. 113:569-580.

Heumann, R., S. Korsching, C. Bandtlow, and H. Thoenen. 1987. Changes of nerve growth factor synthesis in nonneuronal cells in response to sciatic nerve transection. *The Journal of cell biology*. 104:1623-1631.

Hieda, M., M. Isokane, M. Koizumi, C. Higashi, T. Tachibana, M. Shudou, T. Taguchi, Y. Hieda, and S. Higashiyama. 2008. Membrane-anchored

growth factor, HB-EGF, on the cell surface targeted to the inner nuclear membrane. *The Journal of cell biology*. 180:763-769.

Higashiyama, S., K. Lau, G.E. Besner, J.A. Abraham, and M. Klagsbrun. 1992. Structure of heparin-binding EGF-like growth factor. Multiple forms, primary structure, and glycosylation of the mature protein. *The Journal of biological chemistry*. 267:6205-6212.

Hinkle, C.L., S.W. Sunnarborg, D. Loiselle, C.E. Parker, M. Stevenson, W.E. Russell, and D.C. Lee. 2004. Selective roles for tumor necrosis factor alpha-converting enzyme/ADAM17 in the shedding of the epidermal growth factor receptor ligand family: the juxtamembrane stalk determines cleavage efficiency. *The Journal of biological chemistry*. 279:24179-24188.

Hirata, K., and M. Kawabuchi. 2002. Myelin phagocytosis by macrophages and nonmacrophages during Wallerian degeneration. *Microscopy research and technique*. 57:541-547.

Ho, M.K., and T.A. Springer. 1982. Mac-2, a novel 32,000 Mr mouse macrophage subpopulation-specific antigen defined by monoclonal antibodies. *Journal of immunology*. 128:1221-1228.

Hobson, M.I., C.J. Green, and G. Terenghi. 2000. VEGF enhances intraneural angiogenesis and improves nerve regeneration after axotomy. *Journal of anatomy*. 197 Pt 4:591-605.

Hoffman, P.N. 2010. A conditioning lesion induces changes in gene expression and axonal transport that enhance regeneration by increasing the intrinsic growth state of axons. *Experimental neurology*. 223:11-18.

Hoke, A. 2006. Mechanisms of Disease: what factors limit the success of peripheral nerve regeneration in humans? *Nature clinical practice. Neurology*. 2:448-454.

Hoke, A., C. Cheng, and D.W. Zochodne. 2000. Expression of glial cell line-derived neurotrophic factor family of growth factors in peripheral nerve injury in rats. *Neuroreport*. 11:1651-1654.

Hoke, A., T. Gordon, D.W. Zochodne, and O.A. Sulaiman. 2002. A decline in glial cell-line-derived neurotrophic factor expression is associated with impaired regeneration after long-term Schwann cell denervation. *Experimental neurology*. 173:77-85.

Hoke, A., R. Redett, H. Hameed, R. Jari, C. Zhou, Z.B. Li, J.W. Griffin, and T.M. Brushart. 2006. Schwann cells express motor and sensory phenotypes that regulate axon regeneration. *The Journal of neuroscience : the official journal of the Society for Neuroscience*. 26:9646-9655.

Howarth, G.S., S.E. Bastian, A.J. Dunbar, and C. Goddard. 2003. Betacellulin promotes growth of the gastrointestinal organs and effects a diuresis in normal rats. *Growth factors*. 21:79-86.

Huerta, J.J., R. Diaz-Trelles, F.J. Naves, M.M. Llamosas, M.E. Del Valle, and J.A. Vega. 1996. Epidermal growth factor receptor in adult human dorsal root ganglia. *Anatomy and embryology*. 194:253-257.

Huntzinger, E., and E. Izaurralde. 2011. Gene silencing by microRNAs: contributions of translational repression and mRNA decay. *Nature reviews. Genetics*. 12:99-110.

Hutson, T.H., W.J. Buchser, J.L. Bixby, V.P. Lemmon, and L.D. Moon. 2011. Optimization of a 96-Well Electroporation Assay for Postnatal Rat CNS Neurons Suitable for Cost-Effective Medium-Throughput Screening of Genes that Promote Neurite Outgrowth. *Frontiers in molecular neuroscience*. 4:55.

Hynes, N.E., and H.A. Lane. 2005. ERBB receptors and cancer: the complexity of targeted inhibitors. *Nature reviews. Cancer*. 5:341-354.

Jackson, L.F., T.H. Qiu, S.W. Sunnarborg, A. Chang, C. Zhang, C. Patterson, and D.C. Lee. 2003. Defective valvulogenesis in HB-EGF and TACE-null mice is associated with aberrant BMP signaling. *The EMBO journal*. 22:2704-2716.

Jangouk, P., T. Dehmel, G. Meyer Zu Horste, A. Ludwig, H.C. Lehmann, and B.C. Kieseier. 2009. Involvement of ADAM10 in axonal outgrowth and myelination of the peripheral nerve. *Glia*. 57:1765-1774.

Jessen, K.R., and R. Mirsky. 2008. Negative regulation of myelination: relevance for development, injury, and demyelinating disease. *Glia*. 56:1552-1565.

Jia, Q., Z. Jia, Z. Zhao, B. Liu, H. Liang, and H. Zhang. 2007. Activation of epidermal growth factor receptor inhibits KCNQ2/3 current through two distinct pathways: membrane PtdIns(4,5)P2 hydrolysis and channel phosphorylation. *The Journal of neuroscience : the official journal of the Society for Neuroscience*. 27:2503-2512.

Jimenez-Andrade, J.M., M.B. Herrera, J.R. Ghilardi, M. Vardanyan, O.K. Melemedjian, and P.W. Mantyh. 2008. Vascularization of the dorsal root ganglia and peripheral nerve of the mouse: implications for chemical-induced peripheral sensory neuropathies. *Molecular pain*. 4:10.

Johnson, G.L., and R. Lapadat. 2002. Mitogen-activated protein kinase pathways mediated by ERK, JNK, and p38 protein kinases. *Science*. 298:1911-1912.

Jones, J.T., R.W. Akita, and M.X. Sliwkowski. 1999. Binding specificities and affinities of egf domains for ErbB receptors. *FEBS letters*. 447:227-231.

Jorissen, R.N., F. Walker, N. Pouliot, T.P. Garrett, C.W. Ward, and A.W. Burgess. 2003. Epidermal growth factor receptor: mechanisms of activation and signalling. *Experimental cell research*. 284:31-53.

Jung, H., B.C. Yoon, and C.E. Holt. 2012. Axonal mRNA localization and local protein synthesis in nervous system assembly, maintenance and repair. *Nature reviews. Neuroscience*. 13:308-324.

Jungnickel, J., P. Claus, K. Gransalke, M. Timmer, and C. Grothe. 2004. Targeted disruption of the FGF-2 gene affects the response to peripheral nerve injury. *Molecular and cellular neurosciences*. 25:444-452.

Jungnickel, J., K. Haase, J. Konitzer, M. Timmer, and C. Grothe. 2006. Faster nerve regeneration after sciatic nerve injury in mice over-expressing basic fibroblast growth factor. *Journal of neurobiology*. 66:940-948.

Kaiserling, E., J.C. Xiao, P. Ruck, and H.P. Horny. 1993. Aberrant expression of macrophage-associated antigens (CD68 and Ki-M1P) by Schwann cells in reactive and neoplastic neural tissue. Light- and electron-microscopic findings. *Modern pathology : an official journal of the United States and Canadian Academy of Pathology, Inc*. 6:463-468.

Kataoka, H. 2009. EGFR ligands and their signaling scissors, ADAMs, as new molecular targets for anticancer treatments. *Journal of dermatological science*. 56:148-153.

Kawaguchi, M., R. Hosotani, M. Kogire, J. Ida, R. Doi, T. Koshiba, Y. Miyamoto, S. Tsuji, S. Nakajima, H. Kobayashi, T. Masui, and M. Imamura. 2000. Auto-induction and growth stimulatory effect of betacellulin in human pancreatic cancer cells. *International journal of oncology*. 16:37-41.

Kersten, C., and M.G. Cameron. 2012. Cetuximab alleviates neuropathic pain despite tumour progression. *BMJ case reports*. 2012.

Kersten, C., M.G. Cameron, and S. Mjåland. 2013. Epithelial growth factor receptor (EGFR)-inhibition for relief of neuropathic pain—A case series. *Scandinavian Journal of Pain*. 4:3-7.

Keys, D.N., J.K. Au-Young, and R.A. Fekete. 2010. TaqMan Array Cards in pharmaceutical research. *Methods in molecular biology*. 632:87-97.

Kigerl, K.A., J.C. Gensel, D.P. Ankeny, J.K. Alexander, D.J. Donnelly, and P.G. Popovich. 2009. Identification of two distinct macrophage subsets with divergent effects causing either neurotoxicity or regeneration in the injured mouse spinal cord. *The Journal of neuroscience : the official journal of the Society for Neuroscience*. 29:13435-13444.

Kim, H.S., H.S. Shin, H.J. Kwak, C.H. Cho, C.O. Lee, and G.Y. Koh. 2003. Betacellulin induces angiogenesis through activation of mitogen-activated protein kinase and phosphatidylinositol 3'-kinase in endothelial cell. *FASEB journal : official publication of the Federation of American Societies for Experimental Biology*. 17:318-320.

Kim, S.H., and J.M. Chung. 1992. An experimental model for peripheral neuropathy produced by segmental spinal nerve ligation in the rat. *Pain*. 50:355-363.

Kimpinski, K., R.B. Campenot, and K. Mearow. 1997. Effects of the neurotrophins nerve growth factor, neurotrophin-3, and brain-derived neurotrophic factor (BDNF) on neurite growth from adult sensory neurons in compartmented cultures. *Journal of neurobiology*. 33:395-410.

Kirsch, M., U. Terheggen, and H.D. Hofmann. 2003. Ciliary neurotrophic factor is an early lesion-induced retrograde signal for axotomized facial motoneurons. *Molecular and cellular neurosciences*. 24:130-138.

Kobayashi, H., and A.P. Mizisin. 2001. Nerve growth factor and neurotrophin-3 promote chemotaxis of mouse macrophages in vitro. *Neuroscience letters*. 305:157-160.

Koeppen, A.H. 2004. Wallerian degeneration: history and clinical significance. *Journal of the neurological sciences*. 220:115-117.

Kojima, A., and C.H. Tator. 2002. Intrathecal administration of epidermal growth factor and fibroblast growth factor 2 promotes ependymal proliferation and functional recovery after spinal cord injury in adult rats. *Journal of neurotrauma*. 19:223-238.

Koprivica, V., K.S. Cho, J.B. Park, G. Yiu, J. Atwal, B. Gore, J.A. Kim, E. Lin, M. Tessier-Lavigne, D.F. Chen, and Z. He. 2005. EGFR activation mediates inhibition of axon regeneration by myelin and chondroitin sulfate proteoglycans. *Science*. 310:106-110.

Krenz, N.R., S.O. Meakin, A.V. Krassioukov, and L.C. Weaver. 1999. Neutralizing intraspinal nerve growth factor blocks autonomic dysreflexia caused by spinal cord injury. *The Journal of neuroscience : the official journal of the Society for Neuroscience*. 19:7405-7414.

Kreutzberg, G. 1982. Acute neural reaction to injury. *In* Repair and Regeneration of the Nervous System. Springer. 57-69.

Krivosheya, D., L. Tapia, J.N. Levinson, K. Huang, Y. Kang, R. Hines, A.K. Ting, A.M. Craig, L. Mei, S.X. Bamji, and A. El-Husseini. 2008. ErbB4-neuregulin signaling modulates synapse development and dendritic arborization through distinct mechanisms. *The Journal of biological chemistry*. 283:32944-32956.

Kubicek, L., R. Kopacik, I. Klusakova, and P. Dubovy. 2010. Alterations in the vascular architecture of the dorsal root ganglia in a rat neuropathic pain model. *Annals of anatomy = Anatomischer Anzeiger : official organ of the Anatomische Gesellschaft*. 192:101-106.

Kubo, T., T. Yamashita, A. Yamaguchi, K. Hosokawa, and M. Tohyama. 2002. Analysis of genes induced in peripheral nerve after axotomy using cDNA microarrays. *Journal of neurochemistry*. 82:1129-1136.

LaCroix-Fralish, M.L., J.S. Austin, F.Y. Zheng, D.J. Levitin, and J.S. Mogil. 2011. Patterns of pain: meta-analysis of microarray studies of pain. *Pain*. 152:1888-1898.

Lagunoff, D. 2002. Portraits of science. A Polish, Jewish scientist in 19th-century Prussia. *Science*. 298:2331.

Lamb, D.J., H. Modjtahedi, N.J. Plant, and G.A. Ferns. 2004. EGF mediates monocyte chemotaxis and macrophage proliferation and EGF receptor is expressed in atherosclerotic plaques. *Atherosclerosis*. 176:21-26.

Langley, J.N., and M. Hashimoto. 1917. On the suture of separate nerve bundles in a nerve trunk and on internal nerve plexuses. *The Journal of physiology*. 51:318-346.

Lentz, S.I., C.M. Knudson, S.J. Korsmeyer, and W.D. Snider. 1999. Neurotrophins support the development of diverse sensory axon morphologies. *The Journal of neuroscience : the official journal of the Society for Neuroscience*. 19:1038-1048.

Levy, D., M. Tal, A. Hoke, and D.W. Zochodne. 2000. Transient action of the endothelial constitutive nitric oxide synthase (ecNOS) mediates the development of thermal hypersensitivity following peripheral nerve injury. *The European journal of neuroscience*. 12:2323-2332.

Li, H., G. Terenghi, and S.M. Hall. 1997. Effects of delayed re-innervation on the expression of c-erbB receptors by chronically denervated rat Schwann cells in vivo. *Glia*. 20:333-347.

Li, K.X., Y.M. Lu, Z.H. Xu, J. Zhang, J.M. Zhu, J.M. Zhang, S.X. Cao, X.J. Chen, Z. Chen, J.H. Luo, S. Duan, and X.M. Li. 2012. Neuregulin 1 regulates excitability of fast-spiking neurons through Kv1.1 and acts in epilepsy. *Nature neuroscience*. 15:267-273.

Lindsay, R.M. 1988. Nerve growth factors (NGF, BDNF) enhance axonal regeneration but are not required for survival of adult sensory neurons. *The Journal of neuroscience : the official journal of the Society for Neuroscience*. 8:2394-2405.

Lindsay, R.M., E.M. Shooter, M.J. Radeke, T.P. Misko, G. Dechant, H. Thoenen, and D. Lindholm. 1990. Nerve Growth Factor Regulates Expression of the Nerve Growth Factor Receptor Gene in Adult Sensory Neurons. *The European journal of neuroscience*. 2:389-396.

Liu, K., A. Tedeschi, K.K. Park, and Z. He. 2011a. Neuronal intrinsic mechanisms of axon regeneration. *Annual review of neuroscience*. 34:131-152.

Liu, M., S. Guo, and J.K. Stiles. 2011b. The emerging role of CXCL10 in cancer (Review). *Oncology letters*. 2:583-589.

Livak, K.J., and T.D. Schmittgen. 2001. Analysis of relative gene expression data using real-time quantitative PCR and the 2(-Delta Delta C(T)) Method. *Methods*. 25:402-408.

Lopez-Vales, R., X. Navarro, T. Shimizu, C. Baskakis, G. Kokotos, V. Constantinou-Kokotou, D. Stephens, E.A. Dennis, and S. David. 2008. Intracellular phospholipase A(2) group IVA and group VIA play important roles in Wallerian degeneration and axon regeneration after peripheral nerve injury. *Brain : a journal of neurology*. 131:2620-2631.

Lowenstein, E.J., R.J. Daly, A.G. Batzer, W. Li, B. Margolis, R. Lammers, A. Ullrich, E.Y. Skolnik, D. Bar-Sagi, and J. Schlessinger. 1992. The SH2

and SH3 domain-containing protein GRB2 links receptor tyrosine kinases to ras signaling. *Cell*. 70:431-442.

Lubinska, L. 1977. Early course of Wallerian degeneration in myelinated fibres of the rat phrenic nerve. *Brain research*. 130:47-63.

Mandolesi, G., F. Madeddu, Y. Bozzi, L. Maffei, and G.M. Ratto. 2004. Acute physiological response of mammalian central neurons to axotomy: ionic regulation and electrical activity. *FASEB journal : official publication of the Federation of American Societies for Experimental Biology*. 18:1934-1936.

Mantovani, A., A. Sica, S. Sozzani, P. Allavena, A. Vecchi, and M. Locati. 2004. The chemokine system in diverse forms of macrophage activation and polarization. *Trends Immunol*. 25:677-686.

Marchand, F., M. Perretti, and S.B. McMahon. 2005. Role of the immune system in chronic pain. *Nature reviews. Neuroscience*. 6:521-532.

Martinez, F.O., S. Gordon, M. Locati, and A. Mantovani. 2006. Transcriptional profiling of the human monocyte-to-macrophage differentiation and polarization: new molecules and patterns of gene expression. *Journal of immunology*. 177:7303-7311.

Martinez, F.O., L. Helming, and S. Gordon. 2009. Alternative activation of macrophages: an immunologic functional perspective. *Annual review of immunology*. 27:451-483.

Martini, R., M. Schachner, and T.M. Brushart. 1994. The L2/HNK-1 carbohydrate is preferentially expressed by previously motor axon-associated Schwann cells in reinnervated peripheral nerves. *The Journal of neuroscience : the official journal of the Society for Neuroscience*. 14:7180-7191.

Mashima, H., H. Ohnishi, K. Wakabayashi, T. Mine, J. Miyagawa, T. Hanafusa, M. Seno, H. Yamada, and I. Kojima. 1996. Betacellulin and activin A coordinately convert amylase-secreting pancreatic AR42J cells into insulin-secreting cells. *The Journal of clinical investigation*. 97:1647-1654.

Massague, J. 1990. Transforming growth factor-alpha. A model for membrane-anchored growth factors. *The Journal of biological chemistry*. 265:21393-21396.

Matsuura, H., M. Sakaue, K. Subbaramaiah, H. Kamitani, T.E. Eling, A.J. Dannenberg, T. Tanabe, H. Inoue, J. Arata, and A.M. Jetten. 1999. Regulation of cyclooxygenase-2 by interferon gamma and transforming growth factor alpha in normal human epidermal keratinocytes and squamous carcinoma cells. Role of mitogen-activated protein kinases. *The Journal of biological chemistry*. 274:29138-29148.

McGinn, M.J., D. Sun, S.L. Schneider, J.K. Alexander, and R.J. Colello. 2004. Epidermal growth factor-induced cell proliferation in the adult rat striatum. *Brain research*. 1007:29-38.

McIntyre, E., E. Blackburn, P.J. Brown, C.G. Johnson, and W.J. Gullick. 2010. The complete family of epidermal growth factor receptors and their ligands are co-ordinately expressed in breast cancer. *Breast cancer research and treatment*. 122:105-110.

McKerracher, L., S. David, D.L. Jackson, V. Kottis, R.J. Dunn, and P.E. Braun. 1994. Identification of myelin-associated glycoprotein as a major myelin-derived inhibitor of neurite growth. *Neuron*. 13:805-811.

McKillop, D., A.D. McCormick, G.S. Miles, P.J. Phillips, K.J. Pickup, N. Bushby, and M. Hutchison. 2004. In vitro metabolism of gefitinib in human liver microsomes. *Xenobiotica; the fate of foreign compounds in biological systems*. 34:983-1000.

McLachlan, E.M., W. Janig, M. Devor, and M. Michaelis. 1993. Peripheral nerve injury triggers noradrenergic sprouting within dorsal root ganglia. *Nature*. 363:543-546.

McNamara, C.R., J. Mandel-Brehm, D.M. Bautista, J. Siemens, K.L. Deranian, M. Zhao, N.J. Hayward, J.A. Chong, D. Julius, M.M. Moran, and C.M. Fanger. 2007. TRPA1 mediates formalin-induced pain. *Proceedings of the National Academy of Sciences of the United States of America*. 104:13525-13530.

McQuarrie, I.G., B. Grafstein, and M.D. Gershon. 1977. Axonal regeneration in the rat sciatic nerve: effect of a conditioning lesion and of dbcAMP. *Brain research*. 132:443-453.

Meyer zu Horste, G., W. Hu, H.P. Hartung, H.C. Lehmann, and B.C. Kieseier. 2008. The immunocompetence of Schwann cells. *Muscle & nerve*. 37:3-13.

Michael, G.J., S. Averill, P.J. Shortland, Q. Yan, and J.V. Priestley. 1999. Axotomy results in major changes in BDNF expression by dorsal root ganglion cells: BDNF expression in large trkB and trkC cells, in pericellular baskets, and in projections to deep dorsal horn and dorsal column nuclei. *The European journal of neuroscience*. 11:3539-3551.

Michaelevski, I., Y. Segal-Ruder, M. Rozenbaum, K.F. Medzihradszky, O. Shalem, G. Coppola, S. Horn-Saban, K. Ben-Yaakov, S.Y. Dagan, I. Rishal, D.H. Geschwind, Y. Pilpel, A.L. Burlingame, and M. Fainzilber. 2010. Signaling to transcription networks in the neuronal retrograde injury response. *Science signaling*. 3:ra53.

Mifune, M., H. Ohtsu, H. Suzuki, G.D. Frank, T. Inagami, H. Utsunomiya, P.J. Dempsey, and S. Eguchi. 2004. Signal transduction of betacellulin in growth and migration of vascular smooth muscle cells. *American journal of physiology. Cell physiology*. 287:C807-813.

Mishima, K., S. Higashiyama, Y. Nagashima, Y. Miyagi, A. Tamura, N. Kawahara, N. Taniguchi, A. Asai, Y. Kuchino, and T. Kirino. 1996. Regional distribution of heparin-binding epidermal growth factor-like growth factor mRNA and protein in adult rat forebrain. *Neuroscience letters*. 213:153-156.

Miyata, Y., Y. Kashihara, S. Homma, and M. Kuno. 1986. Effects of nerve growth factor on the survival and synaptic function of Ia sensory neurons axotomized in neonatal rats. *The Journal of neuroscience : the official journal of the Society for Neuroscience*. 6:2012-2018.

Moalem, G., K. Xu, and L. Yu. 2004. T lymphocytes play a role in neuropathic pain following peripheral nerve injury in rats. *Neuroscience*. 129:767-777.

Mogil, J.S. 2009. Animal models of pain: progress and challenges. *Nature reviews. Neuroscience*. 10:283-294.

Mokarram, N., A. Merchant, V. Mukhatyar, G. Patel, and R.V. Bellamkonda. 2012. Effect of modulating macrophage phenotype on peripheral nerve repair. *Biomaterials*. 33:8793-8801.

Monaco, S., J. Gehrmann, G. Raivich, and G.W. Kreutzberg. 1992. MHC-positive, ramified macrophages in the normal and injured rat peripheral nervous system. *Journal of neurocytology*. 21:623-634.

Moon, W.S., H.S. Park, K.H. Yu, M.Y. Park, K.R. Kim, K.Y. Jang, J.S. Kim, and B.H. Cho. 2006. Expression of betacellulin and epidermal growth factor receptor in hepatocellular carcinoma: implications for angiogenesis. *Human pathology*. 37:1324-1332.

Moore, K.A., T. Kohno, L.A. Karchewski, J. Scholz, H. Baba, and C.J. Woolf. 2002. Partial peripheral nerve injury promotes a selective loss of GABAergic inhibition in the superficial dorsal horn of the spinal cord. *The*

Journal of neuroscience : the official journal of the Society for Neuroscience. 22:6724-6731.

Moore, K.J., V.V. Kunjathoor, S.L. Koehn, J.J. Manning, A.A. Tseng, J.M. Silver, M. McKee, and M.W. Freeman. 2005. Loss of receptor-mediated lipid uptake via scavenger receptor A or CD36 pathways does not ameliorate atherosclerosis in hyperlipidemic mice. *The Journal of clinical investigation*. 115:2192-2201.

Mosley, K., and M.L. Cuzner. 1996. Receptor-mediated phagocytosis of myelin by macrophages and microglia: effect of opsonization and receptor blocking agents. *Neurochemical research*. 21:481-487.

Mueller, M., C. Leonhard, K. Wacker, E.B. Ringelstein, M. Okabe, W.F. Hickey, and R. Kiefer. 2003. Macrophage response to peripheral nerve injury: the quantitative contribution of resident and hematogenous macrophages. *Laboratory investigation; a journal of technical methods and pathology*. 83:175-185.

Mueller, M., K. Wacker, E.B. Ringelstein, W.F. Hickey, Y. Imai, and R. Kiefer. 2001. Rapid response of identified resident endoneurial macrophages to nerve injury. *The American journal of pathology*. 159:2187-2197.

Mummery, R.S., B. Mulloy, and C.C. Rider. 2007. The binding of human betacellulin to heparin, heparan sulfate and related polysaccharides. *Glycobiology*. 17:1094-1103.

Myers, R.R., H.M. Heckman, and M. Rodriguez. 1996. Reduced hyperalgesia in nerve-injured WLD mice: relationship to nerve fiber phagocytosis, axonal degeneration, and regeneration in normal mice. *Experimental neurology*. 141:94-101.

Nadeau, S., M. Filali, J. Zhang, B.J. Kerr, S. Rivest, D. Soulet, Y. Iwakura, J.P. de Rivero Vaccari, R.W. Keane, and S. Lacroix. 2011. Functional

recovery after peripheral nerve injury is dependent on the pro-inflammatory cytokines IL-1beta and TNF-: implications for neuropathic pain. *The Journal of neuroscience : the official journal of the Society for Neuroscience*. 31:12533-12542.

Nakahashi, T., H. Fujimura, C.A. Altar, J. Li, J. Kambayashi, N.N. Tandon, and B. Sun. 2000. Vascular endothelial cells synthesize and secrete brain-derived neurotrophic factor. *FEBS letters*. 470:113-117.

Namaka, M.P., M. Sawchuk, S.C. MacDonald, L.M. Jordan, and S. Hochman. 2001. Neurogenesis in postnatal mouse dorsal root ganglia. *Experimental neurology*. 172:60-69.

Napoli, I., L.A. Noon, S. Ribeiro, A.P. Kerai, S. Parrinello, L.H. Rosenberg, M.J. Collins, M.C. Harrisingh, I.J. White, A. Woodhoo, and A.C. Lloyd. 2012. A central role for the ERK-signaling pathway in controlling Schwann cell plasticity and peripheral nerve regeneration in vivo. *Neuron*. 73:729-742.

Neumann, S., and C.J. Woolf. 1999. Regeneration of dorsal column fibers into and beyond the lesion site following adult spinal cord injury. *Neuron*. 23:83-91.

Oh, Y.S., S. Shin, Y.J. Lee, E.H. Kim, and H.S. Jun. 2011. Betacellulin-induced beta cell proliferation and regeneration is mediated by activation of ErbB-1 and ErbB-2 receptors. *PloS one*. 6:e23894.

Olayioye, M.A. 2001. Update on HER-2 as a target for cancer therapy: intracellular signaling pathways of ErbB2/HER-2 and family members. *Breast cancer research : BCR*. 3:385-389.

Osterloh, J.M., J. Yang, T.M. Rooney, A.N. Fox, R. Adalbert, E.H. Powell, A.E. Sheehan, M.A. Avery, R. Hackett, M.A. Logan, J.M. MacDonald, J.S. Ziegenfuss, S. Milde, Y.J. Hou, C. Nathan, A. Ding, R.H. Brown, Jr., L. Conforti, M. Coleman, M. Tessier-Lavigne, S. Zuchner, and M.R.

Freeman. 2012. dSarm/Sarm1 is required for activation of an injury-induced axon death pathway. *Science*. 337:481-484.

Palmer, R.M., D.S. Ashton, and S. Moncada. 1988. Vascular endothelial cells synthesize nitric oxide from L-arginine. *Nature*. 333:664-666.

Park, J.Y., Y.Q. Su, M. Ariga, E. Law, S.L. Jin, and M. Conti. 2004. EGF-like growth factors as mediators of LH action in the ovulatory follicle. *Science*. 303:682-684.

Parkinson, D.B., A. Bhaskaran, P. Arthur-Farraj, L.A. Noon, A. Woodhoo, A.C. Lloyd, M.L. Feltri, L. Wrabetz, A. Behrens, R. Mirsky, and K.R. Jessen. 2008. c-Jun is a negative regulator of myelination. *The Journal of cell biology*. 181:625-637.

Passaniti, A., R.M. Taylor, R. Pili, Y. Guo, P.V. Long, J.A. Haney, R.R. Pauly, D.S. Grant, and G.R. Martin. 1992. A simple, quantitative method for assessing angiogenesis and antiangiogenic agents using reconstituted basement membrane, heparin, and fibroblast growth factor. *Laboratory investigation; a journal of technical methods and pathology*. 67:519-528.

Pastore, S., F. Mascia, V. Mariani, and G. Girolomoni. 2008. The epidermal growth factor receptor system in skin repair and inflammation. *The Journal of investigative dermatology*. 128:1365-1374.

Patapoutian, A., and L.F. Reichardt. 2001. Trk receptors: mediators of neurotrophin action. *Current opinion in neurobiology*. 11:272-280.

Pearson, R.J., Jr., and S.L. Carroll. 2004. ErbB transmembrane tyrosine kinase receptors are expressed by sensory and motor neurons projecting into sciatic nerve. *The journal of histochemistry and cytochemistry : official journal of the Histochemistry Society*. 52:1299-1311.

Perkins, N.M., and D.J. Tracey. 2000. Hyperalgesia due to nerve injury: role of neutrophils. *Neuroscience*. 101:745-757.

Perlson, E., S. Hanz, K. Ben-Yaakov, Y. Segal-Ruder, R. Seger, and M. Fainzilber. 2005. Vimentin-dependent spatial translocation of an activated MAP kinase in injured nerve. *Neuron*. 45:715-726.

Perrin, F.E., S. Lacroix, M. Aviles-Trigueros, and S. David. 2005. Involvement of monocyte chemoattractant protein-1, macrophage inflammatory protein-1alpha and interleukin-1beta in Wallerian degeneration. *Brain : a journal of neurology*. 128:854-866.

Perry, V.H., M.C. Brown, and S. Gordon. 1987. The macrophage response to central and peripheral nerve injury. A possible role for macrophages in regeneration. *The Journal of experimental medicine*. 165:1218-1223.

Perry, V.H., J.W. Tsao, S. Fearn, and M.C. Brown. 1995. Radiation-induced reductions in macrophage recruitment have only slight effects on myelin degeneration in sectioned peripheral nerves of mice. *The European journal of neuroscience*. 7:271-280.

Pezet, S., and S.B. McMahon. 2006. Neurotrophins: mediators and modulators of pain. *Annual review of neuroscience*. 29:507-538.

Piiper, A., I. Dikic, M.P. Lutz, J. Leser, B. Kronenberger, R. Elez, H. Cramer, W. Muller-Esterl, and S. Zeuzem. 2002. Cyclic AMP induces transactivation of the receptors for epidermal growth factor and nerve growth factor, thereby modulating activation of MAP kinase, Akt, and neurite outgrowth in PC12 cells. *The Journal of biological chemistry*. 277:43623-43630.

Pinkas-Kramarski, R., A.E. Lenferink, S.S. Bacus, L. Lyass, M.L. van de Poll, L.N. Klapper, E. Tzahar, M. Sela, E.J. van Zoelen, and Y. Yarden. 1998. The oncogenic ErbB-2/ErbB-3 heterodimer is a surrogate receptor of the epidermal growth factor and betacellulin. *Oncogene*. 16:1249-1258.

Podhajsky, R.J., and R.R. Myers. 1993. The vascular response to nerve crush: relationship to Wallerian degeneration and regeneration. *Brain research*. 623:117-123.

Pratt, J.M., J. Petty, I. Riba-Garcia, D.H. Robertson, S.J. Gaskell, S.G. Oliver, and R.J. Beynon. 2002. Dynamics of protein turnover, a missing dimension in proteomics. *Molecular & cellular proteomics : MCP*. 1:579-591.

Quinn, S.M., W.M. Walters, A.L. Vescovi, and S.R. Whittemore. 1999. Lineage restriction of neuroepithelial precursor cells from fetal human spinal cord. *Journal of neuroscience research*. 57:590-602.

Raivich, G., R. Hellweg, and G.W. Kreutzberg. 1991. NGF receptor-mediated reduction in axonal NGF uptake and retrograde transport following sciatic nerve injury and during regeneration. *Neuron*. 7:151-164.

Raivich, G., L.L. Jones, C.U. Kloss, A. Werner, H. Neumann, and G.W. Kreutzberg. 1998. Immune surveillance in the injured nervous system: T-lymphocytes invade the axotomized mouse facial motor nucleus and aggregate around sites of neuronal degeneration. *The Journal of neuroscience : the official journal of the Society for Neuroscience*. 18:5804-5816.

Raivich, G., and M. Makwana. 2007. The making of successful axonal regeneration: genes, molecules and signal transduction pathways. *Brain research reviews*. 53:287-311.

Ramer, M.S., G.D. French, and M.A. Bisby. 1997. Wallerian degeneration is required for both neuropathic pain and sympathetic sprouting into the DRG. *Pain*. 72:71-78.

Ramm, P., Y. Alexandrov, A. Cholewinski, Y. Cybuch, R. Nadon, and B.J. Soltys. 2003. Automated screening of neurite outgrowth. *Journal of biomolecular screening*. 8:7-18.

Reichert, F., R. Levitzky, and S. Rotshenker. 1996. Interleukin 6 in intact and injured mouse peripheral nerves. *The European journal of neuroscience*. 8:530-535.

Reichert, F., and S. Rotshenker. 2003. Complement-receptor-3 and scavenger-receptor-AI/II mediated myelin phagocytosis in microglia and macrophages. *Neurobiology of disease*. 12:65-72.

Reichert, F., A. Saada, and S. Rotshenker. 1994. Peripheral nerve injury induces Schwann cells to express two macrophage phenotypes: phagocytosis and the galactose-specific lectin MAC-2. *The Journal of neuroscience : the official journal of the Society for Neuroscience*. 14:3231-3245.

Remak, R. 1844. Neurologische Erläuterungen. *Arch Anat Physiol wiss Med*. 12:463-472.

Rieff, H.I., L.T. Raetzman, D.W. Sapp, H.H. Yeh, R.E. Siegel, and G. Corfas. 1999. Neuregulin induces GABA(A) receptor subunit expression and neurite outgrowth in cerebellar granule cells. *The Journal of neuroscience : the official journal of the Society for Neuroscience*. 19:10757-10766.

Rishal, I., and M. Fainzilber. 2010. Retrograde signaling in axonal regeneration. *Experimental neurology*. 223:5-10.

Rosenberg, A.F., M.A. Wolman, C. Franzini-Armstrong, and M. Granato. 2012. In vivo nerve-macrophage interactions following peripheral nerve injury. *The Journal of neuroscience : the official journal of the Society for Neuroscience*. 32:3898-3909.

Rossi, F., S. Gianola, and L. Corvetti. 2007. Regulation of intrinsic neuronal properties for axon growth and regeneration. *Progress in neurobiology*. 81:1-28.

Rotshenker, S. 2003. Microglia and macrophage activation and the regulation of complement-receptor-3 (CR3/MAC-1)-mediated myelin phagocytosis in injury and disease. *Journal of molecular neuroscience : MN*. 21:65-72.

Rotshenker, S. 2011. Wallerian degeneration: the innate-immune response to traumatic nerve injury. *Journal of neuroinflammation*. 8:109.

Saada, A., F. Reichert, and S. Rotshenker. 1996. Granulocyte macrophage colony stimulating factor produced in lesioned peripheral nerves induces the up-regulation of cell surface expression of MAC-2 by macrophages and Schwann cells. *The Journal of cell biology*. 133:159-167.

Sahin, U., G. Weskamp, K. Kelly, H.M. Zhou, S. Higashiyama, J. Peschon, D. Hartmann, P. Saftig, and C.P. Blobel. 2004. Distinct roles for ADAM10 and ADAM17 in ectodomain shedding of six EGFR ligands. *The Journal of cell biology*. 164:769-779.

Saito, H., Y. Nakao, S. Takayama, Y. Toyama, and H. Asou. 2005. Specific expression of an HNK-1 carbohydrate epitope and NCAM on femoral nerve Schwann cells in mice. *Neuroscience research*. 53:314-322.

Sanderson, M.P., S.N. Erickson, P.J. Gough, K.J. Garton, P.T. Wille, E.W. Raines, A.J. Dunbar, and P.J. Dempsey. 2005. ADAM10 mediates ectodomain shedding of the betacellulin precursor activated by p-aminophenylmercuric acetate and extracellular calcium influx. *The Journal of biological chemistry*. 280:1826-1837.

Sato, S., C. St-Pierre, P. Bhaumik, and J. Nieminen. 2009. Galectins in innate immunity: dual functions of host soluble beta-galactoside-binding lectins as damage-associated molecular patterns (DAMPs) and as receptors for

pathogen-associated molecular patterns (PAMPs). *Immunological reviews*. 230:172-187.

Scaltriti, M., and J. Baselga. 2006. The epidermal growth factor receptor pathway: a model for targeted therapy. *Clinical cancer research : an official journal of the American Association for Cancer Research*. 12:5268-5272.

Scapini, P., J.A. Lapinet-Vera, S. Gasperini, F. Calzetti, F. Bazzoni, and M.A. Cassatella. 2000. The neutrophil as a cellular source of chemokines. *Immunological reviews*. 177:195-203.

Schmittgen, T.D., and K.J. Livak. 2008. Analyzing real-time PCR data by the comparative C(T) method. *Nature protocols*. 3:1101-1108.

Schneider, M.R., M. Antsiferova, L. Feldmeyer, M. Dahlhoff, P. Bugnon, S. Hasse, R. Paus, E. Wolf, and S. Werner. 2008. Betacellulin regulates hair follicle development and hair cycle induction and enhances angiogenesis in wounded skin. *The Journal of investigative dermatology*. 128:1256-1265.

Schneider, M.R., M. Dahlhoff, N. Herbach, I. Renner-Mueller, C. Dalke, O. Puk, J. Graw, R. Wanke, and E. Wolf. 2005. Betacellulin overexpression in transgenic mice causes disproportionate growth, pulmonary hemorrhage syndrome, and complex eye pathology. *Endocrinology*. 146:5237-5246.

Schneider, M.R., and E. Wolf. 2009. The epidermal growth factor receptor ligands at a glance. *Journal of cellular physiology*. 218:460-466.

Scholz, J., and C.J. Woolf. 2007. The neuropathic pain triad: neurons, immune cells and glia. *Nature neuroscience*. 10:1361-1368.

Sebert, M.E., and E.M. Shooter. 1993. Expression of mRNA for neurotrophic factors and their receptors in the rat dorsal root ganglion and sciatic

nerve following nerve injury. *Journal of neuroscience research*. 36:357-367.

Shamash, S., F. Reichert, and S. Rotshenker. 2002. The cytokine network of Wallerian degeneration: tumor necrosis factor-alpha, interleukin-1alpha, and interleukin-1beta. *The Journal of neuroscience : the official journal of the Society for Neuroscience*. 22:3052-3060.

Shelton, D.L., and L.F. Reichardt. 1984. Expression of the beta-nerve growth factor gene correlates with the density of sympathetic innervation in effector organs. *Proceedings of the National Academy of Sciences of the United States of America*. 81:7951-7955.

Shim, S., and G.L. Ming. 2010. Roles of channels and receptors in the growth cone during PNS axonal regeneration. *Experimental neurology*. 223:38-44.

Shing, Y., G. Christofori, D. Hanahan, Y. Ono, R. Sasada, K. Igarashi, and J. Folkman. 1993. Betacellulin: a mitogen from pancreatic beta cell tumors. *Science*. 259:1604-1607.

Shoyab, M., V.L. McDonald, J.G. Bradley, and G.J. Todaro. 1988. Amphiregulin: a bifunctional growth-modulating glycoprotein produced by the phorbol 12-myristate 13-acetate-treated human breast adenocarcinoma cell line MCF-7. *Proceedings of the National Academy of Sciences of the United States of America*. 85:6528-6532.

Shubayev, V.I., and R.R. Myers. 2002. Endoneurial remodeling by TNF-alph- and TNF-alpha-releasing proteases. A spatial and temporal co-localization study in painful neuropathy. *Journal of the peripheral nervous system : JPNS*. 7:28-36.

Siebert, H., N. Dippel, M. Mader, F. Weber, and W. Bruck. 2001. Matrix metalloproteinase expression and inhibition after sciatic nerve axotomy. *Journal of neuropathology and experimental neurology*. 60:85-93.

Silverstein, R.L., and M. Febbraio. 2009. CD36, a scavenger receptor involved in immunity, metabolism, angiogenesis, and behavior. *Science signaling*. 2:re3.

Singer, A.J., and R.A. Clark. 1999. Cutaneous wound healing. *The New England journal of medicine*. 341:738-746.

Singh, A.B., and R.C. Harris. 2005. Autocrine, paracrine and juxtacrine signaling by EGFR ligands. *Cellular signalling*. 17:1183-1193.

Sirotnak, F.M., M.F. Zakowski, V.A. Miller, H.I. Scher, and M.G. Kris. 2000. Efficacy of cytotoxic agents against human tumor xenografts is markedly enhanced by coadministration of ZD1839 (Iressa), an inhibitor of EGFR tyrosine kinase. *Clinical cancer research : an official journal of the American Association for Cancer Research*. 6:4885-4892.

Soilu-Hanninen, M., P. Ekert, T. Bucci, D. Syroid, P.F. Bartlett, and T.J. Kilpatrick. 1999. Nerve growth factor signaling through p75 induces apoptosis in Schwann cells via a Bcl-2-independent pathway. *The Journal of neuroscience : the official journal of the Society for Neuroscience*. 19:4828-4838.

Sommer, C., and M. Schafers. 1998. Painful mononeuropathy in C57BL/Wld mice with delayed wallerian degeneration: differential effects of cytokine production and nerve regeneration on thermal and mechanical hypersensitivity. *Brain research*. 784:154-162.

Sondell, M., G. Lundborg, and M. Kanje. 1999. Vascular endothelial growth factor has neurotrophic activity and stimulates axonal outgrowth, enhancing cell survival and Schwann cell proliferation in the peripheral

nervous system. *The Journal of neuroscience : the official journal of the Society for Neuroscience*. 19:5731-5740.

Spreyer, P., H. Schaal, G. Kuhn, T. Rothe, A. Unterbeck, K. Olek, and H.W. Muller. 1990. Regeneration-associated high level expression of apolipoprotein D mRNA in endoneurial fibroblasts of peripheral nerve. *The EMBO journal*. 9:2479-2484.

Srinivasan, R., E. Benton, F. McCormick, H. Thomas, and W.J. Gullick. 1999. Expression of the c-erbB-3/HER-3 and c-erbB-4/HER-4 growth factor receptors and their ligands, neuregulin-1 alpha, neuregulin-1 beta, and betacellulin, in normal endometrium and endometrial cancer. *Clinical cancer research : an official journal of the American Association for Cancer Research*. 5:2877-2883.

Stapleton, J.A., K. Endo, Y. Fujita, K. Hayashi, M. Takinoue, H. Saito, and T. Inoue. 2012. Feedback control of protein expression in mammalian cells by tunable synthetic translational inhibition. *ACS synthetic biology*. 1:83-88.

Stassart, R.M., R. Fledrich, V. Velanac, B.G. Brinkmann, M.H. Schwab, D. Meijer, M.W. Sereda, and K.A. Nave. 2013. A role for Schwann cell-derived neuregulin-1 in remyelination. *Nature neuroscience*. 16:48-54.

Stoll, G., J.W. Griffin, C.Y. Li, and B.D. Trapp. 1989. Wallerian degeneration in the peripheral nervous system: participation of both Schwann cells and macrophages in myelin degradation. *Journal of neurocytology*. 18:671-683.

Strachan, L., J.G. Murison, R.L. Prestidge, M.A. Sleeman, J.D. Watson, and K.D. Kumble. 2001. Cloning and biological activity of epigen, a novel member of the epidermal growth factor superfamily. *The Journal of biological chemistry*. 276:18265-18271.

Subang, M.C., and P.M. Richardson. 2001. Synthesis of leukemia inhibitory factor in injured peripheral nerves and their cells. *Brain research*. 900:329-331.

Sulaiman, O.A., and T. Gordon. 2000. Effects of short- and long-term Schwann cell denervation on peripheral nerve regeneration, myelination, and size. *Glia*. 32:234-246.

Tada, H., R. Sasada, Y. Kawaguchi, I. Kojima, W.J. Gullick, D.S. Salomon, K. Igarashi, M. Seno, and H. Yamada. 1999. Processing and juxtacrine activity of membrane-anchored betacellulin. *Journal of cellular biochemistry*. 72:423-434.

Tamura, R., J. Miyagawa, M. Nishida, S. Kihara, R. Sasada, K. Igarashi, A. Nakata, K. Yamamori, K. Kameda-Takemura, S. Yamashita, and Y. Matsuzawa. 2001. Immunohistochemical localization of Betacellulin, a member of epidermal growth factor family, in atherosclerotic plaques of human aorta. *Atherosclerosis*. 155:413-423.

Taniuchi, M., H.B. Clark, J.B. Schweitzer, and E.M. Johnson, Jr. 1988. Expression of nerve growth factor receptors by Schwann cells of axotomized peripheral nerves: ultrastructural location, suppression by axonal contact, and binding properties. *The Journal of neuroscience : the official journal of the Society for Neuroscience*. 8:664-681.

Terenghi, G. 1999. Peripheral nerve regeneration and neurotrophic factors. *Journal of anatomy*. 194 (Pt 1):1-14.

Tessier-Lavigne, M., and C.S. Goodman. 1996. The molecular biology of axon guidance. *Science*. 274:1123-1133.

Tetzlaff, W. 1982. Tight junction contact events and temporary gap junctions in the sciatic nerve fibres of the chicken during Wallerian degeneration and subsequent regeneration. *Journal of neurocytology*. 11:839-858.

Thowfeequ, S., K.L. Ralphs, W.Y. Yu, J.M. Slack, and D. Tosh. 2007. Betacellulin inhibits amylase and glucagon production and promotes beta cell differentiation in mouse embryonic pancreas. *Diabetologia*. 50:1688-1697.

Todd, A.J. 2010. Neuronal circuitry for pain processing in the dorsal horn. *Nature reviews. Neuroscience*. 11:823-836.

Toma, J.G., S. Pareek, P. Barker, T.C. Mathew, R.A. Murphy, A. Acheson, and F.D. Miller. 1992. Spatiotemporal increases in epidermal growth factor receptors following peripheral nerve injury. *The Journal of neuroscience : the official journal of the Society for Neuroscience*. 12:2504-2515.

Tonra, J.R., R. Curtis, V. Wong, K.D. Cliffer, J.S. Park, A. Timmes, T. Nguyen, R.M. Lindsay, A. Acheson, and P.S. DiStefano. 1998. Axotomy upregulates the anterograde transport and expression of brain-derived neurotrophic factor by sensory neurons. *The Journal of neuroscience : the official journal of the Society for Neuroscience*. 18:4374-4383.

Toyoda, H., T. Komurasaki, D. Uchida, Y. Takayama, T. Isobe, T. Okuyama, and K. Hanada. 1995. Epiregulin. A novel epidermal growth factor with mitogenic activity for rat primary hepatocytes. *The Journal of biological chemistry*. 270:7495-7500.

Trapp, B.D., P. Hauer, and G. Lemke. 1988. Axonal regulation of myelin protein mRNA levels in actively myelinating Schwann cells. *The Journal of neuroscience : the official journal of the Society for Neuroscience*. 8:3515-3521.

Tse, A.C., and W. Ge. 2009. Differential regulation of betacellulin and heparin-binding EGF-like growth factor in cultured zebrafish ovarian follicle cells by EGF family ligands. *Comparative biochemistry and physiology. Part A, Molecular & integrative physiology*. 153:13-17.

Tsien, R.Y. 1981. A non-disruptive technique for loading calcium buffers and indicators into cells. *Nature*. 290:527-528.

Turner, P.V., E. Vaughn, J. Sunohara-Neilson, J. Ovari, and F. Leri. 2012. Oral gavage in rats: animal welfare evaluation. *Journal of the American Association for Laboratory Animal Science : JAALAS*. 51:25-30.

Udina, E., M. Furey, S. Busch, J. Silver, T. Gordon, and K. Fouad. 2008. Electrical stimulation of intact peripheral sensory axons in rats promotes outgrowth of their central projections. *Experimental neurology*. 210:238-247.

Ueda, H. 2006. Molecular mechanisms of neuropathic pain-phenotypic switch and initiation mechanisms. *Pharmacology & therapeutics*. 109:57-77.

Ullrich, A., and J. Schlessinger. 1990. Signal transduction by receptors with tyrosine kinase activity. *Cell*. 61:203-212.

Umezawa, H., M. Imoto, T. Sawa, K. Isshiki, N. Matsuda, T. Uchida, H. Iinuma, M. Hamada, and T. Takeuchi. 1986. Studies on a new epidermal growth factor-receptor kinase inhibitor, erbstatin, produced by MH435-hF3. *The Journal of antibiotics*. 39:170-173.

Valyi-Nagy, I., P.J. Jensen, S.M. Albelda, and U. Rodeck. 1992. Cytokine-induced expression of transforming growth factor-alpha and the epidermal growth factor receptor in neonatal skin explants. *The Journal of investigative dermatology*. 99:350-356.

Vandesompele, J., K. De Preter, F. Pattyn, B. Poppe, N. Van Roy, A. De Paepe, and F. Speleman. 2002. Accurate normalization of real-time quantitative RT-PCR data by geometric averaging of multiple internal control genes. *Genome biology*. 3:RESEARCH0034.

Vargas, M.E., and B.A. Barres. 2007. Why is Wallerian degeneration in the CNS so slow? *Annual review of neuroscience*. 30:153-179.

Vargas, M.E., J. Watanabe, S.J. Singh, W.H. Robinson, and B.A. Barres. 2010. Endogenous antibodies promote rapid myelin clearance and effective axon regeneration after nerve injury. *Proceedings of the National Academy of Sciences of the United States of America*. 107:11993-11998.

Vaskovsky, A., Z. Lupowitz, S. Erlich, and R. Pinkas-Kramarski. 2000. ErbB-4 activation promotes neurite outgrowth in PC12 cells. *Journal of neurochemistry*. 74:979-987.

Vega, J.A., E. Vazquez, F.J. Naves, B. Calzada, M.E. del Valle, and J.J. Represa. 1994. Expression of epidermal growth factor receptor (EGFr) immunoreactivity in human cutaneous nerves and sensory corpuscles. *The Anatomical record*. 240:125-130.

Verkhratsky, A., and H. Kettenmann. 1996. Calcium signalling in glial cells. *Trends in neurosciences*. 19:346-352.

Vlaicu, P., P. Mertins, T. Mayr, P. Widschwendter, B. Ataseven, B. Hogel, W. Eiermann, P. Knyazev, and A. Ullrich. 2013. Monocytes/macrophages support mammary tumor invasivity by co-secreting lineage-specific EGFR ligands and a STAT3 activator. *BMC cancer*. 13:197.

Wagner, R., and R.R. Myers. 1996. Schwann cells produce tumor necrosis factor alpha: expression in injured and non-injured nerves. *Neuroscience*. 73:625-629.

Waller, A. 1850. Experiments on the section of the glossopharyngeal and hypoglossal nerves of the frog, and observations of the alterations produced thereby in the structure of their primitive fibres. *Philosophical Transactions of the Royal Society of London*. 140:423-429.

Wang, Y., J. Li, C. Ying Wang, A.H. Yan Kwok, and F.C. Leung. 2007. Epidermal growth factor (EGF) receptor ligands in the chicken ovary: I. Evidence for heparin-binding EGF-like growth factor (HB-EGF) as a potential oocyte-derived signal to control granulosa cell proliferation and HB-EGF and kit ligand expression. *Endocrinology*. 148:3426-3440.

Werner, M.H., L.B. Nanney, C.M. Stoscheck, and L.E. King. 1988. Localization of immunoreactive epidermal growth factor receptors in human nervous system. *The journal of histochemistry and cytochemistry : official journal of the Histochemistry Society*. 36:81-86.

White, F.V., A.D. Toews, J.F. Goodrum, D.L. Novicki, T.W. Bouldin, and P. Morell. 1989. Lipid metabolism during early stages of Wallerian degeneration in the rat sciatic nerve. *Journal of neurochemistry*. 52:1085-1092.

White, R.E., F.Q. Yin, and L.B. Jakeman. 2008. TGF-alpha increases astrocyte invasion and promotes axonal growth into the lesion following spinal cord injury in mice. *Experimental neurology*. 214:10-24.

Whitworth, I.H., G. Terenghi, C.J. Green, R.A. Brown, E. Stevens, and D.R. Tomlinson. 1995. Targeted delivery of nerve growth factor via fibronectin conduits assists nerve regeneration in control and diabetic rats. *The European journal of neuroscience*. 7:2220-2225.

Wiberg, M., C. Ljungberg, A. O'Byrne, R. Brown, I. Whitworth, A. Liss, and G. Terenghi. 1999. Primary sensory neuron survival following targeted administration of nerve growth factor to an injured nerve. *Scandinavian journal of plastic and reconstructive surgery and hand surgery / Nordisk plastikkirurgisk forening [and] Nordisk klubb for handkirurgi*. 33:387-392.

Wildering, W.C., P.M. Hermann, and A.G. Bulloch. 2001. Lymnaea epidermal growth factor promotes axonal regeneration in CNS organ culture. *The*

Journal of neuroscience : the official journal of the Society for Neuroscience. 21:9345-9354.

Wilhelm, J.C., M. Xu, D. Cucoranu, S. Chmielewski, T. Holmes, K.S. Lau, G.J. Bassell, and A.W. English. 2012. Cooperative roles of BDNF expression in neurons and Schwann cells are modulated by exercise to facilitate nerve regeneration. *The Journal of neuroscience : the official journal of the Society for Neuroscience*. 32:5002-5009.

Woolf, C.J., and M.W. Salter. 2000. Neuronal plasticity: increasing the gain in pain. *Science*. 288:1765-1769.

Wu, G., M. Ringkamp, T.V. Hartke, B.B. Murinson, J.N. Campbell, J.W. Griffin, and R.A. Meyer. 2001. Early onset of spontaneous activity in uninjured C-fiber nociceptors after injury to neighboring nerve fibers. *The Journal of neuroscience : the official journal of the Society for Neuroscience*. 21:RC140.

Wu, Y.Y., and R.A. Bradshaw. 1996. Synergistic induction of neurite outgrowth by nerve growth factor or epidermal growth factor and interleukin-6 in PC12 cells. *The Journal of biological chemistry*. 271:13033-13039.

Xia, M., and Y. Zhu. 2011. Signaling pathways of ATP-induced PGE2 release in spinal cord astrocytes are EGFR transactivation-dependent. *Glia*. 59:664-674.

Xian, C.J., L. Li, Y.S. Deng, S.P. Zhao, and X.F. Zhou. 2001. Lack of effects of transforming growth factor-alpha gene knockout on peripheral nerve regeneration may result from compensatory mechanisms. *Experimental neurology*. 172:182-188.

Xian, C.J., and X.F. Zhou. 1999a. Neuronal-glial differential expression of TGF-alpha and its receptor in the dorsal root ganglia in response to sciatic nerve lesion. *Experimental neurology*. 157:317-326.

Xian, C.J., and X.F. Zhou. 1999b. Roles of transforming growth factor-alpha and related molecules in the nervous system. *Molecular neurobiology*. 20:157-183.

Xing, W., M. Deng, J. Zhang, H. Huang, O. Dirsch, and U. Dahmen. 2009. Quantitative evaluation and selection of reference genes in a rat model of extended liver resection. *Journal of biomolecular techniques : JBT*. 20:109-115.

Yan, Q., J. Elliott, and W.D. Snider. 1992. Brain-derived neurotrophic factor rescues spinal motor neurons from axotomy-induced cell death. *Nature*. 360:753-755.

Yang, H., P. Lu, H.M. McKay, T. Bernot, H. Keirstead, O. Steward, F.H. Gage, V.R. Edgerton, and M.H. Tuszynski. 2006a. Endogenous neurogenesis replaces oligodendrocytes and astrocytes after primate spinal cord injury. *The Journal of neuroscience : the official journal of the Society for Neuroscience*. 26:2157-2166.

Yang, H., Z. Wang, J.E. Capo-Aponte, F. Zhang, Z. Pan, and P.S. Reinach. 2010. Epidermal growth factor receptor transactivation by the cannabinoid receptor (CB1) and transient receptor potential vanilloid 1 (TRPV1) induces differential responses in corneal epithelial cells. *Experimental eye research*. 91:462-471.

Yang, P., K.A. Baker, and T. Hagg. 2006b. The ADAMs family: coordinators of nervous system development, plasticity and repair. *Progress in neurobiology*. 79:73-94.

Yarden, Y., and G. Pines. 2012. The ERBB network: at last, cancer therapy meets systems biology. *Nature reviews. Cancer*. 12:553-563.

Yarden, Y., and M.X. Sliwkowski. 2001. Untangling the ErbB signalling network. *Nature reviews. Molecular cell biology*. 2:127-137.

Ydens, E., A. Cauwels, B. Asselbergh, S. Goethals, L. Peeraer, G. Lornet, L. Almeida-Souza, J.A. Van Ginderachter, V. Timmerman, and S. Janssens. 2012. Acute injury in the peripheral nervous system triggers an alternative macrophage response. *Journal of neuroinflammation*. 9:176.

Zhang, J.Y., X.G. Luo, C.J. Xian, Z.H. Liu, and X.F. Zhou. 2000. Endogenous BDNF is required for myelination and regeneration of injured sciatic nerve in rodents. *The European journal of neuroscience*. 12:4171-4180.

Zhang, X., and A.H. Neufeld. 2005. Activation of the epidermal growth factor receptor in optic nerve astrocytes leads to early and transient induction of cyclooxygenase-2. *Investigative ophthalmology & visual science*. 46:2035-2041.

Zhou, F.Q., M. Walzer, Y.H. Wu, J. Zhou, S. Dedhar, and W.D. Snider. 2006. Neurotrophins support regenerative axon assembly over CSPGs by an ECM-integrin-independent mechanism. *Journal of cell science*. 119:2787-2796.

Zhou, F.Q., J. Zhou, S. Dedhar, Y.H. Wu, and W.D. Snider. 2004. NGF-induced axon growth is mediated by localized inactivation of GSK-3beta and functions of the microtubule plus end binding protein APC. *Neuron*. 42:897-912.

Zhuang, Z.Y., Y. Kawasaki, P.H. Tan, Y.R. Wen, J. Huang, and R.R. Ji. 2007. Role of the CX3CR1/p38 MAPK pathway in spinal microglia for the development of neuropathic pain following nerve injury-induced cleavage of fractalkine. *Brain, behavior, and immunity*. 21:642-651.

Zigmond, S.H., E.F. Foxman, and J.E. Segall. 2001. Chemotaxis assays for eukaryotic cells. *Current protocols in cell biology / editorial board, Juan S. Bonifacino ... [et al.]*. Chapter 12:Unit 12 11.

Zochodne, D.W., and D. Levy. 2005. Nitric oxide in damage, disease and repair of the peripheral nervous system. *Cellular and molecular biology*. 51:255-267.

Zuo, Y., N.M. Perkins, D.J. Tracey, and C.L. Geczy. 2003. Inflammation and hyperalgesia induced by nerve injury in the rat: a key role of mast cells. *Pain*. 105:467-479.